Vladimir I. Erofeev
Igor S. Pavlov

Structural Modeling of Metamaterials

Springer

Advanced Structured Materials

Volume 144

Series Editors

Andreas Öchsner, Faculty of Mechanical Engineering, Esslingen University of Applied Sciences, Esslingen, Germany

Lucas F. M. da Silva, Department of Mechanical Engineering, Faculty of Engineering, University of Porto, Porto, Portugal

Holm Altenbach , Faculty of Mechanical Engineering, Otto von Guericke University Magdeburg, Magdeburg, Sachsen-Anhalt, Germany

Common engineering materials reach in many applications their limits and new developments are required to fulfil increasing demands on engineering materials. The performance of materials can be increased by combining different materials to achieve better properties than a single constituent or by shaping the material or constituents in a specific structure. The interaction between material and structure may arise on different length scales, such as micro-, meso- or macroscale, and offers possible applications in quite diverse fields.

This book series addresses the fundamental relationship between materials and their structure on the overall properties (e.g. mechanical, thermal, chemical or magnetic etc.) and applications.

The topics of *Advanced Structured Materials* include but are not limited to

- classical fibre-reinforced composites (e.g. glass, carbon or Aramid reinforced plastics)
- metal matrix composites (MMCs)
- micro porous composites
- micro channel materials
- multilayered materials
- cellular materials (e.g., metallic or polymer foams, sponges, hollow sphere structures)
- porous materials
- truss structures
- nanocomposite materials
- biomaterials
- nanoporous metals
- concrete
- coated materials
- smart materials

Advanced Structured Materials is indexed in Google Scholar and Scopus.

Vladimir I. Erofeev · Igor S. Pavlov

Structural Modeling of Metamaterials

Vladimir I. Erofeev [ID]
Mechanical Engineering Research Institute
of the Russian Academy of Sciences
Federal Research Center 'Institute of
Applied Physics of the Russian Academy
of Sciences'
Nizhny Novgorod, Russia

Igor S. Pavlov [ID]
Mechanical Engineering Research Institute
of the Russian Academy of Sciences
Federal Research Center 'Institute of
Applied Physics of the Russian Academy
of Sciences'
Nizhny Novgorod, Russia

Preface

At present, technologies of creating advanced structural materials with micro- and nanostructure are intensively developed. One example of such materials is *meta-materials*—a new class of substances with a complexly organized internal structure (microstructure) and possessing unique physical and mechanical properties [1]. They first appeared in the field of optics and photonics [2], but now they are increasingly found in other areas. For example, acoustic metamaterials are widely used [3–7]. In particular, they are applied as acoustic absorbers [8]. In addition, among porous media, granular materials, polymers, composites, and crystalline media, there are materials with a negative Poisson's ratio (auxetic materials) [9–17].

However, the creation of metamaterials is extremely difficult without adequate mathematical models.

In this monograph, the method of structural modeling is proposed to use for constructing mathematical models of metamaterials. This method enables one both revealing the qualitative effect of the internal structure of a material on its effective elastic moduli and performing quantitative estimates of the moduli. Results of the performed research can be used for the design of advanced metamaterials with predetermined physical and mechanical properties.

This book has been written on the basis of studies carried out over the past two decades in Mechanical Engineering Research Institute of the Russian Academy of Sciences (Nizhny Novgorod, Russia), which is a branch of the Federal State Budget Scientific Institution "Federal Research Center Institute of Applied Physics of the Russian Academy of Sciences" since 2016.

We are very grateful to our colleagues who, unfortunately, have already passed away:

to Prof. Alexander Ivanovich Potapov (1949–2010), who was the founder of this scientific direction at our institute;
to Prof. Nadezhda Evgenievna Nikitina (1951–2016), who was an acoustoelasticity specialist and made a significant contribution to obtaining the results of Chap. 7, where prestressed media are considered;

Nizhny Novgorod, Russia   Vladimir I. Erofeev
                                                                                   Igor S. Pavlov
                                                          Lobachevsky State University
                                                                   of Nizhny Novgorod

References

1. Gulyaev, Yu.V., Lagar'kov, A.N., Nikitov, S.A.: Metamaterials: basic research and potential applications. Herald Russ. Acad. Sci. **78**, 268–278 (2008)
2. Zhu, S., Zhang, X.: Metamaterials: artificial materials beyond nature. Natl. Sci. Rev. **5**(2), 131 (2018)
3. Bobrovnitskii, YuI: An acoustic metamaterial with unusual wave properties. Acoust. Phys. **60**(4), 371–378 (2014)
4. Bobrovnitskii, YuI: Models and general wave properties of two-dimensional acoustic meta-materials and media. Acoust. Phys. **61**(3), 255–264 (2015)
5. Cummer, S.A., Christensen, J., Alù, A.: Controlling sound with acoustic metamaterials. Nat. Rev. Mater. **1**, 16001 (2016)
6. Fedotovskii, V.S.: A porous medium as an acoustic metamaterial with negative inertial and elastic properties. Acoust. Phys. **64**(5), 548–554 (2018)
7. Zhou, L., Jiang, H.: Auxetic composites made of 3D textile structure and polyurethane foam. Phys. Status Solidi B **253**(7), 1331–1341 (2016)
8. Bobrovnitskii, Yu.I., Tomilina, T.M.: Sound absorption and metamaterials: a review. Acoust. Phys. **64**(5), 519–526 (2018)
9. Engelbrecht J.K., Fridman V.E., Pelinovsky E.N.: Nonlinear Evolution Equations. Pitman, London. (1988)
10. Evans, K.E.: Auxetic polymers: a new range of materials. Endeavour New Ser. **4**, 170–174 (1991)
11. Goldstein R.V., Gorodtsov V.A., Lisovenko D.S. Auxetic mechanics of crystalline materials. Mechanics of Solids. **45**(4), 529–545 (2010)
12. Goldstein, R.V., Gorodtsov, V.A., Lisovenko, D.S.: Average Poisson's ratio for crystals. Hexagonal Auxetics. Letters on Materials. **3**(1), 7–11 (2013)
13. Goldstein, R.V., Gorodtsov, V.A., Lisovenko, D.S.: Classification of cubic auxetics. Physica Status Solidi B. **250**(10), 2038–2043 (2013)
14. Goldstein R.V., Gorodtsov V.A., Lisovenko D.S.: Cubic auxetics. Doklady Physics. **56**(7), 399–402 (2011)
15. Goldstein R.V., Gorodtsov V.A., Lisovenko D.S. Longitudinal elastic tension of two-layered plates from isotropic auxetics–nonauxetics and cubic crystals. European J. of Mech. – A: Solids. **63**, 122–127 (2017)
16. Goldstein, R.V., Gorodtsov, V.A., Lisovenko, D.S.: The elastic properties of hexagonal auxetics under pressure. Phys. Status Solidi B **253**(7), 1261–1269 (2016)
17. Koniok, D.A., Voitsekhovsky, K.V., Pleskachevsky, Yu.M., Shilko, S.V.: Materials with negative Poisson's ratio (The review). Composite Mech. Des. **10**, 35–69 (2004)

Introduction

Prediction of physical and mechanical properties of media with microstructure and adequate description of dynamic (wave) processes necessitate mathematical models taking into account the presence of several scales (structural levels) in a medium, their self-consistent interaction, and the possibility of energy transfer from one level to another. The following scales are usually distinguished [1, 2]: *atomic* or *microscopic* level (characteristic sizes are angstroms and nanometers), *mesoscopic* level (from 10^{-8} to 10^{-6} m), *submacroscopic* level (from 10^{-6} to 10^{-4} m), and *macroscopic* level (over 10^{-4} m).

Mental breaking of a material into parts is restricted by some limit consisting in a qualitative change of physical properties on a given scale level; i.e., in this case, a *size effect* [3, 4] arises. During studying of wave processes in materials, the size effects start to be shown, when the characteristic spatial scale of effect (e.g., length of an elastic or electromagnetic wave) becomes comparable with the characteristic spatial scale of a material—the size of grain, the lattice period, etc.

In process of accumulation of knowledge about microstructure of a material, there arises a transition to new level of knowledge—a theory is created that enables one to explain mechanical behavior of a material from new positions. It should be emphasized that the actual values of the "microstructure" of the medium in a specific problem can lie both in the range of nano- or micrometers and in the larger scales. However, from the viewpoint of the methodology of theoretical research, the absolute values of the "microstructure" are not so important, as the smallness of some scales with respect to others.

Frequently, different physical properties of the medium are manifested at different scales. For example, it concerns media such as rocks, particularly, hydrocarbon reservoirs. The internal structure of the rocks determines at different scales not only various elastic properties, but also physical properties such as thermal and electrical conductivity, and hydraulic and dielectric constant [5, 6].

In the mathematical simulation of microstructured media, two approaches can be distinguished: "from micro to meso" and "from macro to meso." The first approach consists in the passage from atomic-level models to mesoscale models and is based on the laws of quantum theory. In this case, the medium is considered as a discrete

system of particles coupled by the interaction forces determined from the first principles (quantum postulates). This approach allows one to understand the nature of physical laws and to explain the origin of some properties having no substantiation in the classical theory.

Until the middle of twentieth century, the quantum mechanics was considered, basically, as the microworld mechanics. Being constructed on the basis of quantum postulates, it does not appear at all on the macroscales, where the continuum mechanics is valid, which is created on the basis of the laws of conservation of mass, momentum, kinetic momentum, and the thermodynamics laws (the macroscopic first principles). The first fundamental step of the quantum mechanics in the field of macroscopic phenomena was the creation of the hydrodynamic theory of superfluidity of helium-II by L. D. Landau in 1941 and the idea of L. Onsager (1948) to quantize vortex motion in it [7]. The next step in this direction was made by A. F. Andreev and I. M. Lifshits, who developed in 1969 the phenomenological theory of defects in quantum crystals [8]. According to this theory, defects are considered as delocalized excitations (defectons) that move дефекты almost freely through the crystal. A crystal with defectons is neither a liquid nor a solid. Two different types of motion are possible in it. The first type of motion is associated with small vibrations of the lattice sites near the equilibrium states and is described by the classical equations of elastic solid mechanics. The second type is characteristic for a liquid and is associated with quantum diffusion that leads to mass transfer by defectons, when lattice sites are fixed. At present, such studies are the subject of quantum macrophysics [9].

The second approach to modeling of microstructured media means passing from description of a medium on a macrolevel to mesoscale models. Within its scope, the elaboration of mathematical models of such media proceeds in three directions. The first of them—the *continuum-phenomenological direction*—is associated with the construction of generalized continuum models (*generalized continua*) of the mechanics of a deformable solid and is based on the classical physics laws. It involves expanding of the concept of a representative volume of the medium and taking into account the rotational degrees of freedom of microparticles (polarity of the material), as well as affine deformations of the mesovolume and non-locality of the material [10–11]. Polarity indicates that rigid rotation is allowed, which is not related to the field of displacements in the general case, whereas non-locality testifies the dependence of the physical properties of the material on the influence of environmental particles. Continual theories are elaborated by the deductive way: All the results are consequences of a system of fundamental assumptions—axioms or postulates. The advantages of this elaboration are logical consistency, a rigor of the derivation of various particular versions of the models, and the possibility of a consistent classification of theories according to selected attributes. A decisive contribution to the development of this direction was made by the works of E. and F. Cosserat [12], C. Truesdell and R. Toupin [13, 14], E. L. Aero and E. V. Kuvshinskii [15, 16], R. Mindlin [17], A. C. Eringen [18–21], W. Nowacky [22], V. A. Palmov [23, 24], L. I. Sedov [25–27], V. I. Erofeev [28], A. I. Potapov [29], V. P. Matveenko, I. N. Shardakov, M. A. Kulesh, and E. F. Grekova [30, 31],

S. A. Lurie [32, 33], etc. At present, structurally heterogeneous materials are frequently simulated by the generalized micropolar theories of the Cosserat continuum type [34–39]. However, these theories involve a large number of material constants, which have to be determined experimentally. Moreover, relationships between these constants and the material structure are not always clear.

The second direction—*structural modeling*, which is the subject of study of this monograph, is devoid of such a drawback. In accordance with this method, a material is represented by a regular or quasiregular lattice consisting of finite-sized particles. The elaboration of a structural model starts with selection in the material of some minimal volume—a structural cell that is an analog of the periodicity cell in a crystalline material. The cell is capable of characterizing the basic features of the macroscopic behavior of the material [40–43]. As a rule, a structural cell is a particle, which behavior is characterized by interaction with the environment and is described by kinematic variables [44–61]. The role of these body particles can be played by domains, grains, fullerenes, nanotubes, or clusters consisting of nanoparticles. Sometimes, particles are represented as material points, i.e., force centers possessing the properties of mass, charge, etc. The interaction forces are assumed to be rapidly decreased with growing distance, so they can be neglected if the distance between the points exceeds "the radius of molecular action." This direction originates from Max Born's works on the theory of crystal lattices and until recently has developed mainly in the framework of the solid-state physics [62, 63]. The founder of the structural modeling method in Russia is a professor of Moscow State University Nikolai Pavlovich Kasterin (1869–1947). He was a student of a great Russian physicist Alexander Grigorievich Stoletov (1839–1896). N. P. Kasterin studied the dispersion of sound waves by means of this method [64, 65].

Special attention in the structural modeling method is paid to studying the propagation and interaction of elementary excitations—quasiparticles (phonons, magnons, excitons, etc.)—and various defects inherent in real bodies [66, 67]. Both quantum and classical approaches to the analysis of dynamic processes coexist organically within the scope of this direction [68].

As distinct from the continual models, the structural ones explicitly contain the geometric parameters of the structure—the size and shape of the particles. Finally, the effective elastic moduli of various orders depend on these parameters [69, 70]. Structural models enable one not only to reveal the qualitative influence of local structure on the effective moduli of elasticity but also to perform numerical estimations of their quantities and even to control physical and mechanical properties of a medium, these being generally unavailable from continuum-phenomenological theories.

The clear coupling between a structure of a medium and its macroparameters discloses major opportunities for the purposeful design of materials with given physical–mechanical properties. Shortcomings of the structural modeling are absence of universality of modeling procedure and complexity of the accounting of nonlinear and non-local effects of interparticle interactions. A significant contribution to the development of the structural modeling method was made by the works of I. A. Kunin [71], E. Kroner [72], A. Askar [73–75], G. Maugin and

J. Pouget [76–80], E. L. Aero and A. V. Porubov [81–88], N. F. Morozov and A. M. Krivtsov [89–94], D. A. Indeytsev [95], L. I. Manevich and V. V. Smirnov [96–98], Askes H., A. Suiker, A. V. Metrikine, and R. de Borst [99–101], Chinyu Li and Tsu-Wei Chou [102], A. I. Potapov [103–112], A. A. Vasiliev, S. V. Dmitriev, and A. E. Miroshnichenko [113–116], and others.

The third direction is related to the method of statistical averaging and is used mainly for constructing models of a medium with arbitrary packing of particles [117]. In the framework of this direction, equations of micromotion are first made up, i.e., equations of motion of microparticles taking into account their interaction with the environment, and then, using averaging, "macrovariables" are introduced that describe various types of collective forms of motion of the medium and averaged dynamic equations are derived [118–120]. Averaged equations of motion have much in common with the generalized continuum models. This direction includes elements of the first two directions, and its advantage is the ability to simulate the dynamics of disordered systems. The disadvantages include the substantial complexity of deriving the averaged equations of motion and calculating the constants containing in these equations. The works by V. A. Lomakin, A. A. Ilyushin [121–123], V. N. Nikolaevsky [124, 125], T. D. Shermergor [126], and others made a significant contribution to the development of this direction.

Further, let us consider the advantages of applying the method of structural modeling to metamaterials.

References

1. Ghoniem, N.M., et al.: Multiscale modelling of nanomechanics and micromechanics: an over-view. Phil. Mag. **83**(31–34), 3475–3528 (2003)
2. Li S., Wang G.: Introduction to micromechanics and nanomechanics. Singapore; Hackensack: World Scientific, (2008)
3. Miller, R.E., Shenoy, V.B.: Size-dependent elastic properties of nanosized structural elements. Nanotechnology **11**, 139–147 (2000)
4. Solyaev, Yu., Lurie, S.: Numerical predictions for the effective size-dependent properties of piezoelectric composites with spherical inclusions. Compos. Struct. **202**, 1099–1108 (2018)
5. Bayuk, I., Ammerman, M., Chesnokov, E.: Upscaling of elastic properties of anisotropic sedimentary rocks. Geophys. J. Int. **172**, 842–860 (2008)
6. Yalaev T., Bayuk I., Tarelko N., Abashkin A. Connection of elastic and thermal properties of Bentheimer sandstone using effective medium theory (rock physics). ARMA-2016-128. 50th U.S. Rock Mechanics/Geomechanics Symposium, 26-29 June, Houston, Texas, 1–7 (2016)
7. Landau L.D. and Lifshitz E.M. *Course of Theoretical Physics*, Vol. 6: Fluid Mechanics (Fizmatlit, Moscow, 2003; Butterworth–Heinemann, Oxford, 2005).
8. Andreev A.F., Lifshitz I.M. Quantum theory of defects in crystals. Soviet Physics JETP. **29**(6) 1107–1113 (1969)
9. Tsipenyuk Yu.M. *Quantum micro- and macrophysics*. Fizmatkniga, Moscow, (in Russian). 640 (2006)
10. Eringen, A.C.: Microcontinuum Field Theories. 1: Foundation and Solids. Springer. New York (1999)

11. Lisina, S.A., Potapov, A.I.: Generalized continuum models in nanomechanics. Doklady Phys. **53**, 275–277 (2008). https://doi.org/10.1134/S1028335808050091
12. Cosserat E. et F. Theorie des Corps Deformables. – Paris: Librairie Scientifique A. Hermann et Fils, 1909. – 226p. (Reprint, 2009)
13. Toupin, R.A.: Theories of elasticity with couple-stresses Arch. Rat. Mech. Anal. **17**, 85–112 (1964)
14. Truesdell, C., Toupin, R.A.: The classical field theories. Springer, Handbuch der Physik. III/I. Berlin (1960)
15. Aero, E.L., Kuvshinskii, E.V.: Fundamental equations of the theory of elastic media with rotationally interacting particles. Soviet Phys. Solid State **2**, 1272–1281 (1961)
16. Kuvshinskiy, E.V., Aero, E.L.: Continuum theory of asymmetric elasticity—the problem of internal rotation. Soviet Phys. Solid State **5**, 1892–1897 (1964)
17. Mindlin, R.D.: Microstructure in linear elasticity. Arch. Rat. Mech. Anal. **16**(7), 51–78 (1964)
18. Eringen, A.C.: Microcontinuum Field Theories. 1: Foundation and solids. Springer, New York (1999)
19. Eringen, A.C.: Nonlinear theory of continuous media, 477 p. McGraw-Hill, New York (1962)
20. Eringen, A.C., Edelen, D.G.B.: On non-local elasticity. Int J. Eng. Sci. **10**(3), 233–248 (1972)
21. Eringen, A.C., Suhubi, E.S.: Nonlinear theory of simple micro-elastic solids. Int. J. Eng. Sci. **2**, 189–203, 389–404 (1964)
22. Nowacki, W.: Theory of Micropolar Elasticity. J. Springer, Wien (1970)
23. Palmov, V.A.: Basic equations of the theory of asymmetrical elasticity. Prikl. Matem. Mekh. **28**(3), 401–408 (1964)
24. Palmov, V.A.: On a model of a medium with complex structure. Prikl. Matem. Mekh. **33**(4), 768–773 (1969)
25. Sedov, L.I.: Mathematical methods for constructing new models of continuous media. Russ. Math. Surv. **20**(5), 123–182 (1965)
26. Sedov, L.I.: Models of continuous media with internal degrees of freedom. J. Appl. Math. Mech. **32**(5), 803–819 (1968)
27. Sedov, L.I.: Mechanics of Continuous Medium, vol. 1. World Scientific Publ, Singapore (1997)
28. Erofeev, V.I.: Wave Processes in Solids with Microstructure. World Scientific Publishing. New Jersey, London, Singapore, Hong Kong, Bangalore, Taipei (2003)
29. Lisina, S.A., Potapov, A.I.: Generalized continuum models in nanomechanics. Doklady Phys. **53**, 275–277 (2008). https://doi.org/10.1134/S1028335808050091
30. Kulesh, M.A., Matveenko, V.P., Shardakov, I.N.: Propagation of surface elastic waves in the Cosserat medium. Acoust. Phys. **52**(2), 186–193 (2006). https://doi.org/10.1134/s1063771006020114
31. Kunin, I.A.: Elastic Media with Microstructure, 2 volumes. Springer, Berlin (1983)
32. Solyaev, Yu., Lurie, S.: Numerical predictions for the effective size-dependent properties of piezoelectric composites with spherical inclusions. Compos. Struct. **202**, 1099–1108 (2018)
33. Solyaev, Yu., Lurie, S., Ustenko, A.: Numerical modeling of a composite auxetic metamaterials using micro-dilatation theory. Continuum Mech. Thermodyn. **31**, 1099–1107 (2019)
34. Altenbach, H., Maugin, G.A., Erofeev, V.I. (eds.): Mechanics of Generalized Continua. Springer, Berlin, Heidelberg, 350 p. (2011)
35. Erofeev V.I., Leontieva A.V., Malkhanov A.O.: Stationary longitudinal thermoelastic waves and the waves of the rotation type in the non-linear micropolar medium. ZAMM – J. Appl. Math. Mech. **97**(9), 1064–1071 (2017)
36. Erofeev V.I., Malkhanov A.O.: Macromechanical modelling of elastic and visco-elastic Cosserat continuum. ZAMM – J. Appl. Math. Mech. **97**(9), 1072–1077 (2017)
37. Maugin, G.A., Metrikine, A.V. (eds.): Mechanics of Generalized Continua. One Hundred Years After the Cosserats. Springer, 337 p. (2010)

38. Mechanics of generalized continua. Proceedings of the IUTAM-symposium on the general-ized Cosserat continuum and the continuum theory of dislocations with applications. Freudenstadt and Stuttgart, 1967, ed. E. Kroner, Springer-Verlag, Berlin, Heidelberg, New York (1968)

39. Suvorov, Y.M., Tarlakovskii, D.V., Fedotenkov, G.V.: The plane problem of the impact of a rigid body on a half-space modelled by a Cosserat medium. J. Appl. Math. Mech. **76**(5), 511–518 (2012)

40. Blank X., Bris C.Le, Lions P.-L. From molecular models to continuum mechanics. Arch. Rational Mech. Anal. **164**, 341–381 (2002)

41. Broberg, K.B.: The cell model of materials. Comput. Mech. **19**, 447–452 (1997)

42. Ghoniem, N.M., et al.: Multiscale modelling of nanomechanics and micromechanics: an over-view. Phil. Mag. **83**, 31–34, 3475–3528 (2003)

43. Pavlov, I.S., Potapov, A.I.: Structural models in mechanics of nanocrystalline media. Doklady Phys. **53**(7), 408–412 (2008)

44. Berglund K. Structural Models of Micropolar Media. in: Mechanics of Micropolar Media. Eds. O. Brulin and R.K.T. Hsieh. World Scientific, Singapore, 35–86 (1982)

45. Fisher-Hjalmars, I.: Micropolar phenomena in ordered structures. In: Brulin, O., Hsieh, R.K. T. (eds.) Mechanics of Micropolar Media. World Scientific, Singapore, 1–33 (1982)

46. Gendelman, O.V., Manevitch, L.I.: Linear and nonlinear excitations in a polyethylene crystal. Part I. Vibrational modes and linear equations. Macromol. Theor. Simul. **7**, 579–589 (1998)

47. Gendelman O.V, Manevitch L.I.: Linear and nonlinear excitations in a polyethylene crystal. Part II. Nonhomogeneous states and nonlinear excitations. Macromol. Theor. Simul. **7**, 591–598 (1998)

48. Gendelman O.V., Manevitch L.I. The description of polyethylene crystal as a continuum with internal degrees of freedom. Int. J. Solids Struct. **33**(12) 1781–1798 (1996)

49. Pavlov, I.S., Potapov, A.I.: Two-dimensional model of a granular medium. Mech. Solids **42**(2), 250–259 (2007)

50. Porubov, A.V.: Two-dimensional modeling of diatomic lattice. In: dell'Isola F. et al. (eds.) Advances in Mechanics of Microstructured Media and Structures, Advanced Structured Materials vol. 87. Springer International Publishing AG, part of Springer Nature, 263─272 (2018). https://doi.org/10.1007/978-3-319-73694-5_15

51. Porubov, A.V., Berinskii, I.E.: Nonlinear plane waves in materials having hexagonal internal structure. Int. J. Non-Linear Mech. **67**, 27–33 (2014)

52. Porubov, A.V., Berintskii, I.E.: Two-dimensional nonlinear shear waves in materials having hexagonal lattice structure. Math. Mech. Solids **21**(1), 94–103 (2016)

53. Porubov, A.V., Krivtsov, A.M., Osokina, A.E.: Two-dimensional waves in extended square lattice. Int. J. Non-Linear Mech. **99**, 281–287 (2018)

54. Porubov, A.V., Osokina, A.E.: On two-dimensional longitudinal nonlinear waves in graphene lattice. In: Berezovski A., Soomere T. (eds.) Applied Wave Mathematics II. Mathematics of Planet Earth, vol. 6, pp. 151–166. Springer, Cham (2019)

55. Pouget, J.: Lattice dynamics and stability of modulated-strain structures for elastic phase transitions in alloys. Phys. Rev. B. **48**(2), 864–875 (1993)

56. Pouget, J., Askar, A., Maugin, G.A.: Lattice model for elastic ferroelectric crystals: Microscopic approach. Phys. Rev. B. **33**(9), 6304–6325 (1986)

57. Pouget, J., Maugin, G.A.: Nonlinear dynamics of oriented elastic solid. Part 1,2 J. Elasticity **22**, 135–155, 157–183 (1989)

58. Suiker, A.S.J., Metrikine, A.V., de Borst, R.: Comparison of wave propagation characteristics of the Cosserat continuum model and corresponding discrete lattice models. Int. J. Solids Struct. **38**, 1563–1583 (2001)

59. Suiker, A.S.J., Metrikine, A.V., de Borst, R.: Dynamic behaviour of a layer of discrete particles. Part 1: Analysis of body waves and eigenmodes. J. Sound Vib. **240**(1), 1–18 (2001)

60. Vasiliev, A.A., Pavlov, I.S.: Models and some properties of Cosserat triangular lattices with chiral microstructure. Lett. Mater. **9**(1), 45–50 (2019). www.lettersonmaterials.com https://doi.org/10.22226/2410-3535-2019-1-45-50

61. Vasiliev, A.A., Pavlov, I.S.: Structural and mathematical modeling of Cosserat lattices composed of particles of finite size and with complex connections. IOP Conf. Ser.: Mater. Sci. Eng. **447**, 012079 (2018)

62. Born, M., Huang, K.: Dynamical Theory of Crystal Lattices. Clarendon Press, Oxford (1954)

63. Brillouin, L., Parodi, M.: Wave Propagation in Periodic Structures. McGrawHill, New York (1946)

64. Kasterin N.P.: On dispersion of sound waves in a heterogeneous medium. Zhurnal russkogo fiziko-khimicheskogo obshestva. J. Russian Physical-Chemical Society. **30**(3A), 61–78 (1898) (in Russian)

65. Kasahara, K.: Earthquake Mechanics. Cambridge University Press, Cambridge (1981)

66. Bogomolov V.N., Parfen'eva L.S., Smirnov I.A., Misiorek H., and Jzowski A.: Phonon Propagation through Photonic Crystals — Media with Spatially Modulated Acoustic Properties. Phys. Solid State. **44**, 181–185 (2002)

67. Kaganov M.I. Electrons, Phonons, Magnons, 268 pp. English Translation. Mir Publishers, Moscow (1981)

68. Kosevich, A.M.: 1999. The Crystal Lattice, Wiley-VCH, Berlin (1999)

69. Pavlov, I.S., Potapov, A.I.: Structural models in mechanics of nanocrystalline media. Doklady Phys. **53**(7), 408–412 (2008)

70. Potapov, A.I., Pavlov, I.S., Lisina, S.A.: Acoustic identification of nanocrystalline media. J. Sound Vib. **322**(3), 564–580 (2009)

71. Kushwaha, M.S., Halevi, P., Martinez, G., Dobrzynski, L., Djafari-Rouhani, B.: Theory of band structure of periodic elastic composites. Phys. Rev. B. **49**, 2313 (1994)

72. Kroner, E., Datta, B.K.: Non-local theory of elasticity for a finite inhomogeneous medium—a derivation from lattice theory. In: J. Simmons, R. de Wit (eds.) Fundamental aspects, of dislocation theory (Conference Proc.), **2**, 737–746. National Bureau of Standards, Washington (1970)

73. Askar, A.: A model for coupled rotation-displacement mode of certain molecular crystals. Illustration for KNO_3. J. Phys. Chem. Solids **34**, 1901–1907 (1973)

74. Askar, A.: Lattice Dynamics Foundation of Continuum Theory. World-Scientific, Singapore (1985)

75. Askar, A.: Molecular crystals and the polar theories of continua: experimental values of material coefficients for KNO_3. Int. J. Eng. Sc. **10**, 293–300 (1972)

76. Maugin, G.A.: Continuum Mechanics of Electromagnetic Solids. North-Holland Amsterdam (1988)

77. Pouget, J.: Lattice dynamics and stability of modulated-strain structures for elastic phase transitions in alloys. Phys. Rev. B. **48**(2), 864–875 (1993)

78. Pouget, J., Askar, A., Maugin, G.A.: Lattice model for elastic ferroelectric crystals: Microscopic approach. Phys. Rev. B. **33**(9), 6304–6325 (1986)

79. Pouget, J., Maugin, G.A.: Nonlinear dynamics of oriented elastic solid. Part 1,2 J. Elasticity **22**, 135–155, 157–183 (1989)

80. Sayadi, M.K., Pouget, J.: Soliton dynamics in a microstructured lattice model. J. Phys. A: Math. Gen. **24**, 2151–2172 (1991)

81. Aero E.L., Bulygin A.N.: Strongly nonlinear theory of nanostructure formation owing to elastic and nonelastic strains in crystalline solids. Mech. Solids. **42**, 807–822 (2007)

82. Porubov, A.V.: Two-dimensional modeling of diatomic lattice. In: dell'Isola F. et al. (eds.) Advances in Mechanics of Microstructured Media and Structures, Advanced Structured Materials vol. 87. Springer International Publishing AG, part of Springer Nature, 263–272 (2018). https://doi.org/10.1007/978-3-319-73694-5_15

83. Porubov A.V., Aero E.L., Andrievsky B.R.: Dynamic Properties of Essentially Nonlinear Generalized Continua. In: Maugin G., Metrikine A. (eds) Mechanics of Generalized Continua. Advances in Mechanics and Mathematics. Springer, New York, NY. V. **21** 161–168 (2010). https://doi.org/10.1007/978-1-4419-5695-8_17
84. Porubov A.V., Aero E.L., Maugin G.A.: Two approaches to study essentially nonlinear and dispersive properties of the internal structure of materials. Physical Review E79. 046608 (2009)
85. Porubov, A.V., Berinskii, I.E.: Nonlinear plane waves in materials having hexagonal internal structure. Int. J. Non-Linear Mech. **67**, 27–33 (2014)
86. Porubov, A.V., Berintskii, I.E.: Two-dimensional nonlinear shear waves in materials having hexagonal lattice structure. Math. Mech. Solids **21**(1), 94–103 (2016)
87. Porubov, A.V., Krivtsov, A.M., Osokina, A.E.: Two-dimensional waves in extended square lattice. Int. J. Non-Linear Mech. **99**, 281–287 (2018) (без ротационных степеней, учет нелокальности, дискретная модель)
88. Porubov, A.V., Osokina, A.E.: On two-dimensional longitudinal nonlinear waves in graphene lattice. In: Berezovski A., Soomere T. (eds.) Applied Wave Mathematics II. Mathematics of Planet Earth, **6**, 151–166. Springer, Cham (2019)
89. Berinskii, I.E., Ivanova, E.A., Krivtsov, A.M., Morozov, N.F.: Application of moment interaction to the construction of a stable model of graphite crystal lattice. Mech. Solids **42**(5), 663–671 (2007)
90. Ivanova, E.A., Krivtsov, A.M., Morozov, N.F.: Derivation of macroscopic relations of the elasticity of complex crystal lattices taking into account the moment interactions at the microlevel. J. Appl. Math. Mech. **71**(4), 543–561 (2007)
91. Ivanova, E.A., Krivtsov, A.M., Morozov, N.F., Firsova, A.D.: Description of crystal packing of particles with torque interaction. Mech. Solids **38**(4), 76–88 (2003)
92. Ivanova E.A., Morozov N.F., Semenov B.N., Firsova A.D.: On determination of elasticity modules of nanostructures: theoretical calculations and experiment methods. Mech. Solids. **40**(4), 60–68 (2005)
93. Krivtsov A.M., Morozov N.F.: On mechanical characteristics of nanocrystals. Phys. Solid State. **44**(12), 2260–2265 (2002)
94. Krivtsov, A.M., Podol'skaya, E.A.: Modeling of elastic properties of crystals with hexagonal close-packed lattice. Mech. Solids **45**(3), 370–378 (2010)
95. Indeytsev, D.A., Naumov, V.N., Semenov, B.N.: Dynamic effects in materials of complex structure. Mech. Solids **42**(5), 672–691 (2007)
96. Manevich L.I., Smirnov V.V.: Localized nonlinear oscillations of a planar zigzag. Doklady Phys. Chem. **413**, 69–73 (2007). https://doi.org/10.1134/S0012501607030086
97. Smirnov V.V., Manevich L.I. Localization of torsion vibrations in a discrete model of alkanes. Dokl. Phys. **62**, 165–169 (2017). https://doi.org/10.1134/S1028335817040048
98. Smirnov, V.V., Shepelev, D.S., Manevitch, L.I.: Localization of bending vibrations in the single-wall carbon nanotubes. Nanosyst. Phys. Chem. Math. **2**(2), 102–106 (2011)
99. Askes H., Metrikine A.V. One-dimensional dynamically consistent gradient elasticity models derived from a discrete microstructure Part 1: Generic formulation. European J. of Mech. A/Solids. **21**(4), P. 573–588 (2002)
100. Suiker, A.S.J., Metrikine, A.V., de Borst, R.: Comparison of wave propagation characteristics of the Cosserat continuum model and corresponding discrete lattice models. Int. J. Solids Struct. **38**, 1563–1583 (2001)
101. Suiker, A.S.J., Metrikine, A.V., de Borst, R.: Dynamic behaviour of a layer of discrete particles. Part 1: Analysis of body waves and eigenmodes. J. Sound Vib. **240**(1), 1–18 (2001)
102. Pavlov, I.S.: Acoustic identification of the anisotropic nanocrystalline medium with non-dense packing of particles. Acoust. Phys. **56**(6), 924–934 (2010)
103. Lisina, S.A., Potapov, A.I., Nesterenko, V.F.: Nonlinear granular medium with rotations of the particles. One-dimensional model. Phys. Acoust. **47**(5), 666–674 (2001)

104. Pavlov, I.S., Potapov, A.I.: Structural models in mechanics of nanocrystalline media. Doklady Phys. **53**(7), 408–412 (2008)
105. Pavlov, I.S., Potapov, A.I.: Two-dimensional model of a granular medium. Mech. Solids **42**(2), 250–259 (2007)
106. Pavlov, I.S., Potapov, A.I., Maugin, G.A.: A 2D granular medium with rotating particles. Int. J. Solids Struct. **43**(20), 6194–6207 (2006)
107. Potapov, A.I., Pavlov, I.S.: Nonlinear waves in 1D oriented media. Acoust. Lett. **19**(6), 110–115 (1996)
108. Potapov, A.I., Pavlov, I.S., Gorshkov, K.A., Maugin, G.A.: Nonlinear interactions of solitary waves in a 2D lattice. Wave Motion **34**(1), 83–95 (2001)
109. Potapov, A.I., Pavlov, I.S., Lisina, S.A.: Acoustic Identification of Nanocrystalline Media. J. Sound Vib. **322**(3), 564–580 (2009)
110. Potapov, A.I., Pavlov, I.S., Maugin, G.A.: Nonlinear wave interactions in 1D crystals with complex lattice. Wave Motion 29, 297–312 (1999)
111. Potapov, A.I., Pavlov, I.S., Lisina, S.A.: Identification of nanocrystalline media by acoustic spectroscopy methods. Acoust. Phys. **56**(4), 588–596 (2010)
112. Potapov A.I., Pavlov I.S., Nikitenkova S.P., Shudyaev A.A. Structural models in nanoacoustics: control of dispersion properties of phonon crystals. Acoustics of inhomogeneous media. Proceedings of the Russian acoustic society. Issue 10. Moscow: GEOS, 9–16 (2009) (in Russian)
113. Vasiliev, A.A, Dmitriev, S.V., Miroshnichenko, A.E.: Multi-field approach in mechanics of structural solids. Int. J. Solids Struct. **47**, 510–525 (2010)
114. Vasiliev, A.A, Dmitriev, S.V., Miroshnichenko, A.E.: Multi-field continuum theory for medium with microscopic rotations. Int. J. Solids Struct. **42**, 6245–6260 (2005)
115. Vasiliev, A.A, Miroshnichenko, A.E., Ruzzene, M.: Multifield model for Cosserat media. J. Mech. Mater. Struct. **3**(7), 1365–1382 (2008)
116. Vasiliev, A.A., Miroshnichenko, A.E., Dmitriev, S.V.: Multi-field modeling of a Cosserat lattice: models, wave filtering, and boundary effects. Euro. J. Mech. A/Solids **46**, 96–105 (2014)
117. Christoffersen, J., Mehrabadi, M.M., Nemat-Nasser, S.A.: A micromechanical description of granular material behavior. Trans. ASME. J. Appl. Mech. **48**(2), 339–344 (1981)
118. Chang, C.S., Ma, L.: A micromechanical-based micropolar theory for deformation of granular solids. Int. J. Solids Struct. **28**(1), 67–87 (1994)
119. Christoffersen, J., Mehrabadi, M.M., Nemat-Nasser, S.A.: A micromechanical description of granular material behavior. Trans. ASME. J. Appl. Mech. **48**(2), 339–344 (1981)
120. Nikolaevsky V.N.: Stress tensor and averaging in mechanics of continuous media. J. Appl. Math. Mech. **39**(2) 351–356 (1975)
121. Ilyushin, A.A.: Mechanics of Continuous Media. Moscow State Univ, Publ, Moscow (1990). (in Russian)
122. Ilyushin, A.A., Lomakin, V.A.: Moment theories in mechanics of solids. Strength and Plasticity. Moscow, Nauka, 54–60 (1971)
123. Lomakin, V.A.: Static Problems in Mechanics of Deformable Solids. Nauka, Moscow (1970). (in Russian)
124. Nikolaevsky, V.N.: Geomechanics and Fluidodynamics. Kluwer Academic Publishers, Dordrecht (1996)
125. Nikolaevsky V.N.: Stress tensor and averaging in mechanics of continuous media. J. Appl. Math. Mech. **39**(2), 351–356 (1975)
126. Shermergor, T.D.: Theory of Elasticity of Micro-Inhomogeneous Media. Nauka, Moscow (1977).(in Russian)

Contents

Chapter 1
Theoretical Basis of the Structural Modeling Method

The principles of the structural modeling method, the development of the theoretical foundations of which this monograph is devoted, are formulated in the first chapter. Moreover, the problem of the applicability of the classical mechanics laws to a theoretical description of media with micro- and nanostructure is discussed here.

1.1 Review of References

One of the main hypotheses of the classical continuum mechanics is the Cauchy stress principle, which postulates that the effect of all the internal forces applied to an elementary area is equivalent to the effect of their resultant force applied to the center of this area [1]. However, in the general case, the action of an arbitrary system of forces is equivalent to the action of the main vector and the main moment. In this case, couple stresses also appear in the medium, forming, generally speaking, asymmetric tensors [2, 3]. Thus, the rejection of the Cauchy stress principle makes possible taking into account the presence in the medium of internal pairs of forces and moment interactions that arise naturally when considering a physically infinitely small volume (over which the medium's properties are averaged) not as a material point, but as a more complex object with new degrees of freedom: rotational, oscillatory, or the ability to microdeforming. The assumption about the existence of an internal structure (microstructure) of a physically infinitesimal object, which is provided by the discreteness or fibrous structure of real materials, leads to a significant expansion of the spectrum of properties of a continuous medium. In particular, this assumption enables one describing some experimentally observed acoustic effects, for example, the dispersion of shear waves [4]. A brief description of the history of studies of microstructured media is given below.

1.1.1 Discrete and Continuum Models of Solids: A Brief Historical Review

Isaak Newton was the first to use a discrete model in problems of the mechanics of continuous deformable media [5]. He considered a one-dimensional lattice consisting of pointwise particles and calculated the speed of sound in air using this model. His model represented a chain of particles of uniform mass located at equal distances from each other on a straight-line coinciding with the wave propagation direction. According to his assumption, a force proportional to their relative displacement acts on each particle from the side of its neighboring particles.

The reason, due to which I. Newton had to consider a chain of point particles, was that the study of continuous media wosuld lead to partial differential equations, which had been then unknown. The motion of the mechanical model chosen by Newton was described by the set of ordinary differential equations already known at that time. However, as it will be shown in Chap. 3, only longitudinal waves can be considered in the framework of this model, whereas the study of transverse waves principally necessitates taking into account either an additional degree of freedom provided by the rotation of anisotropic particles or the initial deformation of the springs (see [6, 7] and Sect. 7.2).

A systematic study of one-dimensional lattices began in 1727 from the works of Johann Bernoulli and his son—Daniel Bernoulli. They revealed that a one-dimensional system of *n* point particles possesses *n* independent types of vibrations and, as a consequence, *n* natural frequencies.

In 1753, D. Bernoulli established the superposition principle, according to which any movement of the oscillatory system can be represented as a superposition of its own vibrations. This most important principle is one of the particular consequences of Fourier expansion. Later, it was generalized. Now it is known as "Fourier theorem."

After Johann and Daniell Bernoulli gave a complete solution to the problem about a one-dimensional lattice consisting of point particles, and Leonard Euler solved the problem of an oscillating string, their results were interconnected in 1759 by J. L. Lagrange, who established the transition from the continuous model to the discrete one. The related work was published in the Proceedings of the Turin Academy. Later, it was developed in the famous book "Analytical Mechanics" by J. L. Lagrange (1788).

In 1830, O. L. Cauchy, using a discrete model of the medium (ether), tried to explain the dispersion of light under the assumption that light is elastic waves with a very high frequency [8]. He showed that for wavelengths much larger than the distance between neighboring particles in a one-dimensional lattice, the wave velocity does not depend on the wavelength. For short wavelengths (i.e., at high frequencies), the wave velocity is a function of wavelength and can vary drastically. In 1839, W.R. Hamilton, considering waves in a discrete chain, introduced the concept of the group wave velocity.

Cauchy's ideas expressed in [8] served as the starting point for the studies of Baden Powell, who, based on Newton's model of a one-dimensional lattice, derived

a formula related the wave propagation velocity and its length [9]. However, he did not notice one of the most important properties of such systems, namely the existence of a maximum frequency at which the waves can still propagate in a lattice. This discovery was made in 1881 by Lord Kelvin (W. Thomson), who paid attention to the fact that frequency is a function of the wavenumber [10]. Using a model of a chain of particles of two kinds, Kelvin was able to explain the phenomenon of dispersion, avoiding the difficulties that arose in Cauchy's theory.

Since the middle of nineteenth century, most of the results of the deformable solid mechanics had been obtained in the framework of the continuum theory of elasticity, whereas discrete models were used in the solid-state physics and in the crystal lattice theory [11, 12]. The emphasis on continuum models was associated with successes in the theory of functions of the real and complex variables, the theory of boundary and initial-boundary value problems of differential equations in ordinary and partial derivatives, with the development of the theory of integral equations, i.e., with those branches of science that operate mainly continuous and continuously differentiable functions.

Historically, one of the first continuum models of an elastic medium that cannot be described in the framework of the classical theory of elasticity considering a medium as a continuum of material points possessing, in general, three translational degrees of freedom is the Cosserat medium, which consists of solid non-deformable bodies-particles possessing three translational and three rotational degrees of freedom. The microdisplacement tensor acquires an antisymmetric part, which can be expressed through the vector of particle rotation with respect to the particle axis. The role of such rotations increases with increasing frequency, whereas as the frequency decreases, the translational displacements of the centers of mass of the particles (elements of the medium) become the governing factor [2]. The theoretical foundations of such a continuum were laid by the brothers Eugène and François Cosserat [13] in 1909. It is traditionally assumed that the work [13] exists as if in a vacuum, without any predecessors or, until the beginning of the 1960s, followers. But this is not true.

So, yet in 1839, J. Mac Cullagh's work [14] had been published, which was devoted to construction of an elastic medium model capable describing both the observed reflection and refraction. In the Mac Cullagh continuum, the strain energy depends on the rotational components of the strain.

Ideas distinguishing from the classical continuum canons were contained in books by Mossoti (1851) [15], Clebsh (1862) [16], Kirchhoff (1874) [17], Duhem (1891) [18], and Hertz (1894) [19]. So, the concepts of "couple stresses" and "the rotational energy" were introduced in their works by A. Clebsch in 1862 [16] and by G. Kirchhoff in 1874 [17]. The importance of taking into account couple stresses was also mentioned by W. Voigt in 1887 in Ref. [20], and in 1891 P. Duhem [18] introduced the rotational measure of deformation. Thus, in 1909, the Cosserat brothers generalized and developed works of G. Kirchhoff, A. Clebsch, P. Duhem, and W. Voigt. But the Cosserat theory remained forgotten until the middle of 1960s years.

However, discrete models of media consisting of non-point particles possessing rotational degrees of freedom began to be developed after the elaboration of the Cosserat continuum theory. So, in the late 1930s Ya.I. Frenkel considered a model of

a chain of oriented dipoles with fixed mass centers and showed that "waves of rotational oscillations" [21] (i.e., orientational waves) can propagate in such a chain. The first model of the interaction of translational and rotational oscillations in a molecular lattice was proposed by Anselm and Porfiryeva in 1949 [22]. Only the linear interaction of orientational waves with one type of translational oscillations—longitudinal waves—was taken into account in this model. Nevertheless, the authors showed that, basically, mixed orientational–translational oscillations, which frequencies depend both on the mass and the moment of inertia of molecules, propagate in molecular crystal lattices. There exist four branches of the rotational–translational oscillation spectrum in a one-dimensional molecular lattice model with two molecules in a unit cell. In the long-wavelength range, one branch (acoustic) corresponds to purely translational oscillations, the second branch—to purely rotational oscillations depending only on the moment of inertia, and the other two ones are responsible for mixed rotational–translational oscillations depending on both the mass and the moment of inertia. Further research by N. N. Porfiryeva [23] showed that these results obtained for a one-dimensional lattice model are, in general, saved for a three-dimensional crystal lattice.

From the beginning of the 1960s generalized models of the Cosserat continuum are intensively developed [24]: the theory of oriented media, asymmetric, multipolar, micromorphic, gradient theories of elasticity. So, on the basis of assumption of the rotational interaction of particles of elongated shape in an anisotropic elastic medium, Aero and Kuvshinsky [25, 26] generalized the phenomenological theory of elasticity in order to explain some anomalies in the dynamic behavior of plastics, to which the classical theory of elasticity did not provide a satisfactory treatment. Later, the idea of an "oriented" continuum, each point of which is assigned a direction (the field of a director), was developed in the theory of liquid crystals [27–29], where the director waves in liquid crystals are, in fact, analogs of rotational waves in solids, like spin waves in ferromagnets [30]. A significant contribution to the development of moment theories was also made by the works of Hermann and Gunther [24], Green and Rivlin [31], Koiter [32], Ilyushin and Lomakin [33–35], Mindlin [36], Nowacky [3], Palmov [37, 38], Savin [39], Toupin and Truesdell [40, 41], Eringen [42–45], Kunin [2], and others (see also the List of references in [46]). By the middle of 1960s, a new direction was formed that was closely related to the theory of the crystal lattice—the nonlocal theory of elasticity, containing generalized Cosserat continuum models as a long-wavelength approximation (Kroner [47], Krumhansl [48], Kunin [2]). The nonlocal theory of elasticity was further developed by Green et al. [49], Eringen [44, 50], and other authors [2, 47, 51].

On the other hand, the classical theory of elasticity was shown to be insufficient in the solid-state physics when studying the thermodynamic properties of materials. In 1952, Lifshits [52], when considering the thermal properties of chain and layered structures at low temperatures, paid attention to the influence of the transverse rigidity of atomic layers or chains on the dispersion law of acoustic oscillations of a layered crystal in the long-wavelength section of the spectrum, where it should be absent according to the laws of the theory of elasticity. In this paper, the dispersion laws for longitudinal and transverse (bending) waves are given. Later on, bending waves

in the crystal lattice were studied in more detail by Kosevich [53]. He remarked that bending waves, in contrast to longitudinal waves provided by central forces of interaction, are caused by weaker noncentral forces arising due to transverse displacements of particles. He also showed that a more accurate description of the nonlinear dynamics of the crystal lattice necessitates taking into account in the governing equations the couple stresses described by the fourth spatial derivatives of the transverse displacements of the particles. It should be noted that couple stresses can also be taken into account if one considers the rotational degree of freedom of particles and then, using the method of step-by-step approximations, reduces the three-mode system to a two-mode system admitting only translational displacements of particles (see Chap. 4).

In mechanics, interest in discrete models has resumed since the mid-twentieth century (see, for example, the works of M.Ya. Leonov [54], L.I. Slepyan [55, 56], M.R. Korotkina [57], S.A. Nazarov and M.V. Paukshto [58]) and continues in the current century (see, particularly, the works of A.M. Krivtsov and N.F. Morozov et al. [59–62], A.V. Porubov et al. [63–67], A.A. Vasiliev, S.V. Dmitriev, and A.E. Miroshnichenko [68–71], A. Suiker, A.V. Metrikine and R. de Borst [72, 73]).

According to N.F. Morozov and M.V. Paukshto [74], interest in discrete models is associated with the following circumstances:

- A lot of scientists believed that employing of discrete methods is more justified due to discreteness of computing processes.
- The development of personal computers currently enables one solving systems containing great amount of equations. This fact partially disproves hypothesis about the inadequacy of real and computing situations.
- Discrete methods had allowed, for example, in problems of fracture [54–56, 75, 76], to discover some effects that could not be found by continual methods. And this is not accidental, because a continuum model is a certain concept of the long-wavelength approach of the discrete model, whereas the destruction occurs at the microstructure level and is described by the long-wavelength asymptotics only approximately.
- Discrete models simulate a real atomic structure of substances.

1.1.2   Development of Models of Microstructured Solids with Account of Particle Rotation

In recent decades, more and more models are being developed taking into account the rotational degrees of freedom of particles and the moment interactions between them. For example, in [77], J. Pouget and G. Maugin studied the nonlinear dynamics of oriented media using the microscopic theory, modeling the medium as a system of material objects with translational and rotational degrees of freedom. M. Sayadi and J. Pouget proposed a one-dimensional chain of rotating dipoles as a model of an oriented medium [78]. But this model took into account only one of the possible types of

anharmonic interactions between the nearest neighbors in the chain, associated only with the rotational movements of dipoles (dipole interaction). A lattice consisting of identical particles with both transverse and rotational degrees of freedom was studied by A. Askar [79, 80]. The central forces of interaction between the particles were simulated by tensile springs, whereas the noncentral forces were modeled by flexible beams (rods). Later, this model was generalized to the case of a lattice consisting of particles of two types with different masses and moments of inertia [81]. The cubic lattice, consisting of identical dipoles, was considered by Japanese scientists K. Fujii, T. Fuka, H. Kondo, and K. Ishii in [82], where the interaction between the particles was described by the Lennard–Jones potential. In the linear approximation, a three-dimensional model of a granular medium consisting of spherical particles interacting by means of elastic springs of three types was constructed by K. Berglund [83].

One of the variants of the theory describing the moment dynamics of a deformable solid has been proposed by A.G. Ugodchikov in [84]. Based on the physical and mechanical properties of geomaterials with complex structure, V.N. Nikolaevsky [85–87] elaborated mathematical models of the deformation and destruction of mountain massifs and layers under external influences.

The academician of the Russian Academy of Sciences V.E. Panin and his students were actively developing an alternative way to construct mathematical models of microstructured media—*the method of movable cellular automata* [88–92]. This is a discrete modeling method that describes the behavior of materials at the meso- and macrolevels. In its framework, a rotation is taken into account as an independent degree of freedom of the automat along with the translational motion of its mass center.

At present, the concept of the existence of rotational degrees of freedom and various types of interactions in a crystal lattice is widely used in the study of dynamic processes in microstructured media [7, 14, 71, 77, 78, 93–101].

1.1.3 Experimental Research of Dynamic Properties of Microstructured Media

In the middle of 1930s and early 1940s, experimental physicists paid attention to the importance of taking into account the rotational degrees of freedom of the elements (particles) of the medium. Thus, the experiments of B. Bauer and M. Mag are very interesting (see References in [102]). They compared the scattering spectra for heavy and light water. From the comparison of spectra of these two substances, which molecules have approximately the same mass, but different moments of inertia, the authors made a conclusion about existence of both translational and rotational oscillations of molecules. J. Bernal and J. Tamm [103] explained the differences between some physical properties of light and heavy water under the assumption about the existence of rotational oscillations.

In 1940 E.F. Gross [102] observed the effect of variation of the wavelength of scattered light in a liquid associated with orientation fluctuations of anisotropic molecules. He remarked that the axes of molecules can rotate by a significant angle, if the oscillation period is much larger than the relaxation time. Later, E.F. Gross and A.V. Korshunov established experimentally [104] that in crystals of some organic substances (for instance, benzene and naphthalene) the scattering spectrum of small frequencies is associated with rotational vibrations of molecules. The scattering spectrum is the most intensive in substances, which molecules have a large optical anisotropy (carbon disulfide, naphthalene, benzene). The crystal lattices of such substances consist of large molecules. In them, the intermolecular forces are usually much larger than the van der Waals forces acting between the molecules; therefore, the molecules can be regarded as solid bodies oscillating with respect to each other. Among molecular crystals, the most popular objects for study are naphthalene crystals [104–106]. There are translational oscillations of molecules, rotational oscillations, as well as mixed translational–rotational oscillations. Experimental studies of oscillations in such crystals, carried out by Raman scattering, have shown that in the vicinity of the Rayleigh lines there are characteristic scattering lines due to the rotational nature of molecular oscillations [105, 106]. In experiments on spectrograms of light scattering in organic substances, estimates have been obtained for the threshold frequency of benzene and naphthalene [105].

In the late 1950s, some experiments were performed to observe the optical–acoustic effect in liquids and solids. So, in [107], experiments are described to study the spectral dependence of the optical-acoustic effect in ferroelectric crystals (in particular, Rochelle salt). The study of the spectral dependence of such an effect in a Rochelle salt crystal and the comparison of the results with the infrared absorption spectrum was interesting from the viewpoint of problems associated with the molecular mechanism of the piezoelectric phenomenon. However, the degree of influence of oscillation types on the excitation of the optical–acoustic effect has not been still studied.

The first experiments on acoustics of microstructured solids were performed yet in 1970 by G.N. Savin et al. [4, 108]. The authors established the correlation between the grain size in different metals and aluminum alloys and the dispersion of the acoustic wave. In these works, they used the Cosserat and Mindlin models. Based on the Mindlin model [36], where each of the material points of an elastic continuum can both rotate and be deformed, the presence of wave dispersion for both shear and longitudinal waves propagating in a microstructured medium was explained in [4]. A nonlinear problem for an isotropic elastic Cosserat continuum was considered in [108]. The inclusion of microrotations caused the appearance of an additional elastic constant with the dimension of length, as well as to the dispersion of shear waves.

Dispersion of the ultrasound waves was observed by V.I. Erofeev and V.M. Rodyushkin in an artificial composite—ferrite pellets in epoxy resin [109]. The appearance of a wave dispersion "forbidden" by the classical theory of elasticity can be explained, in particular, by the influence of rotational modes. Moreover, A.I. Potapov and V.M. Rodyushkin [110] experimentally observed the transfer of momentum in a microstructured material with the velocity that is distinct from the

longitudinal wave velocity. A clear separation of the impact pulse into two components was observed in this case. This fact indicates that pulse is carried by two types of oscillations differing from each other in velocity. Nevertheless, still nobody could observe experimentally the propagation of rotational waves in "laboratory conditions."

It should be noted that in microstructured media there are several types of waves— the so-called *acoustic* and *optical* phonons, and it is possible to transfer energy from one type of wave to another [111]. This fact should be taken into account both for theoretical and experimental studies. So, in the monograph by V.E. Lyamov [112], it was shown that the account of microrotations in crystals leads to the appearance of the spatial dispersion and new wave modes. Chapter 4 of the monograph [30] by A.I. Akhiezer, V.G. Barjahtar, and S.V. Peletminsky deals with the analysis of coupled spin and acoustic waves in ferromagnets. Elastic waves are considered in the framework of the classical theory without taking into account microrotations, but it is shown that, due to the relatedness of the elastic deformations with the magnetic field of spins, the stress tensor is no longer symmetric; i.e., in an elastic ferromagnet, there appear couple stresses at the excitation of the spin waves. The analysis of the dispersion properties showed that the acoustic wave with the "left" circular polarization interacts with the spin wave much stronger than the acoustic wave with the "right" polarization.

In the last thirty years, the processes of propagation and interaction of elastic (acoustic) waves in microstructured solids have been extensively studied theoretically and experimentally (see, e.g., [110, 113–118]). However, the main attention is paid to the analysis of the propagation of the longitudinal and shift waves, and the propagation of rotational waves (waves of microrotations) is studied less. Thereby, some articles by V.N. Nikolaevsky et al. [85, 86], where the nonlinear interactions of longitudinal and microrotational waves were studied in relation to seismic acoustics problems (in the framework of a gradient-consistent model of a medium with complex structure, they attempted to explain the generation of ultrasound during the propagation of seismic waves), and by A.I. Potapov et al. [7, 119–123], including a co-author of this monograph, in which the processes of propagation and interaction of longitudinal, transverse, and rotational waves in crystalline media were investigated, should be remarked.

1.2 Methods of Description of Different Scale Levels

An adequate description of wave processes in a structurally heterogeneous material necessitates, as a rule, consideration of several scale levels, which continuously interact with each other due to internal connections [124]. The following scales are usually distinguished [125]: *atomic* or *microscopic* level (characteristic sizes are angstroms and nanometers), *mesoscopic* level (from 10^{-8} to 10^{-6} m), *submacroscopic* level (from 10^{-6} to 10^{-4} m), and *macroscopic* level (over 10^{-4} m). Their brief

Table 1.1 Methods for mathematical description of a continuous medium

The structural level of a substance	The spatial structure of a medium	Mathematical model
Microscopic (atomic) level $(10^{-10}$–10^{-8} m)	A discrete medium consisting of interacting particles, which sizes are much smaller than the lattice period	Quantum theories based on the first principles Semi-empirical quantum models containing fitting parameters Molecular dynamics models
Mesoscopic (nanostructural) level $(10^{-8}$–10^{-6} m)	A microinhomogeneous medium consisting of structural elements (particles, clusters, domains) with internal degrees of freedom	Phenomenological theory of the crystal lattice. Multipolar continual theories
Submacroscopic level $(10^{-6}$–10^{-4} m)	A piecewise-inhomogeneous medium represented by structural elements (domains, grains) without internal degrees of freedom	Statistical theory of elasticity Nonlocal and higher-order gradient theories of elasticity
Macroscopic level (over 10^{-4} m)	A continuous medium, where discreteness is ignored and only averaged effects are taken into account	Classical (continual) theory of elasticity

description is given in Table 1.1. Let us start with extreme situations, as they are the most developed.

Microscopic (*atomic*) level: a physical solid body is represented as a set of a large number of particles—atoms interacting with each other and with a field of external forces [125]. An atom is considered as a point mass (nucleus) enclosed in an elastic, almost inertialess sphere simulating an electron cloud. The properties of the atom model can be refined by introducing a charge, mechanical, and magnetic moments, etc. The interaction between two arbitrary particles of the system does not admit their collision, but enables them to be removed at any distance. A model of a solid at normal temperature and pressure is a system of almost densely packed particles that perform small thermal vibrations near the equilibrium states [126, 127]. The task of modeling the system at this level is the derivation of equations of motion based on the first principles (laws) of quantum theory [128] and the analysis of interatomic interactions [125]. Atomic-molecular systems are assumed to be simulated within the scope of Schrödinger models. The Hamiltonian of such models contains the kinetic energy of nuclei and electrons, the potential energy of the Coulomb interaction between electrons, between nuclei and electrons, and between all nuclei.

The complete realization of this approach would enable us revealing the reasons for the existence of many properties and phenomena that have no justification in the classical theory. However, a meaningful analysis of quantum–mechanical models for real systems consisting of a large number of particles is a very difficult problem even for modern computing tools. One of the main problems along this path is that the direct calculation of the Schrödinger equations for a system of many particles requires

gigantic computational resources. When the number of particles grows, the required calculation time increases exponentially. Therefore, for real systems consisting of 10^8–10^{10} particles, this approach does not allow solving this problem even using high-performance computers [129].

The *macroscopic* (*phenomenological*) level of description of a material is a subject of the continuum mechanics. At this level, a material is regarded as a continuous medium, its discreteness is ignored, and only averaged macroeffects are taken into account. A solid is represented as a continuous substance that is called *the material continuum* and continuously fills a geometric space volume. On the base of experience, the concept of a physically infinitesimal volume of a solid is introduced and the number of variables, which are necessary for description of the system, is determined. "The macroscopic first principles" (i.e., the laws of conservation of mass, momentum, kinetic moment and energy, as well as the first and second principles of thermodynamics) are used to derive the motion equations [1]. In order to close the set of motion equations, equations of state of the medium should be used, which establish relationships between strains, internal stresses, and temperature and ultimately reflect the averaged statistics of motion and interaction of atoms. Since phenomenological theories are much simpler than microscopic ones, they are usually used, if it is known that they are true in this case. The brightest examples of this are the Landau hydrodynamic theory of superfluidity and the Ginzburg–Landau–Abrikosov–Gorkov phenomenological theory of superconductivity. So, L.D. Landau was awarded the Nobel Prize in 1962 for creating the hydrodynamic theory of superfluid helium. The great importance of the phenomenological theory of superconductivity for modern physics was noted by awarding of the Nobel Prize in 2003 to V. L. Ginzburg and A. A. Abrikosov for the pioneer contribution to its development, whereas L. Cooper, J. Bardin, and J. R. Schriffer were already awarded by the Nobel Prize in 1972 for the development of the microscopic theory of superconductivity.

The *mesoscopic* level of the description of a medium is intermediate. At this level, the medium is assumed to be composed of small-sized structural elements (clusters) possessing internal degrees of freedom. In this case, the task of mathematical modeling is to derive equations of motion of a medium taking into account the self-consistent interaction between micro-, meso-, and macroscale processes. The difficulty in constructing models of this level consists in that, on the one hand, they must take into account the quantum–mechanical properties of small particles, and, on the other hand, they must degenerate into the classical macrocontinuum models, when the scales of the studied phenomenon are much larger than the scales of the "microstructure" of the medium. Since in most practical situations they are dealing not with individual quantum events, but with large ensembles of particles, collective processes begin to play a leading role that can be fairly accurately described in the framework of semi-empirical and classical representations [60, 130]. Mathematical models of this level can be continual [42, 131–133] or structural [64–68, 77, 83, 98, 122, 123, 134–146].

At the *submacroscopic* level, the spatial structure of a medium is considered to be piecewise-inhomogeneous and represented by structural elements (domains, grains) that do not have internal degrees of freedom. The methods of statistical averaging of

Fig. 1.1 Regular structure consisting of spherical silica particles [151]
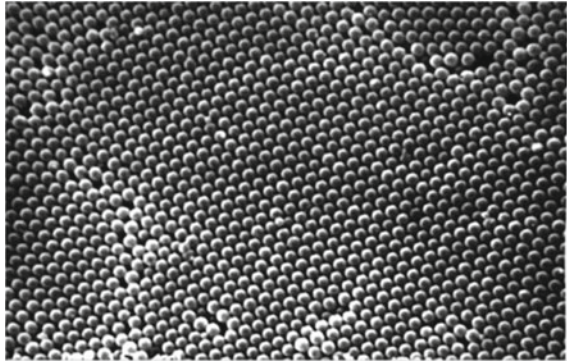
"microinhomogeneous" media are used for constructing of mathematical models of this level [33–35, 147].

Frequently, in structurally inhomogeneous materials, a qualitative change in their physical properties occurs at a certain scale level; i.e., a *size effect* [148, 149] arises. There are materials, where qualitative changes occur gradually, but in *metamaterials* this limit is expressed rather accurately and takes place in the field of nanometers. A metamaterial is a complex periodic structure [150] with small-sized bodies (rather than material points) possessing internal degrees of freedom occupying the lattice sites. Granules, domains, fullerenes, nanotubes, or clusters of nanoparticles can play the role of such bodies.

Figure 1.1 shows a typical regular structure—a dense packing of spherical silica particles with a diameter of 250 nm, formed by centrifugal deposition.

Another example of metamaterials is *fullerites*—solid-state structures formed on the base of fullerenes (both C_{60} and higher fullerenes—C_{70}, C_{76}, C_{78}, C_{80}, C_{82}, etc.) [152]. As fullerites belong to crystals of the molecular type, it is possible to consider the fullerenes forming them like molecules.

Usually, the determining parameters for forming fullerites are pressure and temperature [153]. So, in the case of the formation of fullerites based on C_{60} fullerenes at pressure of 1.5 GPa, dimers $C_{60} = C_{60}$ are formed even at room temperature (Fig. 1.2). As the temperature grows, a crystal lattice consisting of dimers begins to form.

A further increase in temperature leads to the decomposition of dimers and to the generation of polymer structures [154], the same is for increase in pressure.

A distinctive property of fullerites is orientational disorder associated with the ability of fullerenes to easily change relative spatial orientation during thermal motion even in presence of crystalline environment, i.e. to make the so-called orientation phase transitions. This ability of fullerenes is provided by their highly symmetric, almost spherical shape. The orientation of fullerenes changes when they, performing torsional vibrations, overcome a certain energy barrier and pass to pseudorotation. In particular, C_{60} fullerenes are in a crystal in a state of almost free rotation with three degrees of freedom [152]. The nature of the rotational movements of a fullerene with
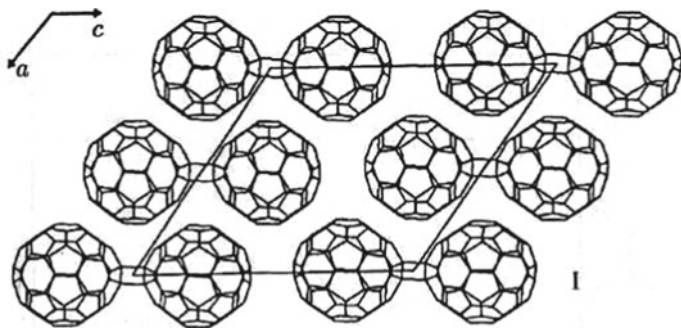
Fig. 1.2 Fullerene dimers $C_{60} = C_{60}$ [111]

account of influence of the constant thermal motion of other fullerenes in the crystal resembles the jump-like movement of the ratchet of a clockwork.

Super- and ultrahard fullerites are characterized by uniquely high longitudinal elastic wave velocities and by a wide range of these values from 11 km/s to 26 km/s depending on their structure determined by the synthesis conditions [155, 156]. The value of 26 km/s measured in one of the fullerite phases is a record—it is almost 20% higher than the longitudinal wave velocity in graphite along atomic layers, equal to 21.6 km/s (until recently, this value was the highest one for all known substances) and 40% more than the corresponding velocity in diamond (18.6 km/s). The shear wave velocities in solid fullerite phases are also great (their values are in the interval from 7 km/s to 9.7 km/s), but still they are lower than ones in diamond (11.6–12.8 km/s) that still remain a record for all the currently known substances.

Experimental data show [152] that C_{60}-fullerenes crystallize at room temperature and form a face-centered cubic lattice (fcc) with the lattice constant $a = 1.417$ nm.[1] This is the most densely packed lattice among all cubic lattices. The distance between the centers of the nearest C_{60} fullerenes in the crystal structure equals 1.002 nm, the fullerite density is 1.72 g/sm^3. As the temperature decreases till 250 K, there occurs a first-order phase transition of the crystal structure of fullerite C_{60}, during which a fcc lattice is rearranged into a simple cubic (sc) lattice [157]. At the same time, dynamics of fullerene movement changes substantially, namely fullerenes lose two of the three rotational degrees of freedom, and the rotation axes corresponding to the remaining degree of freedom acquire a certain average direction with respect to the coordinate system of the crystal.

For C_{60} with sc-lattice, the following values of second-order elasticity constants were theoretically determined in [158]: $C_{11} = 14.9$ GPa, $C_{12} = 6.9$ GPa, $C_{44} = 8.1$ GPa. The data on the elastic constants for C_{60} with fcc lattice at temperature of 300 K, given in various sources and obtained by different (both experimental and theoretical) methods, differ markedly from each other [159]. So, C_{11} ranges from 11.76 [159] to 16.1 GPa [160], C_{12}—from 6.0 [161] to 8.86 GPa [159], and C_{44}—from 5.88 [159] to 8.2 GPa [160].

---

[1]For comparison—$a = 0.54$ nm in silicon and $a = 0.57$ nm in germanium.

A 3D model of a crystalline medium, similar in structure to fullerite, will be considered in Chapter 6 of this monograph. Using experimental data on the second-order elasticity constants in C_{60} with sc-lattice, numerical estimates of the velocity and threshold frequency of rotational waves, as well as nonlinear coefficients of such a medium will be also obtained in this chapter.

1.3   Limits of Applicability of the Classical Mechanics Laws to Modeling of Generalized Continua

In this section, we will find out whether the classical mechanics laws are applicable to modeling of nanostructures.

1.3.1   Quantum and Classical Descriptions of Microparticles

The classical physics introduces us to two types of motion—*corpuscular* and *wave.* The first one is characterized by the localization of an object in space and the existence of a certain trajectory of movement, which can be calculated using Newton's equations. For a wave motion, on the contrary, delocalization in space is typical. This motion is associated with the propagation of a certain disturbance in the medium that arose due to displacement of particles from the equilibrium state [162]. This type of motion is described using wave equations. From the viewpoint of the corpuscular concept, the properties of macroscopic solid bodies can be considered as the properties of a set of material particles interacting with each other. In physics and mechanics of continuous media, the concept of corpuscles is achieved during "fragmentation" of bodies into small particles. Each such particle is usually called a *physically infinitesimal particle* or a *representative volume of a medium* [42, 139]. According to the definition, such a particle must possess all the physical properties of the original material. Therefore, there is no sense to break the body into separate molecules or atoms, since the properties of the original material are lost. Hence, in the macroscopic description, there must be a certain spatial scale, beyond which the process of fragmentation of a body becomes physically senseless.

If in classical physics a corpuscle (particle) and a wave are two mutually exclusive opposites—either a particle or a wave, then at the microlevel these opposites are unified in a single object—a microparticle. On the one hand, a microparticle is characterized by a certain rest mass and charge, which brings it closer to the classical corpuscle; on the other hand, it does not have a trajectory, which is an obligatory attribute of a classical particle. The use of such characteristics as coordinate, momentum, moment, and energy for description of a microparticle is restricted by the

framework of Heisenberg's uncertainty relations. In the quantum theory, microparticles are neither "pure" particles, nor "pure" waves. This circumstance is commonly called a *wave-particle dualism* [128].

The idea of dualism was originally applied to electromagnetic radiation. In 1917, A. Einstein proposed to consider the radiation quanta introduced by M. Planck as especial particles possessing both an energy and a momentum. Later, these particles began to be called *photons*. In 1924, de Broglie suggested to extend the idea of dualism not only to radiation, but also to all microobjects in general; namely, he offered to associate with each micro-object, on the one hand, corpuscular characteristics (energy E and momentum p), and on the other hand,—wave characteristics (frequency ω and wavelength λ). The relationship between the characteristics of different types is provided by Planck's constant $h \approx 6.626 \times 10^{-34}\,\text{J} \cdot \text{s} = 4.136 \times 10^{-15}\,\text{eV} \cdot \text{s}$:

$$E = h\omega/2\pi, \quad p = h/\lambda = hk/2\pi. \tag{1.1}$$

In quantum mechanics, a particle has a certain probability distribution described by a complex wave function $\psi(\mathbf{r}, t)$ satisfying the Schrödinger equation

$$i\hbar \frac{\partial \psi}{\partial t} = \left[-\frac{\hbar^2}{2m}\nabla^2 + U(\mathbf{r}, t) \right]\psi, \tag{1.2}$$

where U is the potential energy of the particle, m is the particle mass, $\hbar = h/2\pi$ is the reduced Planck constant ($\hbar \approx 1,055 \cdot 10^{-34}\text{J} \cdot \text{sec} == 6,582 \cdot 10^{-16}\text{eV} \cdot \text{sec}$). In quantum mechanics, the Schrödinger equation plays the same role as the Newton equation in classical mechanics [128]. It is a linear partial differential equation with a variable coefficient. If to take into account that the particle operator $\mathbf{p}$ corresponds to the differential operator $-i\hbar\nabla$ in quantum mechanics, then the expression in the right-hand side of Eq. (1.2) can be considered as a quantum analog of the system Hamiltonian, which equals to the sum of the kinetic energy $E = p^2/2m$ and the potential energy of the particle. Solution of Eq. (1.2) in the form of a traveling harmonic wave

$$\psi(x, t) = \psi_0 \exp[i(\mathbf{kr} - \omega t)] = \psi_0 \exp\left[\frac{i}{\hbar}(\mathbf{pr} - Et) \right] \tag{1.3}$$

corresponds to a freely moving particle ($U(r) = 0$) with momentum $\mathbf{p}$ and energy E and is called de Broglie wave. Substitution of (1.3) into (1.2) leads to the dispersion relation between its frequency and wavenumber

$$\omega = \frac{\hbar k^2}{2m}. \tag{1.4}$$

Using Eq. (1.1), it is possible to obtain from Eq. (1.4) the relationship between the energy and momentum of the de Broglie wave

Table 1.2 Quantum–mechanical characteristics of microparticles

The particle	Rest mass, g	Energy, eV	De Broigle wavelength, nm	Initial width x_0, nm	«Life time» T, sec	Mean free path $L(x_0)$
Electron	10^{-27}	1	1.171	3×10^{-5}	3×10^{-26}	$4.4 \times 10^{-5} x_0$
Atom	1.66×10^{-24}	1	0.029	0.1	10^{-13}	$6.0 \, x_0$
Molecule C_{60}	1.195×10^{-21}	1	1.072×10^{-3}	0.714	1.59×10^{-9}	$1154 \, x_0$

$$E(p) = \frac{p^2}{2m}, \tag{1.5}$$

which is also called the dispersion relation. This implies the relationship between the wavelength and the microparticle energy

$$\lambda = 2\pi \hbar / p = 2\pi \hbar / \sqrt{2mE}. \tag{1.6}$$

Here we meet with the first difference of the quantum description of microparticle motion from the wave theory. In the wave theory, the length of a linear wave does not depend on energy, whereas the de Broglie wavelength depends on energy, although the Schrödinger equation is linear. Estimates of the characteristic de Broglie wavelengths for some microparticles are given in Table 1.2 (see Sect. 1.3.3).

1.3.2 The Uncertainty Relation

In the classical mechanics, the movement of a microparticle (material point) is uniquely described by values of its coordinate and velocity (momentum). In the case of quantum microparticles, it is necessary to take into account their wave nature, so the situation is another: a microparticle is "smeared" in space and its motion cannot be described by a trajectory of a point in the classical sense. In 1927, on the base of quantum mechanical calculations, Werner Heisenberg showed that the coordinate and momentum of a microparticle can be determined only with some accuracy [128]:

$$\Delta x \, \Delta p \geq \hbar. \tag{1.7}$$

Here Δx and Δp mean not measurement errors, but fundamentally unrecoverable uncertainties, deviations of the coordinate and momentum from their average values. Quantities Δx and Δp cannot be equal to zero at the same time. This means that the coordinate and momentum cannot have completely definite values at the same time, for example, de Broglie wave with a definite momentum (i.e., $\Delta p \to 0$) must fill the entire space ($\Delta x \to \infty$ and $\Delta p \to 0$). The classical concepts of a

spatial location and a momentum magnitude are applicable to a microparticle only within the scope of Heisenberg's relations. This circumstance is related to the very nature of microparticles, namely to their particle-wave properties. The uncertainty relation plays an important heuristic role, since many results of problems considered in quantum mechanics can be obtained and understood on the basis of a combination of the classical mechanics laws and the uncertainty relation [128]. States minimizing the uncertainty relation (i.e., corresponding to the equal sign) are called *coherent* states of the system.

1.3.3   A Microparticle as a Localized Wave Packet

At first view, it may seem unclear how the motion of the wave (1.3) is associated with the mechanical laws of the microparticle motion. However, there is an exact quantitative analogy between the Heisenberg uncertainty relations and the wave properties. The de Broglie wave cannot describe a localized particle, since $|\psi|^2 = const$ for it. Therefore, the probability of detecting a particle is the same for all points of space. It is known from the wave theory [162, 163] that a localized particle is described by a wave packet occupying a small area of space. It is possible to construct a group of de Broglie plane waves with an amplitude different from zero in a narrow range of wavenumbers:

$$\psi(x, t) = \int\limits_{k_0-\Delta k/2}^{k_0+\Delta k/2} F(k) \, \exp\{-i[\omega(k)t - kx]\} \, dk.$$

Figure 1.3 shows a wave packet with a normal (Gaussian) density distribution $|\psi|^2 = \psi_0^2 \exp(-x^2/x_0^2)$, where $x_0 = \Delta x/2$—is the initial half-width of the pulse. The spatial spectrum of such a packet $F(k) = (x_0/\sqrt{2\pi}) \exp(-k^2 x_0^2/2)$ has a width $\Delta k = \sqrt{2}/x_0$.

The movement of the envelope of a wave packet in space occurs with a group velocity

$$v_{\text{gr}} = \frac{d\omega}{dk} = \frac{1}{\hbar}\frac{dE}{dk} = \frac{dE}{dp}. \tag{1.8}$$

Taking into account relation $\omega(k) = \hbar k^2/2m = p^2/2\hbar m$, from Eq. (1.8), one can obtain an equality $v_{gr} = \hbar k/m = v$, which means that the group velocity of the packet of de Broglie waves is equal to the microparticle velocity v. From the spectral analysis, the relationship is known between the wave packet width Δx and its spectrum width Δk:

$$\Delta x \cdot \Delta k \geq 1.$$
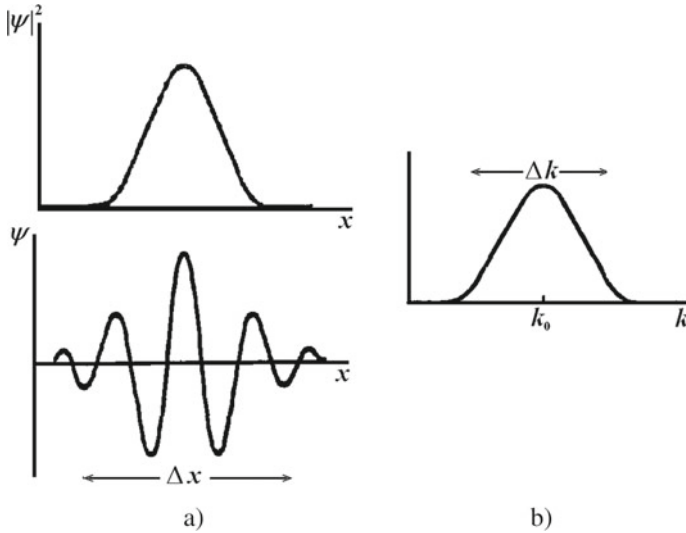
Fig. 1.3 Wave packet ψ, square of its envelope $|\psi|^2$ (a) and spectrum (**b**)

If we now use the second relation in (1.1), then the spread of the coordinate Δx will correspond to the spread of momentum $\Delta p = \hbar\,\Delta k$ and, therefore, $\Delta x \cdot \Delta p \geq \hbar$ that coincides with the Heisenberg uncertainty relation (1.8). Since the wave packet velocity is equal to the particle velocity and the uncertainty relation is valid for it, there appears an idea of representing the particle as a wave packet. This idea seems especially attractive because it enables unifying a wave and a particle in one object. Another argument in its support is the Ehrenfest theorem, according to which the dynamic equations for average values of quantum–mechanical operators have the form of Newton's equations for a classical particle [128]. However, this idea turned out to be wrong, as a particle is a stable formation and does not change during its motion, but a wave packet does not possess this property. Due to dispersion, it spreads over time, since the phase velocity of the various monochromatic components of the wave packet is different. The condition for the applicability of the group approximation is known from the theory of waves [163]. The characteristic distance L and time T, when the spreading of the wave packet can still be neglected, are equal to [162]

$$L \leq v_{\mathrm{gr}} T = \frac{\pi\, v_{\mathrm{gr}}(k_0)}{(\mathrm{d}v_{\mathrm{gr}}(k_0)/\mathrm{d}k)\,(\Delta k)^2},$$

where $k_0 = \sqrt{2mE}/\hbar$ is the wavenumber of the central component of the packet spectrum and Δk is its width. If the dispersion law and the wave packet width are known, one can estimate the characteristic time of spreading of the wave packet. For a wave packet with a Gaussian density distribution, its width will be doubled in time.

$$T = \frac{\sqrt{3}mx_0^2}{2\pi\hbar}, \quad L = Tv_{gr} = \frac{\sqrt{3m\,E}x_0^2}{\sqrt{2}\pi\hbar} = \frac{\sqrt{3}x_0^2}{\lambda}, \tag{1.9}$$

where λ is the de Broigle wavelength (see Eq. (1.6) and Table 1.2).

Expressions (1.9) can be considered as conditions, under which a quantum particle is described by a wave packet. Or, in other words, they determine the applicability limits of the classical description of a microparticle. Estimates of characteristic "lifetimes" and mean free paths (1.9) of some microparticles are listed as examples in Table 1.2.

These examples show that if for a particle with an atomic mass the applicability time of classical consideration is comparable with the "lifetime" of phonons in a solid, and the mean free path of such a particle is comparable with its initial width, then for electrons, the classical wave consideration is unsatisfactory from the very beginning [111]. Perhaps, the situation can be corrected due to consideration of nonlinear wave packets, in which the lifetimes can theoretically be infinite, but this is beyond the scope of this research.

1.3.4 The Conformity Principle

The quantum mechanics contains the classical mechanics as a limiting case. If the particle wavelength is small in comparison with the characteristic sizes L, which determine the conditions of this particular problem, then the properties of the system should be close to classical ones. These requirements constitute the correspondence principles in quantum mechanics [128]. For simplicity, we will consider the motion of one particle in an external field with a potential $U(\mathbf{r})$. The wave function of a particle in the limiting case $\lambda \to 0$ should have the form:

$$\psi(\mathbf{r},\,t) = a(\mathbf{r},\,t)\,\exp\left(\frac{i}{\hbar}S(\mathbf{r},\,t)\right), \tag{1.10}$$

where a is the amplitude, S is the action. Substituting in Eq. (1.2) the limiting expression of the wave function (1.10), one can find:

$$a\frac{\partial S}{\partial t} - i\hbar\frac{\partial a}{\partial t} + \frac{a}{2m}(\nabla S)^2 - \frac{i\hbar}{2m}a\,\Delta S - \frac{i\hbar}{m}\nabla S\,\nabla a - \frac{\hbar^2}{2m}\Delta a + Ua = 0.$$

Equating the imaginary and real parts separately to zero, we receive two equations:

$$\frac{\partial S}{\partial t} + \frac{1}{2m}(\nabla S)^2 + U - \frac{\hbar^2}{2ma}\Delta a = 0,$$
$$\frac{\partial a}{\partial t} + \frac{a}{2m}\Delta S + \frac{1}{m}\nabla S\nabla a = 0.$$

Neglecting the term containing $\hbar^2$ in the first of these equations, one can obtain the Hamilton–Jacobi equation for the material particle action S:

$$\frac{\partial S}{\partial t} + \frac{1}{2m}(\nabla S)^2 + U = 0. \tag{1.11}$$

The second of the obtained equations after multiplying by $2a$ can be rewritten in the form of a continuity equation:

$$\frac{\partial a^2}{\partial t} + \nabla\left(a^2 \frac{\nabla S}{m}\right) = 0. \tag{1.12}$$

Equation (1.12) shows the probability density of a particle in space $a^2 = |\psi|^2$ to "move" according to the classical mechanics laws with velocity $\mathbf{v} = \nabla S/m = \mathbf{p}/m$. In the classical limit, the particle trajectory is determined by the action minimum. The generalized momentum $\mathbf{p}$ and the Hamilton function H of the particle are equal to:

$$\mathbf{p} = \nabla S, \quad H = -\frac{\partial S}{\partial t}.$$

Thus, at $S/\hbar \gg 1$, the classical mechanics is valid up to the first-order values with respect to the parameter $\hbar$ inclusive, but it does not describe the second-order effects with respect to $\hbar$. Hence, the criterion for the applicability of the methods of classical mechanics can be formulated.

If in a physical system the numerical value of a dynamic variable having the dimension of action S (J·sec) is large in comparison with the Planck constant, then it can be described with sufficient accuracy by the classical physics laws.

As an example, let us estimate this quantity for a nanostructure representing a lattice of fullerenes. The most common molecule of fullerene C_{60} contains 60 carbon atoms. Its diameter equals 0.714 nm [152]. Under certain conditions, C_{60} molecules can order and form molecular crystals with fcc lattice (see Fig. 1.4 and Sect. 1.2) with parameter $a = 1.417$ nm. The dimension of the action S in such a system is the product of the oscillation period T and the oscillation energy E. It was proved by nuclear magnetic resonance that at room temperature, C_{60} molecules rotate around the equilibrium state with frequency $\omega = 2\pi/T = 10^{12}$ s^{-1}, and the energy E has an order of 0.1 eV $= 1.6 \times 10^{-20}$ J. Then, the magnitude of the action is equal to $S = 2\pi E/\omega \approx 10^{-31}$ J sec, and its relation to Planck's constant is large—$S/\hbar \approx 10^3$. Consequently, elastic vibrations of such a lattice can be described with a sufficient degree of accuracy by the classical physics laws.

Fig. 1.4 Fcc lattice of
fullerite C_{60}
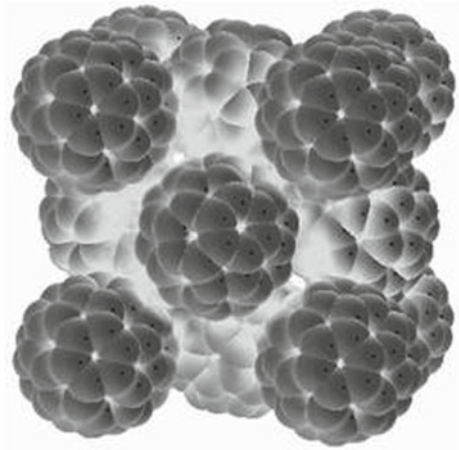
1.4   Principles of the Structural Modeling Method

The closely related to each other mechanics of media with microstructure and theory
of generalized continua remained unclaimed for many years due to their complexity
and lack of practical needs. Now there is a next stage of development of these
theories after the Cosserat brothers work [13] and after the boom of the 1960s,
when great success was expected from them in the field of the continuous theory
of dislocations and the mechanics of composites. Interest in these theories began to
increase again from the middle of 1990s (fracture mechanics [54–56, 74–76, 164],
geomechanics [87, 165], mechanics of granular materials [166–168], higher-order
gradient theory of plasticity [169]). This interest continued in the first decade of the
twenty-first century, primarily, due to development of nanotechnology and creation of
metamaterials [150, 170–177]—a new class of substances with a complex internal
structure (see Sect. 1.2). At present, generalized continua, such as micropolar or
oriented media, higher-order gradient materials, micromorphic media, composites,
solids with weak or strong nonlocal interactions, are intensively studied by both theo-
rists and experimenters specializing in various branches of mechanics and physics
[178, 179]. The wave dynamics of microstructured media is developed [116, 123,
180] that allows, in particular, to propose new methods of non-destructive testing of
the stress–strain state, structure, and properties of materials [6, 75, 122, 181, 182].
However, an adequate description of intense two-dimensional and three-dimensional
processes in structured materials by means of the nonlinear wave dynamics necessi-
tates development of new mathematical models. The method of structural modeling
should be used to construct such models [83, 124, 139, 141, 142, 183], since the
structural models contain parameters characterizing the geometry of a material (a
lattice period, sizes and a shape of the particles, etc.), and therefore, they are the most
suitable models for studying the influence of size effects on the macroproperties of
a material.

During the structural modeling, penetration into the depth of a material is multi-level (multiscale), although it is often difficult to attribute one or another theory (model) to any specific scale expressed in units of distance. Nevertheless, such classifications exist and they are useful for assessing the areas of applicability of various theories [124].

The structural theory of the continuum mechanics is based on the molecular, atomistic, or subatomistic structure of a solid. Most of the early structural theories, which are used in the solid mechanics, considered particles of a medium as centers of forces possessing mass. These elements of a solid act on each other using the central forces. It is assumed that the forces of interaction between the structural elements of a solid rapidly decrease with distance and they can be neglected if the distance between the elements exceeds "the radius of molecular action." Applying of the method of central forces to crystalline media, depending on their symmetry, leads to certain relations between the second-order elasticity constants. These relations are called *Cauchy relations*. Within the scope of structural models, the Cauchy relations between the elasticity constants can be not valid.

It should be noted that as early as in 1842, Poisson made the assumption that molecules of a crystal can be not points, but small solid bodies possessing both translational and rotational degrees of freedom [184]. In 1887, this idea was developed by Voigt [20]. In 1890, W. Thomson (Lord Kelvin) remarked that the Cauchy relations could be eliminated if to represent a crystal as two homogeneous point formations (two sublattices) penetrating into each other. In 1915, Max Born proposed more general structural schemes of crystalline materials, where each crystal element—the unit cell—consists of attracting and repelling particles [11]. Inside each cell, the particles are uniformly located with respect to each other. Crystal structures are classified according to the type of crystal lattice and the nature of the interparticle (interatomic) connections. The classification by crystalline systems gives an idea of the geometric characteristics of crystals, but does not consider the question about the nature of the forces holding particles (atoms, ions, molecules, or nanoclusters) in the lattice sites. The classification based on the types of connection forces enables one performing some generalizations of the properties and behavior of crystals that was impossible by considering only the geometry of the lattices.

Elaboration of a structural model starts with the selection of a certain minimum volume—a structural cell (that is analog of the periodicity cell in the crystalline material) in the bulk of a material. Such a cell is capable of reflecting the main features of the macroscopic behavior of this material. As a rule, a structural cell represents a particle, which behavior is characterized by interaction with its environment and is described by kinematic variables [83, 136, 185]. In contrast to the standard theory of crystal lattices [11, 53], the structural modeling involves the presence in the lattice sites of finite-size bodies having internal degrees of freedom instead of material points. For instance, domains, granules, fullerenes, nanotubes, or clusters of nanoparticles can play the role of such bodies. If to consider their micromotions, then new types of motion arise in a microstructured medium. For example, account of microrotations with respect to the mass centers of particles leads to the appearance of microrotations in granular media [140].

The force interaction between elements is described by means of model potentials used in the molecular mechanics and the solid-state physics. Due to the presence of finite-sized bodies in lattice sites, it is possible to introduce into consideration the central and moment interactions between particles. The method of structural modeling takes into account the parameters characterizing the lattice period, the size, and shape of particles. Therefore, this is the most suitable method for studying the influence of size effects on material properties.

The discreteness of a medium can be taken into account in two ways. In one of them, the medium is represented as a regular lattice, which sites contain finite-sized bodies rather than material points [77, 97, 98, 119, 122, 140, 141, 143, 186, 187]. Bodies, unlike points, possess not only translational, but also rotational degrees of freedom that significantly expands the kinematic capabilities of the model. In the second method [114, 166, 167], a representative volume of the medium is considered as an ensemble of N contacting bodies. The tangential and normal forces in the contact area are introduced, and the equations of particle motion are derived from Newton's laws. As a result, the movement of a representative volume of the medium is described by a set of N interrelated equations, which can be reduced to partial differential equations using the averaging procedure.

Let us formulate basic principles of the structural modeling [135]:

1. *Minimality of generalizations.* Such generalizations are necessary, which would lead to qualitatively new results. At the same time, the number of new parameters containing in a model should be as small as possible.
2. *Variability* of *the model.* The possibility of a fairly wide variation of linear and nonlinear parameters of the model due to the choice of kinematic and force schemes of the interaction of structural elements.
3. Identification *and verification of the model.* Verification of the adequacy of the constructed model to real systems and determination of relationships between the model parameters and the physical constants of a material (density, porosity, macro- and microelasticity modules, etc.). For this purpose, the relationships between the parameters of the micromodel and the main physical and mechanical characteristics of a medium should be found.
4. *The principle of compliance.* In the limiting cases, a new model, as a rule, should be degenerated into the known (classical) theories of a deformable solid.

The advantages of the structural modeling are the clear coupling between a structure and macroparameters of a medium and the possibility of purposeful design of materials with specified properties. Shortcomings of the structural modeling are absence of universality of modeling procedure and complexity of the accounting of nonlinear and nonlocal effects of interparticle interactions.

The structural modeling consists of the following stages.

1st stage. *The* geometric *description of a structure.* In a regular lattice consisting of particles of a given shape, a periodicity cell is determined, and its characteristic sizes and kinematic variables describing the current state of the cell are introduced. A kinetic energy is calculated.

2nd stage. *The simulation of force interactions.* Since small deviations of the particles from the equilibrium states are considered, the force and moment interactions of the particles can be described by a power-law potential. In the harmonic approximation, the interaction potential is a quadratic form of the variables of a state of the system. The potential energy per lattice cell is equal to the potential energy of the particle interacting with its neighbors and, particularly, for a system with two spatial variables it can be represented by the following expression:

$$
U\left(\Delta_{nr}q^k, \varphi, \Delta_{nr}\varphi\right) = \sum_{k,s=1}^{2} \sum_{n,r,l,m} \frac{\partial^2 U}{\partial\left(\Delta_{nr}q^k\right)\partial(\Delta_{lm}q^s)} \Delta_{nr}q^k \Delta_{lm}q^s
$$

$$
+ \sum_{n,r,l,m} \frac{\partial^2 U}{\partial(\Delta_{nr}\varphi)\partial(\Delta_{lm}\varphi)} \Delta_{nr}\varphi \Delta_{lm}\varphi +
$$

$$
+ \sum_{k=1}^{2} \sum_{n,r,l,m} \frac{\partial^2 U}{\partial\left(\Delta_{nr}q^k\right)\partial(\Delta_{lm}\varphi)} \Delta_{nr}q^k \Delta_{lm}\varphi
$$

$$
+ \sum_{k=1}^{2} \sum_{n,r} \frac{\partial^2 U}{\partial\left(\Delta_{nr}q^k\right)\partial\varphi} \Delta_{nr}q^k \varphi + \frac{\partial^2 U}{(\partial\varphi)^2}\varphi^2. \qquad (1.13)
$$

Here $q^k = \{q^1,\ q^2\} = \{u_{i,j},\ w_{i,j}\}$ are the components of the vector of the mass center displacements of a particle located at a site with indices (i, j), $\Delta_{nr}q^k = \left(q^k_{i+n, j+r} - q^k_{i,j}\right)\big/a$ are quantities for the relative variation of the distances between the interacting particles, $\Delta_{nr}\varphi = \left(\varphi_{i+n, j+r} - \varphi_{i,j}\right)\big/a$ are quantities for the relative variation of the orientation angles of the particles, and coefficients n and r, as well as l and m determine the spatial positions of neighbouring particles. Summarizing is performed over all quasi-elastic connections in the cell. The second-order derivatives of the potential energy are the constants of quasi-elastic interactions of the particles and represent elements of force matrices of the crystalline structure [188].

In the phenomenological theories, the force constants should be found experimentally. Their connection with the geometrical structure and with the scheme of force interactions in a concrete crystalline lattice is not clear. From general energy reasoning and the requirements of symmetry of the lattice, it is possible to receive only some restrictions on the values of the force constants. Usage of the structural approach enables one to find an explicit dependence between the elements of the force matrices and the parameters characterising the inner structure of the lattice, i.e., its period, sizes, and shape of its particles.

For structural modeling of solids, an equivalent force scheme is introduced as a system of rods, beams, or springs that incorporates the transmission of forces and moments between the structural elements instead of a field description of the interaction of the particles [71–73, 76, 83, 100, 146, 189]. The mechanical characteristics of the connecting rods and springs should be generally determined from the requirement of equality of the strain energy in the investigated object and in its model.

Spring models are used in this monograph. When introducing the scheme of force interactions, round particles are replaced for convenience by inscribed polygons, which shape repeats the cell shape. Springs simulating transmission of force interactions between particles are assumed to be fixed at the vertices of polygons and have different elasticity constants [97, 122]. Next, mainly, two-dimensional models of media will be considered, in which sites there are bodies possessing internal degrees of freedom.

3rd stage. *Derivation of dynamical equations for a discrete system.* Due to expressions for the kinetic and potential energy that were obtained at the previous stages, it is possible to make up differential–difference equations describing the lattice dynamics. Such equations represent Lagrange equations of the second kind.

$$\frac{\mathrm{d}}{\mathrm{d}t}\left(\frac{\partial L}{\partial \dot{q}_{i,j}^{(l)}}\right) - \frac{\partial L}{\partial q_{i,j}^{(l)}} = 0, \tag{1.14}$$

where $L = T_{i,j} - U_{i,j}$ is the Lagrange function, which is equal to the difference between the kinetic and potential energy of a cell, $q_{i,j}^{(l)}$ are the generalized coordinates, $(q_{i,j}^{(1)} = u_{i,j}, q_{i,j}^{(2)} = w_{i,j}, q_{i,j}^{(3)} = \varphi_{i,j})$, $\dot{q}_{i,j}^{(l)}$ are the generalized velocities.

4th stage. *The continuum approximation.* A transition from discrete models to continual ones is performed by extrapolating the functions specified at discrete points by continuous fields of displacements and microrotations. For long-wavelength perturbations, when $\lambda \gg a$ (where λ is a characteristic spatial scale of deformation), discrete labels i and j can be changed by means of a continuous spatial variables $x = ia$ and $y = ja$. In this case, the functions specified at discrete points are interpolated by the continuous functions and their partial derivatives in accordance with the standard Taylor formula. Depending on the number of interpolation terms, one can consider various approximations of a discrete model of a microstructured medium and elaborate a hierarchy of quasi-continuum models.

5th stage. *Identification of a model.* The goal of identification is the construction of the best (optimal) model on the basis of experimental observations. Identification is divided by *structural* and *parametric*. *The structural identification* is a choice of the optimal form of equations for a mathematical model. *The parametric identification* is a determination by the experimental data of the values of the parameters of the mathematical model ensuring the agreement of the model values with the experimental data, provided that the model and the object are subjected to similar influences. Such identification also includes a numerical simulation of experiment and a choice of the model parameters from the condition of the best coincidence of calculation and experimental results.

The main problem of parametric identification is the choice of variables possessing information about the medium. Such variables should be measured experimentally. For example, in acoustic spectroscopy, the measured values are the acoustic characteristics of a microstructured medium, using which the parameters of its micromodel can be determined. In the linear approximation, the acoustic characteristics of the medium can be determined due to dispersion dependences between the frequency and

the length of the elastic wave. In order to determine the nonlinear characteristics of the medium, it is necessary to consider the anharmonic interactions of acoustic waves of various types with each other [119, 121, 123, 180], as well as their interaction with the magnetic [190] and electric fields [191].

1.5 Conclusions

In this chapter, methods for describing a continuous medium at various scale levels and the basic principles of the structural modeling are formulated, and applicability of the classical mechanics laws for a theoretical description of media with micro- and nanostructure is justified.

The following chapters of the monograph are devoted to construction, in accordance with the principles of structural modeling described here, of a hierarchy of mathematical models of microstructured media (generalized continua) for various periodic structures, frequencies, and wavelengths. Moreover, by the microstructure, we mean not so much the smallness of the absolute values, but the smallness of some scales of the medium with respect to others.

Based on the foregoing, the models constructed in this work can be applied both to nanocrystalline materials and to media which particle sizes are several orders of magnitude greater than the characteristic sizes of nanoparticles. The only condition is that the particles are supposed to be non-deformable and homogeneous, not having their own internal structure inherent in real materials. In other words, the models proposed here are applicable in those cases when microstructure of particles of a medium can be neglected. Moreover, a wave dissipation and effects of wave reflection from a boundary of a medium are not considered in in this monograph. It should be noted that the generalized variational principle for taking into account dissipative effects in continuum mechanics was proposed by G.A. Maksimov in Ref. [192]. In addition, all the media simulated here are assumed to be boundless. When it is necessary to consider bounded media, the boundary conditions can be taken as for the Cosserat medium, since the models of microstructured media considered in Chapters 2–5 generally coincide with the Cosserat continuum equations. For example, the conditions of the absence of forces and moments directed along the normal line are taken in Ref. [193] as the boundary conditions of a half-space composed of the Cosserat medium.

References

1. Sedov, L.I.: Mechanics of Continuous Medium, vol. 1. World Scientific Publ, Singapore (1997)
2. Kunin, I.A.: Elastic Media with Microstructure, 2 volumes. Springer, Berlin (1983)
3. Nowacki, W.: Theory of Micropolar Elasticity. J. Springer, Wien (1970)

4. Savin, G.N., Lukashev, A.A., Lysko, E.M.: Propagation of elastic waves in a solid with microstructure. Prikl. Mekh. (Appl. Mech.) **6**(7), 48–52 (1970) (in Russian)
5. Newton, I.: Philosophical Naturalis Principia Mathematica. London, 419 p (1686)
6. Nikitina, N.Ye., Pavlov, I.S.: Specificity of the phenomenon of acoustoelasticity in a two-dimensional internally structured medium. Acoust. Phys. **59**(4), 399–405 (2013). © Pleiades Publishing, Ltd. https://doi.org/10.1134/S106377101304012X
7. Potapov, A.I., Pavlov, I.S., Maugin, G.A.: Nonlinear wave interactions in 1D crystals with complex lattice. Wave Motion 29, 297–312 (1999)
8. Cauchy, A.L.: Memoire sur la dispersion de la lumiere. Paris (1830)
9. Powell, B.: An abstract of the essential principles of A.Cauchy's view of the undulatory theory, leading to an explanation of the dispersion of light; with remarks. Phil. Mag. **6**(3), 31 (1835)
10. Tomson, S.W.: Popular Lectures and Addresses, vol. I. MacMilan and Co and New York, Constitution of Matter. London (1889)
11. Born, M., Huang, K.: Dynamical Theory of Crystal Lattices. Clarendon Press, Oxford (1954)
12. Brillouin, L., Parodi, M.: Wave Propagation in Periodic Structures. McGrawHill, New York (1946)
13. Cosserat, E., Cosserat, F.: Theorie des Corps Deformables. Librairie Scientifique A. Hermann et Fils, Paris, 226p (1909) (Reprint, 2009)
14. Mac Cullagh, J.: An essay towards a dynamical theory of crystalline reflection and refraction. Trans. R. Irish. Acad. Sci. 21, 17–50 (1839)
15. Mossoti, E.: Lezioni di Meccanica Razionale, Firenze (1851)
16. Clebsch, A.: Theorie der Elastizität tester Korper, Leipzig, 424 p (1862)
17. Kirchhoff, G.: Vorlesungen uber mathematische Physik, p. 466p. Mechanik, Leipzig (1874)
18. Duhem, P.: Hidrodynamique, Elasticité. Acoustique, Paris (1891)
19. Hertz, K.: Die Prinzipien der Mechanik. Leipzig (1894)
20. Voigt, W.: Theoretische Studien uber die Elastizitatsverhältnisse der Krystalle. Abn. Ges.Wiss. Gottingen, vol. 34 (1887).
21. Frenkel, Ya.I.: The Kinetic Theory of Liquids. USSR Academic Press, Moscow (1945) (in Russian).
22. Anselm, A.I., Porfiryeva, N.N.: Orientational-translational waves in molecular crystals. Soviet Phys. JETP. **19**(5), 438–446 (1949) ((in Russian))
23. Porfiryeva, N.N.: Orientational-translational waves in molecular crystals. Part 2. Dynamics of 2D and 3D lattices. JETP 19(8), 692–702 (1949) (in Russian).
24. Mechanics of generalized continua. Proceedings of the IUTAM-symposium on the generalized Cosserat continuum and the continuum theory of dislocations with applications. Freudenstadt and Stuttgart, 1967, ed. E. Kroner, Springer-Verlag, Berlin, Heidelberg, New York (1968)
25. Aero, E.L., Kuvshinskii, E.V.: Fundamental equations of the theory of elastic media with rotationally interacting particles. Soviet Phys. Solid State **2**, 1272–1281 (1961).
26. Kuvshinskiy, E.V., Aero, E.L.: Continuum theory of asymmetric elasticity—the problem of internal rotation. Soviet Phys. Solid State **5**, 1892–1897 (1964).
27. Kapustina, O.A.: Acousto-optics of liquid crystals: yesterday, today, and tomorrow. Crystallogr. Rep. **59**, 635–649 (2014). https://doi.org/10.1134/S1063774514050071
28. Lee, J.D., Eringen, A.C.: Continuum theory of smectic liquid crystal. J. Chem. Phys. **58**(10), 4203–4211 (1973)
29. Lee, J.D., Eringen, A.C.: Wave propagation in nematic liquid crystals. J. Chem. Phys. **54**(12), 5027–5034 (1971)
30. Akhiezer, A.I., Bar'yakhtar, V.G., Peletminskii, S.V.: Spin Waves. North Holland, Amsterdam (1968)
31. Green, A.E., Rivlin, R.S.: Multipolar continuum mechanics. Arch. Rat. Mech. Anal. **17**, 113–147 (1964)
32. Koiter, W.T.: Couple-stresses in the theory of elasticity. Proc. Konikl Acad. Wet., Ser. B67, 17 (1964)
33. Ilyushin, A.A.: Mechanics of Continuous Media. Moscow State Univ, Publ, Moscow (1990).((in Russian))

34. Ilyushin, A.A., Lomakin, V.A.: Moment theories in mechanics of solids. Strength and Plasticity. Moscow, Nauka, pp. 54–60 (1971)
35. Lomakin, V.A.: Static Problems in Mechanics of Deformable Solids. Nauka, Moscow (1970).((in Russian))
36. Mindlin, R.D.: Microstructure in linear elasticity. Arch. Rat. Mech. Anal. **16**(7), 51–78 (1964)
37. Palmov, V.A.: Basic equations of the theory of asymmetrical elasticity. Prikl. Matem. Mekh. **28**(3), 401–408 (1964)
38. Palmov, V.A.: On a model of a medium with complex structure. Prikl. Matem. Mekh. **33**(4), 768–773 (1969)
39. Savin, G.N.: Foundations of the Plane Problem of the Couple Stress Theory of Elasticity. Izd-vo Kiev. Univ, Kiev (1965).((in Russian))
40. Toupin, R.A.: Theories of elasticity with couple-stresses Arch. Rat. Mech. Anal. **17**, 85–112 (1964)
41. Truesdell, C., Toupin, R.A.: The classical field theories. Springer, Handbuch der Physik. III/I. Berlin (1960)
42. Eringen, A.C.: Microcontinuum Field Theories. 1: Foundation and solids. Springer, New York (1999).
43. Eringen, A.C.: Nonlinear theory of continuous media, p. 477p. McGraw-Hill, New York (1962)
44. Eringen, A.C., Edelen, D.G.B.: On non-local elasticity. Int J. Eng. Sci. **10**(3), 233–248 (1972)
45. Eringen, A.C., Suhubi, E.S.: Nonlinear theory of simple micro-elastic solids. Int. J. Eng. Sci. **2**, 189–203, 389–404 (1964)
46. Kushwaha, M.S., Halevi, P., Martinez, G., Dobrzynski, L., Djafari-Rouhani, B.: Theory of band structure of periodic elastic composites. Phys. Rev. B. **49**, 2313 (1994)
47. Kroner, E., Datta, B.K.: Non-local theory of elasticity for a finite inhomogeneous medium— a derivation from lattice theory. In: J. Simmons, R. de Wit (eds.) Fundamental aspects, of dislocation theory (Conference Proc.), vol. 2, pp. 737–746. National Bureau of Standards, Washington (1970)
48. Krumhansl, J.A.: Some considerations of the relation between solid state physics and generalized continuum mechanics. Eur. J. Mech. A/Solids **15**, 1049–1075 (1996)
49. Edelen, D.G.B., Green, A.E., Laws, N.: Nonlocal continuum mechanics. Arch. Rat. Mech. Anal. **43**(1), 36–44 (1971)
50. Green, A.E.: Micro-materials and multipolar continuum mechanics. Int. J. Eng. Sci. **3**(5), 533–537 (1965)
51. Bardenhagen, S., Triantafyllidis, N.: Derivation of higher order gradient continuum theories in 2,3-D non-linear elasticity from periodic lattice models. J. Mech. Phys. Solids. **42**(1), 111–139 (1994)
52. Lifshits, I.M.: On heat properties of chain and layered structures at low temperatures. J. Exp. Theoret. Phys. **22**(4), 475–486 (1952) (in Russian)
53. Kosevich, A.M.: 1999. The Crystal Lattice, Wiley-VCH, Berlin (1999)
54. Leonov, M.Y.: The Mechanics of Deformations and Fracture. Ilim, Frunze (1981).((in Russian))
55. Slepyan, L.I.: Models and Phenomena in Fracture Mechanics. Springer, Berlin (2002)
56. Slepyan, L.I.: On discrete models in fracture mechanics. Mech. Solids **45**(6), 803–814 (2011)
57. Korotkina, M.R.: Remark about moment stresses in discrete media. Moscow University Mechanics Bulletin. Allerton Press, Inc. no. 5, pp. 103–109 (1969)
58. Nazarov, S.A., Paukshto, M.V.: Discrete Models and Averaging in Problems of the Elasticity Theory. Izd. Leningr. Univ, Leningrad (1984).((in Russian))
59. Berinskii, I.E., Ivanova, E.A., Krivtsov, A.M., Morozov, N.F.: Application of moment inter-action to the construction of a stable model of graphite crystal lattice. Mech. Solids **42**(5), 663–671 (2007)
60. Ivanova, E.A., Krivtsov, A.M., Morozov, N.F.: Derivation of macroscopic relations of the elasticity of complex crystal lattices taking into account the moment interactions at the microlevel. J. Appl. Math. Mech. **71**(4), 543–561 (2007)

61. Ivanova, E.A., Krivtsov, A.M., Morozov, N.F., Firsova, A.D.: Description of crystal packing of particles with torque interaction. Mech. Solids **38**(4), 76–88 (2003)
62. Krivtsov, A.M., Podol'skaya, E.A.: Modeling of elastic properties of crystals with hexagonal close-packed lattice. Mech. Solids **45**(3), 370–378 (2010)
63. Porubov, A.V.: Two-dimensional modeling of diatomic lattice. In: dell'Isola F. et al. (eds.) Advances in Mechanics of Microstructured Media and Structures, Advanced Structured Materials vol. 87. Springer International Publishing AG, part of Springer Nature, pp. 263–272 (2018). https://doi.org/10.1007/978-3-319-73694-5_15
64. Porubov, A.V., Berinskii, I.E.: Nonlinear plane waves in materials having hexagonal internal structure. Int. J. Non-Linear Mech. **67**, 27–33 (2014)
65. Porubov, A.V., Berintskii, I.E.: Two-dimensional nonlinear shear waves in materials having hexagonal lattice structure. Math. Mech. Solids **21**(1), 94–103 (2016)
66. Porubov, A.V., Krivtsov, A.M., Osokina, A.E.: Two-dimensional waves in extended square lattice. Int. J. Non-Linear Mech. **99**, 281–287 (2018)
67. Porubov, A.V., Osokina, A.E.: On two-dimensional longitudinal nonlinear waves in graphene lattice. In: Berezovski A., Soomere T. (eds.) Applied Wave Mathematics II. Mathematics of Planet Earth, vol. 6, pp. 151–166. Springer, Cham (2019)
68. Vasiliev, A.A, Dmitriev, S.V., Miroshnichenko, A.E.: Multi-field approach in mechanics of structural solids. Int. J. Solids Struct. **47**, 510–525 (2010)
69. Vasiliev, A.A, Dmitriev, S.V., Miroshnichenko, A.E.: Multi-field continuum theory for medium with microscopic rotations. Int. J. Solids Struct. **42**, 6245–6260 (2005)
70. Vasiliev, A.A, Miroshnichenko, A.E., Ruzzene, M.: Multifield model for Cosserat media. J. Mech. Mater. Struct. **3**(7), 1365–1382 (2008)
71. Vasiliev, A.A., Miroshnichenko, A.E., Dmitriev, S.V.: Multi-field modeling of a Cosserat lattice: models, wave filtering, and boundary effects. Euro. J. Mech. A/Solids **46**, 96–105
72. Suiker, A.S.J., Metrikine, A.V., de Borst, R.: Comparison of wave propagation characteristics of the Cosserat continuum model and corresponding discrete lattice models. Int. J. Solids Struct. **38**, 1563–1583
73. Suiker, A.S.J., Metrikine, A.V., de Borst, R.: Dynamic behaviour of a layer of discrete particles. Part 1: Analysis of body waves and eigenmodes. J. Sound Vib. **240**(1), 1–18
74. Morozov, N.F., Paukshto, M.V.: On the crack simulation and solution in the lattice. ASME J. Appl. Mech. **58**, 290–292 (1991)
75. Krivtsov, A.M.: Deformation and destruction of microstructured solids. Moscow, Fizmatlit Publ., 304 p. (2007) (in Russian)
76. Ostoja-Starzewski, M., Sheng, P.Y., Alzebdeh, K.: Spring network models in elasticity and fracture of composites and polycrystals. Comput. Materi. Sci. **7**, 82–93 (1996)
77. Pouget, J., Maugin, G.A.: Nonlinear dynamics of oriented elastic solid. Part 1,2 J. Elasticity **22**, 135–155, 157–183 (1989)
78. Sayadi, M.K., Pouget, J.: Soliton dynamics in a microstructured lattice model. J. Phys. A: Math. Gen. **24**, 2151–2172 (1991)
79. Askar, A.: A model for coupled rotation-displacement mode of certain molecular crystals. Illustration for KNO_3. J. Phys. Chem. Solids **34**, 1901–1907 (1973)
80. Askar, A.: Molecular crystals and the polar theories of continua: experimental values of material coefficients for KNO_3. Int. J. Eng. Sc. **10**, 293–300 (1972)
81. Fisher-Hjalmars, I.: Micropolar phenomena in ordered structures. In: Brulin, O., Hsieh, R.K.T. (eds.) Mechanics of Micropolar Media. World Scientific, Singapore, pp. 1–33 (1982)
82. Fujii, K., Fuka, T., Kondo, H., Ishii, K.: Orientational phase transition in molecular crystal N_2. J. Phys. Soc. Jpn. **66**, 125–129 (1997)
83. Berglund, K.: Structural models of micropolar media. In: Brulin, O., Hsieh, R.K.T. (eds.) Mechanics of Micropolar Media. World Scientific, Singapore, pp. 35–86 (1982)
84. Ugodchikov, A.G.: Moment dynamics of a linearly elastic body. Dokl. Phys. **340**(1), 56–58 (1995)

85. Krylov, A.L., Mazur, N.G., Nikolayevskii, V.N., El', G.A.: Gradient-consistent non-linear model of the generation of ultrasound in the propagation of seismic waves. J. Appl. Math. Mech. **57**(6), 1057–1066 (1993)

86. Krylov, A.L., Nikolayevskii, V.N., El', G.A.: Mathematical model of nonlinear generation of ultrasound by seismic waves. Dokl. Akad. Nauk SSSR **318**(6), 1340–1345 (1991)

87. Nikolaevsky, V.N.: Geomechanics and Fluidodynamics. Kluwer Academic Publishers, Dordrecht (1996)

88. Popov, V.L., Psakhie, S.G.: Theoretical aspects of computer simulation of elastic-plastic media on the basis of movable cellular automata I. Homogeneous Media. Phys. Mesomech. **3**(1), 17 (2000)

89. Psakhie, S.G., Horie, Y., Korostelev, S.Y., Smolin, A.Y., Dmitriev, A.I., Shilko, E.V., Alekseev, S.V.: Method of movable cellular automata as a tool for simulation within the framework of mesomechanics. Russ. Phys. J. **38**(11), 1157–1168 (1995). https://doi.org/10.1007/BF00559396

90. Psakhie, S.G., Horie, Y., Ostermeyer, G.P., Korostelev, S.Y., Smolin, A.Y.: Movable cellular automata method for simulating materials with mesostructure. Theoret. Appl. Fract. Mech. **37**(1–3), 311–334 (2001)

91. Smolin, AYu., Dobrynin, S.A., Psahie, S.G., Roman, N.V.: On rotation in the movable cellular automation method. Phys. Mesomech. **12**(3–4), 124–129 (2009)

92. Smolin, AYu., Smolin, IYu., Eremina, G., Smolina, IYu.: Multiscale simulation of porous ceramics based on movable cellular automaton method. J. Phys. Conf. Ser. **894**, 012087 (2017)

93. Askar, A.: Lattice Dynamics Foundation of Continuum Theory. World-Scientific, Singapore (1985)

94. Erofeyev, V.I., Potapov, A.I.: Longitudinal strain waves in nonlinearly elastic media with couple stresses. Int. J. Non-Linear Mech. **28**(4), 483–489 (1993)

95. Erofeyev, V.I., Potapov, A.I.: Nonlinear wave processes in elastic media with inner structure. Nonlinear World, vol. 2, pp. 1197–1215. World-Scientific, Singapore (1990)

96. Gendelman, O.V., Manevitch, L.I.: Linear and nonlinear excitations in a polyethylene crystal. Part I. Vibrational modes and linear equations. Macromol. Theor. Simul. **7**, 579–589 (1998)

97. Lisina, S.A., Potapov, A.I., Nesterenko, V.F.: Nonlinear granular medium with rotations of the particles. One-dimensional model. Phys. Acoust. **47**(5), 666–674 (2001)

98. Pouget, J.: Lattice dynamics and stability of modulated-strain structures for elastic phase transitions in alloys. Phys. Rev. B. **48**(2), 864–875 (1993)

99. Sargsyan, A.H., Sargsyan, S.H.: Dynamic model of micropolar elastic thin plates with independent fields of displacements and rotations. J. Sound Vib. **333**(18), 4354–4375 (2014)

100. Sargsyan, S.H.: Micropolar beam model for nanocrystalline material consisting of linear chains of atoms. Phys. Mesomech. **20**(4), 425–431 (2017)

101. Sargsyan, S.H., Sargsyan, A.A.: General dynamic theory of micropolar elastic thin plates with free rotation and special features of their natural oscillations. Acoust. Phys. **57**(4), 473–481 (2011)

102. Gross, E.F.: Light scattering and relaxation phenomena in liquids Doklady Akademii Nauk SSSR 28(9), 788–793 (1940) (in Russian)

103. Bernal, J.D., Tamm, G.R.: Zero point energy and physical properties of H_2O and D_2O. Nature **135**, 229 (1935)

104. Gross, E.F., Korshunov, A.V.: Rotational oscillations of molecules in a crystal lattice of organic substances and scattering spectra. JETP. **16**(1), 53–59 (1946)

105. Gross, E.F.: Izbrannye Trudy (Selected Papers). Nauka, Leningrad (1976).((in Russian))

106. Gross, E.F., Korshunov, A.V., Sel'kin, V.A.: Raman spectra of small frequencies of crystals of para-, meta- and orthoiodiobenzenes. JETP **20**, 293–296 (1950)

107. Abolinsh, Y.Y., Gross, E.F., Shultin, A.A.: Optic-acoustic effect in crystals. Soviet Phys. Tech. Phys. **28**, 2255 (1958)

108. Savin, G.N., Lukashev, A.A., Lysko, E.M., Veremeenko, S.V., Agas'ev, G.G.: Propagation of elastic waves in the Cosserat continuum with constrained particle rotation. Prikl. Mekh. (Appl. Mech.) **6**(6), 37–40 (1970) (in Russian)

109. Erofeyev, V.I., Rodyushkin, V.M.: Observation of the dispersion of elastic waves in a granular composite and a mathematical model for its description. Sov. Phys. Acoust. **38**(6), 611–612 (1992)
110. Potapov, A.I., Rodyushkin, V.M.: Experimental investigation of strain waves in materials with microstructure. Acoust. Phys. **47**(1), 347–352 (2001)
111. Stroscio, M.A., Dutta, M.: Phonons in Nanostructures. Cambridge University Press, 274 p. (2001)
112. Lyamov, V.E.: Polarization Effects and Anisotropy of the Interaction of Acoustic Waves in Crystals. Mosk. Gos. Univ., Moscow, 224 p. (1983) (in Russian)
113. Bagdoev, A.G., Erofeyev, V.I., Shekoyan, A.V.: Wave Dynamics of Generalized Continua. Advanced Structured Materials, vol. 24, 274 p. Springer, Berlin, Heidelberg (2016)
114. Belyaeva, IYu., Zaitsev, VYu., Ostrovsky, L.A.: Nonlinear acoustical properties of granular media. Acoust. Phys. **39**, 11–16 (1993)
115. Bykov, V.G.: Solitary shear waves in a granular medium. Acoust. Phys. **45**(2), 138–142 (1999)
116. Erofeev, V.I.: Wave Processes in Solids with Microstructure. World Scientific Publishing. New Jersey, London, Singapore, Hong Kong, Bangalore, Taipei (2003)
117. Nazarov, V.E., Radostin, A.V. Nonlinear Acoustic Waves in Micro-Inhomogeneous Solids. Wiley, 251 p. (2015)
118. Qiu, C., Zhang, X., Liu, Z.: Far-field imaging of acoustic waves by a two-dimensional sonic crystal. Phys. Rev. B **71**, 054302–054311 (2005)
119. Dragunov, T.N., Pavlov, I.S., Potapov, A.I.: Anharmonic interaction of elastic and orientation waves in one-dimensional crystals. Phys. Solid State **39**, 118–124 (1997)
120. Potapov, A.I., Pavlov, I.S.: Nonlinear waves in 1D oriented media. Acoust. Lett. **19**(6), 110–115 (1996)
121. Potapov, A.I., Pavlov, I.S., Gorshkov, K.A., Maugin, G.A.: Nonlinear interactions of solitary waves in a 2D lattice. Wave Motion **34**(1), 83–95 (2001)
122. Potapov, A.I., Pavlov, I.S., Lisina, S.A.: Acoustic Identification of Nanocrystalline Media. J. Sound Vib. **322**(3), 564–580 (2009)
123. Potapov, A.I., Pavlov, I.S., Lisina, S.A.: Identification of nanocrystalline media by acoustic spectroscopy methods. Acoust. Phys. **56**(4), 588–596 (2010)
124. Ghoniem, N.M., et al.: Multiscale modelling of nanomechanics and micromechanics: an over-view. Phil. Mag. **83**(31–34), 3475–3528 (2003)
125. Cleland, A.N.: Foundations of nanomechanics: from solid-state theory to device applications. Springer, Berlin (2003)
126. Kittel, C.: Introduction to Solid State Physics, 8th edn. Wiley, Inc. (2005)
127. Pavlov, P.V., Khokhlov, A.F.: Physics of Solid Body: Textbook, p. 494. Visshaya School, Moscow (2000)
128. Davydov, A.S.: Quantum Mechanics, 637 p. In: Dirk ter Haar (ed.). Pergamon Press (1976)
129. Rieth, M.: Nano-Engineering in Science and Technology. An Introduction to the World of Nano-Design. World Scientific, 151 p. (2003)
130. Golovneva, E.I., Golovnev, I.F., Fomin, V.M.: Peculiarities of application of continuum mechanics methods to the description of nano-structures. Phys. Mesomech. **8**(5), 41–48 (2005)
131. Lisina, S.A., Potapov, A.I.: Generalized continuum models in nanomechanics. Doklady Phys. **53**, 275–277 (2008). https://doi.org/10.1134/S1028335808050091
132. Sedov, L.I.: Mathematical methods for constructing new models of continuous media. Russ. Math. Surv. **20**(5), 123–182 (1965)
133. Sedov, L.I.: Models of continuous media with internal degrees of freedom. J. Appl. Math. Mech. **32**(5), 803–819 (1968)
134. Li, C., Chou, T.W.: Structural mechanics approach for the analysis of carbon nanotubes. Int. J. Solids Struct. **40**, 2487–2499 (2003)
135. Erofeev, V.I., Leontyeva, A.V., Malkhanov, A.O., Pavlov I.S. Structural modeling of nonlinear localized strain waves in generalized continua. In: Wolfgang, H., Altenbach, H., Muller, W.H., Abali, B.E. (eds.) Advanced Structured Materials. 2019/High Gradient Materials and Related Generalized Continua. Springer Nature Switzerland AG. Part of Springer, Cham, Switzerland, pp. 55–68.

136. Moshev, V.V., Garishin, O.K.: Structural mechanics of dispersedly filled elastomeric composites. Uspekhi Mekh. **3**(2), 3–36 (2005)
137. Nikitenkova, S.P., Potapov, A.I.: Dispersion properties of two-dimensional phonon crystals with a hexagonal structure. Acoust. Phys. **56**(6), 909–918 (2010)
138. Pavlov, I.S.: Acoustic identification of the anisotropic nanocrystalline medium with non-dense packing of particles. Acoust. Phys. **56**(6), 924–934 (2010)
139. Pavlov, I.S., Potapov, A.I.: Structural models in mechanics of nanocrystalline media. Doklady Phys. **53**(7), 408–412 (2008)
140. Pavlov, I.S., Potapov, A.I., Maugin, G.A.: A 2D granular medium with rotating particles. Int. J. Solids Struct. **43**(20), 6194–6207 (2006)
141. Pavlov, I.S., Vasiliev, A.A., Porubov, A.V.: Dispersion properties of the phononic crystal consisting of ellipse-shaped particles. J. Sound Vib. **384**, 163–176 (2016)
142. Potapov, A.I., Pavlov, I.S., Nikitenkova, S.P., Shudyaev, A.A.: Structural models in nanoacoustics: control of dispersion properties of phonon crystals. Acoustics of inhomogeneous media. In: Proceedings of the Russian acoustic society. Issue 10. Moscow: GEOS, pp. 9–16 (2009) (in Russian)
143. Pouget, J., Askar, A., Maugin, G.A.: Lattice model for elastic ferroelectric crystals: Microscopic approach. Phys. Rev. B. **33**(9), 6304–6325 (1986)
144. Vasiliev, A.A., Pavlov, I.S.: Auxetic properties of hiral hexagonal cosserat lattices composed of finite-sized particles. Phys. Status Solidi B **3**(257), 1900389 (2020). https://doi.org/10.1002/pssb.201900389
145. Vasiliev, A.A., Pavlov, I.S.: Models and some properties of Cosserat triangular lattices with chiral microstructure. Lett. Mater. **9** (1), 45–50 (2019). www.lettersonmaterials.com DOI: https://doi.org/10.22226/2410-3535-2019-1-45-50
146. Vasiliev, A.A., Pavlov, I.S.: Structural and mathematical modeling of Cosserat lattices composed of particles of finite size and with complex connections. IOP Conf. Ser.: Mater. Sci. Eng. **447**, 012079 (2018)
147. Shermergor, T.D.: Theory of Elasticity of Micro-Inhomogeneous Media. Nauka, Moscow (1977).((in Russian))
148. Miller, R.E., Shenoy, V.B.: Size-dependent elastic properties of nanosized structural elements. Nanotechnology **11**, 139–147 (2000)
149. Solyaev, Yu., Lurie, S.: Numerical predictions for the effective size-dependent properties of piezoelectric composites with spherical inclusions. Compos. Struct. **202**, 1099–1108 (2018)
150. Gulyaev, Yu.V., Lagar'kov, A.N., Nikitov, S.A.: Metamaterials: basic research and potential applications. Herald Russ. Acad. Sci. **78**, 268–278 (2008)
151. Vityaz, P.A., Shelekhina, V.M., Prokhorov, O.A., Gaponenko, N.V.: Preparation of pseudocrystalline materials based on silica. Proc. Natl. Acad. Sci. Belarus. Physical-Technical Ser. **1**, 16–20 (2002) (in Russian)
152. Sidorov, L.N., Yurovskaya, M.A., Borschevskii, A.Y., Trushkov, I.V., Ioffe, I.N.: Fullerenes. Ekzamen, Moscow, 690 p. (2005) (in Russian)
153. Suzdalev, I.P.: Nanotechnology: Physical Chemistry of Nanoclusters, Nanostructures, and Nanomaterials. KomKniga, Moscow (2006).((in Russian))
154. Morozov, A.N., Skripkin, A.V.: Behaviour of polymer chains and structures under the influence of random forces. Nonlinear World. **13**(7), 33–37 (2015) ((in Russian))
155. Blank, V.D., Levin, V.M., Prokhorov, V.M., Buga, S.G., Dubitskii, G.A., Serebryanaya, N.R.: Elastic properties of ultrahard fullerites. J. Exp. Theoret. Phys. **87**, 741–746 (1998)
156. Kulbachinskii, V.A., Buga, S.G., Blank, V.D., Dubitsky, G.A., Serebryanaya, N.R.: Superconducting superhard composites based on C_{60}, diamond or boron nitride and MgB_2. J. Nanostruct. Polym. Nanocompos. **6**(4), 119–122 (2010)
157. Kobelev, N.P., Soifer, Ya.M., Bashkin, I.O., Moravski, A.P.: Elastic and dissipative properties of C_{60} fullerite. Nanostruct. Mater. **6**(5), 909–912 (1995)
158. Yildirim, T., Harris, A.B.: Lattice dynamics of solids C_{60}. Phys. Rev. B **46**, 7878–7896 (1992)
159. Mikhalchenko, V.P., Motskin, V.V.: On elastic properties of fullerite C_{60} f.c.c. phase. J. Thermoelectricity **3**, 31–44 (2004)

160. Koch, E.: Enhancing T_C in field-doped fullerenes by applying uniaxial stress. Phys. Rev. B. **66**, 081401 (2002)
161. Kobelev, N.P., Nikolaev, R.K., Soifer, Ya.M., Khasanov, S.S.: Elastic moduli of single-crystal C_{60}. Phys. Solid State **40**(1), 154–156 (1998)
162. Ostrovsky, L.A., Potapov, A.I.: Modulated Waves: Theory and Applications. The Johns Hopkins University Press, Baltimore, MD (1999)
163. Vinogradova, M.B., Rudenko, O.V., Sukhorukov, A.P.: Theory of Waves. Nauka, Moscow (1990).((in Russian))
164. Grekov, M.A., Morozov, N.F.: Some modern methods in mechanics of cracks. In: Adamyan, V.M. et al. (eds.) Modern Analysis and Applications. Operator Theory: Advances and Applications, vol. 191. Birkhäuser, Basel (2009). https://doi.org/10.1007/978-3-7643-9921-4_8
165. Vardoulakis, I., Sulem, J.: Bifurcation Analysis in Geomechanics, p. 459. Blackie Academic and Professional, London (1995)
166. Chang, C.S., Ma, L.: A micromechanical-based micropolar theory for deformation of granular solids. Int. J. Solids Struct. **28**(1), 67–87 (1994)
167. Christoffersen, J., Mehrabadi, M.M., Nemat-Nasser, S.A.: A micromechanical description of granular material behavior. Trans. ASME. J. Appl. Mech. **48**(2), 339–344 (1981)
168. Sadovskaya, O., Sadovskii, V.: Mathematical Modeling in Mechanics of Granular Materials. Springer, Heidelberg, New York, Dordrecht, London, 390 p. (2012)
169. Lippman, H.: Cosserat plasticity and plastic spin. Appl. Mech. Rev. **48**(11) Part 1, 753–762 (1995)
170. Bobrovnitskii, Yu.I.: An acoustic metamaterial with unusual wave properties. Acoust. Phys. **60**(4), 371–378 (2014)
171. Bobrovnitskii, Yu.I.: Models and general wave properties of two-dimensional acoustic metamaterials and media. Acoust. Phys. **61**(3), 255–264 (2015)
172. Bobrovnitskii, Yu.I., Tomilina, T.M.: Sound absorption and metamaterials: a review. Acoust. Phys. **64**(5), 519–526 (2018)
173. Cummer, S.A., Christensen, J., Alù, A.: Controlling sound with acoustic metamaterials. Nat. Rev. Mater. **1**, 16001 (2016)
174. Fedotovskii, V.S.: A porous medium as an acoustic metamaterial with negative inertial and elastic properties. Acoust. Phys. **64**(5), 548–554 (2018)
175. Kolken, H.M.A., Zadpoor, A.A.: Auxetic mechanical metamaterials. RSC Adv. **7**(9), 5111–5129 (2017)
176. Zhu, S., Zhang, X.: Metamaterials: artificial materials beyond nature. Natl. Sci. Rev. **5**(2), 131 (2018)
177. Solyaev, Yu., Lurie, S., Ustenko, A.: Numerical modeling of a composite auxetic metamaterials using micro-dilatation theory. Continuum Mech. Thermodyn. **31**, 1099–1107 (2019)
178. Altenbach, H., Maugin, G.A., Erofeev, V.I. (eds.): Mechanics of Generalized Continua. Springer, Berlin, Heidelberg, 350 p. (2011)
179. Maugin, G.A., Metrikine, A.V. (eds.): Mechanics of Generalized Continua. One Hundred Years After the Cosserats. Springer, 337 p. (2010)
180. Vakhnenko, V.A.: Diagnosis of the properties of a structurized medium by long nonlinear waves. J. Appl. Mech. Tech. Phys. **37**(5), 643–649 (1996)
181. Destrade, M., Gilchrist, M.D., Saccomandi, G.: Third- and fourth-order constants of incompressible soft solids and the acousto-elastic effect. J. Acoust. Soc. Am. **127**(5), 2759–2763 (2010)
182. Nikitina, N.E.: Acoustoelasticity. Experience of Practical Application. TALAM, Nizhny Novgorod, 208 p (2005) (in Russian)
183. Erofeev, V.I., Pavlov, I.S.: Rotational waves in microstructured materials. In: dell'Isola, F., Eremeyev, V.A., Porubov, A.V. (eds.) Advances in Mechanics of Microstructured Media and Structures, Advanced Structured Materials, vol. 87, pp. 103–124. Springer, Cham (2018)

184. Love, A.E.H.: A treatise on the mathematical theory of elasticity, 4th edn. Cambridge University Press, Cambridge (1927)
185. Broberg, K.B.: The cell model of materials. Comput. Mech. **19**, 447–452 (1997)
186. Gendelman, O.V., Manevitch, L.I.: The description of polyethylene crystal as a continuum with internal degrees of freedom. Int. J. Solids Struct. **33**(12), 1781–1798 (1996)
187. Pavlov, I.S., Potapov, A.I.: Two-dimensional model of a granular medium. Mech. Solids **42**(2), 250–259 (2007)
188. Fedorov, V.I.: Theory of Elastic Waves in Crystals. Nauka, Moscow (1965); Plenum Press, New York (1968)
189. Goldshtein, R.V., Chentsov, A.V.: A discrete-continual model for a nanotube. Mech. Solids **4**, 57–74 (2005)
190. Erofeev, V.I., Malkhanov, A.O., Zemlyanukhin, A.I., Catcon, V.M.: Nonlinear magnetoelastic waves in a plate. In: Altenbach, H., Eremeyev, V.A. (eds.) Shell-like Structures. Non-classical Theories and Applications. Advanced Structured Materials, vol. 15, pp. 125–134. Springer, Heidelberg, Dordrecht, London, New York (2011)
191. Maugin, G.A.: Continuum Mechanics of Electromagnetic Solids. North-Holland Amsterdam (1988)
192. Maximov, G.A.: Generalized variational principle for dissipative continuum mechanics. In: Maugin, G., Metrikine, A. (eds.) Mechanics of Generalized Continua. Advances in Mechanics and Mathematics, vol. 21. Springer, New York, NY (2010). https://doi.org/10.1007/978-1-4419-5695-8_31
193. Kulesh, M.A., Matveenko, V.P., Shardakov, I.N.: Propagation of surface elastic waves in the Cosserat medium. Acoust. Phys. **52**(2), 186–193 (2006). https://doi.org/10.1134/s1063771006020114

Chapter 2
A 2D Lattice with Dense Packing of the Particles

Mechanical properties of a granular consolidated medium depend on the geometry of the microparticles, their location, and the forces of interaction between them. One of the main goals of mathematical modeling of such media is obtaining equations of motion and equations of state, which are capable to describe a discrete nature of a medium. Investigations of the dynamic behavior of granular media with regular and random packings without taking into account the rotation of particles were carried out in Refs. [1–3]. Models of granular media with allowance for particle rotation were considered in Refs. [4–9].

In this chapter, discrete and continual models of a crystalline medium with a hexagonal symmetry are elaborated, and the analytical interrelation between the medium macroparameters and the parameters of its microstructure is determined and dispersion properties of the developed models are analyzed.

2.1 The Discrete Model for a Hexagonal Lattice Consisting of Round Particles

We will start the structural modeling with consideration of a two-dimensional hexagonal closed-packed lattice [10] (or *triangle*, as it is mentioned in [11]) consisting of homogeneous round particles[1] with masses M and diameter d. In the initial state ($t = 0$), they are located in the lattice sites and the distance between the mass centers of the neighboring granules is equal to a, see Fig. 2.1a. It is assumed that each particle interacts only with six nearest neighbors in the lattice, which mass centers are located at the vertices of a regular hexagon inscribed in a circle of radius a (*the first coordination sphere*) (Fig. 2.1a, b). Simulation of the central and non-central interactions

---

[1]Hereinafter, we will use the terms "grains" and "granules" as synonyms for the word "particles." However, these terms do not have such a meaning, as in materials science.
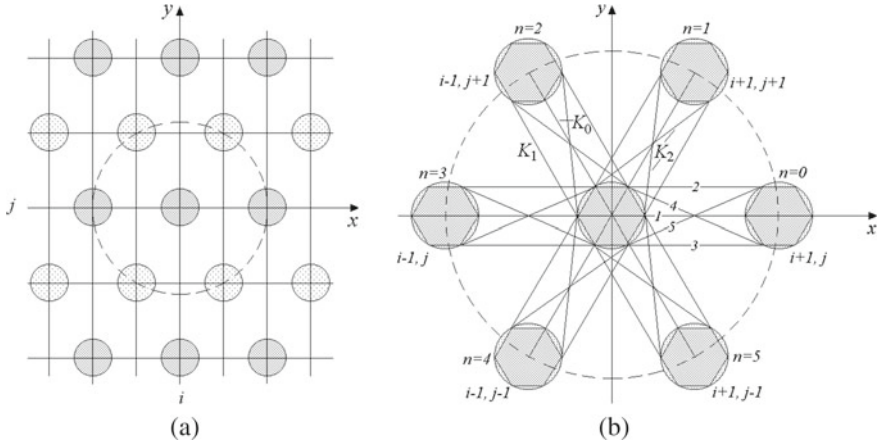
Fig. 2.1 Hexagonal lattice consisting of round particles (**a**) and scheme of force interactions (**b**)

between the particles is performed by means of the so-called spring model [8, 12–16]. The interactions of the neighboring granules are simulated by elastic springs of three types [17–20]: Central (the corresponding spring is designated in Fig. 2.1b by number 1 and has rigidity K_0), non-central (2 and 3 with rigidity K_1), and "diagonal" (4 and 5 with rigidity K_2). The interactions of tension/compression type are modeled by the central and non-central springs. Figure 2.1b Besides, the torques of the particles are provided by the springs of the K_1 type. Springs with the rigidity K_2 characterize the force interactions of the particles at the shear deformations in the material. The points of junctions of the springs K_1 and K_2 coincide with the apexes of the regular hexagon inscribed in the round particle Fig. 2.1b.

It should be noted that six pairs of diagonal springs connecting the central particle with the six nearest neighbors in the lattice have the same rigidity K_2. But if the rigidities of the diagonal springs in pairs are different, then there is a lattice with a chiral microstructure. Dynamical properties of such lattices were discussed, particularly, in Refs. [21, 22].

Each particle has three degrees of freedom, when it moves in its plane: the displacement of the mass center of the particle with the number $N = N(i, j)$ по осям x и y (translational degrees of freedom $u_{i,j}$ and $w_{i,j}$) and the rotation with respect to the mass center (the rotational degree of freedom $\varphi_{i,j}$ (Fig. 2.2). The kinetic energy of the particle $N(i, j)$ equals

$$T_{i,j} = \frac{M}{2}\left(\dot{u}_{i,j}^2 + \dot{w}_{i,j}^2\right) + \frac{J}{2}\dot{\varphi}_{i,j}^2. \tag{2.1}$$

Here, $J = Md^2/8$ is the moment of inertia of the particle about the axis passing through its mass center. The upper dot denotes derivatives with respect to time.

The displacements of the granules are supposed to be small in comparison with the sizes of the elementary cell of the lattice. The energy of each particle provided by
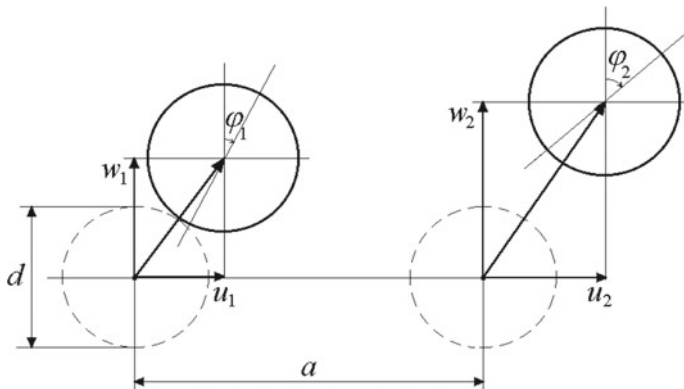
Fig. 2.2 Kinematic scheme

deviation of the particle from the equilibrium state is determined by the strain energy of the springs connecting this particle with the six nearest neighbors in the lattice. These six particles can be numbered by two ways: either by the number of the row, where the particle is located (Fig. 2.1b), or by the coordinates of the mass centers of these particles on the circle of unit radius. In order to construct a discrete model, it is more convenient to use the first method. In this case, 1 is added to the first index of the particles, if they are located to the right of the particle $N(i, j)$ (in Fig. 2.1b, these particles have the numbers $n = 0, 1, 5$), and -1 is added, if the particles are to the left of it (these are particles $n = 2, 3, 4$). Similarly, 1 is added to the second index of the particles located above the particle $N(i, j)$ and -1 is added, if the particles are below it (respectively, for particles with numbers $n = 0$ and $n = 5$, the second index remains equal to j). Thus, the potential energy due to the interaction of the particle $N(i, j)$ with six nearest neighbors in the lattice $(i + m_1, \ j + m_2)$, where $m_1 = \pm 1$ is the shift of the number along the horizontal axis and $m_2 = 0, \ \pm 1$ is the shift of the number along the vertical axis and is described by the formula

$$U_{i,j} = \frac{1}{2} \sum_{(m_1, m_2)} \left(\frac{K_0}{2} D^2_{1(m_1, m_2)} + \frac{K_1}{2} \left(D^2_{2(m_1, m_2)} + D^2_{3(m_1, m_2)} \right) \right.$$
$$\left. + \frac{K_2}{2} \left(D^2_{4(m_1, m_2)} + D^2_{5(m_1, m_2)} \right) \right) \tag{2.2}$$

Here, $D_{l(m_1, m_2)}$ $(l = 1, 2, 3, 4, 5)$ are the elongations of the springs connecting the central particle N with its six neighbors, l is the spring number in Fig. 2.1b. Equation (2.2) contains an additional factor 1/2, since the potential energy of each spring is equally divided between two particles connected by this spring. Expressions for the elongations of the springs, $D_{l(m_1, m_2)}$, calculated in the approximation of smallness of the quantities $\Delta u_{m_1 m_2} = (u_{i+m_1, j+m_2} - u_{i,j})/a \sim \Delta w_{m_1 m_2} = (w_{i+m_1, j+m_2} - w_{i,j})/a \sim \varphi_{i,j} \sim \varepsilon$ (here $\varepsilon \ll 1$ is a measure of the cell deformation) and $\Phi_{m_1 m_2} = (\varphi_{i,j} + \varphi_{i+m_1, j+m_2})/2 = \varphi_{i,j} - 0,5a\Delta\varphi_{m_1 m_2} \ll \pi/2$ are given in

Appendix A, see Eq. (A.1). Substitution of these expressions into Eq. (2.2) leads to the following expression for the potential energy per cell with the number $N = N(i, j)$ with accuracy up to quadratic terms:

$$
\begin{aligned}
U_{i,j} &= \gamma_1(\Delta u_{10}^2 + \Delta u_{-10}^2) + \gamma_2(\Delta u_{11}^2 + \Delta u_{-1-1}^2 + \Delta u_{1-1}^2 + \Delta u_{-11}^2) \\
&+ \gamma_3(\Delta w_{10}^2 + \Delta w_{-10}^2 + \Phi_{10}^2 + \Phi_{-10}^2 + \Phi_{11}^2 + \Phi_{-1-1}^2 + \Phi_{1-1}^2 + \Phi_{-11}^2 \\
&+ \Delta w_{11}\Phi_{11} - \Delta w_{-1-1}\Phi_{-1-1} + \Delta w_{1-1}\Phi_{1-1} - \Delta w_{-11}\Phi_{-11}) \\
&+ \sqrt{3}\gamma_3(-\Delta u_{11}\Phi_{11} + \Delta u_{-1-1}\Phi_{-1-1} + \Delta u_{1-1}\Phi_{1-1} - \Delta u_{-11}\Phi_{-11}) \\
&+ 2\gamma_3(\Delta w_{10}\Phi_{10} - \Delta w_{-10}\Phi_{-10}) + \gamma_4(\Delta w_{11}^2 + \Delta w_{-1-1}^2 + \Delta w_{1-1}^2 + \Delta w_{-11}^2) \\
&+ \gamma_5 d^2(\Delta \varphi_{10}^2 + \Delta \varphi_{-10}^2 + \Delta \varphi_{11}^2 + \Delta \varphi_{-1-1}^2 + \Delta \varphi_{1-1}^2 + \Delta \varphi_{-11}^2) \\
&+ \gamma_6(\Delta u_{11}\Delta w_{11} + \Delta u_{-1-1}\Delta w_{-1-1} - \Delta u_{1-1}\Delta w_{1-1} - \Delta u_{-11}\Delta w_{-11}).
\end{aligned}
\tag{2.3}
$$

Here, the coefficients $\gamma_1,\ldots, \gamma_6$ are determined in terms of the parameters of the internal structure of a material:

$$
\begin{aligned}
\gamma_1 &= \frac{a^2}{2}\left(K_0 + 2K_1 + \frac{(2a-d)^2}{2r_0^2}K_2\right), \\
\gamma_2 &= \frac{a^2}{8}\left(K_0 + 2K_1 + \frac{2a^2 - 2ad + 5d^2}{r_0^2}K_2\right), \\
\gamma_3 &= \frac{3a^2 d^2}{4r_0^2}K_2, \quad \gamma_4 = \frac{3}{8}a^2\left(K_0 + 2K_1 + \frac{2a^2 - 2ad + d^2}{r_0^2}K_2\right), \\
\gamma_5 &= \frac{3a^2}{16}K_1, \quad \gamma_6 = \frac{\sqrt{3}}{4}a^2\left(2K_1 - \frac{2a^2 - 2ad - d^2}{r_0^2}K_2\right),
\end{aligned}
\tag{2.4}
$$

where $r_0 = \sqrt{a^2 - ad + d^2}$ is the length of the undisturbed spring K_2.

Differential–difference equations describing the lattice dynamics, as it has been mentioned above, can be obtained from the Lagrange equations of the second kind (1.14) using Eqs. (2.1) and (2.3):

$$
\begin{aligned}
&M\ddot{u}_{i,j} - \frac{2\gamma_1}{a^2}(u_{i+1,j} - 2u_{i,j} + u_{i-1,j}) \\
&- \frac{2\gamma_2}{a^2}(u_{i+1,j+1} + u_{i-1,j-1} + u_{i+1,j-1} + u_{i-1,j+1} - 4u_{i,j}) \\
&- \frac{\gamma_6}{a^2}(w_{i+1,j+1} + w_{i-1,j-1} - w_{i+1,j-1} - w_{i-1,j+1}) \\
&- \frac{\sqrt{3}\gamma_3}{2a}(-\varphi_{i+1,j+1} + \varphi_{i-1,j-1} + \varphi_{i+1,j-1} - \varphi_{i-1,j+1}) = 0, \\
&M\ddot{w}_{i,j} - \frac{2}{a^2}\gamma_1(w_{i+1,j} - 2w_{i,j} + w_{i-1,j})
\end{aligned}
$$

$$-\frac{2}{a^2}\gamma_2(u_{i+1,j+1}+u_{i-1,j-1}+u_{i+1,j-1}+u_{i-1,j+1}-4u_{ij})$$

$$-\frac{1}{a^2}\gamma_6(w_{i+1,j+1}+w_{i-1,j-1}-w_{i+1,j-1}-w_{i-1,j+1})$$

$$-\frac{1}{a}\gamma_3(\varphi_{i+1,j}-\varphi_{i-1,j})$$

$$-\frac{1}{2a}\gamma_3(\varphi_{i+1,j+1}-\varphi_{i-1,j-1}+\varphi_{i+1,j-1}-\varphi_{i-1,j+1})=0, \qquad (2.5)$$

$$M\ddot{\varphi}_{i,j}-\left(\frac{16d^2}{a^2}\gamma_5-4\gamma_3\right)(\varphi_{i+1,j}+\varphi_{i-1,j}+\varphi_{i+1,j+1}$$

$$+\varphi_{i-1,j-1}+\varphi_{i+1,j-1}+\varphi_{i-1,j+1}-6\varphi_{i,j})$$

$$+48\gamma_3\varphi_{i,j}-\frac{4\sqrt{3}}{a}\gamma_3(u_{i+1,j+1}-u_{i-1,j-1}-u_{i+1,j-1}+u_{i-1,j+1})$$

$$+\frac{8}{a}\gamma_3(w_{i+1,j}-w_{i-1,j})$$

$$-\frac{4}{a}\gamma_3(-w_{i+1,j+1}+w_{i-1,j-1}-w_{i+1,j-1}+w_{i-1,j+1})=0.$$

Differential–difference Eq. (2.5) can be used for numerical simulation of the response of the system to the external dynamic forcing in the wide range of frequencies up to the threshold values [23]. However, for a comparison of the proposed mathematical model of a crystalline medium with the known theories of solids, it is convenient to pass over from the discrete to the continuous description.

2.2 The Continual Approximation

For long-wavelength perturbations, when $\lambda \gg a$ (where λ is a characteristic spatial scale of deformation) discrete labels i and j can be changed by means of continuous spatial variables $x = ia$ and $y = ja$. In this case, the functions specified at discrete points are interpolated by the continuous functions and their partial derivatives in accordance with the standard Taylor formula:

$$u_{i+l_1,j+l_2}(t) = u(x + l_1 a,\ y + l_2 a,\ t) = u(x, y, t) + a\left(l_1\frac{\partial u}{\partial x} + l_2\frac{\partial u}{\partial y}\right)$$

$$+\frac{a^2}{2}\left(l_1^2\frac{\partial^2 u}{\partial x^2} + 2l_1 l_2\frac{\partial u}{\partial x}\frac{\partial u}{\partial y} + l_2^2\frac{\partial^2 u}{\partial y^2}\right)$$

$$+\frac{a^3}{6}\left(l_1^3\frac{\partial^3 u}{\partial x^3} + 3l_1^2 l_2\frac{\partial^2 u}{\partial x^2}\frac{\partial u}{\partial y} + 3l_1 l_2^2\frac{\partial u}{\partial x}\frac{\partial^2 u}{\partial y^2} + l_2^3\frac{\partial^3 u}{\partial y^3}\right)+\dots,$$

$$(2.6)$$

where $l_1 = \cos\frac{\pi n}{3}$ is the abscissa of the center of the nth particle (among the six nearest neighbors) on a circle of unit radius, $l_2 = \sin\frac{\pi n}{3}$ is the ordinate of the center of this particle, $n = 0, 1, 2, 3, 4, 5$ (Fig. 2.1b). Thus, $l_1(0) = 1, l_2(0) = 0; l_1(1) = 1/2, l_2(1) = \sqrt{3}/2; l_1(2) = -1/2, l_2(2) = \sqrt{3}/2; l_1(3) = -1, l_2(3) = 0; l_1(4) = -1/2, l_2(4) = -\sqrt{3}/2; l_1(5) = 1, l_2(5) = -\sqrt{3}/2$. Similar expansions are also used for functions $w_{i\pm1,j\pm1}(t)$ and $\varphi_{i\pm1,j\pm1}(t)$. Depending on the number of terms kept in Eq. (2.6), one can consider various approximations of the discrete model for a granular medium. If only quantities of order $O(a)$ are taken into consideration in expansions (2.6) (it corresponds to the local theory of elasticity), then, after substituting these expansions into Eq. (2.3), the 2D Lagrange function L (Lagrangian) takes on the form:

$$L = \frac{\rho}{2}\left(u_t^2 + w_t^2 + R^2\varphi_t^2\right) - \frac{\rho}{2}[c_1^2(u_x^2 + w_y^2) + c_2^2(w_x^2 + u_y^2) + R^2c_3^2(\varphi_x^2 + \varphi_y^2)$$
$$+ s^2(u_x w_y + u_y w_x) + 2\beta(w_x - u_y)\varphi + R^2\omega_0^2\varphi^2]. \tag{2.7}$$

Here, the following notations have been introduced: c_i ($i = 1$ to 3)—are the velocities of propagation of longitudinal, transverse, and rotational waves $\varphi(x, y, t)$, respectively, s is the coefficient of coupling between the longitudinal and transverse deformations, β is the parameter of coupling of microrotations with the transverse and longitudinal waves, ω_0 is the threshold frequency of the microrotation wave, below which it does not propagate, $R = d/\sqrt{8}$ is the radius of the mass moment of inertia of the medium microparticles relative to the mass center, and $\rho = 2M/a^2\sqrt{3}$ is the surface density of a 2D medium with a hexagonal symmetry [11].

Using the Lagrange function (2.7), a set of differential equations of the first approximation describing the dynamic processes in a crystalline medium is derived in agreement with Hamilton's variational principle:

$$u_{tt} = c_1^2 u_{xx} + c_2^2 u_{yy} + s^2 w_{xy} - \beta\varphi_y,$$
$$w_{tt} = c_2^2 w_{xx} + c_1^2 w_{yy} + s^2 u_{xy} + \beta\varphi_x,$$
$$\varphi_{tt} = c_3^2(\varphi_{xx} + \varphi_{yy}) - \omega_0^2\varphi + \frac{\beta}{R^2}(u_y - w_x). \tag{2.8}$$

The squares of the wave velocities containing in Eq. (2.8) are expressed in terms of the density, ρ, force constants of the micromodel, K_0, K_1, K_2, K_3, the distance between the particles a, and their diameter d:

$$c_1^2 = \frac{3\sqrt{3}}{4\rho}\left(K_0 + 2K_1 + (2 - \frac{d^2}{a^2 - ad + d^2})K_2\right),$$
$$c_2^2 = \frac{\sqrt{3}}{4\rho}\left(K_0 + 2K_1 + \left(2 + \frac{3d^2}{a^2 - ad + d^2}\right)K_2\right),$$
$$c_3^2 = \frac{3\sqrt{3}}{4\rho}\left(2K_1 + \frac{a^2}{a^2 - ad + d^2}K_2\right),$$

$$\beta = \frac{3d^2\sqrt{3}}{2\rho(a^2 - ad + d^2)}K_2, \quad s^2 = c_1^2 - c_2^2. \tag{2.9}$$

The threshold frequency ω_0 depends on parameter β and on the radius of gyration of particles, $R = d/\sqrt{8}$:

$$\omega_0 = \sqrt{2|\beta|/R^2} = 4\sqrt{|\beta|/d^2}, \tag{2.10}$$

and parameters c_2, β, and s are interrelated by the following relationship:

$$\beta = c_2^2 - s^2/2. \tag{2.11}$$

And due to the last Eq. (2.9)

$$\beta = \frac{1}{2}(3c_2^2 - c_1^2). \tag{2.12}$$

Equation (2.8) describe the dynamics of a granular (crystalline) medium accounting for local interactions of granules and coincide with the dynamic equations of a two-dimensional Cosserat continuum consisting of centrally symmetric particles (see Sect. 4.3). This system differs from the equations of the classical theory of elasticity by the appearance of an additional equation for the rotational wave. This equation differs from the first two equations, as it has a solution that is homogeneous in space and oscillating in time with frequency ω_0. In the continuous approach, this equation follows from the conservation law of moment of momentum (or angular momentum), if the internal moments of the particles of the medium are introduced into the consideration [24, 25].

It should be also noted that due to substitution of expansions (2.6) into differential–difference Eq. (2.5), it is possible to obtain differential Eq. (2.8) immediately, bypassing the stage of derivation of the Lagrange function (2.7).

2.3 Influence of Microstructure on Acoustic Properties of a Medium

The question arises as to what new features the structural modeling gives us as compared with the phenomenological description. The structural approach establishes a one-to-one relation between parameters of the microstructure and macroscopic properties of the medium, whereas it is impossible for phenomenological theories. Next, let us analyze the relationships between the microstructure of a medium with dense packing of particles and its macroparameters, which have been obtained in the previous section.

The dependencies (2.9) of the velocities of the longitudinal (c_1), transverse (c_2), and rotational (c_3) waves on the relative size of particles d/a are given in Fig. 2.3 for

Fig. 2.3 Dependencies of elastic wave velocities on the relative size of particles in a hexagonal lattice for $K_1/K_0 = 0.1$, $K_2/K_0 = 0.1$ (curves 1), and $K_2/K_0 = 0.5$ (curve 2)
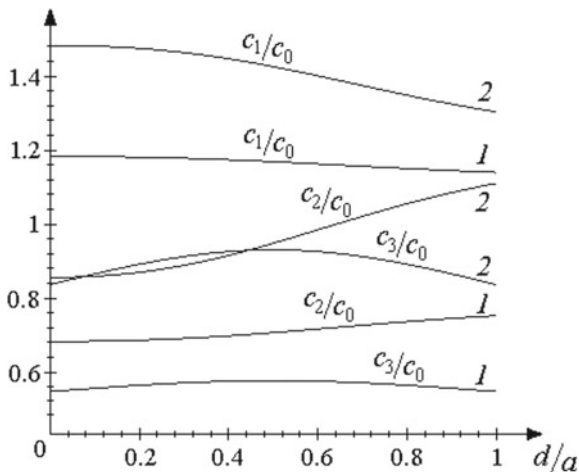
$K_1/K_0 = 0.1$. The curves 1 correspond to the value $K_2/K_0 = 0.1$, while curves 2 stand for the value $K_2/K_0 = 0.5$. All velocities are normalized by the longitudinal wave velocity $c_0 = \sqrt{3K_0\sqrt{3}/4\rho}$ taking account only of the central interactions. From these figures, it is clear that the longitudinal wave velocity decreases monotonically as the grains grow in size, while the transverse wave velocity, c_2, on the contrary, increases monotonously. The rotational wave velocity has a maximum for some value of d/a. In the range of small coupled interactions ($K_2 \ll K_0$), the grain size does not essentially affect the quantities of the wave velocities (see curves 1).

Due to relations (2.9) and (2.11), the parameters of force interactions can be expressed in terms of the acoustic characteristics of the medium:

$$K_2 = \frac{\rho(a^2 - ad + d^2)}{3d^2\sqrt{3}}\left(3c_2^2 - c_1^2\right),$$

$$K_1 = \frac{\rho}{3\sqrt{3}}\left(2c_3^2 - \frac{\beta a^2}{d^2}\right),$$

$$K_0 = \frac{4\rho}{3\sqrt{3}}\left(c_1^2 - c_3^2 - \frac{(a-d)^2}{2d^2}\beta\right). \tag{2.13}$$

Moreover, the particle size can be also expressed in terms of the acoustic characteristics of the medium due to Eqs. (2.10) and (2.11):

$$d = \sqrt{8\left|2c_2^2 - s^2\right|}/\omega_0 = \sqrt{8\left|3c_3^2 - c_1^2\right|}/\omega_0. \tag{2.14}$$

Thus, Eqs. (2.9)–(2.12), on the one hand, and Eqs. (2.13)–(2.14), on the other hand, establish one-to-one correspondences between the micromodel parameters

and macrocharacteristics of a medium. This interrelation can be used, in particular, for diagnostics of metamaterials due to data of wave (acoustic) experiments [18, 26].

2.4 Dispersion Properties of Normal Waves

The physical properties of a medium can be determined by the dispersion dependences of the waves propagating in such a medium. Therefore, let us consider this problem more in detail both for the discrete and continual models.

2.4.1 Dispersion Properties of the Discrete Model

The term "photonic crystals" appeared in the early 1990s for media having a periodic system of dielectric inhomogeneities giving rise to emergence of zones opaque both for light and electromagnetic waves [27–29]. From a general viewpoint, a photonic crystal is a superlattice or a medium, in which an additional field has been artificially created, and its period is of some orders greater than the basic lattice period. The behavior of photons is radically different from their behavior in the ordinary crystal lattice if the optical superlattice period is comparable with the length of the electromagnetic wave. They do not transmit the light with a wavelength comparable with the lattice period of the photonic crystal and determine the effect of the light localization. Photonic lattices are in the gap between the atomic crystal lattices and the macroscopic artificial periodic structures.

Subsequently, natural or artificial periodic structures became known as "phononic" crystals (acoustic superlattices) by analogy if they consist of non-pointwise particles, in which the length of the acoustic waves is comparable with the lattice period [27, 30, 31]. The velocity of propagation of elastic waves in solids is about 10^5 times less than the light wave velocity. Therefore, all effects inherent to photonic crystals should take place in acoustics, but for significantly lower frequencies. High interest in materials of this type is caused by the unique properties of the materials that enables one to apply them in many fields, primarily, in nano-electronics. At present, the propagation characteristics of acoustic waves of various types, both bulk and surface, are intensively studied in artificial two-dimensional and three-dimensional composite materials.

The ordering of the geometric structure is typical for the periodic (crystalline) media. It is a decisive factor leading to anisotropy of the properties of crystals and to the predominance of the collective motions of the wave type in the crystal lattice [31]. It is usually assumed that particles located in lattice sites do not have their own degrees of freedom. However, in artificial periodic structures (for example, in synthetic opals [32]), like in the medium considered in this chapter, nodes can contain non-point particles possessing rotational degrees of freedom, for example, molecular clusters or nanoparticles [27, 33].

The lattice with round particles considered in this chapter represents a system with N degrees of freedom, which is described by coupled Eq. (2.5). Introduction of normal mode variables makes equations of motion independent [34]. Each of them describes one normal vibration, and the arbitrary motion of the system can be represented as a superposition of normal vibrations. This approach is very convenient both for the theoretical analysis of the problem and for the physical interpretation of the obtained results. Similar concepts can be also introduced for distributed systems, where interacting waves of various types can propagate. A generalization of the concept of the normal vibrations of concentrated systems to "not closed" wave systems (boundless media, waveguides, tubes, rods, strings, etc.) gives rise to the *normal waves* [35–38].

The normal waves are called traveling harmonic waves in the linear systems with constant parameters, in which an absorption and scattering of energy are negligible. The normal waves retain their transverse structure and polarization, when they propagate along the direct line [35].

In the hexagonal lattice under consideration, all particles are physically equivalent; therefore, the excitation of any of the particles must be redistributed throughout the medium. In other words, any motion of an individual particle will stimulate the corresponding movements of neighboring particles; as a result, a wave will run across the lattice that is a typical collective motion. In order to study the collective motions arising in an arranged crystalline structure, we will pass to the normal oscillations. Let us consider solutions of the equations of motion representing plane monochromatic waves, for which the displacements can be represented in the following form:

$$
\begin{aligned}
u\left(\overrightarrow{N},t\right) &= u_0 \exp\left[i\left(\omega(\vec{q})\,t - \vec{q}\,\overrightarrow{N}\right)\right] \\
w\left(\overrightarrow{N},t\right) &= w_0 \exp\left[i\left(\omega(\vec{q})\,t - \vec{q}\,\overrightarrow{N}\right)\right] \\
\varphi\left(\overrightarrow{N},t\right) &= \varphi_0 \exp\left[i\left(\omega(\vec{q})\,t - \vec{q}\,\overrightarrow{N}\right)\right]
\end{aligned}
\tag{2.15}
$$

Here, $\omega = \omega(\vec{q})$ is a wave frequency regarded as a continuous function of the wave vector $\vec{q} = (q_1, q_2)$ that defines both the direction of the wave propagation in the Cartesian coordinate system (x, y) and the wavelength $\lambda = 2\pi / q$ $(q = |\vec{q}|)$. The vector $\overrightarrow{N} = (i, j)$ fixes the lattice sites. Arbitrary collective motions can be represented as a superposition of monochromatic waves. Substitution of solutions (2.15) into Eqs. (2.5) results in a set of equations in the matrix form for determination of the amplitudes of displacements

$$
\begin{pmatrix}
M\omega^2 - d_{11} & d_{12} & d_{13} \\
d_{21} & M\omega^2 - d_{22} & d_{23} \\
d_{31} & d_{32} & M\omega^2 - d_{33}
\end{pmatrix}
\times
\begin{pmatrix}
u_0 \\
w_0 \\
\varphi_0
\end{pmatrix}
= 0,
\tag{2.16}
$$

where the matrix elements are:

$$
d_{11} = \frac{8\gamma_1}{a^2}\sin^2\left(\frac{q_1 a}{2}\right) + \frac{8\gamma_2}{a^2}\left(1 - \cos\left(\frac{q_1 a}{2}\right)\cos\left(\frac{q_2 a\sqrt{3}}{2}\right)\right),
$$

$$d_{22} = \frac{16\gamma_3}{a^2} \sin^2\left(\frac{q_1 a}{2}\right) + \frac{8\gamma_4}{a^2}\left(1 - \cos\left(\frac{q_1 a}{2}\right)\cos\left(\frac{q_2 a\sqrt{3}}{2}\right)\right),$$

$$d_{33} = \frac{8}{a^2}\left[\frac{8\gamma_5 + 4a^2\gamma_3}{d^2} + \left(\gamma_6\sqrt{3} - \gamma_3\left(1 + \frac{2a}{d}\right)\right)\left(\sin^2\left(\frac{q_1 a}{2}\right) - \cos\left(\frac{q_1 a}{2}\right)\cos\left(\frac{q_2 a\sqrt{3}}{2}\right)\right)\right],$$

$$d_{12} = d_{21} = \frac{8\sqrt{3}}{3a^2}(\gamma_3 - \gamma_4)\sin\left(\frac{q_1 a}{2}\right)\sin\left(\frac{q_2 a\sqrt{3}}{2}\right),$$

$$d_{13} = -\frac{d^2}{8}d_{31} = i\frac{2\sqrt{3}\gamma_3}{a}\cos\left(\frac{q_1 a}{2}\right)\sin\left(\frac{q_2 a\sqrt{3}}{2}\right),$$

$$d_{23} = -\frac{d^2}{8}d_{32} = -i\frac{2\gamma_3}{a}\sin\left(\frac{q_1 a}{2}\right)\left(\cos\left(\frac{q_2 a\sqrt{3}}{2}\right) + 2\cos\left(\frac{q_1 a}{2}\right)\right). \tag{2.17}$$

The solvability condition for Eqs. (2.16) with coefficients defined by Eq. (2.17) leads to a bi-cubic dispersion equation for

$$M^3\omega^6 + F_1\omega^4 + F_2\omega^2 + F_3 = 0, \tag{2.18}$$

where $F_{1,2,3}$ are the wave vector functions:

$$\begin{aligned}
F_1 &= d_{11} + d_{22} + d_{33}, \\
F_2 &= d_{11}d_{22} + d_{11}d_{33} + d_{22}d_{33} - d_{12}d_{21} - d_{13}d_{31} - d_{23}d_{32}, \\
F_3 &= -d_{11}d_{22}d_{33} + d_{11}d_{23}d_{32} + d_{22}d_{13}d_{31} \\
&\quad + d_{33}d_{12}d_{21} + d_{12}d_{23}d_{31} + d_{13}d_{32}d_{21}.
\end{aligned} \tag{2.19}$$

Thus, the left-hand side of Eq. (2.18) contains three variables: frequency ω and the components of the wave vector, q_1 and q_2. Moreover, the coefficients (2.19) of Eq. (2.18) depend on the relative particle size d/a and on two parameters of the force and couple interactions: K_1/K_0 and K_2/K_0.

Two lattices correspond to each of the crystal structure: a direct lattice and a reciprocal one. A direct lattice is a lattice in ordinary space and a reciprocal one is a lattice in abstract reciprocal space, where distances have a dimension of the reciprocal length, in fact, it is the Fourier transform of the direct lattice [39]. The diffraction pattern represents a reciprocal crystal lattice map, just as the microscopic image is a map of the real crystal structure.

The primitive unit cells which constitute the periodic reciprocal lattice in the Bloch wave vector space are referred to as *Brillouin zones* [39]. The first Brillouin zone can be regarded as a primitive cell of the reciprocal lattice that possesses point symmetry of this lattice. Indeed, if we construct the first Brillouin zone around each node of the reciprocal lattice (the origin should be located in the node), then such zone would entirely fill the entire space without overlapping with each other. From this fact, it follows, in particular, that the volume of the first Brillouin zone is equal to the volume of the primitive cell of the reciprocal lattice.

The structure of the Brillouin zones is defined only by crystal structure and depends neither on the type of particles forming the crystal, nor on their interaction.

The physical meaning of the Brillouin zone boundaries consists in that they show the following values of the wave vectors or the electron quasipulses, in which the electron wave cannot propagate in a solid [39]. Next, we will analyze the dispersion properties of the medium in the first Brillouin zone and on its boundary depending on the values of the microstructure parameters.

Like in the solid-state physics, each normal lattice vibration can be associated with a certain type of quasiparticle—phonon [39, 40]. The considered system has a longitudinal acoustic (LA) phonon, a transverse acoustic (TA) one, and a rotational optical (*RO*) phonon (Fig. 2.4) [41, 42]. We pass to the polar coordinate system $q_1 = q \cos \theta$, $q_2 = q \sin \theta$, in Eq. (2.18), where q is the wave vector module and the angle θ indicates the direction of the plane wave propagation with respect to *x*-axis in the direct lattice. In particular, in the case of propagation of the plane waves, when $q_2 \equiv 0$ and, hence, $d_{12} \equiv d_{13} \equiv d_{21} \equiv d_{31} \equiv 0$, Eq. (2.14) is substantially simplified since the longitudinal phonons become independent in it:

$$\left(\varpi^2 - \frac{d_{11}}{K_0} \right) \left(\left(\varpi^2 - \frac{d_{22}}{K_0} \right) \left(\varpi^2 - \frac{d_{33}}{K_0} \right) - \frac{d_{23}}{K_0} \frac{d_{32}}{K_0} \right) = 0, \qquad (2.20)$$

where $\varpi = \omega/\omega_0$, $\omega_0 = \sqrt{M/K_0}$, and coefficients of Eq. (2.20) have the form:

Fig. 2.4 Dispersion curves of the discrete model
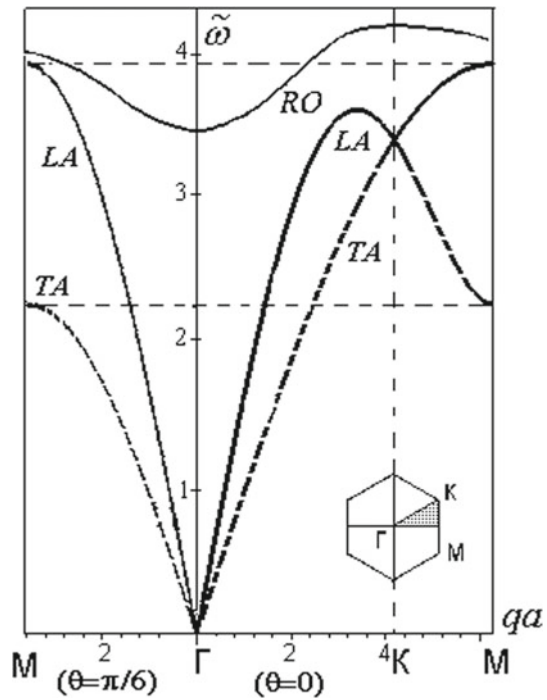
$$d_{11} = \frac{8}{a^2}\left[\gamma_1 \sin^2\left(\frac{qa}{2}\right) + \gamma_2\left(1 - \cos\left(\frac{qa}{2}\right)\right)\right],$$

$$d_{22} = \frac{8}{a^2}\left[2\gamma_3 \sin^2\left(\frac{qa}{2}\right) + \gamma_4\left(1 - \cos\left(\frac{qa}{2}\right)\right)\right],$$

$$d_{33} = \frac{8}{a^2}\left[8\gamma_5 + \frac{4a^2\gamma_3}{d^2} + \left(\gamma_6\sqrt{3} - \gamma_3\left(1 + \frac{2a}{d}\right)\right)\left(\sin^2\left(\frac{qa}{2}\right) - \cos\left(\frac{qa}{2}\right)\right)\right],$$

$$d_{23} = -\frac{d^2}{8}d_{32} = -i\frac{2\gamma_3}{a}\left(\sin\left(\frac{qa}{2}\right) + \sin(qa)\right). \tag{2.21}$$

From Eqs. (2.20) and (2.21), it follows that each wave mode has both minimum and maximum, which values depend on microstructure parameters. Thus, for example, along the Γ-K-axis the frequency of the longitudinal phonons has a local maximum $\omega_{LA}^{max} = \sqrt{2\left(4(\gamma_1 + \gamma_2) + \gamma_2^2/\gamma_1\right)/Ma^2}$ at the point $qa = 2(\pi - \arccos(\gamma_2/2\gamma_1))$ and the frequency of the rotational phonons has a local minimum $\omega_{RO}^{min} = \sqrt{8\left(8\gamma_5 + \gamma_3(1 + 2a/d + 4a^2/d^2) - \gamma_6\sqrt{3}\right)/Ma^2}$ at the point $q = 0$. Consequently, by varying the microstructure parameters (see Eq. (2.4)), it is possible to specify certain dispersion properties of the phonon crystal [23, 26].

Let us perform analysis of solutions of the dispersion Eq. (2.18) for the following values of the microstructure parameters: $d/a = 0.1$, $K_1/K_0 = 0.5$, $K_2/K_0 = 0.3$. The dispersion curves calculated along directions $\theta = 30°$ (Γ–K), $\theta = 30°$ (Γ–M) and along the boundary of the Brillouin zone (K–M) are shown in the dimensionless coordinates (qa, ϖ), where $\varpi = \omega/\omega_0$ and $\omega_0 = \sqrt{K_0/M}$, in Fig. 2.4.

From Fig. 2.4, it is visible that in the Γ-M-direction the frequencies of all three phonons increase monotonically, when the wavenumber grows, up to the boundary of the Brillouin zone. In the Γ-K-direction, the frequency of the longitudinal phonons has a local maximum $\varpi \approx 3.63$ located at the point $qa = 2\left(\pi - \text{arctg}\left(3\sqrt{7}\right)\right)$. In the interval $2\left(\pi - \text{arctg}\left(3\sqrt{7}\right)\right) < qa < 4\pi/3$, the group velocity of rotational phonons is negative: $v_{gr} = d\omega/dq < 0$. This area is called a *backward-wave region* [39]. Usually, a field of the negative group velocity exists for optical phonons in lattices with a complex structure, when more than one particle is present in the Bravais lattice [43]. Here, a similar situation takes place for acoustic phonons in a simple lattice. The presence of a backward wave in a medium is associated with the phenomenon of negative refraction provided that the surface of equal frequencies is convex. The longitudinal mode has the maximum frequency $\varpi \approx 3.93$ that is achieved on the boundary of the first Brillouin zone at point M ($qa = 2\pi/\sqrt{3}$). At this point, the group velocity is equal to zero and therefore a signal with such a frequency cannot propagate in a crystal lattice. This restriction can be dropped only for nonlinear perturbations [37], when anharmonic terms are taken into account in equations of motion (2.5). The frequency of the transverse phonons has the maximal value $\varpi \approx 3.36$ at the point K. The rotational (optical) mode has two threshold frequencies: the minimum $\varpi(0) \approx 3.45$ and maximum $\varpi \approx 4.18$ ones. In the frequency range $0 \leq \varpi \leq 3.36$, the system has *LA*- and *TA*-modes. In the interval

<center>**LA - mode**   **TA – mode**   **RO – mode**</center>
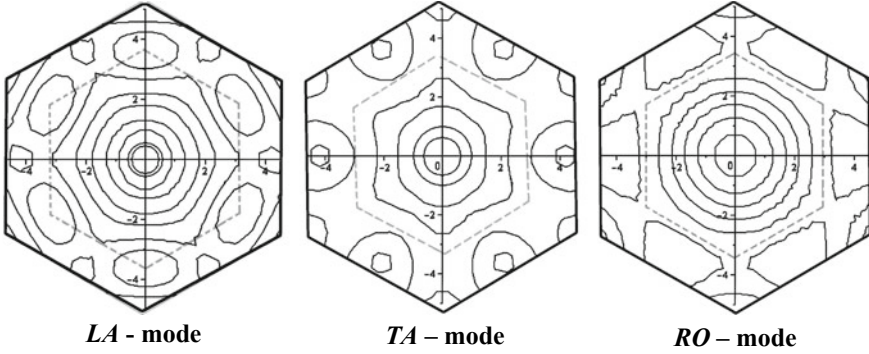
Fig. 2.5 Maps of equal frequencies of acoustic and optical phonons

$3.36 < \varpi < 3.45$ there is only a longitudinal mode and for frequencies $3.45 \leq \varpi \leq 3.93$ there are longitudinal and rotational modes. And, finally, in the high-frequency range $3.93 < \varpi \leq 4.18$, only the rotational mode is present in the system (Fig. 2.4).

Figure 2.5 shows maps of equal frequencies for longitudinal, transverse, and rotational phonons (for *LA*-mode $\varpi = 1.0, 1.5, 2.1, 2.7, 3.0, 3.3, 3.6, 3.8$, for *TA*-mode $\varpi = 0.7, 1.0, 1.5, 2.1, 2.7, 3.0$, and for *RO*-mode $\varpi = 3.65, 3.75, 3.85, 3.95, 4.05, 4.15$) [44]. The horizontal axis represents the projection q_x, of the wave vector, and along the vertical axis—q_y. The boundaries of the first Brillouin zone are indicated by a dashed line.

Figure 2.5 shows that lines of equal frequencies are circles for small values of the wavenumber. Hence, the crystal structure behaves like an isotropic medium in the long-wavelength range. However, when the wavelength decreases (the magnitude of the wave vector increases); the properties of acoustic anisotropy begin to appear. In this case, the transverse waves become anisotropic ones faster than the longitudinal waves do. For a certain frequency, the map of equal frequencies of each mode reproduces completely the structure of the hexagonal lattice at issue.

2.4.2 Dispersion Properties of the Continual Model

After consideration of the dispersion properties of the discrete model, let us analyze the dispersion properties of the continual model. We will seek solutions to Eqs. (2.8) in the form of plane harmonic waves

$$(u, w, \varphi)^T = (A_u, A_w, A_\varphi)^T \exp[i(\omega t - \mathbf{k} \cdot \mathbf{r})], \qquad (2.22)$$

where A_u, A_w, and A_φ are the complex amplitudes of the harmonic waves; ω is the oscillation frequency; and $\mathbf{k} = \{k_x, k_y\}$ is the wave vector. Substitution of expressions (2.22) into Eq. (2.8) yields a system of equations for the amplitudes A_u, A_w, and A_φ.

By setting the determinant of its matrix to zero, we obtain the dispersion relation:

$$\begin{vmatrix} -\omega^2 + c_1^2 k_x^2 + c_2^2 k_y^2 & s^2 k_x k_y & -i\beta k_y \\ s^2 k_x k_y & -\omega^2 + c_2^2 k_x^2 + c_1^2 k_y^2 & i\beta k_x \\ i\beta k_y & -i\beta k_x & R^2(-\omega^2 + c_3^2 k^2 + \omega_0^2) \end{vmatrix} = 0. \quad (2.23)$$

After calculating the determinant, Eq. (2.23) takes on the form:

$$\omega^6 - H_1 \omega^4 + H_2 \omega^2 + H_3 = 0. \quad (2.24)$$

Here, the coefficients H_1, H_2, and H_3 depend on the scalar square of the wave vector $k^2 = k_x^2 + k_y^2$ (i.e., k is the wavenumber) as follows [18, 26]:

$$H_1 = (c_1^2 + c_2^2 + c_3^2)k^2 + \omega_0^2,$$
$$H_2 = (c_1^2 c_2^2 + c_1^2 c_3^2 + c_2^2 c_3^2)k^4 + ((c_1^2 - c_2^2)^2 - s^4)k_x^2 k_y^2 + \omega_0^2(c_1^2 + c_2^2 - \beta/2)k^2,$$
$$H_3 = \omega_0^2 c_1^2(\beta/2 - c_2^2)k^4 + \omega_0^2[\beta(c_2^2 - c_1^2 + s^2) - (c_1^2 - c_2^2)^2 + s^4]k_x^2 k_y^2$$
$$- c_1^2 c_2^2 c_3^2 k^6 + c_3^2(s^4 - (c_1^2 - c_2^2)^2)k^2 k_x^2 k_y^2. \quad (2.25)$$

Transformation into the polar coordinate system $k_x = k\cos\theta$ and $k_y = k\sin\theta$ yields $k_x^2 k_y^2 = \frac{k^4}{4}\sin^2 2\theta$. It is necessary to note that equality $c_1^2 - c_2^2 = s^2$ is valid for the hexagonal lattice, and coefficients of the $k_x^2 k_y^2$ term are equal to zero in this case. This fact indicates isotropy of the medium with hexagonal symmetry. For an isotropic medium, the dispersion Eq. (2.25) can be written in a much simpler form:

$$(\omega^2 - c_1^2 k^2)[R^2(\omega^2 - c_2^2 k^2)(\omega^2 - c_3^2 k^2 - \omega_0^2) - \beta^2 k^2] = 0. \quad (2.26)$$

It is also possible to derive the same equation by consideration of the wave propagating only along the axis of symmetry, when $\theta = 0$ (i.e., $k = k_x$) [45]. Dispersion curves determined by Eq. (2.26) are represented in the normalized form (in $(k/k_0, \omega/\omega_0)$-coordinates, where $k_0 = \omega_0/c_2$) in Fig. 2.6, where L, T, and R indicate the longitudinal, transverse, and rotational modes, respectively. The graphics have been plotted for numerical data corresponding to cadmium crystals: $c_1/c_2 = 1.80$, $c_3/c_2 = 0.69$, $\omega_0 d/c_2 = 1.34$ (see Sect. 4.1).

It follows from Eq. (2.26) and Fig. 2.6 that the dispersion properties of Eq. (2.8) are independent of the wave propagation direction, i.e., in the continuous approximation, the crystal structure is isotropic. The curves for the R- and T-modes have oblique asymptotes $\omega = \pm c_2 k$ and $\omega = \pm c_3 k$, respectively.

Equation (2.26) also yields expressions that relate the phase velocity $v = \omega/k$ to the wavenumber k [26]:

$$(v^2 - c_1^2)[R^2(v^2 - c_2^2)(v^2 - c_3^2 - \omega_0^2/k^2) - \beta^2/k^2] = 0. \quad (2.27)$$

Equation (2.27) specifies the following dispersion curves

Fig. 2.6 Dispersion curves
for the hexagonal lattice
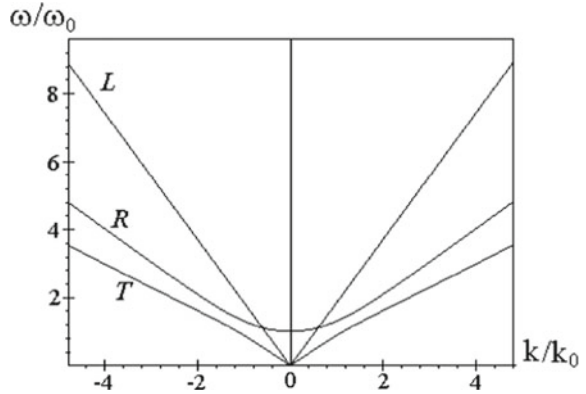
$$v^2 = \frac{1}{2}\left[c_2^2 + c_3^2 + \frac{\omega_0^2}{k^2} \pm \sqrt{\left(c_2^2 - c_3^2 - \frac{\omega_0^2}{k^2}\right)^2 + \frac{\omega_0^4 d^2}{8k^2}}\right] \qquad (2.28)$$

presented in the normalized form in Fig. 2.7 in the coordinate system $(k/k_0, \ v/v_0)$, where $v_0 = \omega_0/k_0$ (the curves for negative v are symmetric to these curves with respect to the axis k). It follows from (2.28) that, as $k \to \infty$, $v^2 \to \frac{1}{2}(c_2^2 + c_3^2 \pm (c_2^2 - c_3^2))$, i.e., phase velocities of the R- and T-modes have horizontal asymptotes $v = \pm c_2$ and $v = \pm c_3$, accordingly. Phase velocity of the R-mode also has a vertical asymptote $k = 0$, whereas the phase velocity of the T-mode takes at $k = 0$ the maximum value—$v = c_2$. As $d \to 0$ $v^2 \to \frac{1}{2}\left(c_2^2 + c_3^2 + \frac{\omega_0^2}{k^2} \pm \left(c_2^2 - c_3^2 - \frac{\omega_0^2}{k^2}\right)\right)$, i.e., in a medium consisting of material points, the phase velocity of the R-mode has the form of horizontal curves $v = \pm c_2$, while the phase velocity of the T-mode has the form $v(k) = \pm c_3\sqrt{1 + \omega_0^2/c_3^2 k^2}$.

Equation (2.27) yields the following relation between complex amplitudes of the transverse and rotational waves [26]:

Fig. 2.7 Phase velocities of
normal waves as a function
of wavenumber at the same
parameters as shown in
Fig. 2.6
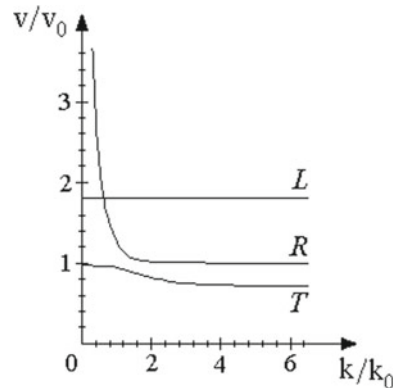
Fig. 2.8 Amplitude ratio of the transverse and rotational oscillations in the normal modes as a function of dimensionless frequency
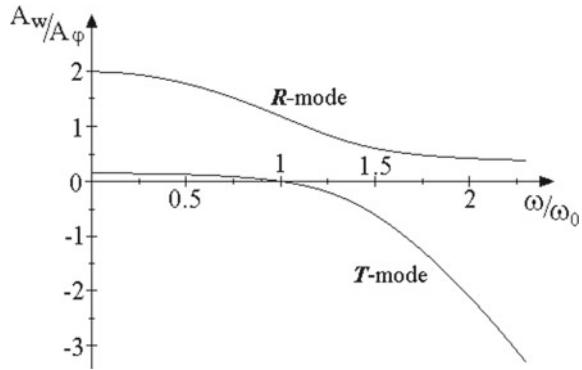
$$\left(\frac{RA_\varphi}{A_w}\right)_{\omega_j(k)} = i\,\frac{R(c_2^2 k^2 - \omega_j^2(k))}{\beta k} \equiv i\,\frac{\beta k}{R(c_3^2 k^2 + \omega_0^2 - \omega_j^2(k))} = i\,g\big(\omega_j(k), k\big),$$

where $g\big(\omega_j(k), k\big)$ is the distribution factor of the transverse and rotational oscillations in the normal modes. Frequency behavior of this coefficient is shown in Fig. 2.8.

Curves R and T characterize the relative contribution of rotational oscillations to the transverse (T) and rotational (R) normal modes of the system. From Fig. 2.8, it is visible that in the interval of low frequencies $\omega/\omega_0 < 0.6$, transverse motion prevails in the T-mode, while in the region of high frequencies $\omega/\omega_0 > 2$, the rotational motion becomes dominating. In other words, at long wavelengths, the T-mode is a purely transverse wave. As the wavelength becomes shorter, it increasingly degenerates into the microrotation wave. In the neighborhood of the synchronism point $\omega_0 = 1$, contributions of both types of waves to the T-mode are approximately the same. The R-mode is a propagating wave at high frequencies $\omega/\omega_0 > 1$. At long wavelengths, the R-mode is mostly a wave of microrotations; at short wavelengths, a transverse wave. Thus, the transverse and rotational waves retain their identity only far from the synchronism point. In its neighborhood, they cannot be separated and must be regarded as a coupled state [34].

2.5 Conclusions

In this chapter, the discrete and continual models have been elaborated that describe the dynamics of a hexagonal lattice of circular particles with a quadratic potential of interaction between them. These models can be used to study the physicomechanical properties of photonic crystals, for example, synthetic opals based on silicon, which consist of spherical particles with a diameter of 200–1000 nm forming a close-packed lattice [32].

The transition from a discrete model to a continuum model makes sense when long-wavelength processes are studied [46–48]. In this case, it also becomes possible to compare the obtained model with well-known continual theories. But if we study short-wavelength processes, it is necessary either to remain within the scope of a discrete model, or to pass to generalized continua, for example, in the framework of the multifield approach [49–52] or on the basis of Pade-approximations [53].

In the framework of the models elaborated in this chapter, the dependences of the elastic wave velocities and the dispersion parameter on the particle size and the parameters of the interactions between them have been found in an analytical form.

Dispersion properties of such a medium have been analyzed for some values of the microstructure parameters. The analysis showed that if in the long-wavelength (continuum) approximation (when the characteristic length of an acoustic wave is much larger than the lattice period) the hexagonal lattice with round particles is isotropic in terms of acoustic properties, then in the short-wavelength (discrete) approximation it is anisotropic, and the transverse waves become anisotropic ones faster than the longitudinal waves do.

In the discrete model, all three wave models have two threshold frequencies: maximum and minimum. In the ranges of low ($0 \leq \varpi < 2.33$) and high ($2.98 < \varpi \leq 3.28$) frequencies, there are two wave modes in the system, whereas for $2.33 < \varpi \leq 2.98$, all three wave modes (longitudinal, transverse, and rotational) are present in the system. The greatest value of the frequency of longitudinal phonons is reached at the boundary of the Brillouin zone at the point M ($q = 2\pi \left/ (a\sqrt{3})\right.$). Moreover, in the discrete model, there exists a backward wave, i.e., the wave whose phase and group velocities are oppositely directed.

In the continuum approximation, all three wave modes increase indefinitely, and the transverse and rotational modes have oblique asymptotes. The rotational wave possesses dispersion of the wave-guide (Klein-Gordon) type, and therefore c_3 represents an asymptotic value of the phase and group velocities of the wave for large frequencies. Analysis of the amplitude ratio of the transverse and rotational oscillations in normal modes showed that the transverse and rotational waves retain their identity only far from the synchronism point. In its neighborhood, they cannot be separated and must be regarded as a coupled state.

References

1. Belyaeva, I.Y., Zaitsev, V.Y., Ostrovsky, L.A.: Nonlinear acoustical properties of granular media. Acoust. Phys. **39**, 11–16 (1993)
2. Bykov, V.G.: Solitary shear waves in a granular medium. Acoust. Phys. **45**(2), 138–142 (1999)
3. Goldstein, R.V., Gorodtsov, V.A., Lisovenko, D.S.: Young's moduli and Poisson's ratio of curvilinear anisotropic hexagonal and rhombohedral nanotubes. Nanotubes-auxetics. Dokl. Phys. **58**(9), 400–404 (2013)
4. Chang, C.S., Gao, J.: Wave propagation in granular rod using high-gradient theory. J. Engn. Mech.-ASCE 1, 52–59 (1997)

5. Chang, C.S., Ma, L.: A micromechanical-based micropolar theory for deformation of granular solids. Int. J. Solids Struct. **28**(1), 67–87 (1994)

6. Christoffersen, J., Mehrabadi, M.M., Nemat-Nasser, S.A.: A micromechanical description of granular material behavior. Trans. ASME J. Appl. Mech. **48**(2), 339–344 (1981)

7. Lisina, S.A., Potapov, A.I., Nesterenko, V.F.: Nonlinear granular medium with rotations of the particles one-dimensional model. Phys. Acoust. **47**(5), 666–674 (2001)

8. Pavlov, I.S., Potapov, A.I., Maugin, G.A.: A 2D Granular Medium With Rotating particles. Int. J. Solids Struct. **43**(20), 6194–6207 (2006)

9. Sadovskaya, O., Sadovskii, V.: Mathematical modeling in mechanics of granular materials. Springer, Heidelberg, New York, Dordrecht, London, 390 p (2012)

10. Krivtsov, A.M., Podol'skaya E.A.: Modeling of elastic properties of crystals with hexagonal close-packed lattice. Mech. Solids. **45**(3), 370–378 (2010)

11. Krivtsov, A.M.: Deformation and destruction of microstructured solids. Fizmatlit Publ., Moscow, 304 p (2007). (in Russian)

12. Askar, A.: Lattice Dynamics Foundation of Continuum Theory. World-Scientific, Singapore (1985)

13. Berglund K.: Structural models of micropolar media. In: Mechanics of Micropolar Media. Brulin, O., Hsieh, R.K.T. (eds.) World Scientific, Singapore, pp. 35–86 (1982)

14. Ostoja-Starzewski, M., Sheng, P.Y., Alzebdeh, K.: Spring network models in elasticity and fracture of composites and polycrystals. Comput. Mater. Sci. **7**, 82–93 (1996)

15. Pavlov, I.S.: Acoustic Identification of the anisotropic nanocrystalline medium with non-dense packing of particles. Acoust. Phys. **56**(6), 924–934 (2010)

16. Pavlov, I.S., Vasiliev, A.A., Porubov, A.V.: Dispersion properties of the phononic crystal consisting of ellipse-shaped particles. J. Sound Vibr. **384**, 163–176 (2016)

17. Pavlov, I.S., Potapov, A.I.: Structural Models in Mechanics of Nanocrystalline Media. Dokl. Phys. **53**(7), 408–412 (2008)

18. Potapov, A.I., Pavlov, I.S., Lisina, S.A.: Acoustic identification of nanocrystalline media. J. Sound Vib. **322**(3), 564–580 (2009)

19. Suiker, A.S.J., Metrikine, A.V., de Borst, R.: Comparison of wave propagation characteristics of the Cosserat continuum model and corresponding discrete lattice models. Int. J. Solids Struct. **38**, 1563–1583 (2001)

20. Suiker, A.S.J., Metrikine, A.V., de Borst, R.: Dynamic behaviour of a layer of discrete particles. Part 1: analysis of body waves and eigenmodes. J Sound Vib. **240**(1), 1–18 (2001)

21. Vasiliev, A.A., Pavlov, I.S.: Auxetic properties of hiral hexagonal cosserat lattices composed of finite-sized particles. Phys. Status Solidi B **3**(257), 1900389 (2020). https://doi.org/10.1002/pssb.201900389

22. Vasiliev, A.A., Pavlov, I.S.: Models and some properties of Cosserat triangular lattices with chiral microstructure. Lett. Mater. **9**(1), 45–50 (2019) www.lettersonmaterials.com, https://doi.org/10.22226/2410-3535-2019-1-45-50

23. Erofeev, V.I., Pavlov, I.S., Vasiliev, A.A., Porubov, A.V.: Dispersion properties of a closed-packed lattice consisting of round particles. In: Altenbach, H., et al. (eds.) Generalized Models and Non-classical Approaches in Complex Materials 2, Advanced Structured Materials 90. © Springer International Publishing AG, part of Springer Nature 2018, pp. 101–117

24. Sedov, L.I.: Models of continuous media with internal degrees of freedom. J. Appl. Math. Mech. **32**(5), 803–819 (1968)

25. Sedov, L.I.: Mechanics of continuous medium. World Scientific Publ, Singapore, vol. 1, (1997)

26. Potapov, A.I., Pavlov, I.S., Maugin, G.A.: Nonlinear wave interactions in 1D crystals with complex lattice. Wave Motion **29**, 297–312 (1999)

27. Bogomolov, V.N., Parfen'eva, L.S., Smirnov, I.A., Misiorek, H., Jzowski, A.: Phonon propagation through photonic crystals—media with spatially modulated acoustic properties. Phys. Solis State **44**, 181–185 (2002)

28. Vetrov, S.Y., Timofeev, I.V., Rudakova, N.V.: Band structure of a two-dimensional resonant photonic crystal. Phys. Solid State **52**, 527–532 (2010)

29. Yablonovitch, E., Gmitter, T.J., Leung, K.M.: Photonic band structure: The face-centered cubic case employing nonspherical atoms. Phys. Rev. Lett. **67**, 2295 (1991)
30. Fujii, M., Kanzaea, Y., Hayashi, S., Yamamoto, K.: Raman scattering from acoustic phonons confined in Si nanocrystals. Phys Rev. B **54**, R8373 (1996)
31. Kushwaha, M.S., Halevi, P., Martinez, G., Dobrzynski, L., Djafari-Rouhani, B.: Theory of band structure of periodic elastic composites. Phys. Rev. B **49**, 2313 (1994)
32. Samusev, K.B., Rybin, M.V., Limonov, M.F., Yushin, G.N.: Structural parameters of synthetic opals: statistical analysis of electron microscopy images. Phys. Solid State **50**(7), 1280–1286 (2008)
33. Stroscio, M.A., Dutta, M.: Phonons in nanostructures. Cambridge University Press, 274 p (2001)
34. Pierce, J.R., Almost All about Waves, Dover Publications (2006)
35. Normal waves. In: Prokhorov, A.M., (ed.) The physical encyclopedia in 5 volumes. The Big Russian encyclopedia, Moscow, vol. 3. p. 360 (1992). (in Russian)
36. Ostrovsky, L.A., Papko, V.V., Pelinovsky, E.N.: Solitary electromagnetic waves in nonlinear lines. Radiophys. Quantum Electron. **15**, 438–446 (1972)
37. Ostrovsky, L.A., Potapov, A.I.: Modulated waves: theory and applications. The Johns Hopkins University Press, Baltimore, MD (1999)
38. Vinogradova, M.B., Rudenko, O.V., Sukhorukov, A.P.: Theory of Waves. Nauka, Moscow (1990). (in Russian)
39. Kittel, C.: Introduction to Solid State Physics. 8th edn. Wiley, Inc., (2005)
40. Kaganov, M.I.: Electrons, Phonons, Magnons, 268 pp. English Translation. Mir Publishers, Moscow (1981)
41. Nikitenkova, S.P., Potapov, A.I.: Dispersion properties of two-dimensional phonon crystals with a hexagonal structure. Acoust. Phys. **56**(6), 909–918 (2010)
42. Potapov, A.I., Pavlov, I.S., Nikitenkova, S.P., Shudyaev, A.A.: Structural models in nanoacoustics: control of dispersion properties of phonon crystals. Acoustics of inhomogeneous media. In: Proceedings of the Russian acoustic society, GEOS, Moscow, no 10, pp. 9–16 (2009). (in Russian)
43. Reisland, J.A.: Physics of Phonons. Wiley, London, New York, Sydney, Toronto (1973)
44. Porubov, A.V., Krivtsov, A.M., Osokina, A.E.: Two-dimensional waves in extended square lattice. Int. J. Non-Linear Mech. **99**, 281–287 (2018) (без ротационных степеней, учет нелокальности, дискретная модель)
45. Potapov, A.I., Pavlov, I.S., Lisina, S.A.: Identification of nanocrystalline media by acoustic spectroscopy methods. Acoust. Phys. **56**(4), 588–596 (2010)
46. Berryman, J.G.: Long-wavelength propagation in composite elastic media I, II. J. Acoust. Soc. Am. **68**(6), 1809–1831 (1980)
47. Goldshtein, R.V., Chentsov, A.V.: A discrete-continual model for a nanotube. Mech. Solids **4**, 57–74 (2005)
48. Porubov, A.V., Aero, E.L., Maugin, G.A.: Two approaches to study essentially nonlinear and dispersive properties of the internal structure of materials. Phys. Rev. E79. 046608 (2009)
49. Vasiliev, A.A., Dmitriev, S.V., Miroshnichenko, A.E.: Multi-field approach in mechanics of structural solids. Int. J. Solids Struct. **47**, 510–525 (2010)
50. Vasiliev, A.A, Dmitriev, S.V., Miroshnichenko, A.E.: Multi-field continuum theory for medium with microscopic rotations. Int. J. Solids Struct. **42**, pp. 6245–6260 (2005)
51. Vasiliev, A.A., Miroshnichenko A.E., Ruzzene, M.: Multifield model for Cosserat media. J. Mech. Mater. Struct. **3**(7), 1365–1382 (2008)
52. Vasiliev, A.A., Miroshnichenko A.E., Dmitriev, S.V.: Multi-field modeling of a cosserat lattice: models, wave filtering, and boundary effects. Eur. J. Mech. A/Solids. **46**, 96–105 (2014)
53. Andrianov, I.V., Kholod, E.G., Weichert, D.: Application of quasi-continuum models for perturbation analysis of discrete kinks. Nonlinear Dyn. **68**, 1–5 (2012)

Chapter 3
A Two-Dimensional Lattice with Non-dense Packing of Particles

In this chapter, we consider a model of a granular medium as a rectangular lattice of rigid ellipse-shaped particles. Each particle of such a lattice possesses two translational and one rotational degrees of freedom. The space between the particles is a massless medium through which the force and coupled interactions are transmitted. In limiting cases, this model degenerates either into a chain of ellipse-shaped particles or into a square lattice of round particles. The main objectives of this chapter are to derive dynamic equations of a granular medium consisting of anisotropic particles and to identify the relationships between the physicomechanical properties of a granular material and the parameters of its microstructure. Using the results obtained in the chapter, it is possible to determine the elastic properties of an anisotropic nanocrystalline (granular) material with non-dense packing of particles by measuring the velocities of elastic waves propagating along different crystallographic directions [1].

3.1 The Discrete Model for an Anisotropic Medium Consisting of Ellipse-Shaped Particles

As a model of a medium with non-dense packing of particles, let us consider a two-dimensional rectangular lattice consisting of homogeneous particles (grains or granules) with masses M having the form of an ellipse with axis lengths equal to d_1 and d_2. In the initial state, they are located in the lattice sites and the distance between the mass centers of the neighboring granules along the x-axis is denoted by a, while b corresponds to the distance along the y-axis; see Fig. 3.1. Each particle, when it moves in its plane, has three degrees of freedom: the displacement of the mass center of the particle with the number $N = N(i, j)$ along the axes x and y (translational
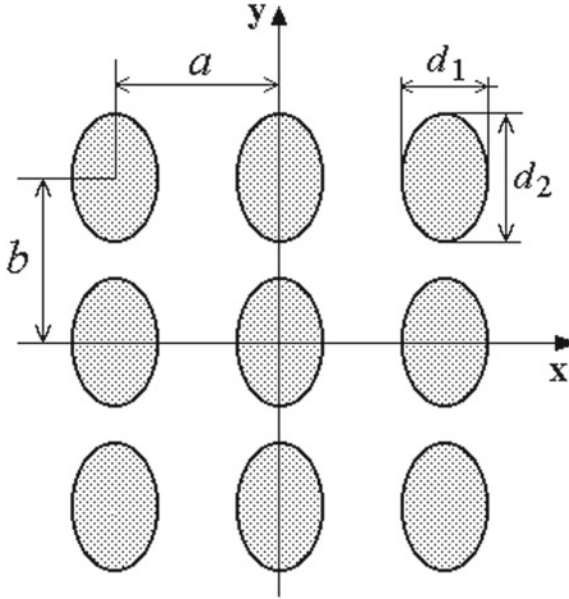
Fig. 3.1 Rectangular lattice consisting of ellipse-shaped particles

degrees of freedom $u_{i,j}$ and $w_{i,j}$) and the rotation with respect to the mass center (the rotational degree of freedom $\varphi_{i,j}$) (Fig. 3.2). The kinetic energy of the particle $N(i, j)$, as in the model of a medium with dense packing, is described by Eq. (2.1), but the moment of inertia of the particle about the axis passing through its mass center is equal to $J = M(d_1^2 + d_2^2)/16$.

It is assumed that the particle N interacts only with eight nearest neighbors in the lattice. The distance between mass centers of four of them and the considered particle is equal to a along x-axis and is equal to b along y-axis (these are the particles of the first coordination sphere). The mass centers of the other four lie at the diagonals of the rectangular lattice (these are the particles of the second coordination sphere); see Fig. 3.2. The central and non-central interactions of the neighboring granules are simulated by elastic springs of four types [2–5]. The springs of the first three types (with rigidity K_0, K_1, and K_2) were also present in the medium with dense packing of particles (see Chap. 2). The springs of the fourth type—with rigidity K_3—simulate the interaction with the grains of the second coordination sphere. The points of junctions of the springs with the particles are in the apexes of the rectangle of the maximum area inscribed in the ellipse (Fig. 3.2). Each rectangle has the size $h_1 \times h_2$, where $h_1 = d_1/\sqrt{2}$ and $h_2 = d_2/\sqrt{2}$.

The displacements of the granules are supposed to be small in comparison with the sizes of the elementary cell of the lattice. Interactions of the particles when they deviate from the equilibrium states are determined by relative elongations of the springs (Fig. 3.2). The potential energy provided by the interaction of the particle $N(i, j)$ with eight nearest neighbors in the lattice equals

$$U_N = \frac{1}{2}\left(\frac{K_0}{2} \sum_{n=1}^{4} D_{0n}^2 + \frac{K_1}{2} \sum_{n=1}^{8} D_{1n}^2 + \frac{K_2}{2} \sum_{n=1}^{8} D_{2n}^2 + \frac{K_3}{2} \sum_{n=1}^{4} D_{3n}^2 \right), \quad (3.1)$$

where D_{ln} ($l = 0, 1, 2, 3$) are the elongations of the springs with rigidity K_0, K_1, K_2, and K_3, respectively. The springs are numbered in the arbitrary order and connect the considered particle with its neighbors. The elongations of the central springs are determined by the changes of the distances between the geometrical centers of the rectangles inscribed in the ellipses (Fig. 3.2), and the tensions of other springs are characterized by the variations of the distances between the apexes of these rectangles. Expression (3.1), similar to Eq. (2.2), contains an additional factor 1/2, since the potential energy of each spring is equally divided between two particles connected by this spring.

We denote $\Delta u_i = u_{i,j} - u_{i-1,j} = \Delta u_{-10}$ and $\Delta u_j = u_{i,j} - u_{i,j-1} = \Delta u_{0-1}$, then $\Delta u_{i+1} = u_{i+1,j} - u_{i,j} = \Delta u_{10}$ and $\Delta u_{j+1} = u_{i,j+1} - u_{i,j} = \Delta u_{01}$. In addition, $\Phi_{m_1 m_2} = (\varphi_{i,j} + \varphi_{i+m_1,j+m_2})/2$, where m_1 and m_2 can take values 0, 1, or -1. Therefore, $\Phi_{-10} = (\varphi_{i-1,j} + \varphi_{i,j})/2 = \varphi_{i,j} - (\varphi_{i,j} - \varphi_{i-1,j})/2 = \varphi_{i,j} - \Delta\varphi_i/2$ and $\Phi_{10} = (\varphi_{i+1,j} + \varphi_{i,j})/2 = \varphi_{i,j} + (\varphi_{i+1,j} - \varphi_{i,j})/2 = \varphi_{i,j} + \Delta\varphi_{i+1}/2$.
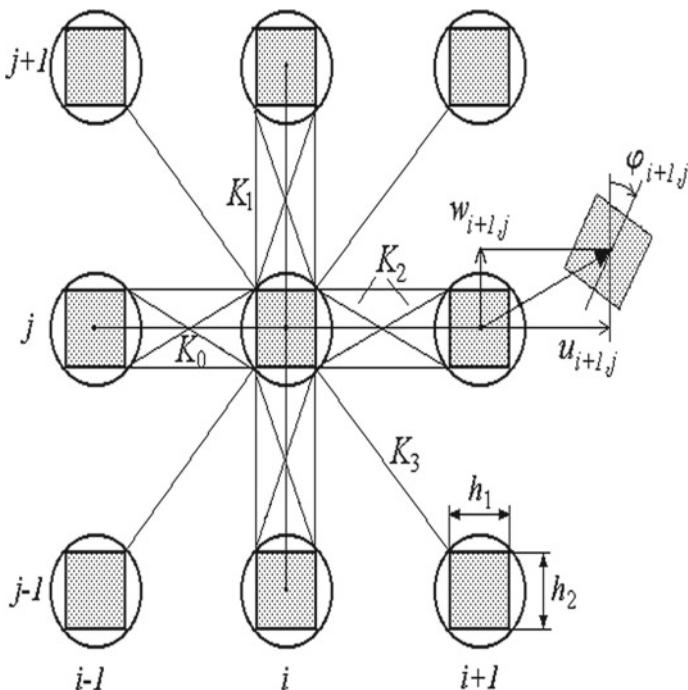

Fig. 3.2 Scheme of the force interactions between the particles and introduced notations

The expressions for the elongations of the springs, which have been calculated for small quantities $\Delta u_i \sim \Delta w_i \sim a\varepsilon$, $\Delta u_j \sim \Delta w_j \sim b\varepsilon$, $\Phi_{m_1 m_2} \sim \varepsilon << \pi/2$, where ε is a measure of the cell deformation, are given in Appendix B; see Eq. (B.2). If in Eq. (B.2) to take into account only linear terms for spring extensions, then it is possible to obtain the following formula for the potential energy per particle numbered as $N = N(i, j)$, up to quadratic terms (cubic terms are taken into account in Chap. 5) [6]:

$$
\begin{aligned}
U_N = {} & \frac{K_0}{2}\left(\Delta u_{10}^2 + \Delta u_{-10}^2 + \Delta w_{01}^2 + \Delta w_{0-1}^2\right) \\
& + K_1\left(\Delta u_{10}^2 + \Delta u_{-10}^2 + \Delta w_{01}^2 + \Delta w_{0-1}^2 + \frac{h_2^2}{4}\left(\Delta\varphi_{10}^2 + \Delta\varphi_{-10}^2\right)\right. \\
& + \frac{h_1^2}{4}\left(\Delta\varphi_{01}^2 + \Delta\varphi_{0-1}^2\right) \\
& + K_2\left(\frac{(a-h_1)^2}{r_1^2}\left(\Delta u_{10}^2 + \Delta u_{-10}^2\right) + \frac{h_1^2}{r_2^2}\left(\Delta u_{01}^2 + \Delta u_{0-1}^2\right)\right. \\
& + \frac{(b-h_2)^2}{r_2^2}\left(\Delta w_{01}^2 + \Delta w_{0-1}^2\right) \\
& + \frac{h_2^2}{r_1^2}\left(\Delta w_{10}^2 + \Delta w_{-10}^2\right) + \frac{a^2 h_2^2}{r_1^2}\left(\Phi_{10}^2 + \Phi_{-10}^2\right) + \frac{b^2 h_1^2}{r_2^2}\left(\Phi_{01}^2 + \Phi_{0-1}^2\right) \\
& + \frac{ah_2^2}{r_1^2}\left(\Delta w_{10}\Phi_{10} - \Delta w_{-10}\Phi_{-10}\right) + \frac{bh_1^2}{r_2^2}\left(-\Delta u_{01}\Phi_{01} + \Delta u_{0-1}\Phi_{0-1}\right)\right) \\
& + \frac{K_3}{2r_3^2}\left((a-h_1)^2\left(\Delta u_{11}^2 + \Delta u_{-1-1}^2 + \Delta u_{1-1}^2 + \Delta u_{-11}^2\right)\right. \\
& + (b-h_2)^2\left(\Delta w_{11}^2 + \Delta w_{-1-1}^2 + \Delta w_{1-1}^2 + \Delta w_{-11}^2\right) \\
& + (ah_2 - bh_1)^2\left(\Phi_{11}^2 + \Phi_{-1-1}^2 + \Phi_{1-1}^2 + \Phi_{-11}^2\right) \\
& + 2(a-h_1)(b-h_2)(\Delta u_{11}\Delta w_{11} + \Delta u_{-1-1}\Delta w_{-1-1} \\
& - \Delta u_{1-1}\Delta w_{1-1} - \Delta u_{-11}\Delta w_{-11}) \\
& + 2(a-h_1)(ah_2 - bh_1)(-\Delta u_{11}\Phi_{11} + \Delta u_{-1-1}\Phi_{-1-1} \\
& + \Delta u_{1-1}\Phi_{1-1} - \Delta u_{-11}\Phi_{-11}) \\
& + 2(b-h_2)(ah_2 - bh_1)(-\Delta w_{11}\Phi_{11} + \Delta w_{-1-1}\Phi_{-1-1} \\
& \left.- \Delta w_{1-1}\Phi_{1-1} + \Delta w_{-11}\Phi_{-11})\right).
\end{aligned}
\tag{3.2}
$$

Here, $r_1 = \sqrt{(a-h_1)^2 + h_2^2}$, $r_2 = \sqrt{(b-h_2)^2 + h_1^2}$, and $r_3 = \sqrt{(a-h_1)^2 + (b-h_2)^2}$ are the distances between the neighboring particles at the initial time moment along the x-axis, the y-axis, and the diagonal, respectively; see Fig. 3.2.

As for the model of a medium with a dense packing of the particles, one can obtain differential–difference equations similar to Eq. (2.4) from the Lagrange equations of the second kind (1.14) to describe the dynamics of the rectangular lattice with anisotropic particles in the linear approximation [6]:

$$
\begin{aligned}
M\ddot{u} &- B_1(u_{1,0} - 2u_{0,0} + u_{-1,0}) - 2B_2'(u_{0,1} - 2u_{0,0} + u_{0,-1}) \\
&- B_5(u_{1,1} + u_{-1,-1} + u_{1,-1} + u_{-1,1} - 4u_{0,0}) - B_4(w_{1,1} \\
&+ w_{-1,-1} - w_{1,-1} - w_{-1,1}) \\
&+ 2bB_2'(\varphi_{0,1} - \varphi_{0,-1}) + \frac{RB_6}{2}(\varphi_{1,1} - \varphi_{-1,-1} - \varphi_{1,-1} + \varphi_{-1,1}) = 0,
\end{aligned}
$$

$$
\begin{aligned}
M\ddot{w} &- B_1'(w_{0,1} - 2w_{0,0} + w_{0,-1}) - 2B_2(w_{1,0} - 2w_{0,0} + w_{-1,0}) \\
&- B_5'(w_{1,1} + w_{-1,-1} + w_{1,-1} + w_{-1,1} - 4w_{0,0}) \\
&- B_4(u_{1,1} + u_{-1,-1} - u_{1,-1} - u_{-1,1}) - 2aB_2(\varphi_{1,0} - \varphi_{-1,0}) \\
&- \frac{RB_6'}{2}(\varphi_{1,1} - \varphi_{-1,-1} + \varphi_{1,-1} - \varphi_{-1,1}) = 0,
\end{aligned}
\tag{3.3}
$$

$$
\begin{aligned}
MR\ddot{\varphi} &- RB_3(\varphi_{1,0} - 2\varphi_{0,0} + \varphi_{-1,0}) - RB_3'(\varphi_{0,1} - 2\varphi_{0,0} + \varphi_{0,-1}) \\
&+ \frac{a^2B_2}{R}(\varphi_{1,0} + 2\varphi_{0,0} + \varphi_{-1,0}) + \frac{b^2B_2'}{2R}(\varphi_{0,1} + 2\varphi_{0,0} + \varphi_{0,-1}) \\
&+ RB_7(\varphi_{1,1} + \varphi_{-1,-1} + \varphi_{1,-1} + \varphi_{-1,1} + 4\varphi_{0,0}) \\
&- \frac{bB_2'}{R}(u_{0,1} - u_{0,-1}) - \frac{B_6}{2}(u_{1,1} - u_{-1,-1} - u_{1,-1} + u_{-1,1}) \\
&+ \frac{aB_2}{R}(w_{1,0} - w_{-1,0}) - \frac{B_6'}{2}(w_{1,1} - w_{-1,-1} + w_{1,-1} - w_{-1,1}) = 0.
\end{aligned}
$$

Here, $R = \sqrt{J/M} = \sqrt{d_1^2 + d_2^2}/4$ is the radius of inertia of the microparticles of the medium with respect to the mass center (obviously, $R = d/\sqrt{8}$ for the round particles with the diameter $d = d_1 = d_2$) and, for brevity, designations u_{m_1,m_2}, w_{m_1,m_2}, and φ_{m_1,m_2} are used instead of quantities $u_{i+m_1,j+m_2}$, $w_{i+m_1,j+m_2}$, and $\varphi_{i+m_1,j+m_2}$, where $m_1 = 0, \pm1$ and $m_2 = 0, \pm1$. Equations (3.3) can be used for numerical simulation of the response of the system to the external dynamic effects in a wide range of frequencies up to the threshold values. The coefficients in Eq. (3.3) have the form:

$$
B_1 = K_0 + 2K_1 + 2K_2\frac{(a - h_1)^2}{r_1^2}, \quad B_1' = K_0 + 2K_1 + 2K_2\frac{(b - h_2)^2}{r_2^2},
$$

$$
B_2 = K_2\frac{h_2^2}{r_1^2}, \quad B_2' = K_2\frac{h_1^2}{r_2^2}, \quad B_3 = \frac{K_1h_2^2}{2R^2}, \quad B_3' = \frac{K_1h_1^2}{2R^2}
$$

$$
B_4 = K_3\frac{(a - h_1)(b - h_2)}{r_3^2},
$$

$$B_5 = K_3 \frac{(a-h_1)^2}{r_3^2}, \; B_5' = K_3 \frac{(b-h_2)^2}{r_3^2},$$

$$B_6 = K_3 \frac{(a-h_1)(ah_2-bh_1)}{Rr_3^2}, \; B_6' = K_3 \frac{(b-h_2)(ah_2-bh_1)}{Rr_3^2},$$

$$B_7 = K_3 \frac{(ah_2-bh_1)^2}{4R^2 r_3^2}. \tag{3.4}$$

Next, we shall consider more in detail a continuum approximation of the model at issue.

3.2 The Continuum Approximation

The transition to the continuum approximation is carried out according to the same procedure as in Sect. 2.2, with one exception: In Eq. (2.6), l_1 and l_2 denote shifts of the numbers of eight particles interacting with the central one. Obviously, $l_1 = 0, \pm 1$ and $l_2 = 0, \pm 1$. Then, if in expansions (2.6) only the rems of $O(a)$-order are taken into account, then the two-dimensional density of the Lagrange function, L, of the medium of anisotropic particles takes on the form:

$$L = \frac{\rho}{2} \left(u_t^2 + w_t^2 + R^2 \varphi_t^2 \right) - \frac{\rho}{2} [c_1^2 (u_x^2 + \delta_1 w_y^2) + c_2^2 (w_x^2 + \delta_2 u_y^2)$$
$$+ R^2 c_3^2 (\varphi_x^2 + \delta_3 \varphi_y^2) + s^2 (u_x w_y + \delta_4 u_y w_x) + 2\beta_1 (w_x - \delta_5 u_y)\varphi + 2\beta_2 \varphi^2]. \tag{3.5}$$

Using the Hamilton–Ostrogradsky variational principle, a set of the first approximation differential equations describing the dynamic processes in the anisotropic crystalline medium is deduced from Lagrangian (3.5) [2]:

$$u_{tt} = c_1^2 u_{xx} + \delta_2 c_2^2 u_{yy} + \frac{1+\delta_4}{2} s^2 w_{xy} - \delta_5 \beta_1 \varphi_y,$$

$$w_{tt} = c_2^2 w_{xx} + \delta_1 c_1^2 w_{yy} + \frac{1+\delta_4}{2} s^2 u_{xy} + \beta_1 \varphi_x,$$

$$\varphi_{tt} = c_3^2 (\varphi_{xx} + \delta_3 \varphi_{yy}) + \frac{\beta_1}{R^2}(\delta_5 u_y - w_x) - \frac{2\beta_2}{R^2}\varphi. \tag{3.6}$$

Here, the following notations are introduced: $c_1 = \sqrt{(B_1 + 2B_5)/\rho}$ is the longitudinal wave velocity, $c_2 = \sqrt{2(B_2 + B_5')/\rho}$ is the transverse wave velocity, $c_3 = \sqrt{(B_3 + a^2 B_2/(2R^2) + 2B_7)/\rho}$ is the rotational wave velocity, $s = 2\sqrt{B_4/\rho}$ is the coefficient of the linear coupling between the longitudinal and shift deformations in the material, $\beta_1 = 2(aB_2 + RB_6')/\rho a$ and $\beta_2 = (a^2 B_2 + b^2 B_2' + R^2 B_7)/\rho a^2$ are the dispersion parameters, $\rho = M/ab$ is the average value of the density of the studied two-dimensional medium, and $\delta_i (i = 1 \div 5)$ are the correction coefficients appearing due to the anisotropy of the studied medium:

$$\delta_1 = \frac{b^2 r_1^2}{a^2 r_2^2} \cdot \frac{r_2^2 r_3^2 (K_0 + 2K_1) + 2(b - h_2)^2 (r_3^2 K_2 + r_2^2 K_3)}{r_1^2 r_3^2 (K_0 + 2K_1) + 2(a - h_1)^2 (r_3^2 K_2 + r_1^2 K_3)},$$

$$\delta_2 = \frac{b^2 r_1^2}{a^2 r_2^2} \cdot \frac{h_1^2 r_3^2 K_2 + (a - h_1)^2 r_2^2 K_3}{h_2^2 r_3^2 K_2 + (b - h_2)^2 r_1^2 K_3},$$

$$\delta_3 = \frac{b^2 r_1^2}{a^2 r_2^2} \cdot \frac{h_1^2 r_2^2 r_3^2 K_1 + b^2 h_1^2 r_3^2 K_2 + (ah_2 - bh_1)^2 r_2^2 K_3}{h_2^2 r_1^2 r_3^2 K_1 + a^2 h_2^2 r_3^2 K_2 + (ah_2 - bh_1)^2 r_1^2 K_3}$$

$$\delta_4 = \frac{b^2}{a^2},$$

$$\delta_5 = \frac{b r_1^2}{a r_2^2} \cdot \frac{b h_1^2 r_3^2 K_2 + (a - h_1)(ah_2 - bh_1) r_2^2 K_3}{a h_2^2 r_3^2 K_2 + (b - h_2)(ah_2 - bh_1) r_1^2 K_3}. \tag{3.7}$$

In the case, when $\delta_i \neq 1$ at least for one i, Eq. (3.6) becomes non-invariant with respect to the rotation of the crystalline lattice by 90° and, therefore, they are a mathematical model of a strongly anisotropic medium [7]. If all anisotropy parameters δ_i are equal to 1, then Eq. (3.6) coincides with Eq. (2.8) for the hexagonal lattice of round particles with accuracy to coefficients.

3.2.1 Dependence of the Anisotropy of the Medium on Its Microstructure

The structural modeling allows one to establish the interrelation between the microstructure and the macroproperties of the medium. In mechanics, this refers, first of all, to the dependence of the anisotropy and moduli of macroelasticity of the medium on its geometrical structure. These problems remain open in the phenomenological theories.

It is seen from expressions (3.7) that the dependences of the anisotropy parameters δ_i on the microstructure parameters are rather complicated, since they contain four force constants (K_0, K_1, K_2, and K_3) and four geometrical parameters (a, b, h_1, and h_2). To simplify these expressions, we decrease the number of the geometrical parameters twice by assuming that the condition of similarity of the form of the particles to the lattice form holds

$$\frac{d_2}{d_1} = \frac{b}{a} \tag{3.8}$$

and introducing two new dimensionless quantities: $f = b/a = h_2/h_1$ is the *similarity coefficient* (or the *shape parameter*), and $p = d_1/a = h_1\sqrt{2}/a = h_2\sqrt{2}/b = d_2/b$ is the *relative particle size*. Then, we consider the analysis of the dependence of δ_i on these two quantities in more detail. Under these assumptions, Eq. (3.7) takes on the form [2]:
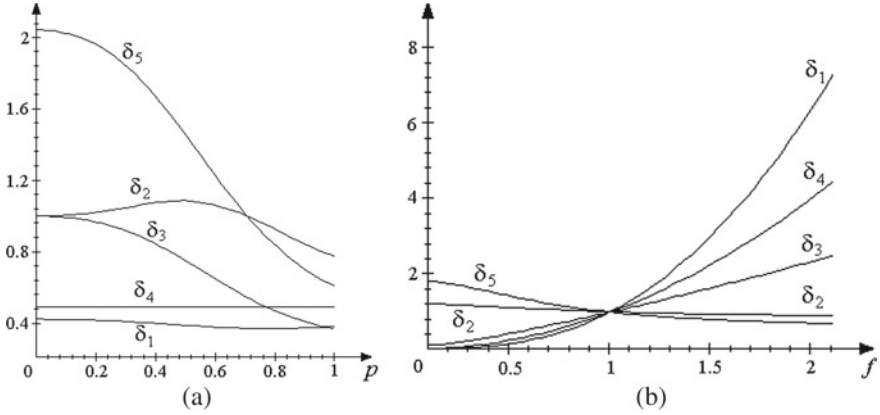
Fig. 3.3 Dependence of the anisotropy parameters δ_i on the relative particle size p (**a**) and on the shape parameter f (**b**)

$$\delta_1 = \frac{f^2 r_1^2}{r_2^2} \cdot \frac{r_2^2(K_0 + 2K_1) + f^2(\sqrt{2} - p)^2 a^2(K_2 + (r_2^2/r_3^2)K_3)}{r_1^2(K_0 + 2K_1) + (\sqrt{2} - p)^2 a^2(K_2 + (r_1^2/r_3^2)K_3)},$$

$$\delta_2 = \frac{p^2(r_3^2/r_2^2)K_2 + (\sqrt{2} - p)^2 K_3}{p^2(r_3^2/r_1^2)K_2 + (\sqrt{2} - p)^2 K_3}, \delta_3 = \frac{K_1 + (f^2 a^2/r_2^2)K_2}{K_1 + (a^2/r_1^2)K_2},$$

$$\delta_4 = f^2, \delta_5 = \frac{r_1^2}{r_2^2} = \frac{(\sqrt{2} - p)^2 + f^2 p^2}{f^2(\sqrt{2} - p)^2 + p^2}.$$

Here, $r_1/a = \sqrt{1 - p\sqrt{2} + p^2(f^2 + 1)/2}$, $r_2/a = \sqrt{f^2(1 - p\sqrt{2}) + p^2(f^2 + 1)/2}$, $r_3/a = \sqrt{(f^2 + 1)(\sqrt{2} - p)^2/2}$.

Figure 3.3a, b shows the dependences of δ_i ($i = 1, 2, 3, 4, 5$) on the relative particle size $0 \le p \le 1$ for $f = 0.7$ (Fig. 3.3a) and on the similarity coefficient f for $p = 0.6$ (Fig. 3.3b). In both figures, $K_1/K_0 = 0.1$, $K_2/K_0 = 0.3$, $K_3/K_0 = 0.5$. It can be seen from Fig. 3.3a, b that variation of f affects deviations of δ_i from 1 (i.e., increasing in the medium anisotropy) more significantly than variation of p. If $f = 1$, then all $\delta_i = 1$ and $\beta_1 = \beta_2$; i.e., Eq. (3.6) degenerates into Eq. (2.8), which, in turn, coincide with the equations of the Cosserat two-dimensional continuum consisting of the central-symmetric particles (see Sect. 4.3).

The coefficients of Eq. (3.6) are expressed in terms of the force constants K_0, K_1, K_2, K_3, the lattice parameters a and b, and the particle sizes h_1 and h_2 as follows:

$$c_1^2 = \frac{a^2}{M}\left(K_0 + 2K_1 + \frac{2(a - h_1)^2}{(a - h_1)^2 + h_2^2}K_2 + \frac{2(a - h_1)^2}{(a - h_1)^2 + (b - h_2)^2}K_3\right),$$

$$c_2^2 = \frac{2a^2}{M}\left(\frac{h_2^2}{(a - h_1)^2 + h_2^2}K_2 + \frac{(b - h_2)^2}{(a - h_1)^2 + (b - h_2)^2}K_3\right),$$

$$c_3^2 = \frac{a^2}{2MR^2}\left(h_2^2 K_1 + \frac{a^2 h_2^2}{(a-h_1)^2+h_2^2}K_2 + \frac{(ah_2-bh_1)^2}{(a-h_1)^2+(b-h_2)^2}K_3 \right),$$

$$s^2 = \frac{4a^2}{M}\frac{(a-h_1)(b-h_2)}{(a-h_1)^2+(b-h_2)^2}K_3,$$

$$\beta_1 = \frac{2a^2}{M}\left(\frac{h_2^2}{(a-h_1)^2+h_2^2}K_2 + \frac{(b-h_2)(ah_2-bh_1)}{a((a-h_1)^2+(b-h_2)^2)}K_3 \right),$$

$$\beta_2 = \frac{1}{M}\left((\frac{a^2 h_2^2}{(a-h_1)^2+h_2^2} + \frac{b^2 h_1^2}{(b-h_2)^2+h_1^2})K_2 + \frac{(ah_2-bh_1)^2}{(a-h_1)^2+(b-h_2)^2}K_3 \right).$$

$$(3.9)$$

It is seen from relations (3.9) that, in the nanocrystalline (granular) media, the velocity of the wave propagation depends on four force constants K_0, K_1, K_2, and K_3, and on four geometric parameters: a, b, h_1, and h_2. To simplify the analysis of such dependence, we assume as above that the condition of similarity of the shape of the particles to lattice form (3.8) holds and substitutes four geometric parameters by two dimensionless quantities: the shape parameter f and the relative particle size p. In this case, expressions (3.9) take the form:

$$c_1^2 = \frac{a^2}{M}\left(K_0 + 2K_1 + \frac{2(\sqrt{2}-p)^2}{(\sqrt{2}-p)^2+f^2 p^2}K_2 + \frac{2}{1+f^2}K_3 \right),$$

$$c_2^2 = \frac{2a^2}{M}\left(\frac{f^2 p^2}{(\sqrt{2}-p)^2+f^2 p^2}K_2 + \frac{f^2}{1+f^2}K_3 \right),$$

$$c_3^2 = \frac{4a^2 f^2}{M(1+f^2)}\left(K_1 + \frac{2}{(\sqrt{2}-p)^2+f^2 p^2}K_2 \right),$$

$$s^2 = \frac{4a^2}{M}\frac{f}{1+f^2}K_3,$$

$$\beta_1 = \frac{2a^2}{M}\left(\frac{f^2 p^2}{(\sqrt{2}-p)^2+f^2 p^2}K_2 \right),$$

$$\beta_2 = \frac{a^2}{M}\left((\frac{f^2 p^2}{(\sqrt{2}-p)^2+f^2 p^2} + \frac{f^2 p^2}{f^2(\sqrt{2}-p)^2+p^2})K_2 \right). \qquad (3.10)$$

It follows from (3.10) that $c_2^2 = \beta_1 + fs^2/2$. This means that $c_2^2 \geq \beta_1$ and the equality is achieved only in two cases: when $f = 0$ (particles are rods elongated along the x-axis) or $K_3 = 0$ (one-dimensional model). If the particles are round, then $\beta_1 = \beta_2 = \beta$ and, independent of the lattice type, $c_2^2 = \beta + s^2/2$.

Next, we will consider the degeneracy of this model into a square lattice of round particles and into a one-dimensional chain of ellipse-shaped particles.

3.2.2 A Square Lattice of Round Particles

For a square lattice of round particles ($a = b$, $h_1 = h_2 = h$), in contrast to the previous case, $\beta_1 = \beta_2 = \beta$ and the dynamic equations will take on the form of Eq. (2.8)—as for a medium with hexagonal symmetry and round particles. Differences will be observed only for the coefficients of these equations:

$$\rho c_1^2 = K_0 + 2K_1 + \frac{2(a-h)^2}{h^2 + (a-h)^2} K_2 + K_3,$$

$$\rho c_2^2 = \frac{2h^2}{h^2 + (a-h)^2} K_2 + K_3, \; \rho c_3^2 = 2\left(K_1 + \frac{a^2}{h^2 + (a-h)^2} K_2\right),$$

$$\rho s^2 = 2K_3, \; \beta_1 = \beta_2 = \beta = c_2^2 - s^2/2 \tag{3.11}$$

Here, $\rho = M/a^2$ is the surface density of the studied medium. The analysis of relations (3.9)–(3.11) shows that if in the square lattice ($a = b$) consisting of round particles ($f = 1$) the rotational wave velocity c_3 and the dispersion parameter β do not depend on the parameter K_3 of the force interaction with the second coordination sphere, then there appears such a dependence for c_3, β_1 and β_2, when the condition (3.8) of similarity of the particle shape to the lattice form does not hold. On the other hand, this analysis implies that this dependence is absent not only in the case of the square lattice of round particles, but also for the rectangular lattice of ellipse-shaped particles under the similarity condition $b/a = d_2/d_1$, although in this case $\beta_1 \neq \beta_2$ still. It is also interesting to note that the last equality (3.11) coincides with (2.11); however, relation $s^2 = c_1^2 - c_2^2$, which is valid for the hexagonal lattice, is not satisfied for rectangular and square lattices. Consequently, in the linear dynamic equations for the rectangular lattice, besides the radius of the particle inertia, R, which makes equal the dimensionality of the translational displacements and rotations, there are six independent constants (c_1, c_2, c_3, s, β_1, and β_2) even if similarity condition (3.8) holds; for the square lattice of round particles, there are five constants (c_1, c_2, c_3, s, β); for the hexagonal lattice of the same particles which is isotropic in the acoustic properties in the long-wave approximation, there are only four independent constants (c_1, c_2, c_3, and β).

3.2.3 A Chain of Ellipse-Shaped Particles

To degenerate the two-dimensional model (3.6) into the one-dimensional one—a chain of ellipses—we should set $K_3 = 0$ and $b = 0$ in coefficients (3.9). Then, $s = 0$ and $\beta_1 = 2\beta_2 = 2c_2^2$. As a result, the dynamic equations of the chain consisting of anisotropic particles take on the form:

$$u_{tt} - c_1^2 u_{xx} = 0,$$

$$w_{tt} - c_2^2 w_{xx} - \beta\varphi_x = 0,$$
$$R^2(\varphi_{tt} - c_3^2\varphi_{xx}) + \beta(\varphi + w_x) = 0. \tag{3.12}$$

Coefficients of Eq. (3.12) have the following form:

$$c_1^2 = \frac{a^2}{M}\left(K_0 + 2K_1 + \frac{2(a-h_1)^2}{(a-h_1)^2 + h_2^2}K_2\right),$$
$$c_2^2 = \frac{2a^2}{M}\left(\frac{h_2^2}{(a-h_1)^2 + h_2^2}K_2\right), \beta = 2c_2^2,$$
$$c_3^2 = \frac{a^2}{2MR^2}\left(h_2^2 K_1 + \frac{a^2 h_2^2}{(a-h_1)^2 + h_2^2}K_2\right). \tag{3.13}$$

Thus, the linear dynamic equations of a chain of ellipses contain only three independent constants: c_1, c_2, and c_3. With allowance for nonlinear terms, similar equations for a chain of rectangular particles were obtained in Lisina et al. [8].

3.3 Influence of Microstructure on Acoustic Properties of the Medium

The interrelation between the microstructure of the anisotropic medium with non-dense packing of particles and its macroparameters was established in the previous section due to the structural modeling method. Now, we will use this interrelation for analysis of the dependence of the acoustic characteristics of the medium on the shape of the particles (using the example of a one-dimensional chain of ellipses), as well as on the parameters of interparticle interaction, particle sizes, and the structure of the lattice (using an example of a square lattice of round particles).

3.3.1 Dependence of the Elastic and Rotational Wave Velocities on the Shape of the Particles in the 1D Lattice

Using the example of a one-dimensional lattice of ellipse-shaped particles, we will analyze the influence of their shape on the velocities of longitudinal, transverse, and rotational waves.

From Eq. (3.10), it is possible to obtain expressions for the velocities of such waves, normalized to the longitudinal wave velocity $c_0 = \sqrt{K_0/M}$ in the chain in the absence of moment interactions between the particles, i.e., when $K_1 = K_2 = 0$:
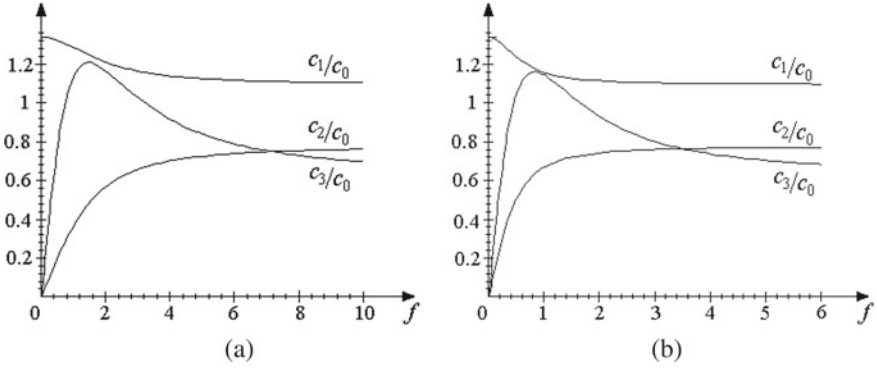
Fig. 3.4 Dependence of the velocities of longitudinal (c_1), transverse (c_2), and rotational waves (c_3) on the shape parameter f at the relative particle size $p = 0.5$ (**a**) and $p = 0.9$ (**b**)

$$\frac{c_1}{c_0} = \sqrt{1 + \frac{2K_1}{K_0} + \frac{2(\sqrt{2} - p)^2}{(\sqrt{2} - p)^2 + p^2 f^2} \frac{K_2}{K_0}},$$

$$\frac{c_2}{c_0} = \sqrt{\frac{2p^2 f^2}{(\sqrt{2} - p)^2 + p^2 f^2} \frac{K_2}{K_0}},$$

$$\frac{c_3}{c_0} = \sqrt{\frac{4f^2}{1 + f^2} \left(\frac{K_1}{K_0} + \frac{2}{(\sqrt{2} - p)^2 + p^2 f^2} \frac{K_2}{K_0} \right)}. \tag{3.14}$$

It is interesting to note that the limit transitions $f \to 0$ (i.e., when $h_2/h_1 \to 0$) and $f \to \infty$ are not equivalent, since in the first case $c_2/c_0 \to 0$ and $c_3/c_0 \to 0$, whereas in the second case $c_2/c_0 \to \sqrt{2K_2/K_0}$ and $c_3/c_0 \to 2\sqrt{K_1/K_0}$. Thus, in a chain of rods connected by springs, transverse waves can propagate only in the presence of non-central interactions (K_2) or by taking into account the preliminary tension of the springs [9, 10].

Figure 3.4a, b shows the dependence of the dimensionless values of the velocities of longitudinal (c_1), transverse (c_2), and rotational waves (c_3) on the shape parameter f (if $f < 1$, then the particles are elongated along x-axis, if $f > 1$—along y-axis, and at $f = 1$ the particles are round) for $K_1/K_0 = 0,1$, $K_2/K_0 = 0,3$ and two values of p: $p = 0.5$ (Fig. 3.4a) and $p = 0.9$ (Fig. 3.4b).

From Fig. 3.4, it is visible that in a chain of ellipse-shaped particles the longitudinal wave velocity decreases and the transverse wave velocity grows monotonously with increase in the shape parameter. Both velocities tend to some limiting values depending on the force constants K_1 and K_2. The rotational wave velocity has a local maximum at a certain value of f depending on the particle size and the parameters of the force interactions. The point of the maximum is shifted to the left with increase in the particle size. For small particle sizes, variations of the wave velocities are smoother than at large values of p. If $f \to \infty$, then all three velocities tend to some limiting values: $c_1/c_0 \to \sqrt{1 + 2K_1/K_0}$, $c_2/c_0 \to \sqrt{2(K_2 + K_3)/K_0}$, and

$c_3/c_0 \rightarrow 2\sqrt{K_1/K_0}$, whereas for $f \rightarrow 0$ (i.e., when $h_2/h_1 \rightarrow 0$) $c_2 \rightarrow 0$ and $c_3 \rightarrow 0$. It also follows from Fig. 3.4 that the longitudinal wave velocity always exceeds the transverse wave velocity, which, in turn, can be either larger or smaller than the rotational wave velocity. The first fact is well known in theory. The second fact is favored by experimental data [11, 12] indicating that in artificial granular materials the rotational wave velocity can exceed the translational wave velocity. However, it should be noted that the practical lack of evidence on the material constants of microstructured media and the poor development of methods for their experimental research [13–15] are the main factors constraining the study of models of non-classical media and their application for calculating the dynamic and strength characteristics of structural materials.

3.3.2 Dependence of the Acoustic Characteristics of the 2D Anisotropic Medium on the Microstructure Parameters

Now let us analyze the dependence of the acoustic characteristics of the medium on the parameters of interparticle interaction, the particle size, and the lattice structure.

In the case of a square lattice of round particles, the squares of the wave velocities contained in Eq. (3.6) are expressed in terms of the force constants of the micromodel K_0, K_1, K_2, and K_3, the distance a between the particles, and their diameter d as follows:

$$c_1^2 = \frac{1}{\rho}\left(K_0 + 2K_1 + \frac{2(a\sqrt{2} - d)^2}{d^2 + (a\sqrt{2} - d)^2}K_2 + K_3\right),$$

$$c_2^2 = \frac{1}{\rho}\left(\frac{2d^2}{d^2 + (a\sqrt{2} - d)^2}K_2 + K_3\right),$$

$$c_3^2 = \frac{2}{\rho}\left(K_1 + \frac{a^2}{d^2 + (a\sqrt{2} - d)^2}K_2\right),$$

$$\beta = \frac{2d^2}{\rho(d^2 + (a\sqrt{2} - d)^2)}K_2, s^2 = \frac{2K_3}{\rho}, \tag{3.15}$$

where $\rho = M/a^2$ is the surface density of this medium (since the hexagonal lattice has a density $\rho = 2M/a^2\sqrt{3}$ (see Sect. 2.2), it represents a denser packing in comparison with a square lattice).

For a medium with hexagonal symmetry, relations similar to Eq. (3.15) have the form of Eq. (2.9). The dependence of the threshold frequency ω_0 on the parameter β and the particle inertia radius $R = d/\sqrt{8}$, as well as the relationship between the parameters c_2, β, and s are the same for both models and are described by Eqs. (2.10) and (2.11). But relation (2.12) is not satisfied for the square lattice [5].

Dependences of the longitudinal (c_1), transverse (c_2), and rotational wave velocities (c_3) on the relative particle size d/a at $K_1/K_0 = 0.1$ in the square lattice are plotted
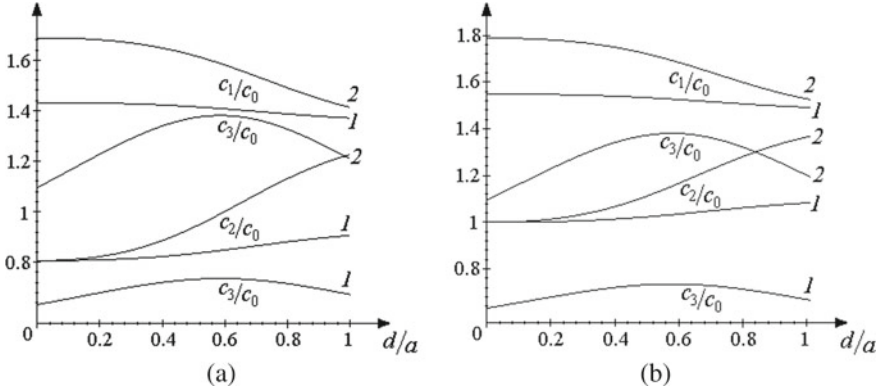
Fig. 3.5 Dependence of the wave velocities on the relative particle size in a square lattice for K_1/K_0 $= 0.1$, $K_2/K_0 = 0.1$ (curves 1), $K_2/K_0 = 0.5$ (curves 2), $K_3/K_0 = 0.65$ (**a**) and $K_3/K_0 = 1$ (**b**)

in Fig. 3.5a, b, where curves 1 correspond to value $K_2/K_0 = 0.1$ and curves 2—to value $K_2/K_0 = 0.5$. It is assumed that $K_3/K_0 = 0.65$ (Fig. 3.5a) or $K_3/K_0 = 1$ (Fig. 3.5b). All velocities are normalized to the longitudinal wave velocity $c_0 = \sqrt{K_0/\rho}$, taking into account only central interactions. It can be seen from Fig. 3.5a, b that the longitudinal wave velocity monotonously decreases with increasing grain size d/a, the shear wave velocity monotonically increases, and the rotational wave velocity has a maximum for some value of d/a. For small values of moment interactions ($K_2 \ll K_0$), the grain size does not significantly affect the wave velocities (see curves 1).

From relations (3.15), one can express the parameters of force interactions in terms of the acoustic characteristics of the medium:

$$K_3 = \rho s^2/2, \quad K_2 = \frac{\rho(d^2 + (a\sqrt{2} - d)^2)}{4d^2}(2c_2^2 - s^2),$$

$$K_1 = \frac{\rho}{2}\left(c_3^2 - \frac{a^2}{d^2}(2c_2^2 - s^2)\right), \quad K_0 = \rho(c_1^2 - c_2^2 - c_3^2) + \frac{\rho a\sqrt{2}}{d}(2c_2^2 - s^2)$$

$$(3.16)$$

In addition, the particle size is expressed in terms of the acoustic characteristics of the medium from Eqs. (2.10) to (2.11) by the same way as in the hexagonal lattice:

$$d = \sqrt{8|2c_2^2 - s^2|}/\omega_0. \tag{3.17}$$

Thus, expressions (3.15) and (3.16)–(3.17) establish one-to-one correspondences between the micromodel parameters and the macrocharacteristics of the medium. Such a relationship can be used, in particular, for testing nanomaterials on the base of wave (acoustic) experiments.

3.4 Dispersion Properties of Normal Waves

This section is devoted to analysis of the dispersion properties of the developed models of a granular medium with non-dense packing of particles under the assumption that the similarity condition (3.8) is valid. Then, as follows from the last three equalities (3.4), $B_6 = B_6' = B_7 = 0$.

3.4.1 Dispersion Properties of the Discrete Model

As in Sect. (2.4.1), we consider solutions of the equations of motion that are plane monochromatic waves, for which the displacement can be represented in the form (2.15). Substitution of solutions (2.15) into Eq. (3.3) yields Eq. (2.16) in a matrix form for determining the displacement amplitudes, where the matrix elements have the following form [6]:

$$d_{11} = 2B_1(\cos(q_1 a) - 1) + 2B_2'(\cos(q_2 b) - 1) + 4B_5(\cos(q_1 a)\cos(q_2 b) - 1),$$
$$d_{12} = -4B_4 \sin(q_1 a)\sin(q_2 b), d_{13} = ibB_2'\sin(q_2 b), d_{21} = d_{12},$$
$$d_{22} = 2B_1'(\cos(q_2 b) - 1) + 2B_2(\cos(q_1 a) - 1) + 4B_5'(\cos(q_1 a)\cos(q_2 b) - 1),$$
$$d_{23} = -iaB_2 \sin(q_1 a), d_{31} = \frac{-d_{13}}{R^2}, d_{32} = \frac{-d_{23}}{R^2},$$
$$d_{33} = \frac{1}{R^2}\left[\left(2B_3 - a^2\frac{B_2}{2}\right)(\cos(q_1 a) - 1)\right.$$
$$\left. + \left(2B_3' - b^2\frac{B_2'}{2}\right)(\cos(q_2 b) - 1) - a^2 B_2 - b^2 B_2'\right]. \tag{3.18}$$

The solvability condition for Eq. (2.16) with coefficients (3.18) leads to dispersion Eq. (2.18):

$$M^3\omega^6 + F_1\omega^4 + F_2\omega^2 + F_3 = 0,$$

where $F_{1,2,3}$ are the wave vector functions defined by relations (2.19). Dividing Eq. (2.18) by K_0^3 and introducing the substitution $\varpi = \omega\sqrt{M/K_0}$, one can obtain the dispersion equation in the dimensionless form (2.20):

$$\varpi^6 - f_1\varpi^4 + f_2\varpi^2 + f_3 = 0,$$

in which $f_1 = \frac{F_1}{K_0}$, $f_2 = \frac{F_2}{K_0^2}$, $f_3 = \frac{F_3}{K_0^3}$.

Next, we will analyze the dispersion properties of the considered medium in the first Brillouin zone (see Sect. 2.4.1 and [16]) and on its boundary.

The left-hand side of the dispersion Eq. (2.20) contains three variables: the frequency ω and the wave vector components q_1 and q_2. In addition, coefficients
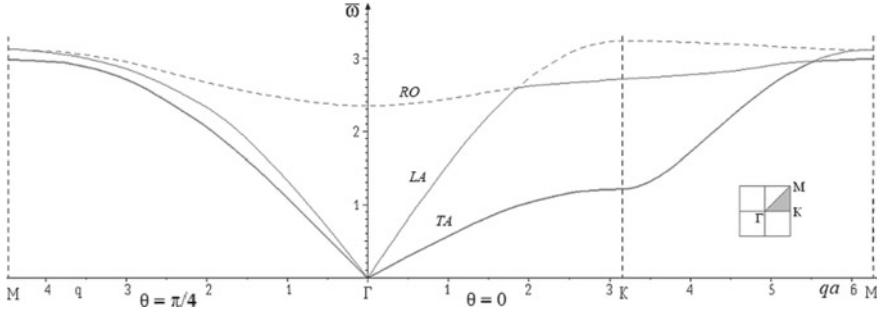
Fig. 3.6 Dependence of the oscillation frequency on the wave vector module for $f = 1$

(3.18) of Eq. (2.20) depend on two geometric parameters: the relative particle size $\tilde{d} = h_1/a = h_2/b$ and the lattice shape parameter $f = b/a = h_2/h_1$ and three parameters of the force interactions of the springs, K_1/K_0, K_2/K_0, and K_3/K_0. Analysis of the dispersion Eq. (2.20) will be carried out for the case when

$$\tilde{d} = \frac{1}{2\sqrt{2}}, \frac{K_1}{K_0} = 0.6, \frac{K_2}{K_0} = 0.2, \frac{K_3}{K_0} = 0.3. \tag{3.19}$$

As in the hexagonal lattice (see Sect. 2.4.1), the system under consideration contains acoustic longitudinal (LA) and transverse (TA) phonons, as well as an optical rotational (RO) phonon (Fig. 3.6). In Eq. (2.20), we pass to the polar coordinate system by setting $q_1 = q \cos \theta$ and $q_2 = q \sin \theta$, where q is the wave vector module, and angle θ indicates the direction of propagation of the plane wave with respect to x-axis in the direct lattice.

The dispersion curves calculated with account of conditions (3.19) along directions $\theta = 0°$ (Γ–K), $\theta = $ arctg f (Γ–M), and along the Brillouin zone boundary $q_1 = \pi/a$ (K–M) are plotted in Fig. 3.6 (in this case $f = 1$, i.e., the lattice is square and the particles are round) and in Fig. 3.7 (in this case, the lattice is rectangular, the particles are ellipse-shaped, and $f = 1.5$).
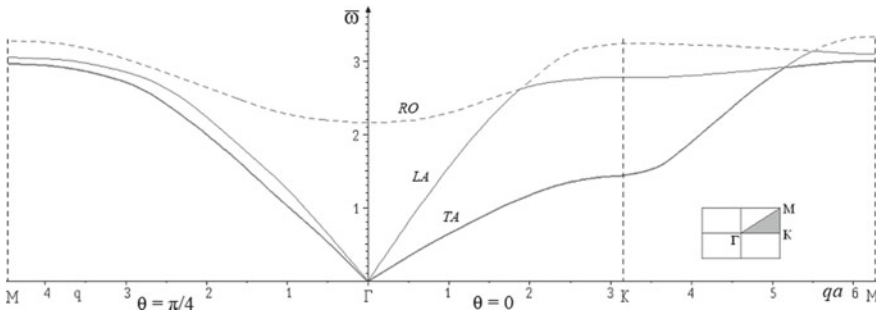
Fig. 3.7 Dependency of the wave frequency on the wave vector module for $f = 1.5$

From Fig. 3.6, it is seen that the frequency increases monotonically along Γ–K- and Γ–M-directions with the wave number growing up to the Brillouin zone boundary. At point $(q_1 = \pi/a, q_2 = 0)$, the frequency of the rotational mode has a maximum

$$\varpi_{\max}^{RO} = 2\sqrt{(B_1 + 2B_5)/K_0}$$
$$= 2\sqrt{1 + 2K_1/K_0 + 2(a-h)^2 K_2/(r^2 K_0) + K_3/K_0}. \quad (3.20)$$

In K-M-direction, the group velocity of rotational phonons is negative: $v_{gr} = d\omega/dq < 0$; i.e., this is a *backward-wave region* (see Sect. 2.4.1). The rotational mode has the minimum threshold frequency that is achieved at point $(q_1 = 0, q_2 = 0)$ [17]:

$$\varpi_{\min}^{RO} = \frac{a}{R}\sqrt{\frac{2B_2}{K_0}} = \frac{2a}{h}\sqrt{\frac{2h^2 K_2}{((a-h)^2 + h^2)K_0}} = \sqrt{\frac{8a^2 K_2}{((a-h)^2 + h^2)K_0}}. \quad (3.21)$$

It follows from Eq. (3.21) that $\varpi_{\min}^{RO} = \sqrt{\frac{8K_2}{K_0}} \neq 0$ for degeneration of the medium particles in the material points ($h \to 0$), if $K_2 \neq 0$. On the other hand, when there are no couple interactions ($K_2 = 0$), then $\varpi_{\min}^{RO} = 0$, even if the particles are not material points. Under assumptions (3.19), the maximum and minimum frequencies of the rotational mode are $\varpi \approx 3.35$ and $\varpi \approx 2.42$, respectively (see Fig. 3.6).

Both acoustic modes have the largest value at the boundary point of the Brillouin zone ($q_1 = \pi/a, q_2 = \pi/b$). The maximum frequency of the longitudinal mode equals [17]

$$\varpi_{\max}^{LA} = 2\sqrt{\frac{B_1 + B_2}{K_0}} = 2\sqrt{1 + \frac{2K_1}{K_0} + \frac{K_2}{K_0}\left(1 + \frac{(a-h)^2}{(a-h)^2 + h^2}\right)} \approx 3.22, \quad (3.22)$$

and the maximum frequency of the transverse mode is equal to

$$\varpi_{\max}^{TA} = 2\sqrt{K_1/K_0} \approx 3,09. \quad (3.23)$$

At this point, the group velocity is equal to zero and therefore a signal with such a frequency cannot propagate in a crystal lattice. This restriction can be dropped only for nonlinear perturbations [18], when anharmonic terms are taken into account in equations of motion (3.3). In the frequency ranges $0 \leq \varpi < 2.42$ and $3.09 < \varpi \leq 3.22$, the system has two wave modes (LA and TA at low frequencies, and LA and RO in the high-frequency field) and all three wave modes (LA, TA, and RO) are present in the system, when $2.42 < \varpi \leq 3.09$; see Fig. 3.6.

It is possible to obtain inverse dependences from Eqs. (3.20) to (3.23), i.e., to express the parameters of force and couple interactions through the threshold frequencies of the acoustic and optical phonons [6]:

$$\frac{K_0}{a} = \frac{\rho a^2}{4}\left(\omega_{\text{max}}^{\text{LA}}\right)^2 - \frac{\rho a^2}{2}\left(\omega_{\text{max}}^{\text{TA}}\right)^2 - \frac{\rho\left(h^2 + 2(a-h)^2\right)}{8}\left(\omega_{\text{min}}^{\text{RO}}\right)^2,$$

$$\frac{K_1}{a} = \frac{\rho a^2}{4}\left(\omega_{\text{max}}^{\text{TA}}\right)^2,$$

$$\frac{K_2}{a} = \frac{\rho\left((a-h)^2 + h^2\right)}{8}\left(\omega_{\text{min}}^{\text{RO}}\right)^2,$$

$$\frac{K_3}{a} = \frac{\rho a^2}{4}\left(\omega_{\text{max}}^{\text{RO}}\right)^2 - \frac{\rho a^2}{4}\left(\omega_{\text{max}}^{\text{LA}}\right)^2 + \frac{\rho h^2}{8}\left(\omega_{\text{min}}^{\text{RO}}\right)^2. \tag{3.24}$$

On the other hand, these parameters are expressed in terms of elasticity constants C_{11}, C_{12}, and C_{44} of the classical theory of elasticity:

$$\frac{K_3}{a} = C_{12}, \quad \frac{K_2}{a} = (C_{44} - C_{12})\left(1 + \left(\frac{a}{h} - 1\right)^2\right),$$

$$\frac{K_0 + 2K_1}{a} = C_{11} - C_{12} - 2(C_{44} - C_{12})\left(\frac{a}{h} - 1\right)^2. \tag{3.25}$$

It should be noted that four parameters of force and couple interactions in the short-wavelength approximation are uniquely expressed in terms of the macroparameters of the medium, namely, through four threshold frequencies of the acoustic and optical phonons [see Eq. (3.24)], whereas there are only three macroparameters in the long-wavelength approximation—elasticity constants C_{11}, C_{12}, and C_{44}. A fourth parameter is needed to account for the rotational degrees of freedom of anisotropic particles. Therefore, it is possible to relate only three threshold frequencies to the elastic moduli of the second order without any additional assumptions using Eqs. (3.24) and (3.25):

$$\omega_{\text{min}}^{RO} = 4\sqrt{\frac{C_{44} - C_{12}}{\rho d^2}},$$

$$\omega_{\text{max}}^{RO} = 2\sqrt{\frac{C_{11} + (C_{44} - C_{12})(a/h - 1)^2}{\rho a^2}},$$

$$\omega_{\text{max}}^{LA} = 2\sqrt{\frac{C_{11} + C_{44} - 2C_{12}}{\rho a^2}}. \tag{3.26}$$

Introducing an additional assumption about the relationship between K_1 and K_0 in the third equality (3.25) enables one to calculate also the maximum frequency of the transverse waves. In particular, if $K_1 = K_0/4$, then

$$\omega_{\text{max}}^{TA} = \sqrt{\frac{2\left(C_{11} + C_{12} - 2C_{44} + 2(C_{44} - C_{12})\left(2a/h - a^2/h^2\right)\right)}{3\rho a^2}}. \tag{3.27}$$

Analysis of Eqs. (3.26) and (3.27) shows that the minimum frequency of the rotational phonons can exceed the maximum frequency of the transverse phonons or be lower than it.

Thus, Eq. (3.24) can be used for estimation of predetermined dispersion properties of artificial periodic structures (metamaterials): One can estimate the values of the threshold frequencies for metamaterials due to Eq. (3.26). In addition, by choosing the elasticity constants it is possible to vary the threshold frequencies.

In contrast to the case, when $f = 1$, for $f = 1.5$ the frequency of the rotational vibrations takes the maximal value at the point ($q_1 = \pi/a$, $q_2 = \pi/b$) (Fig. 3.7) [6]:

$$\varpi_{\max}^{RO} = 2\sqrt{\frac{B_1' + B_2}{K_0}} = 2\sqrt{1 + \frac{2K_1}{K_0} + \left(\frac{2(b - h_2)^2}{r_2^2} + \frac{h_2^2}{r_1^2}\right)\frac{K_2}{K_0}} \approx 3.29. \quad (3.28)$$

A minimal value of the rotational phonon frequency is achieved, like in the previous case, in the zero point and still does not depend on the parameters of force interactions K_1 and K_3:

$$\varpi_{\min}^{RO} = \sqrt{\frac{a^2 B_2 + b^2 B_2'}{R^2 \cdot K_0}} = \frac{\sqrt{a^2 h_2^2 r_2^2 + b^2 h_1^2 r_1^2}}{R r_1 r_2}\sqrt{\frac{K_2}{K_0}} \approx 2.29. \quad (3.29)$$

The greatest value of the longitudinal mode is also located on the Brillouin zone boundary at the point ($q_1 = \pi$, $q_2 \approx 2.4$), and its value is equal to $\varpi \approx 3.2$. In fact, this point divides the backward-wave field between the longitudinal and rotational modes; see Fig. 3.7. The maximum of transverse vibrations does not change its position and quantity: $\varpi = 2\sqrt{K_1/K_0} \approx 3.09$ at the point ($q_1 = \pi/a$, $q_2 = \pi/b$). Thus, the system has two wave modes (longitudinal LA and transverse TA acoustic modes at low frequencies, and longitudinal acoustic LA and rotational optical RO in the high-frequency field) in the frequency ranges $0 \leq \varpi < 2.29$ and $3.09 < \varpi < 3.2$, and all three wave modes (LA, TA, and RO) are present in the system, when $2.29 < \varpi < 3.09$.

It should be also noted that the maximum values of all three modes and the minimum value of the rotational mode vary insignificantly in comparison with the considered ones in the previous case.

It is convenient to study isotropic and anisotropic properties of this lattice using the maps of equal frequencies. Such maps for longitudinal, transverse, and rotational phonons at different fixed values of the frequency are shown in Fig. 3.8 (for $f = 1$) and in Fig. 3.10 (for $f = 1.5$).

Figure 3.8 shows that anisotropy of the longitudinal mode is most evident when $\varpi > 2.7$, and the longitudinal mode is almost isotropic for $\varpi < 1.5$, whereas the transverse mode is anisotropic even for small ϖ. The rotational mode is isotropic for $2.42 < \varpi < 2.8$. However, all modes are anisotropic even in the low-frequency range in the case of the rectangular lattice with ellipse-shaped particles; see Fig. 3.10.
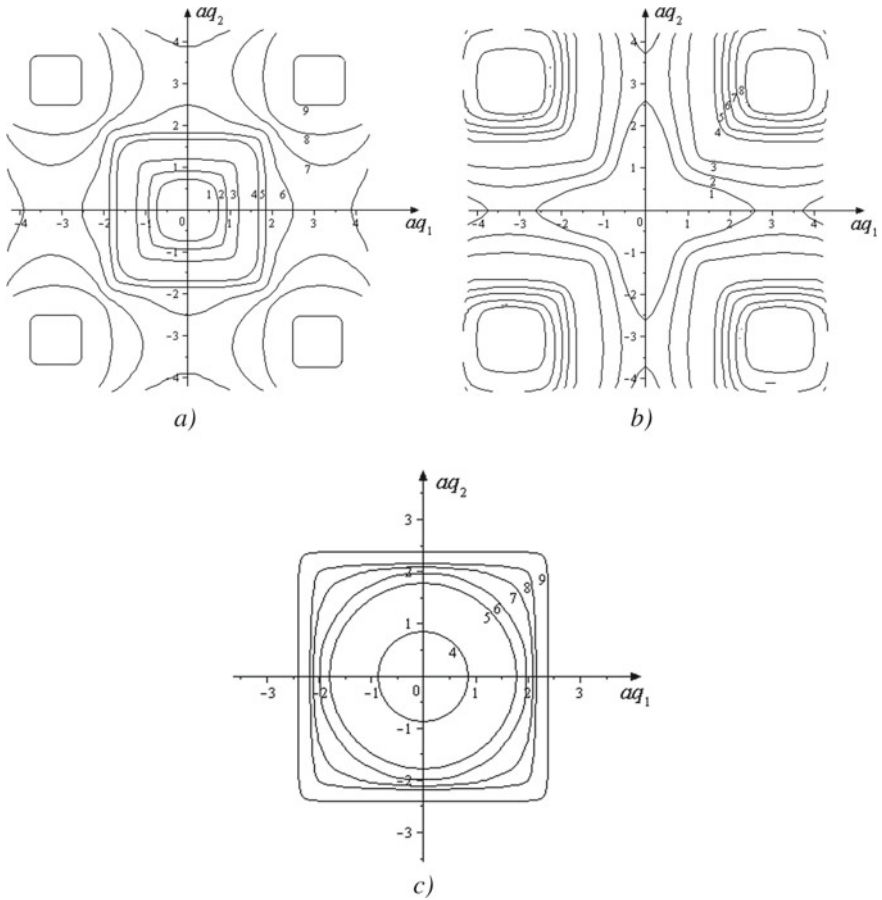
Fig. 3.8 Maps of equal frequencies for the square lattice of round particles ($f = 1$): **a** LA-mode; **b** TA-mode; **c** RO-mode. Curves 1 correspond to $\varpi = 1.2; 2-\varpi = 1.5; 3-\varpi = 1.9; 4-\varpi = 2.5; 5-\varpi = 2.65; 6-\varpi = 2.75; 7-\varpi = 2.85; 8-\varpi = 2.95; 9-\varpi = 3.1$

Two modes (LA and RO) are presented at frequency $\varpi = 3.1$ in Fig. 3.10 in addition to Fig. 3.9, where all three modes are separately plotted in the frequency range $1.2 < \varpi < 3.05$. Here, small "rectangles" correspond to the LA-mode and large "rectangles" stand for the RO-mode. As it was mentioned above, the third mode (TA) is absent in the system at this frequency.

Figure 3.10 shows that the map of equal frequencies reproduces completely the structure of the rectangular lattice at issue. Figure 3.11 contains squares instead of rectangles for the square lattice.
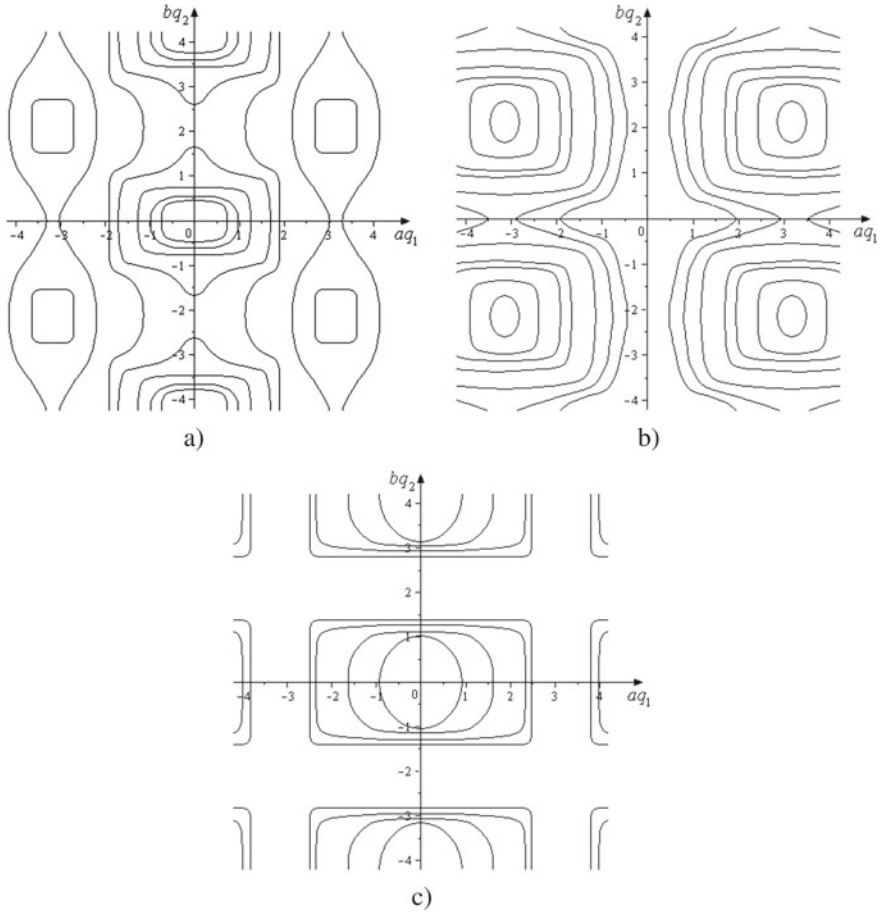
Fig. 3.9 Maps of equal frequencies for the rectangular lattice of ellipse-shaped particles ($f = 1.5$): **a** LA-mode; **b** TA-mode; **c** RO-mode. Curves 1 correspond to $\varpi = 1.2$; $2 - \varpi = 1.5$; $3 - \varpi = 1.9$; $4 - \varpi = 2.45$; $5 - \varpi = 2.65$; $6 - \varpi = 2.95$; $7 - \varpi = 3.05$

3.4.2 Dispersion Properties of the Continual Model

As it was mentioned in Sect. 3.2.2, dynamic Eq. (2.8) is valid both for the hexagonal lattice and for the square lattice of round particles. If to search for their solutions in the form of plane harmonic waves (2.22)

$$(u, w, \varphi)^T = (A_u, A_w, A_\varphi)^T \exp[i(\omega t - \mathbf{k} \cdot \mathbf{r})],$$

where A_u, A_w, and A_φ are the complex amplitudes of harmonic waves, ω is the oscillation frequency, and $\mathbf{k} = \{k_x, k_y\}$ is the wave vector, then, according to the procedure described in Sect. 2.4.2, it is possible to derive Eq. (2.24)
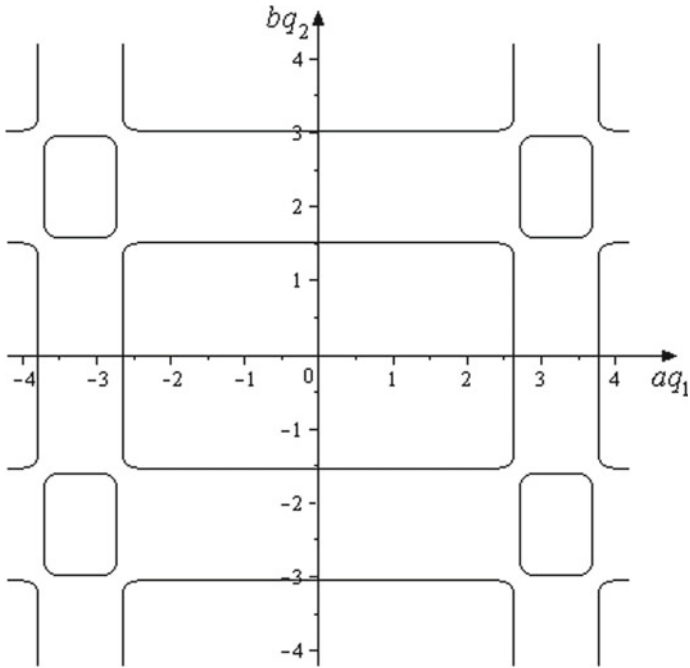
Fig. 3.10 Isolines of frequency $\varpi = 3.1$
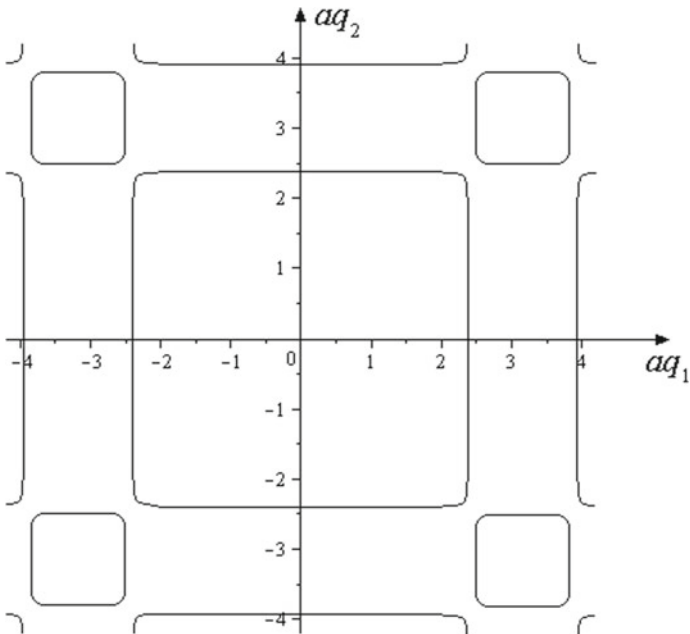
Fig. 3.11 Isolines of frequency $\varpi = 3.1$

$$\omega^6 - H_1\omega^4 + H_2\omega^2 + H_3 = 0,$$

where the dependences of the coefficients H_1, H_2, and H_3 on the scalar square of the wave vector $k^2 = k_x^2 + k_y^2$ (k is the wavenumber) are determined by relations (2.25):

$$H_1 = (c_1^2 + c_2^2 + c_3^2)k^2 + \omega_0^2,$$
$$H_2 = (c_1^2c_2^2 + c_1^2c_3^2 + c_2^2c_3^2)k^4 + ((c_1^2 - c_2^2)^2 - s^4)k_x^2k_y^2 + \omega_0^2(c_1^2 + c_2^2 - \beta/2)k^2,$$
$$H_3 = \omega_0^2c_1^2(\beta/2 - c_2^2)k^4 + \omega_0^2[\beta(c_2^2 - c_1^2 + s^2) - (c_1^2 - c_2^2)^2 + s^4]k_x^2k_y^2$$
$$- c_1^2c_2^2c_3^2k^6 + c_3^2(s^4 - (c_1^2 - c_2^2)^2)k^2k_x^2k_y^2.$$

It should be noted that if equality $c_1^2 - c_2^2 = s^2$ is valid in the hexagonal lattice and the coefficients of $k_x^2k_y^2$ vanish that indicates the isotropy of the medium with hexagonal symmetry, then the medium with cubic symmetry is anisotropic in this approximation. The dispersion curves determined by Eq. (2.24) are represented in the normalized form (in the reference frame $(k/k_0, \omega/\omega_0)$, where $k_0 = \omega_0/c_2$) in Fig. 3.12.

Here, the following designations are introduced: L is the longitudinal mode, T is the transverse mode, and R is the rotational one. Graphs have been plotted for numerical data corresponding to sodium fluoride crystals: $c_1/c_2 = 1.79$, $c_3/c_2 = 0.69$, $\beta/c_2^2 = 0.158$ (see Fig. 3.12 and Table 4.1 in Sect. 4.2). R- and T-mode curves have oblique asymptotes $\omega = \pm c_2 k$ and $\omega = \pm c_3 k$, respectively. The dispersion dependences for the waves propagating along x-axis ($\theta = 0$) are plotted in Fig. 3.12 in the left-hand half plane, and for the waves traveling at angle $\theta = \pi/6$ to x-axis are shown in the same figure in the right-hand half plane. It is visible from this figure that the transverse mode dispersion is more pronounced when the waves propagate at angle $\theta = \pi/6$.

Fig. 3.12 Dispersion curves for the square lattice
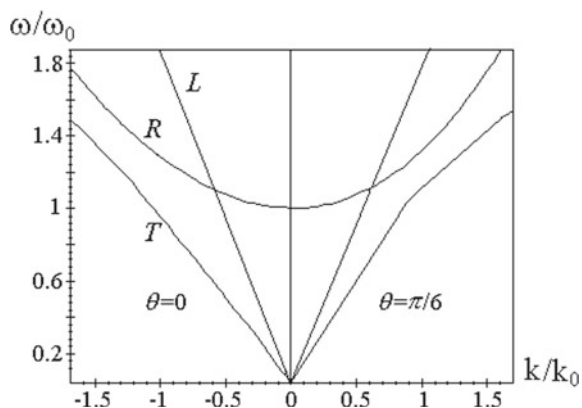
Fig. 3.13 Experimentally
measured dependencies of
dispersion curves of
magnons and phonons in a
ferromagnet FeF_2. *TA* and
LA are the transverse and
longitudinal acoustic
phonons, respectively, and *M*
are magnons
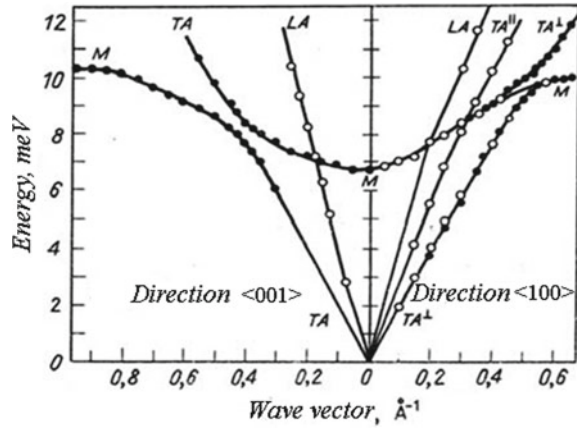
The dispersion curves plotted in Fig. 3.12 qualitatively coincide with the dependences of the energy of magnons and phonons in ferromagnet FeF_2 on the magnitude of the wave vector at temperature of 4.2 K (Fig. 3.13), which were obtained experimentally by the method of inelastic neutron scattering [19].

Comparison of plots 3.12 and 3.13 yields coincidence of the dispersion curves for the microrotation wave and for the spin wave (magnons[1]). This fact is not unexpected, if to take into account that in a ferromagnetic material a change in the angular momentum of a system of microparticles leads to a change in the magnetic moment of this system (the Barnett effect [21]), and vice versa, a change in the magnetic moment of a free body causes this body to rotate (the Einstein–de Haas effect [22]). It was shown in Akhiezer et al. [23] that the antisymmetric part of the stress tensor determines an additional moment of elastic forces arising from a local rotation of the crystallographic axes with respect to magnetization. This leads to appearance of the non-reciprocity effect consisting in the fact that the velocities of two transverse sound waves, in which the directions of the wave vectors and polarizations are mutually changed, turn out to be different. The existence of such magnetoacoustic phenomena in solids is another argument for revising the basic concepts of continuum mechanics and constructing new models of media that take into account their internal structure and rotational degrees of freedom of particles. The fourth chapter in the book [24] by A.I. Akhiezer, V.G. Baryakhtar, and S.V. Peletminsky is devoted to theoretical analysis of coupled spin and elastic waves in ferromagnets.

---

[1]Magnon is a quasiparticle corresponding to a quantum of spin waves in magnetically ordered systems [20]. Magnon plays the same role with respect to spin vibrations as phonon plays with respect to crystal lattice vibrations.

3.5 Conclusions

In this chapter, the discrete and continuous models describing the dynamics of the rectangular lattice of ellipse-shaped particles with a quadratic interaction potential between them have been elaborated. Analytical dependences of the elastic wave velocities on the size of the particles and the parameters of the interaction between them have been found. The longitudinal wave velocity is shown to be always greater than the transverse wave velocity, which, in its turn, can be either larger or less than the rotational wave velocity.

In the particular case of such a lattice—a chain of anisotropic particles—the longitudinal wave velocity monotonously decreases with growing the shape parameter, whereas the transverse wave velocity monotonically increases, and both velocities tend to certain limit values depending on force constants K_1 and K_2. The rotational wave velocity has a local maximum for a certain value of f depending on the size of the particles and the parameters of the force interactions. With increasing particle size, the point of this maximum shifts to the left. For small particle sizes, changes in the wave velocities occur more smoothly than for large values of p. The longitudinal wave velocity monotonously decreases with increasing grain size d/a, the shear wave velocity monotonically increases, and the rotational wave velocity has a maximum at some d/a. For small moment interactions ($K_2 \ll K_0$), the grain size does not exert significant influence on the wave velocities.

The dispersion properties of the discrete medium have been analyzed in this chapter for various values of the lattice shape parameters. For a square lattice with round particles, there are two wave modes in the frequency ranges $0 \leq \varpi < 2.42$ and $3.09 < \varpi \leq 3.22$ (the longitudinal and transverse modes in the low-frequency region and the longitudinal and rotational modes in the high-frequency region). And all three wave modes (the longitudinal, transverse, and rotational ones) are present in the medium in the interval $2.42 \leq \varpi \leq 3.09$. In the case of a rectangular lattice of anisotropic particles, the picture is qualitatively remained, but the length of the three abovementioned intervals changes.

For any values of shape parameter f, the rotational mode has two threshold frequencies: the minimal—at zero—and the maximal—at the boundary of the Brillouin zone, and the magnitude of the minimal frequency does not depend on parameters K_1 and K_3.

When the lattice degenerates into a square lattice with round particles, the longitudinal mode remains isotropic for $\varpi < 1.5$ and the rotational mode does for $\varpi < 2.8$. In the arbitrary case, all three modes are anisotropic even in the low-frequency range.

Comparison of the dispersion properties of the hexagonal and square lattices consisting of round particles in the long-wavelength (continuum) approximation showed that the hexagonal lattice is isotropic in acoustic properties, whereas the square lattice of round particles is anisotropic. When waves propagate in the square lattice at angle $\theta = \pi/6$, the dispersion of the transverse mode is more pronounced.

In the continuum approximation, the dispersion curves of the square lattice qualitatively coincide with the experimentally obtained dependences of the energy

of magnons and phonons in FeF_2 ferromagnet on the reflected wave vector at temperature 4.2 K [19].

The results, which have been obtained in this chapter, can be used for construction of artificial periodic structures with predetermined dispersion properties, namely, taking into account the given maximal and minimal values of the rotational mode frequency, due to the relations obtained in this work, one can find values of the microstructure parameters of the medium at issue.

References

1. Fedorov, V.I.: Theory of Elastic Waves in Crystals. Nauka, Moscow, 1965; Plenum Press, New York, 1968
2. Pavlov, I.S.: Acoustic identification of the anisotropic nanocrystalline medium with non-dense packing of particles. Acoust. Phys. **56**(6), 924–934 (2010)
3. Pavlov, I.S., Potapov, A.I.: Two-dimensional model of a granular medium. Mech. Solids **42**(2), 250–259 (2007)
4. Pavlov, I.S., Potapov, A.I., Maugin, G.A.: A 2D granular medium with rotating particles. J. Solids Struct. **43**(20), 6194–6207 (2006)
5. Potapov, A.I., Pavlov, I.S., Lisina, S.A.: Acoustic identification of nanocrystalline media. J. Sound Vib. **322**(3), 564–580 (2009)
6. Pavlov, I.S., Vasiliev, A.A., Porubov, A.V.: Dispersion properties of the phononic crystal consisting of ellipse-shaped particles. J. Sound Vibr. **384**, 163–176 (2016)
7. Nowacki, W.: Theory of Micropolar Elasticity. Springer, Wien (1970)
8. Lisina, S.A., Potapov, A.I., Nesterenko, V.F.: Nonlinear granular medium with rotations of the particles. One-dimensional model. Phys. Acoust. **47**(5), 666–674 (2001)
9. Dragunov, T.N., Pavlov, I.S., Potapov, A.I.: Anharmonic interaction of elastic and orientation waves in one-dimensional crystals. Phys. Solid State. **39**, 118–124 (1997)
10. Potapov, A.I., Pavlov, I.S., Lisina, S.A.: Identification of Nanocrystalline Media by Acoustic Spectroscopy Methods. Acoust. Phys. **56**(4), 588–596 (2010)
11. Gauthier, R.D.: Experimental investigations on micropolar media. Mechanics of Micropolar Media, pp. 395–463. World Scientific, Singapore (1982)
12. Gauthier, R.D., Jashman W.E.: A quest for micropolar constants. Arch. Mech. **33**(N5), 717–737 (1981)
13. Erofeyev, V.I., Rodyushkin, V.M.: Observation of the dispersion of elastic waves in a granular composite and a mathematical model for its description. Sov. Phys. Acoust. **38**(6), 611–612 (1992)
14. Potapov, A.I., Rodyushkin, V.M.: Experimental investigation of strain waves in materials with microstructure. Acoust. Phys. **47**(1), 347–352 (2001)
15. Vakhnenko, V.A.: Diagnosis of the properties of a structurized medium by long nonlinear waves. J. Appl. Mech. Tech. Phys. **37**(5), 643–649 (1996)
16. Kittel, C.: Introduction to Solid State Physics, 8th edn. Wiley (2005)
17. Suiker, A.S.J., Metrikine, A.V., de Borst, R.: Dynamic behaviour of a layer of discrete particles. Part 1: analysis of body waves and eigenmodes. J. Sound Vibr. **240**(N1), 1–18 (2001)
18. Vinogradova, M.B., Rudenko, O.V., Sukhorukov, A.P.: Theory of Waves. Nauka, Moscow (1990). (in Russian)
19. Prokhorov, A.M.: Inelastic scattering of neutrons. Magnetic inelastic scattering. In: The physical encyclopedia in 5 volumes, vol. 3, p. 345. The Big Russian encyclopedia, Moscow (1992). (in Russian)
20. Kaganov M.I. Electrons, Phonons, Magnons, 268 pp. English Translation. Mir Publishers, Moscow (1981)

21. Barnett, S.J.: Gyromagnetic and electron-inertia effects. Rev. Mod. Phys. **7**, 129–166 (1935)
22. Vonsovsky, S.V.: Magnetism. Wiley, New York (1974)
23. Akhiezer, A.I., Bar'yakhtar, V.G., Vlasov, K.B., Peletminskii, S.V.: Rotational invariance, coupled magnetoelastic waves, and magnetoacoustic resonance. Sov. Phys. Usp. **27**, 641–642 (1984)
24. Akhiezer, A.I., Bar'yakhtar, V.G., Peletminskii, S.V.: Spin Waves. North Holland, Amsterdam (1968)

Chapter 4
Application of the 2D Models of Media with Dense and Non-dense Packing of the Particles for Solving the Parametric Identification Problems

Theoretical estimates [1] and experimental data [2–5] show that rotational waves can exist in solids in the high-frequency field ($>10^9 – 10^{11}$ Hz), where it is rather difficult to carry out acoustic experiments with the technical viewpoint. The question arises: is it possible to obtain some information about the microstructure of a medium from acoustic measurements in the low-frequency range ($10^6 –10^7$ Hz), when the rotational waves do not propagate in the medium? To this purpose, we will consider in this chapter the low-frequency approximation of Eqs. (2.8) and (3.6), in which the microrotations of the particles of the medium are not independent and are determined by the displacement field. Further, by comparing the obtained equations describing the propagation and interaction of longitudinal and transverse waves in a granular medium in the low-frequency approximation with the equations of the classical theory of elasticity, we will consider the problem of parametric identification of the developed models.

4.1 Reduced (Gradient) Models of the Theory of Elasticity

In the Cosserat theory, rotation of the Nth element of a medium is divided into two types: macrorotation θ_N (rotation of the representative volume of a medium as a whole) given by the antisymmetric (common asymmetric) part of the strain tensor and microrotation of the medium element (local rotations of microelements relative to the mass center of the representative volume), which is described by independent quantity ϕ_N [6, 7]. It can be shown that in the long-wave approximation, the potential energy density of the medium depends only on the difference between the macrorotation and microrotation angles [8], since in the small-strain approximation, the macrostrain and microstrain tensors, $e_{kl} = \frac{1}{2}\left(u_{k,l} + u_{l,k}\right)$ and $\varepsilon_{kl} = u_{k,l} + \in_{klN} \phi_N$ (here, $\in_{klN}$ is the Levi-Civita antisymmetric tensor), respectively, are not independent—they are interconnected by the following relation:

V. Erofeev et al., *Structural Modeling of Metamaterials*,

$$\varepsilon_{kl} = e_{kl} + \epsilon_{klN} \, (\theta_N - \phi_N),$$

where $\theta_N = \frac{1}{2} \, \epsilon_{Nij} \, u_{i,j}$ [6, 7]. In the coincide with the rotation of the representative volume as a solid whole, i.e., $\theta_N = \phi_N$, the microstrain and macrostrain tensors are equal: $\varepsilon_{kl} = e_{kl}$. Then, the Cosserat continuum model is simplified and called *the continuum with constrained particle rotation* or *the Cosserat pseudo-continuum* [6, 7, 9]. In this case, the microrotations of the particles of the medium are not independent and are determined by the displacement field, and the relationship between the microrotations φ and the displacements u and w can be found from the equation for the rotational mode by the successive approximation method. So, for a rectangular lattice of ellipse-shaped particles, one can obtain in the first approximation from the third Eq. (3.6):

$$\varphi(x, t) \approx \frac{\beta_1}{2\beta_2} \big(\delta_5 u_y - w_x \big). \tag{4.1}$$

It should be remarked that for the square and hexagonal lattices consisting of round particles, relation (4.1) has a simpler form:

$$\varphi(x, t) \approx \frac{1}{2} \big(u_y - w_x \big) = -\frac{1}{2} rot_z \vec{U}, \tag{4.1a}$$

where $\vec{U}$ is the displacement vector. Relation (4.1a), which relates the rotations of the particles of the medium with the vorticity of the displacement field, is a characteristic feature of the Cosserat pseudo-continuum model. Taking this relation into account leads to a "freezing" of the rotational degree of freedom. As a result, perturbations caused by microrotations do not propagate; however, microrotations affect the propagation of longitudinal and shear waves. In this case, the Lagrange function L is simplified and for a rectangular lattice of anisotropic particles looks like [10]

$$
\begin{aligned}
L = \frac{M}{2} & \left(u_t^2 + w_t^2 + \frac{R^2 \beta_1^2}{4\beta_2^2} (\delta_5 u_{yt} - w_{xt})^2 \right) \\
& - \frac{M}{2} \Big[c_1^2 (u_x^2 + \delta_1 w_y^2) + c_2^2 (w_x^2 + \delta_2 u_y^2) \\
& + \frac{R^2 \beta_1^2}{4\beta_2^2} c_3^2 ((\delta_5 u_{xy} - w_{xx})^2 + \delta_3 (\delta_5 u_{yy} - w_{xy})^2) \\
& + s^2 (u_x w_y + \delta_4 u_y w_x) - \frac{\beta_1^2}{2\beta_2} (w_x - \delta_5 u_y)^2 \Big].
\end{aligned}
\tag{4.2}
$$

In Lagrangian (4.2), there appear additional terms containing the second-order derivatives of the displacement field, which are absent in the classical theory of elasticity. They contain information about the medium microstructure. The terms with mixed derivatives with respect to time and space, u_{yt} and w_{xt}, take into account

the contribution of rotational motions into the kinetic energy, and the terms with spatial derivatives u_{xy}, w_{xx}, etc., describe the contribution of the stresses caused by bending of the lattice into the potential energy.

From Lagrange function (4.2), one can obtain the so-called *equations of the second-order gradient elasticity* [11–13] that contain terms with high-order derivatives (in this case, the fourth order):

$$u_{tt} - c_1^2 u_{xx} - (\delta_2 c_2^2 - \frac{\delta_5^2 \beta_1^2}{2\beta_2}) u_{yy} - \left(\frac{1 + \delta_4}{2} s^2 + \frac{\delta_5 \beta_1^2}{2\beta_2} \right) w_{xy}$$

$$= \frac{R^2 \beta_1^2}{4\beta_2^2} \frac{\partial}{\partial y} \left[\frac{\partial^2}{\partial t^2} (\delta_5 u_y - w_x) - c_3^2 \Delta (\delta_5 u_y - w_x) \right],$$

$$w_{tt} - \left(c_2^2 - \frac{\beta_1^2}{2\beta_2} \right) w_{xx} - \delta_1 c_1^2 w_{yy} - \left(\frac{1 + \delta_4}{2} s^2 + \frac{\delta_5 \beta_1^2}{2\beta_2} \right) u_{xy}$$

$$= -\frac{R^2 \beta_1^2}{4\beta_2^2} \frac{\partial}{\partial x} \left[\frac{\partial^2}{\partial t^2} (\delta_5 u_y - w_x) - c_3^2 \Delta (\delta_5 u_y - w_x) \right]. \tag{4.3}$$

Here, the symbol Δ denotes a differential operator $\Delta = \partial^2/\partial x^2 + \delta_3 \partial^2/\partial y^2$, which is transformed into a two-dimensional Laplacian at $\delta_3 = 1$.

For the square and hexagonal lattices consisting of round particles, the equations of the higher-order gradient theory of elasticity (4.3) take the following form:

$$u_{tt} - c_1^2 u_{xx} - \left(c_2^2 - \frac{\beta}{2} \right) u_{yy} - \left(s^2 + \frac{\beta}{2} \right) w_{xy}$$

$$= \frac{R^2}{4} \frac{\partial}{\partial y} \left[\frac{\partial^2}{\partial t^2} (u_y - w_x) - c_3^2 \Delta (u_y - w_x) \right],$$

$$w_{tt} - \left(c_2^2 - \frac{\beta}{2} \right) w_{xx} - c_1^2 w_{yy} - \left(s^2 + \frac{\beta}{2} \right) u_{xy}$$

$$= -\frac{R^2}{4} \frac{\partial}{\partial x} \left[\frac{\partial^2}{\partial t^2} (u_y - w_x) - c_3^2 \Delta (u_y - w_x) \right]. \tag{4.4}$$

From Eq. (4.4), it follows that in this low-frequency approximation, the transverse wave velocity is diminished by quantity $\beta/2$, and the coupling parameter s^2 increases by the same quantity.

It should be noted that non-neighboring interactions are frequently introduced, even if the particles are the material points. It also leads to appearance of the fourth-order derivatives in the governing equations [14]. So, the corresponding terms take into account the coupled stresses arising at the translational displacements of the particles.

Applying to Eq. (4.4), the algorithm given in Sect. 2.4.2, it is possible to derive a dispersion equation for this approximation:

$$\left(4 + R^2 k^2\right)\omega^4 - \left(R^2(c_1^2 + c_3^2)k^4 + (5c_1^2 + c_2^2)k^2\right)\omega^2$$
$$+ c_1^2(c_1^2 + c_2^2)k^4 + R^2 c_1^2 c_3^2 k^6 = 0 \tag{4.5}$$

Equation (4.5) defines the following dispersion curves:

$$\omega = \pm c_1 k \tag{4.6a}$$

for the longitudinal mode L and

$$\omega = \pm k \sqrt{\frac{8(c_1^2 + c_2^2) + c_3^2 d^2 k^2}{32 + d^2 k^2}} \tag{4.6b}$$

for the transverse mode T. These curves are presented in the normalized form in the reference frame $(k/k_0, \; \omega/\omega_0)$ in Fig. 4.1. Graphs are plotted for numerical data corresponding to cadmium crystals: $c_1/c_2 = 1.80$, $c_3/c_2 = 0.69$, $\omega_0 d/c_2 = 1.34$ (see Table 4.1 in Sect. 4.2.1). The T-mode curves have oblique asymptotes (in the dimensionless form $\frac{\omega}{\omega_0} = \pm \frac{c_3}{c_2} \frac{k}{k_0}$) and are located below the L-mode curve.

It should be noted that the dispersion properties of the equations of the low-frequency long-wavelength approximation (4.4), as in the case of the complete three-mode system (2.8), are independent on the direction of wave propagation, i.e., the crystal structure under consideration is isotropic in this approximation.

Fig. 4.1 Dispersion curves for the two-mode model (4.4)
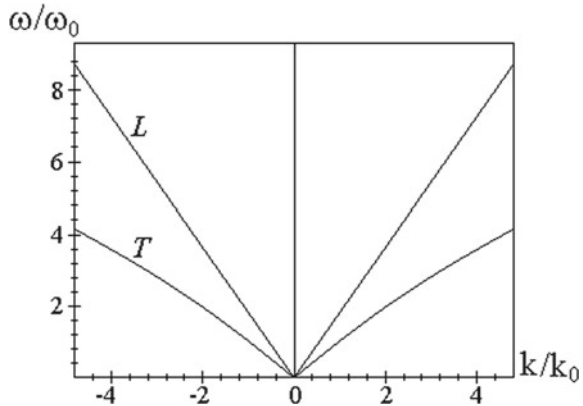
Table 4.1 Structure parameters for crystals with hexagonal symmetry

			Crystals			
	The structure parameters		Be	Cd	Mg	Zn
Experimental data	Density (kg/m^3)	ρ_V	1816	8642	1740	7140
	Elasticity constants (GPa)	C_{11}	292.3	114.5	58.6	161.1
		C_{12}	26.7	39.5	25.0	34.2
Calculated characteristics	Wave velocities (m/s)	c_1	12,687	3640	5803	4750
		c_2	11,470	2027	2223	3603
		c_3	9317	1404	880	2823
	The normalized threshold frequency of the rotational waves $\omega_0 d$ (m/s)	$\omega_0 d$	43,239	2721	12,280	11,450
	The Cosserat constants (GPa)	λ	26.7	39.5	25.0	34.2
		μ	132.8	37.5	16.8	63.5
		γ / R^2	157.7	17.0	1.35	56.9
		κ	212.2	−4.0	−16.4	58.5
	Parameters of force interactions between the particles (GPa)	K_0/a	83.81	61.28	36.05	65.28
		K_1/a	8.381	6.128	3.605	6.528
		K_2/a	74.921	−1.412	−5.79	20.654

4.2 Problems of the Material Identification

An identification problem is a construction of a mathematical model of a material on the base of experimental observations. There are structural and parametric identifications. The first identification consists in the choice of the type of equations of the mathematical model, and the second one is to find the values of the parameters that ensure consistency of the values calculated due to the model with the experimental data. The following approaches to model identification are distinguished:

1. Selection of model parameters from experimentally obtained material deformation diagrams.
2. Numerical simulation of the experiment and selection of model parameters from the condition of the best match between the calculation results and the experiment.
3. The optimization problem of selecting the constants included in the model from the condition of approaching of the analytical curve to experimental points.

Let us consider a problem of finding the values of parameters ensuring the consistency of the two-dimensional models of granular media considered above with the

classical theory of elasticity. It should be noted that the effective moduli of macroe-lasticity are determined experimentally for three-dimensional media in the frame-work of the classical theory. The role of a "bridge" from two-dimensional to three-dimensional models can be played by equations that are two-dimensional degener-ation of the classical Lame equations. Next, we will consider the parametric iden-tification problems for media with hexagonal (Sect. 4.2.1) and cubic (Sect. 4.2.2) symmetry.

4.2.1 Identification of the Medium with Hexagonal Symmetry

Lame equations for media with hexagonal symmetry have the form [15, 16]:

$$\rho_V u_{tt} = C_{11} u_{xx} + C_{66} u_{yy} + \frac{1}{2}(C_{11} + C_{12}) w_{xy},$$

$$\rho_V w_{tt} = C_{66} w_{xx} + C_{11} w_{yy} + \frac{1}{2}(C_{11} + C_{12}) u_{xy}. \tag{4.7}$$

Here, $\rho_V = \rho\sqrt{6}/2a$ is a "volume" density of the medium (note that in this case the volume of the two-dimensional unit cell is equal to $V_2 = 0.5a^2\sqrt{3}$, and the volume of the three-dimensional unit cell equals $V_3 = 0.5a^3\sqrt{2}$ [17]).

The main Eq. (2.8) for the hexagonal lattice was shown in the previous section to degenerate into Eq. (4.4) in the long-wavelength low-frequency range, and those, in turn, coincide with Eq. (4.7) up to the terms containing the fourth-order derivatives. From comparison of the coefficients in Eq. (4.7) and in the left-hand sides of Eq. (4.4), relationships can be found between the longitudinal and shear wave velocities, c_1 and c_2, and the parameters s and β, on the one hand, and the elastic constants of the second-order C_{11}, C_{12}, and C_{66}, on the other hand:

$$c_1^2 = \frac{C_{11}}{\rho_V}, \quad c_2^2 - \frac{\beta}{2} = \frac{C_{66}}{\rho_V} = \frac{C_{11} - C_{12}}{2\rho_V}. \tag{4.8}$$

Hence, it is possible to express the elastic constants in terms of the parameters of a material microstructure:

$$C_{11} = \frac{9\sqrt{2}}{8}\left(\frac{K_0 + 2K_1}{a} + \frac{2(a^2 - ad) + d^2}{a^2 - ad + d^2}\frac{K_2}{a}\right),$$

$$C_{12} = \frac{3\sqrt{2}}{8}\left(\frac{K_0 + 2K_1}{a} + \frac{2(a^2 - ad) - d^2}{a^2 - ad + d^2}\frac{K_2}{a}\right). \tag{4.9}$$

If the following conditions

(1) all the forces of interaction between the particles making up a crystal are central (i.e., they are directed along the line connecting the mass centers of the particles);

(2) the particles are spherically symmetric and are located at the centers of symmetry of the structure;

(3) in the initial state, there are no stresses in the crystal

are valid for the crystal, then six additional relations between the elastic constants (Cauchy relations) yield, which are reduced in the two-dimensional case to equality $C_{11} = 3C_{12}$ for crystals with hexagonal symmetry [18].

Obviously, in the problem under consideration, the first of the above conditions is not satisfied. However, as follows from Eq. (4.9), for media consisting of material points ($d = 0$), in which all the interaction forces are obviously central ($K_1 = K_2 = 0$), this equality is really achieved.

In a general case, the equality

$$C_{11} - 3C_{12} = \frac{9d^2\sqrt{2}}{4(a^2 - ad + d^2)}\frac{K_2}{a} \qquad (4.10)$$

is valid for particles with non-zero sizes.

Inequality $C_{11} < 3C_{12}$ is valid for many crystals with hexagonal symmetry. In this case, as follows from Eq. (4.10), the force constant K_2 is negative (see Table 4.1). Hence, parameter $\beta = \frac{3d^2\sqrt{3}}{2\rho(a^2 - ad + d^2)} K_2$ is also negative (see Eq. (2.9)). Such a situation takes place, for example, for some molecular crystals [19].

From Eqs. (4.10) and (4.9), the force constants of the model can be expressed in terms of elastic moduli as follows:

$$\frac{K_2}{a} = \frac{2(1 - p + p^2)\sqrt{2}}{9p^2}(C_{11} - 3C_{12}),$$
$$\frac{K_1}{a} = \frac{2\sqrt{2}}{9(K + 2)}\left[C_{11} + 3C_{12} + \frac{2(p - 1)}{p^2}(C_{11} - 3C_{12})\right]. \qquad (4.11)$$

Here, $K = K_0/K_1$ is the relation between the central and non-central forces of interaction, $p = d/a$ is the relative size of the particle.

Relationships (4.11) can be useful for the estimation of quantities of the force constants contained in the discrete models of microstructured media, if the macroelasticity moduli and typical particle sizes are known. And then, using the found values of the force constants K_1 and K_2, one can calculate those macroparameters of the medium, whose values are absent among the initial data of the considered problem. This is especially true for those macroparameters that are rather difficult to measure experimentally. These, in particular, include the velocity and critical frequency of the rotational wave. At present, there is no direct experimental proof of the existence of microrotational waves in solids. But it is known that spin waves in ferromagnetics [20], dispersion properties of which were considered in Sect. 3.4.2, are close analogs of microrotation waves in solids with a granular structure. So, an estimate of the values of the velocity and critical frequency of such a wave in a granular medium would be of great interest.

An expression for the velocity of a microrotation wave in the medium with hexagonal symmetry can be obtained from Eq. (4.11) and the third relation (2.9):

$$c_3 = \sqrt{\frac{1}{\rho_V(K+2)}\left(C_{11} + 3C_{12} + \frac{4p - 2 + K}{2p^2}(C_{11} - 3C_{12})\right)}. \qquad (4.12)$$

Values of the longitudinal, c_1, and transverse, c_2, wave velocities have been calculated from Eq. (4.8) with account of Eq. (2.12):

$$c_1 = \sqrt{\frac{C_{11}}{\rho_V}}, \quad c_2 = \sqrt{\frac{C_{11} - 2C_{12}}{\rho_V}}, \qquad (4.13)$$

From Eqs. (2.12) and (4.13), it follows that

$$\beta = \frac{C_{11} - 3C_{12}}{\rho_V}. \qquad (4.14)$$

Hence, according to Eq. (2.10),

$$\omega_0 d = 4\sqrt{|C_{11} - 3C_{12}|/\rho_V}. \qquad (4.15)$$

Theoretical estimates of the value of the velocity of a rotational wave, its normalized critical frequency $\omega_0 d$ and the parameters of force interactions between the particles have been obtained for some crystals with hexagonal symmetry (beryllium (Be), cadmium (Cd), zinc (Zn) from known experimental data (the elasticity constants C_{11}, C_{12}, and C_{44} as well as the density ρ_V at normal temperature [21]). These estimates are listed in Table 4.1. The calculations were carried out for $p = 0.9$ and $K = 10$ (for which the central interactions dominate) due to formulas (4.12), (4.15), and (4.11). Analysis showed that for $0.9 < p < 0.99$ quantities c_3, K_0, K_1, and K_2 varied by less than 10%.

It is clear from Table 4.1 that the rotational wave velocity is minimal for all the considered materials, and the threshold frequencies lie in the hypersonic range. Therefore, if it is to be supposed that the size of a crystal grain $d = 10\,\text{nm} = 10^{-8}\,\text{m}$, then for hypothetical nanocrystalline material with elasticity constants and density, as for cadmium, $\omega_0 \approx 2.721 \times 10^{11}\text{s}^{-1}$, and for nanomaterial with parameters of beryllium $\omega_0 \approx 4.324 \times 10^{12}\text{s}^{-1}$. At $d = 100\,\text{nm} = 10^{-7}\,\text{m}$, the critical frequency decreases by an order of magnitude. Therefore, in the sonic and ultrasonic ranges, the microrotation waves can be neglected. However, their presence can be of principal importance for high-frequency processes.

4.2.2 Identification of the Medium with Cubic Symmetry

For media with cubic symmetry, Lame equations have the form [15, 16]:

$$\rho_V u_{tt} = C_{11}u_{xx} + C_{44}u_{yy} + (C_{12} + C_{44})w_{xy},$$
$$\rho_V w_{tt} = C_{44}w_{xx} + C_{11}w_{yy} + (C_{12} + C_{44})u_{xy}. \qquad (4.16)$$

Here, $\rho_V = \rho/a$ is a "volume" density of the medium.

In order to compare Eqs. (4.16) and (4.4), we neglect the fourth-order derivatives in Eq. (4.4). As a result, a relationship is established between the longitudinal and shear wave velocities, c_1 and c_2, and the parameters s and β, on the one hand, and the elastic constants of the second-order C_{11}, C_{12} and C_{44}, on the other hand:

$$c_1^2 = \frac{C_{11}}{\rho_V}, \quad c_2^2 - \frac{\beta}{2} = \frac{C_{44}}{\rho_V}, \quad s^2 + \frac{\beta}{2} = \frac{C_{12} + C_{44}}{\rho_V}. \qquad (4.17)$$

It should be noted that equalities (4.17) differ from the classical ones by the presence of the dispersion parameter $\beta = \frac{2d^2 K_2}{\rho(d^2 + (a\sqrt{2} - d)^2)}$ in them (see Eq. (3.15)). This parameter is proportional to the square of the critical frequency of the rotational waves: $|\beta| = \omega_0^2 d^2/16$ (see Eq. (2.10)). For degeneration into the classical case (i.e., $\beta = 0$) it is enough to fulfill at least one of two conditions: $d = 0$ (point particles) or $K_2 = 0$ (non-central interactions between the particles are not taken into account).

With the allowance for the relation $c_2^2 = \beta + s^2/2$ Eq. (4.17) can be rewritten in the form:

$$c_1^2 = \frac{C_{11}}{\rho_V}, \quad c_2^2 = \frac{2C_{44} - C_{12}}{\rho_V}, \quad s^2 = \frac{2C_{12}}{\rho_V}, \beta = \frac{2(C_{44} - C_{12})}{\rho_V}. \qquad (4.18)$$

The dependences being inverse to Eq. (4.18) have the form:

$$C_{11} = \rho_V c_1^2, C_{12} = \rho_V s^2/2, C_{44} = \rho_V (2c_2^2 + s^2)/4. \qquad (4.19)$$

Using relations (3.15) and (4.19), it is possible to express the elastic constants in terms of the microstructure parameters of the material:

$$C_{11} = \frac{K_0 + 2K_1 + K_3}{a} + \frac{2(a\sqrt{2} - d)^2}{d^2 + (a\sqrt{2} - d)^2}\frac{K_2}{a},$$
$$C_{12} = \frac{K_3}{a}, C_{44} = \frac{d^2}{d^2 + (a\sqrt{2} - d)^2}\frac{K_2}{a} + \frac{K_3}{a}. \qquad (4.20)$$

It follows from Eq. (4.20) that for media with cubic symmetry and consisting of material points ($d = 0$), all the interaction forces between which are central, the equality $C_{12} = C_{44}$ is fulfilled, which is the Cauchy relation for crystals with cubic

symmetry [18]. In a general case, for particles with non-zero sizes, the following relation is valid:

$$C_{44} - C_{12} = \frac{d^2}{d^2 + (a\sqrt{2} - d)^2} \frac{K_2}{a} \tag{4.21}$$

It is seen from Eq. (4.21) that $C_{44} > C_{12}$ for $K_2 > 0$. This fact is confirmed by experimental data for many crystals with cubic symmetry (see Table 4.2). However, there also exist materials, for which the ratio $C_{44} < C_{12}$ is satisfied. In such cases, the force constant K_2 and the parameter β are negative (see Eq. (4.18)). Such a situation is observed, for example, in some molecular crystals [19], and a negative rigidity of connections is present, in particular, in Ref. [22]. The Cauchy relation fairly good fulfill for alkali-galloid crystals (KCl, NaBr). For metals, the Cauchy relation is poorly performed, because the forces of interaction between atoms in metals are not central [23]. This, apparently, indicates the necessity to take into account the moment interactions between particles in metals.

Table 4.2 Structure parameters for crystals with cubic symmetry

	The structure parameters		Crystals			
			LiF	NaF	NaBr	C_{60}
Experimental data	Density(kg/m^3)	ρ_V	2600	2800	3200	1720
	Elasticity constants (GPa)	C_{11}	113.00	97.00	32.55	14.9
		C_{12}	48.00	25.60	13.14	6.9
		C_{44}	63.00	28.00	13.26	8.1
Calculated characteristics	Wave velocities (m/s)	c_1	6593	5890	3190	2943
		c_2	5477	3295	2045	2325
		v_{tr}	3536	3571	1741	1525
		c_3	5659	2896	1092	2036
	The normalized threshold frequency of the rotational waves $\omega_0 d$ (m/s).	$\omega_0 d$	13,587	5237	1095	4781
	The Cosserat constants (GPa)	λ	48.00	25.60	13.14	6.9
		μ	63.00	28.00	13.26	8.1
		γ/R^2	83.28	23.49	3.81	7.1
		κ	30.00	4.8	0.24	2.4
	Parameters of force interactions between the particles (GPa)	K_0/a	46.01	58.19	16.11	6.01
		K_1/a	4.601	5.819	1.611	0.601
		K_2/a	19.897	3.183	0.159	1.592
		K_3/a	48.00	25.60	13.14	6.90

In order to estimate the values of the force constants included in discrete models of media with microstructure, from relations (4.21) and (4.20) by the known macroelasticity moduli and the typical particle size, like for a medium with hexagonal symmetry (see Sect. 4.2.1), one can obtain equalities similar to (4.11):

$$\frac{K_3}{a} = C_{12}, \frac{K_2}{a} = (C_{44} - C_{12})\left(1 + \left(\frac{\sqrt{2}}{p} - 1\right)^2\right),$$

$$\frac{K_1}{a} = \frac{1}{K+2}\left[C_{11} - C_{12} - 2(C_{44} - C_{12})\left(\frac{\sqrt{2}}{p} - 1\right)^2\right]. \tag{4.22}$$

In addition, the force parameters can also be expressed in terms of the velocities of various elastic waves—for this, it is enough to find the dependences of the elastic constants on these velocities. In the square lattice of round particles, there are three independent quantities among the translational wave velocities—according to the number of elastic constants of the second order. Account of relation $C_{11} - C_{12} = 2\rho_V v_{110}^2$ [15], where v_{110} is the shear wave velocity in the crystallographic direction <110>, leads to the following equality:

$$s^2 = 2c_1^2 - 4v_{110}^2. \tag{4.23}$$

Hence, Eq. (4.19) can be rewritten in the form:

$$C_{11} = \rho_V c_1^2, C_{12} = \rho_V (c_1^2 - 2v_{tr}^2),$$
$$C_{44} = \rho_V (c_1^2 + c_2^2 - 2v_{110}^2)/2. \tag{4.24}$$

Formulas (4.24) demonstrate how to determine the effective elastic moduli of a crystalline medium from acoustic measurements. As a result, from Eqs. (4.22) and (4.24), we derive the following dependences of the force parameters on the elastic wave velocities and the size of round particles in the square lattice [1]:

$$\frac{K_3}{a} = \rho_V (c_1^2 - 2v_{110}^2),$$

$$\frac{K_2}{a} = \frac{\rho_V}{2}\left((c_2^2 - c_1^2 + 2v_{110}^2)\left(1 + \left(\frac{\sqrt{2}}{p} - 1\right)^2\right)\right),$$

$$\frac{K_1}{a} = \frac{\rho_V}{K+2}\left[2v_{110}^2 + \left(\frac{\sqrt{2}}{p} - 1\right)^2 (c_1^2 - c_2^2 - 4v_{110}^2)\right]. \tag{4.25}$$

By finding the inverse dependences to Eq. (3.10), it is possible to obtain the similar relations for a rectangular lattice of ellipsoidal particles [10]:

$$K_3 = \frac{Ms^2(1+f^2)}{4a^2 f} = \frac{M(1+f^2)(c_2^2 - \beta_1)}{2a^2 f^2},$$

$$K_2 = \frac{M\beta_1(f^2 p^2 + (\sqrt{2} - p)^2)}{2a^2 f^2 p^2},$$

$$K_0 + 2K_1 = \frac{M}{a^2}\left[c_1^2 - \frac{\beta_1(\sqrt{2} - p)^2}{f^2 p^2} - \frac{s^2}{2f} \right]$$

$$= \frac{M}{a^2}\left[c_1^2 - \frac{c_2^2(\sqrt{2} - p)^2 + f s^2(p\sqrt{2} - 1)}{f^2 p^2} \right]. \tag{4.26}$$

Expressions (4.26) and (3.10) establish the correspondence between the micro-model parameters and the macrocharacteristics of the anisotropic medium. This relationship can be used to identify microstructured materials according to data of acoustic experiments.

Due to Eqs. (4.22), (4.25), and (4.26), as well as the dependences of the rotational wave velocity c_3 on the microstructure parameters (3.15) and (3.10), it is possible to express c_3 through experimentally determined quantities. So, for a rectangular lattice, the microtation wave velocity has the form:

$$c_3 = \sqrt{\frac{2}{K+2}\left(c_1^2 - \frac{c_2^2}{f^2} + \frac{(2c_2^2 - f s^2)(2p\sqrt{2} + K)}{2f^2 p^2} \right)} \tag{4.27}$$

And in the case of a square lattice ($f = 1$), it is expressed in one of the following two ways:

$$c_3 = \sqrt{\frac{2}{K+2}\left(c_1^2 - c_2^2 + \frac{(c_2^2 - c_1^2 + 2v_{110}^2)(2p\sqrt{2} + K)}{p^2} \right)} \tag{4.28}$$

or

$$c_3 = \sqrt{\frac{2}{\rho_V(K+2)}\left[C_{11} + C_{12} - 2C_{44} + \frac{K + 4p\sqrt{2} - 2}{p^2}(C_{44} - C_{12}) \right]} \tag{4.29}$$

Depending on the initial data of the problem to be solved, it is possible to estimate the rotational wave velocity in various crystals with cubic symmetry either by formula (4.28) or by expression (4.29). Let us suppose that elastic constants are given. Then, the elastic wave velocities are determined by the equalities inverse to Eq. (4.24):

$$c_1 = \sqrt{\frac{C_{11}}{\rho_V}}, \quad c_2 = \sqrt{\frac{2C_{44} - C_{12}}{\rho_V}}, \tag{4.30}$$

$$v_{tr} = \sqrt{(C_{11} - C_{12})/2\rho_V}.$$

Table 4.2 contains the theoretical estimates of the values of the rotational wave velocity and the normalized threshold frequency

$$\omega_0 d = 4\sqrt{2|C_{44} - C_{12}|/\rho_V} \tag{4.31}$$

for some crystals with cubic symmetry (lithium fluoride (LiF), sodium fluoride (NaF), sodium bromide (NaBr), and fullerite (C_{60}). In addition, this table contains the values of the elasticity constants C_{11}, C_{12}, and C_{44}, as well as the density ρ_V taken from the known experimental data (see Ref. [21] for alkali-galloid crystals at normal temperature) and the theoretical data (see Ref. [24], where the modified Lennard-Jones intermolecular potential was used to estimate the elastic moduli of sc-lattice of fullerite C_{60} at low temperatures). The rotational wave velocity has been calculated by the formula (4.29), the elastic wave velocities along directions <100> and <110>—by Eq. (4.30) and, finally, the force interaction parameters—by Eq. (4.22). All calculations have been performed for $p = 0.9$ and $K = 10$ (central interactions dominate).

Table 4.2 shows that for most of the considered materials, the rotational wave velocity is minimal and the threshold frequencies lie in the hypersonic range. So, if we take the crystallite size equal to $d = 10$ nm $= 10^{-8}$ m, then for a hypothetical nanocrystalline material with elastic constants and density, like for sodium bromide, we get $\omega_0 \approx 1.095 \times 10^{11} s^{-1}$, and $\omega_0 \approx 1.359 \times 10^{12} s^{-1}$ for a nanomaterial with lithium fluoride parameters. In order of magnitude, these values coincide with theoretical estimates of the critical frequency of rotational waves in crystals with a hexagonal lattice (see Sect. 4.2.1) and experimentally determined values of such a frequency in organic crystals [2–5, 25] (for example, in a naphthalene crystal $\omega_0 \approx 6 \times 10^{11} s^{-1}$). Therefore, as for media with hexagonal symmetry, the account of microrotational waves is necessary for studying high-frequency processes, while in the sound and ultrasonic ranges, they can be neglected.

4.3 Comparison with the Cosserat Continuum Theory

The practical problem of identifying the Cosserat continuum used for modeling of a real heterogeneous material is still relevant [26–28]. However, reliable and confirmed by different researchers results on determining the model parameters are quite rare even in the simplest case of the elastic isotropic Cosserat continuum [29]. For solving this problem, we propose to apply the following procedure for evaluating the medium macroparameters that is based on the structural modeling method.

Let us compare Eq. (3.6) with the dynamic equations for the two-dimensional Cosserat continuum [6–8, 30] consisting of centrally symmetric particles. Lagrange function for such a continuum has the form

$$
\begin{aligned}
L = {} & \frac{\rho_V}{2}\left(u_t^2 + w_t^2 + R^2\varphi_t^2\right) \\
& - \frac{1}{2}\Bigg[B(u_x^2 + w_y^2) + \left(\mu + \frac{\kappa}{2}\right)(w_x^2 + u_y^2) + \gamma(\varphi_x^2 + \varphi_y^2) \\
& + \left(\lambda + \mu - \frac{\kappa}{2}\right)(u_x w_y + u_y w_x) + 2\kappa(w_x - u_y)\varphi + 2\kappa\varphi^2\Bigg].
\end{aligned}
\tag{4.32}
$$

Here, B is a macroelasticity constant of the second order, λ and μ are Lame constants, and γ and κ are phenomenological constants to be found from experiments. In the case of the isotropic Cosserat continuum,

$$
B = \lambda + 2\mu.
\tag{4.33}
$$

In order to compare Lagrange functions (4.32) and (4.2), we will put in Eq. (4.2) all $\delta_i = 1$, $\beta_1 = \beta_2 = \beta$ and neglect the fourth-order derivatives in it. As a result, the acoustic characteristics of a medium can be expressed in terms of the constants of the Cosserat theory:

$$
c_1^2 = \frac{B}{\rho_V}, \quad c_2^2 = \frac{2\mu + \kappa}{2\rho_V}, \quad c_3^2 = \frac{\gamma}{\rho_V R^2}, \quad s^2 = \frac{2\lambda + 2\mu - \kappa}{2\rho_V}, \quad \beta = \frac{\kappa}{\rho_V},
\tag{4.34}
$$

and for a medium with hexagonal symmetry the first Eq. (4.34) taking relation (4.33) into account, takes on the form $2c_2^2 - s^2 = 2\beta$. The dependence inverse to Eq. (4.34), taking into account the relationship $2c_2^2 - s^2 = 2\beta$, has the form

$$
\begin{aligned}
& B = \rho_V c_1^2 = C_{11}, \ \lambda = \rho_V(c_2^2 - \beta) = C_{12}, \ \mu = \rho_V\left(c_2^2 - \frac{\beta}{2}\right) = C_{44}, \\
& \kappa = \rho_V\beta = 2(C_{44} - C_{12}), \ \gamma = \rho_V R^2 c_3^2
\end{aligned}
\tag{4.35a}
$$

for the square lattice and

$$
\begin{aligned}
& \lambda = \frac{\rho_V(c_1^2 - c_2^2)}{2} = C_{12}, \quad \mu = \frac{\rho_V(c_1^2 + c_2^2)}{4} = \frac{C_{11} - C_{12}}{2}, \\
& \kappa = \rho_V\beta = \frac{\rho_V}{2}(3c_2^2 - c_1^2) = C_{11} - 3C_{12}, \quad \gamma = \rho_V R^2 c_3^2
\end{aligned}
\tag{4.35b}
$$

for the hexagonal lattice, taking into account the relation $s^2 = c_1^2 - c_2^2$.

It follows from Eqs. (4.35a) and (4.35b) that not all the constants of the Cosserat medium can be expressed in terms of the elasticity constants of the second order—additional assumptions about the values of $K = K_0/K_1$ and $p = d/a$ are necessary for parameter γ (see Sect. 4.2). It is interesting to note that Eqs. (4.35a) and (4.35b) imply a relation $\mu - \lambda = \kappa/2$ indicating that in the proposed models the Lamé constants λ and μ are interlinked through the parameter κ, which is responsible for the interaction between the microrotations of the particles and shift strains. The value of a threshold frequency of a microrotational wave also depends on parameter κ: $\omega_0 = \sqrt{2|\kappa|/(\rho_V R^2)} = 4\sqrt{|\kappa|/(\rho_V d^2)}$. We also note that the averaged elastic Lamé constants λ and μ [31] are often used in the mechanics of materials to describe anisotropic media.

Relations (4.35a) and (4.35b) enable one to obtain quantitative estimations for the coefficients, which are included in decomposition of the internal energy in the Cosserat theory, for various materials (see, for example, Tables 4.1 and 4.2). Earlier performance of such estimates was impossible without the structural modeling method. It should be noted that similar relations were obtained in Ref. [30]; however, in that work, the dependence of the material constants on the particle size remained unclear.

4.4 Influence of the Microstructure on the Poisson's Ratio of an Isotropic Medium

One of the most important characteristics of elasticity of a material is the Poisson's ratio ν, which is a relation of transverse compression to elongation in the case of pure tension. From the classical theory of elasticity, it is known that theoretically justified values of the Poisson's ratio lie in the range $-1 \leq \nu \leq 0.5$ [32]. The upper limit corresponds to incompressible materials (particularly, rubber), which save their volume during deformation, but their shape changes substantially. The lower limit corresponds to materials, which geometric proportions are constant during deformation, but their volume varies.

Materials with negative Poisson's ratio ν are of special interest. Porous media, granular materials, polymers, composites, and crystalline media are good examples of such materials [32, 33]. The first reliable mention of the experimentally observed negative values of Poisson's ratio (quartz crystals at high temperatures) refers to 1962 [34]. At present, a term *auxetics* (from the Greek "auxetos"—"swelling") is widely used for these materials. This term was proposed by K. Evans in 1991 [35]. Nowadays, in the scientific literature, there appear rather many publications about nanomaterials (see, for example, [36, 37]) and porous materials possessing auxetic properties. Advantages of such materials are their high consumer values (particularly, small density and good insulation properties). An article [32] is devoted to a review of literature published on the subject at the beginning of the twenty-first century.

In addition, many rocks also have a negative Poisson's ratio. Thus, the data processing for about a hundred samples of fractured materials (rocks) carried out in Ref. [38] revealed that about 40% of the examined samples have a negative Poisson's ratio that is assumed as a rare exception. The discovered properties of real cracks based on the auxetic material model explain this fact and greatly change the conclusions about the effect of fracturing on the elastic wave velocities used in seismic exploration. In particular, this model drastically improves the accuracy of predicting the values of elastic moduli due to data from one pressure range to a significantly different one (for example, from <20–30 MPa to ~100 MPa that is not available to traditional models).

However, the description of auxetic properties is impossible without a mathematical model. In the models contained in modern publications, the Poisson's ratio can be negative due to the anisotropy of the elastic properties of a material [39, 40], the presence of rotating rigid links [41, 42], polydispersity [43], fractal structure [44], and the application of negative hydrostatic pressure [45, 46].

In this section, on the base of the model considered in Chap. 2, we will show that the Poisson's ratio of a medium with hexagonal symmetry can be negative for some values of the parameters of its internal structure.

In an isotropic medium, the Poisson's ratio ν is calculated as follows [7, 23]:

$$\nu = \frac{\lambda}{2(\lambda + \mu)}. \tag{4.36}$$

For a medium with hexagonal symmetry, as follows from (4.35b),

$$\lambda = C_{12}, \mu = \frac{C_{11} - C_{12}}{2},$$

therefore,

$$\nu = \frac{C_{12}}{C_{11} + C_{12}}. \tag{4.37}$$

Substitution of Eqs. (4.9) into (4.37) leads to the following expression for the Poisson's ratio:

$$\nu = \frac{1}{4}\left(1 - \frac{3p^2}{2\eta(1 - p + p^2) + (2 - p)^2}\right), \tag{4.38}$$

where $\eta = (K_0 + 2K_1)/K_2$ is the dimensionless force parameter. Obviously, for $p \to 0$ (i.e., when the particles degenerate into material points), the property of auxeticity of the medium disappears and $\nu \to 1/4$. It should be emphasized that in this section, the value of the Poisson's ratio is analyzed not for the two-dimensional lattice considered in Chap. 2 (in a two-dimensional hexagonal lattice consisting of material points $\nu = 1/3$ [17]), but for a three-dimensional medium. Such an analysis

is carried out by extrapolating the two-dimensional model to the three-dimensional case. As a result, expressions (4.37) and (4.38) are obtained.

As it follows from Eq. (4.38), in the model at issue, negative values of the Poisson's ratio $(-1 \leq \nu \leq 0)$ are observed in the interval

$$\frac{-0,2p^2 + 2p - 2}{p^2 - p + 1} \leq \eta \leq \frac{p^2 + 2p - 2}{p^2 - p + 1}, \tag{4.39a}$$

and positive ones $(0 < \nu \leq 0.5)$—at

$$\eta \leq -2 \text{ or } \eta > \frac{p^2 + 2p - 2}{p^2 - p + 1}. \tag{4.39b}$$

For other values of η, the proposed model should be assumed inapplicable, since in this case, the values of the Poisson's ratio lie outside the mentioned above range $-1 \leq \nu \leq 0.5$.

In order to compare theoretical calculations with experimental data, it is sometimes more convenient to use not the relative particle size $p = d/a$, but the parameter q characterizing the porosity of the medium and defined as the ratio of the volume of voids to the representative volume of the medium:

$$q = 1 - \frac{\pi d^2}{2a^2\sqrt{3}}. \tag{4.40}$$

The effective linear density of the medium $\rho = 2M/(a^2\sqrt{3})$, equal to the mass of the substance per unit cell area, is related to the porosity and linear density of the grains, $\rho_1 = 4M/(\pi d^2)$, by the expression $\rho = (1 - q)\rho_1$. The porosity value in the considered medium lies in the range from q_{min} achieved at $d = a$ (grains touch each other) to q_{max}, which corresponds to the case, when $d = 0$ (a medium consists of material points). Thus, $q_{min} = 1 - \frac{\pi}{2\sqrt{3}} \approx 0.093$ and $q_{max} = 1$. Taking into account the relation, which is inverse to Eq. (4.40),

$$p^2 = \frac{2\sqrt{3}(1 - q)}{\pi},$$

expression (4.38) can be rewritten in the form:

$$\nu = \frac{1}{4}\left(1 - \frac{3\sqrt{3}(1 - q)}{\sqrt{3}(1 - q)(1 + 2\eta) + (\eta + 2)(\pi - \sqrt{2\pi\sqrt{3}(1 - q)})}\right). \tag{4.41}$$

The dependence (4.41) of the Poisson's ratio ν on the porosity q for fixed values of the dimensionless force parameter η is shown in Fig. 4.2a (curve 1 corresponds to
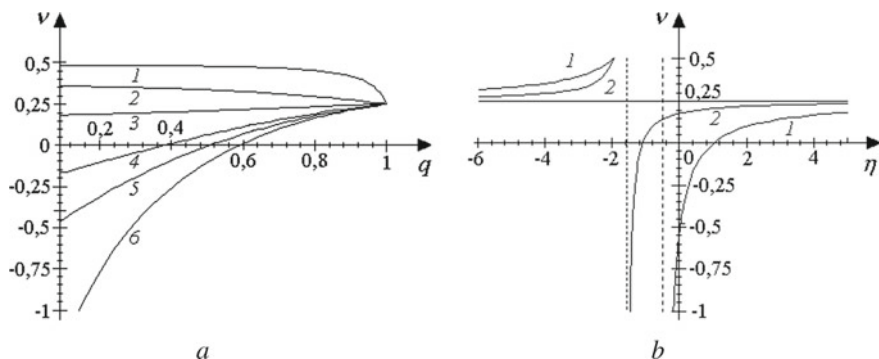
Fig. 4.2 Poisson's ratio versus the porosity of the material (**a**) and the parameter of force interactions (**b**)

Table 4.3 Relationship between the Poisson's ratio, the force parameter η and porosity of the medium (the particle size)

The relative size of particles, p	The medium porosity, q	Values of Poisson's ratio ν	
		$-1 \le \nu \le 0$	$0 < \nu \le 0.5$
0.5	0.773	$-1.4 \le \eta \le -1$	$\eta \le -2$ or $\eta > -1$
0.9	0.265	$-0.398 \le \eta \le 0.670$	$\eta \le -2$ or $\eta > 0.670$
1	0.093	$-0.2 \le \eta \le 1$	$\eta \le -2$ or $\eta > 1$

$\eta = -2.1$; $2 - \eta = -4$; $3 - \eta = 5$; $4 - \eta = 0.4$; $5 - \eta = 0.03$; $6 - \eta = -0.25$) and the dependence of ν on η is plotted at fixed values of porosity in Fig. 4.2b (curves *1* correspond to $q = q_{\min} \approx 0.093$ and curves *2*—to $q = 0.8$). In this figure, all the curves have the same horizontal asymptote $\nu = 0.25$ corresponding to $q = 1$. The vertical asymptotes for a graph of function $\nu(\eta)$ at fixed values of porosity q are found by the formula

$$\eta = \frac{-(\sqrt{2\pi} - \sqrt{(1-q)\sqrt{3}})^2}{(\sqrt{2\sqrt{3}(1-q)} - \sqrt{\pi})^2 + \sqrt{2\pi\sqrt{3}(1-q)}}. \tag{4.42}$$

It follows from Eq. (4.42) that all vertical asymptotes of the function graph $\nu(\eta)$ are located in the left half plane $\eta < 0$.

From Fig. 4.2, it is visible that the Poisson's ratio can be negative for small (in magnitude) η and q, i.e., when the moment interactions are small compared to the central ones ($K_2 < K_0$) and the representative volume of the medium is sufficiently large in comparison with the volume of voids. If η satisfies conditions (4.39b), then the Poisson's ratio is positive for any values of q, moreover, function $\nu(q)$ decreases, when $\eta < 0$, and increases, if $\eta > 0$ (see curves 1–3 in Fig. 4.2a).

For various values of the relative particle size and porosity, Table 4.3 indicates for which η the Poisson's ratio is negative and for which it is positive. The corresponding values of η have been calculated using formulas (4.39a) and (4.39b). Note that $\nu = 0.25$ for $p = 0$ and the condition $0 < \nu \leq 0.5$ is satisfied for any η. But if $\eta = -2$, then $\nu = 0.5$ for any p.

4.5 Influence of the Microstructure on the Poisson's Ratios of the Anisotropic Medium

As distinct from isotropic medium, anisotropic material has several Poisson's ratios, since tension or compression along one axis can substantially differ from tension or compression along an other axis. Different Poisson's ratios are denoted by indices containing the designations of two axes: The first axis is that along which the initial tension or compression occurs and the second one is those along which the response is observed. It should be noted that values of some Poisson's ratios can go beyond the known interval $(-1; 0.5)$ [32, 47], however, the average value of the Poisson's ratios will be sure to locate in this interval.

So, in an anisotropic monocrystalline material with a cubic lattice, the Poisson's ratios in special crystallographic directions <100>, <110>, and <111> are found by known relations [48, 49]:

$$\nu_{<100,\,001>} = \frac{C_{12}}{C_{11} + C_{12}}, \; \nu_{<110,\,001>} = \frac{4C_{12}C_{44}}{2C_{11}C_{44} + (C_{11} - C_{12})(C_{11} + 2C_{12})}, \tag{4.43}$$

$$\nu_{<110,1\bar{1}0>} = \frac{(C_{11} - C_{12})(C_{11} + 2C_{12}) - 2C_{11}C_{44}}{(C_{11} - C_{12})(C_{11} + 2C_{12}) + 2C_{11}C_{44}},$$
$$\nu_{<111,111>} = \frac{C_{11} + 2C_{12} - 2C_{44}}{2(C_{11} + 2C_{12} + C_{44})}. \tag{4.44}$$

Obviously, if the Poisson's ratios (4.43) are always greater than zero for positive elasticity constants, then the Poisson's ratios (4.44) can take on negative values. Substitution of expressions (4.19) into formulas (4.44) gives a possibility to analyze influence of the medium microstructure on the corresponding anisotropic Poisson's ratios. For simplicity, we will also take $K_1 = 0$. Dependences of the Poisson's ratios $\nu_1 = \nu_{<110,\,1\bar{1}0>}$ и $\nu_2 = \nu_{<111,\,111>}$ on the relative size of the particles d/a are plotted for various values of the parameters of force interactions K_2/K_0 and K_3/K_0 in Figs. 4.3 and 4.4.

From Figs. 4.3 and 4.4, it follows that the Poisson's ratios ν_1 and ν_2 monotonically decrease with increasing the particle size and, consequently, the large particle size $d/a \to 1$ contributes to negative values of ν_1 and ν_2 [50].

Note that $\nu_1 < 0$ for
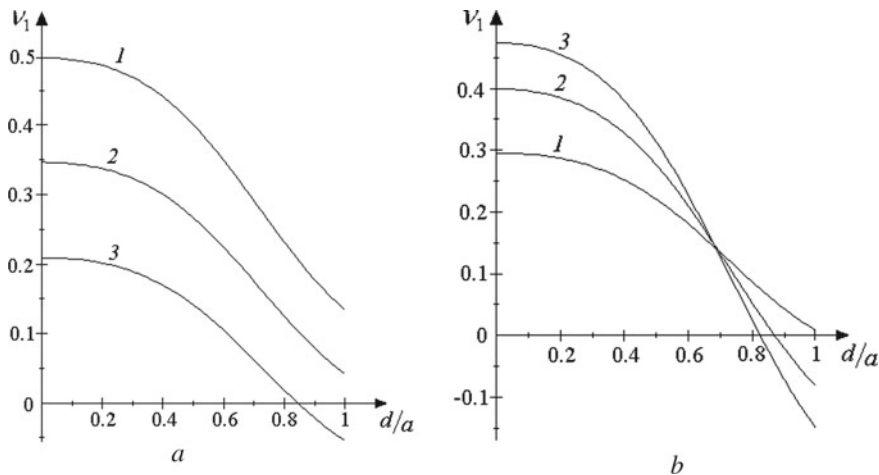
Fig. 4.3 Dependence of the Poisson's ratio $v_1 = v_{<110, \, 1\bar{1}0>}$ on the relative size of the particles: **a** for $K_2/K_0 = 0.3$ (1—$K_3/K_0 = 0.37$; 2—$K_3/K_0 = 0.6$; 3—$K_3/K_0 = 0.9$); **b** for $K_3/K_0 = 0.7$ (1—$K_2/K_0 = 0.3$; 2—$K_2/K_0 = 0.6$; 3—$K_2/K_0 = 0.9$)
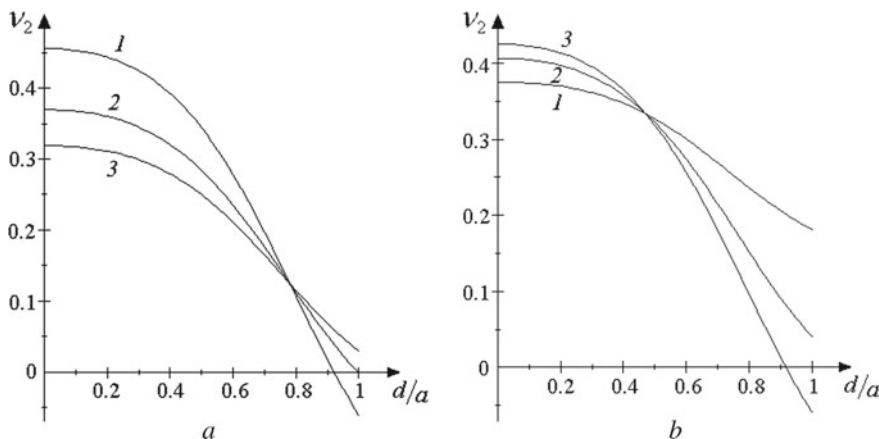
Fig. 4.4 Dependence of the Poisson's ratio $v_2 = v_{<111, \, 111>}$ on the relative size of the particles: **a** for $K_2/K_0 = 1$ (1—$K_3/K_0 = 0.1$; 2—$K_3/K_0 = 0.4$; 3—$K_3/K_0 = 0.7$); **b** for $K_3/K_0 = 0.2$ (1—$K_2/K_0 = 0.3$; 2—$K_2/K_0 = 0.7$; 3—$K_2/K_0 = 1.1$)

$$K_0 + \frac{4\left(1 - p\sqrt{2}\right)K_2}{p^2 + \left(\sqrt{2} - p\right)^2} < \frac{2K_3^2\left(p^2 + \left(\sqrt{2} - p\right)^2\right)}{(K_0 + K_3)\left(p^2 + (\sqrt{2} - p)^2\right) + 2(\sqrt{2} - p)^2 K_2}.$$

$$(4.45)$$

Substitution of the maximum possible value of the relative particle size $p = d/a$ $= 1$ into (4.45) gives the following inequality:

$$2K_{30}^2 + \left(\sqrt{2}K_{20} - 1\right)K_{30} + (\sqrt{2} - 1)K_{20}^2 + \left(\frac{3\sqrt{2}}{2} - 1\right)K_{20} - 1 > 0, \quad (4.46)$$

where $K_{20} = K_2/K_0$ and $K_{30} = K_3/K_0$. In fact, inequality (4.46) is a necessary condition for negativity of ν_1.

An analysis of the expression (4.46) shows that in cases, when $K_{20} < -9.69$ or $K_{20} > 0.71$, $\nu_1 < 0$ for any values of K_{30}. If, then at or, where. But if $-9.69 < K_{20} < 0.71$, then $\nu_1 < 0$ for $K_{30} < \frac{1}{4}\left(1 - \sqrt{2}K_{20} - \sqrt{F}\right)$ or $K_{30} > \frac{1}{4}\left(1 - \sqrt{2}K_{20} + \sqrt{F}\right)$, where $F = (10 - 8\sqrt{2})K_{20}^2 + (8 - 14\sqrt{2})K_{20} + 9$. For example, if $K_{20} = 0.3$, then $F \approx 5.34$ and $K_{30} < -0.43$ or $K_{30} > 0.72$. If $K_{20} = 0.5$, then $F \approx 2.77$ and $K_{30} < -0.34$ or $K_{30} > 0.49$. Finally, if $K_{20} = 0.6$, then $F \approx 1.45$ and $K_{30} < -0.26$ or $K_{30} > 0.34$. These results are confirmed by the shown in Fig. 4.5 dependences of ν_1 on the parameters of force ($K_{30} = K_3/K_0$) and moment ($K_{20} = K_2/K_0$) interactions [50].

In its turn, $\nu_2 < 0$ when

$$(K_0 + K_3)\left(p^2 + (\sqrt{2} - p)^2\right) < 4\sqrt{2}\left(p - 1/\sqrt{2}\right)K_2. \quad (4.47)$$
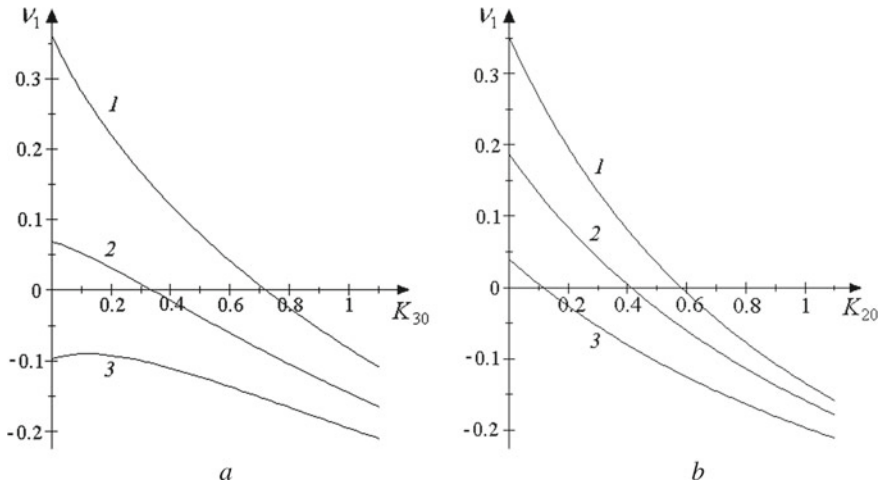
Fig. 4.5 Dependence of the Poisson's ratio $\nu_1 = \nu_{<110,\ 1\bar{1}0>}$ for $d/a = 1$ on the parameters of force **a** and moment **b** interactions: a—$K_{20} = 0.3$ (curve 1), $K_{20} = 0.6$ (curve 2), $K_{20} = 0.9$ (curve 3); 6—$K_{30} = 0.37$ (curve 1), $K_{30} = 0.6$ (curve 2), $K_{30} = 0.9$ (curve 3)

Table 4.4 Poisson's ratios for crystals with cubic symmetry

The structure parameters			Crystals			
			LiF	NaF	NaBr	C_{60}
Experimental data	Density ρ, kg/m^3		2600	2800	3200	1720
	Elasticity constants, GPa	C_{11}	113.00	97.00	32.55	14.9
		C_{12}	48.00	25.60	13.14	6.9
		C_{44}	63.00	28.00	13.26	8.1
Calculated characteristics	Wave velocities, m/s	c_1	6593	5890	3190	2943
		c_2	5477	3295	2045	2325
		v_{110}	3536	3571	1741	1525
		c_3	5659	2896	1092	2036
	The dispersion parameter β, m/s		3396	1309	274	1181
	Parameters of force interactions between the particles, GPa	K_0/a	55.21	69.83	19.33	7.21
		K_2/a	19.90	3.18	0.16	1.59
		K_3/a	48.00	25.60	13.14	6.90
	Poisson's ratios	$v_{<100,\ 001>}$	0.298	0.209	0.288	0.317
		$v_{<110,\ 001>}$	0.435	0.179	0.348	0.474
		$v_{<110,\ 1\bar{1}0>}$	−0.023	0.322	0.139	−0.025
		$v_{<111,\ 111>}$	0.153	0.262	0.224	0.170

Since the Poisson's ratio v_2 decreases with growing of the grain size, inequality (4.47) implies the necessary condition for its negativity, which is obtained by substituting the maximum possible value $p = 1$ into (4.47): $K_3 < \sqrt{2}K_2 - K_0$. Thus, if $\sqrt{2}K_2 < K_0$, then for $K_3 > 0$, the Poisson's ratio v_2 will not be negative at any particle size p.

Table 4.4 contain the values of the Poisson's ratios for some crystals with cubic symmetry (lithium fluoride (LiF), sodium fluoride (NaF), sodium bromide (NaBr), fullerite C_{60}) calculated from known experimental and theoretical data (see Table 4.2). The calculations have been performed for $p = 0.9$ and $K_1 = 0$. From Table 4.4, it is seen that the Poisson's ratio $v_1 = v_{<110,\ 1\bar{1}0>}$ can be negative for two of the four considered materials—LiF and C_{60}.

4.6 Conclusions

In this chapter, the low-frequency approximation of the dynamic equations of granular media obtained in Chaps. 2 and 3 has been considered. In this case, the rotational degrees of freedom of the particles can be neglected, and the original Eqs. (2.8) and (3.6) degenerate into the Lamé equations of the classical theory of elasticity. However, a print of the microstructure is still left in the form of the relationships between the

effective macroscopic characteristic parameters of the medium and the micromodel parameters.

The parametric identification of the elaborated models has been performed by comparing equations describing the propagation and interaction of longitudinal and transverse waves in a granular medium in the low-frequency approximation, with the equations of the classical theory of elasticity and the equations of the two-dimensional Cosserat continuum. As a result, formulas for calculation of the Cosserat constants, as well as the velocity and threshold frequency of the microrotation wave in such a medium have been obtained. Moreover, due to such formulas, quantitative estimates of these parameters have been obtained for some hypothetical materials with parameters similar to certain crystals with hexagonal and cubic symmetry. In addition, the dependence of the Poisson's ratios of both isotropic and anisotropic granular media on the parameters of their microstructure has been established due to parametric identification. An analysis of the dependences showed that the Poisson's ratios monotonously decrease with growing of the relative particle size d/a. So, when this size tends to 1 and the parameter of moment interactions is comparable to the parameters of force interactions K_0 and K_3, with a high probability, the Poisson's ratios $\nu_1 = \nu_{<110,\ 1\bar{1}0>}$ and, to a lesser extent, $\nu_2 = \nu_{<111,\ 111>}$ become negative. This fact concerning $\nu_1 = \nu_{<110,\ 1\bar{1}0>}$ is also confirmed by the quantitative estimates given in Table 4.4 for the Poisson's ratios for some cubic crystals. The performed investigations can serve as a theoretical basis for creating advanced metamaterials with auxetic properties.

It should be also remarked that media possessing auxetic properties are rather often modeled on the base of chiral lattices, particles of which interact on account of non-symmetrical compounds. Such models were considered, particularly, in Refs. [40, 51, 52].

References

1. Potapov, A.I., Pavlov, I.S., Lisina, S.A.: Acoustic identification of nanocrystalline media. J. Sound Vib. **322**(3), 564–580 (2009)
2. Gross, E.F.: Izbrannye Trudy (Selected Papers). Nauka, Leningrad (1976). (in Russian)
3. Gross, E.F.: Light scattering and relaxation phenomena in liquids. Doklady Akademii Nauk SSSR **28**(9), 788–793 (1940) (in Russian)
4. Gross, E.F., Korshunov, A.V.: Rotational oscillations of molecules in a crystal lattice of organic substances and scattering spectra. JETP **16**(1), 53–59 (1946)
5. Gross, E.F., Korshunov, A.V., Sel'kin, V.A.: Raman spectra of small frequencies of crystals of para-iodiobenzenes, meta-iodiobenzenes and ortho-iodiobenzenes. JETP 20, 293–296 (1950)
6. Eringen, A.C.: Microcontinuum Field Theories. 1: Foundation and Solids. Springer. New York (1999)
7. Nowacki, W.: Theory of Micropolar Elasticity. J. Springer, Wien (1970)
8. Kunin, I.A.: Elastic Media with Microstructure, vol. 2. Springer, Berlin
9. Savin, G.N., Lukashev, A.A., Lysko, E.M., Veremeenko, S.V., Agas'ev, G.G.: Propagation of elastic waves in the Cosserat continuum with constrained particle rotation. Prikl. Mekh. (Appl. Mech.) **6**(6), 37–40 (in Russian)

10. Pavlov, I.S.: Acoustic identification of the anisotropic nanocrystalline medium with non-dense packing of particles. Acoust. Phys. **56**(6), 924–934 (2010)
11. Cauchy, A.L.: Memoire sur la dispersion de la lumiere. Paris (1830)
12. Zhu, S., Zhang, X.: Metamaterials: artificial materials beyond nature. Nat. Sci. Rev. **5**(2), 131 (2018)
13. Vanin, G.A.: Gradient theory of elasticity. Mech. Solids **1**, 46–53 (1999)
14. Korotkina, M.R.: Remark About Moment Stresses in Discrete Media, vol. 5, pp. 103–109. Moscow University Mechanics Bulletin. Allerton Press, Inc (1969)
15. Fedorov, V.I.: Theory of Elastic Waves in Crystals. Nauka, Moscow, 1965; Plenum Press, New York, 1968
16. Tucker, J.W., Rampton, V.W.: Microwave Ultrasonics in Solid State Physics. North-Holland Publ. Comp, Amsterdam (1972)
17. Krivtsov, A.M.: Deformation and Destruction of Microstructured Solids, p. 304. Fizmatlit Publ., Moscow (2007) (in Russian)
18. Pavlov, P.V., Khokhlov, A.F.: Physics of Solid Body: Textbook, p. 494. Visshaya School, Moscow (2000)
19. Kitaygorodskiy, A.I.: Molecular Crystals, p. 424. Nauka Publ., Moscow (1971) (in Russian)
20. Akhiezer, A.I., Bar'yakhtar, V.G., Peletminskii, S.V.: Spin Waves. North Holland, Amsterdam (1968)
21. Frantsevich, I.N., Voronov, F.F., Bakuta, S.A.: Elastic constants and elasticity moduli of metals and nonmetals. In: Frantsevich, I.N. (ed.) Reference Book. Naukova Dumka, Kiev (1982). (in Russian)
22. Krivtsov, A.M., Podol'skaya, E.A.: Modeling of elastic properties of crystals with hexagonal close-packed lattice. Mech. Solids **45**(3), 370–378 (2010)
23. Feynman, R.P., Leighton, R.B., Sands, M.: The Feynman Lectures on Physics, vol. 2. Addison-Wesley Publishing Company, Inc, Reading, Massachusetts, Palo Alto, London (1964)
24. Yildirim, T., Harris, A.B.: Lattice dynamics of solids C_{60}. Phys. Rev. B **46**, 7878–7896 (1992)
25. Abolinsh, Y.Y., Gross, E.F., Shultin, A.A.: Optic-acoustic effect in crystals. Sov. Phys. Tech. Phys. **28**, 2255 (1958)
26. Kulesh, M.A., Grekova, E.F., Shardakov, I.N.: The problem of surface wave propagation in a reduced Cosserat medium. Acoust. Phys. **55**(2), 218–226 (2009). https://doi.org/10.1134/S1063771009020110
27. Kulesh, M.A., Matveenko, V.P., Shardakov, I.N.: Propagation of surface elastic waves in the Cosserat medium. Acoust. Phys. **52**(2), 186–193 (2006). https://doi.org/10.1134/s1063771006020114
28. Suvorov, Y.M., Tarlakovskii, D.V., Fedotenkov, G.V.: The plane problem of the impact of a rigid body on a half-space modelled by a Cosserat medium. J. Appl. Math. Mech. **76**(5), 511–518 (2012)
29. Adamov, A.A.: On calculation effects in solving the boundary problems for the isotropic homogeneous Cosserat continuum. In: Proceedings of VI Russian Conference "Mechanics of Microheterogeneous Materials and Fracture". Yekaterinburg (Russia) (2010). http://book.uraic.ru/project/conf/txt/008/2010/mmp2.htm
30. Suiker, A.S.J., Metrikine, A.V., de Borst, R.: Comparison of wave propagation characteristics of the Cosserat continuum model and corresponding discrete lattice models. Int. J. Solids Struct. **38**, 1563–1583 (2001)
31. Hirth, J.P., Lothe, J.: Theory of Dislocations. Mc Graw-Hill Book Company, New York (1970)
32. Koniok, D.A., Voitsekhovsky, K.V., Pleskachevsky, Yu.M., Shilko, S.V.: Materials with negative Poisson's ratio (The review). Composite Mech. Des. **10**, 35–69 (2004)
33. Yang, W.: Review on auxetic materials. J. Mater. Sci. **39**, 3269–3279 (2004)
34. Zubov, V.G., Firsova, M.M.: Elastic properties of quartz near the α-β transition. Sov. Phys. Crystallography **7**, 374–376 (1962)
35. Evans, K.E.: Auxetic polymers: a new range of materials. Endeavour New Ser. **4**, 170–174 (1991)

36. Baimova, J.A., Rysaeva, L.Kh., Dmitriev, S.V., Lisovenko, D.S., Gorodtsov, V.A., Indeitsev, D.A.: Auxetic behaviour of carbon nanostructures. Mater. Phys. Mech. **33**(1), 1–11 (2017)
37. Hall, L.J., Coluci, V.R., Galvão, D.S., Kozlov, M.E., Zhang, M., Dantas, S.O., Baughman, R.H.: Sign change of Poisson's ratio for carbon nanotube sheets. Science **320**(5875), 504–507 (2008)
38. Zaitsev, V.Y., Radostin, A.V., Pasternak, E., Dyskin, A.: Extracting real-crack properties from non-linear elastic behavior of rocks: abundance of cracks with dominating normal compliance and rocks with negative Poisson ratios. Nonlinear Process. Geophys. **24**(3), 543–551 (2017)
39. Goldstein, R.V., Gorodtsov, V.A., Lisovenko, D.S.: Young's moduli and Poisson's ratio of curvilinear anisotropic hexagonal and rhombohedral nanotubes. Nanotubes-auxetics. Doklady Phys. **58**(9), 400–404 (2013)
40. Vasiliev, A.A., Pavlov, I.S.: Auxetic properties of hiral hexagonal Cosserat lattices composed of finite-sized particles. Phys. Status Solidi B **3**(257), 1900389 (2020). https://doi.org/10.1002/pssb.201900389
41. Attard, D., Grima, J.N.: Auxetic behaviour from rotating rhombi. Phys. Status Solidi B **245**(11), 2395–2404 (2008)
42. Grima, J.N., Farrugia, P.-S., Gatt, R., Attard, D.: On the auxetic properties of rotating rhombi and parallelograms: a preliminary investigation. Phys. Status Solidi B **245**(3), 521–529 (2008)
43. Narojczyk, J.W., Wojciechowski, K.W.: Elastic properties of degenerate f.c.c. crystal of polydisperse soft dimers at zero temperature. J. Non-Crystalline Solids **356**(37–40), 2026–2032 (2010)
44. Novikov, V.V., Wojciechowski, K.W.: Negative Poisson coefficient of fractal structures. Phys. Solid State **41**(12), 1970–1975 (1999)
45. Goldstein, R.V., Gorodtsov, V.A., Lisovenko, D.S.: The elastic properties of hexagonal auxetics under pressure. Phys. Status Solidi B **253**(7), 1261–1269 (2016)
46. Wojciechowski, K.W.: Negative Poisson ratios at negative pressures. Mol. Phys. Rep. **10**, 129–136 (1995)
47. Lethbridge, Z.A.D., Walton, R.I., Marmier, A., Smith, C.W., Evans, K.E.: Elastic anisotropy and extreme Poisson's ratios in single crystals. Acta Materialia **58**, 6444–6451 (2010)
48. Belomestnykh, V.N., Soboleva, E.G.: Unconventional approach to determination anisotropic Poisson's ratios in cubic crystals. Lett. Mater. **2**(1), 13–16 (2012)
49. Turley, J., Sines, G.: The anisotropy of Young's modulus, shear modulus and Poisson's ratio in cubic materials. J. Phys. D Appl. Phys. **4**, 264–271 (1971)
50. Erofeev, V.I., Pavlov, I.S.: Parametric identification of crystals having a cubic lattice with negative Poisson's ratios. J. Appl. Mech. Tech. Phys. **56**(6), 1015–1022 (2015)
51. Vasiliev, A.A., Miroshnichenko, A.E., Dmitriev, S.V.: Multi-field modeling of a Cosserat lattice: models, wave filtering, and boundary effects. European J. Mech. A Solids **46**, 96–105 (2014)
52. Vasiliev, A.A., Pavlov, I.S.: Models and some properties of Cosserat triangular lattices with chiral microstructure. Lett. Mater. **9**(1), 45–50 (2019). www.lettersonmaterials.com https://doi.org/10.22226/2410-3535-2019-1-45-50

Chapter 5
Nonlinear Models of Microstructured Media

In Chaps. 2–4, the linear models of microstructured media have been considered, the particles of which have three degrees of freedom. In this chapter, the dynamic equations of a rectangular lattice of ellipse-shaped particles and a square lattice of round particles are generalized to the nonlinear case. Such a generalization is necessary for the study of nonlinear wave processes [1, 2] in microstructured media—the corresponding problems will be considered in Chap. 7. In addition, a nonlinear model of a single-layer medium of nanotubes is developed in this chapter. Such a model represents a square lattice of dipoles with five (three translational and two rotational) degrees of freedom.

5.1 A Rectangular Lattice Consisting of Ellipse-Shaped Particles

This section is devoted to the development of a nonlinear mathematical model of a two-dimensional granular medium, which represents a rectangular lattice of elastically interacting ellipse-shaped particles, and the estimation of the nonlinearity coefficients of this model in the particular case—for the square lattice consisting of round particles.

In Chap. 3, we considered a two-dimensional rectangular lattice consisting of homogeneous particles (grains or granules) of mass M and having the shape of an ellipse with axes of lengths d_1 and d_2 (Fig. 3.1). The interactions of neighboring granules are modeled by four types of elastic springs and are determined by the relative elongations of the springs when the particles deviate from the equilibrium states. In Appendix 2, the elongations of these springs are calculated up to quadratic terms. Taking into account these terms, one can obtain the Lagrange function $L = T_{i,j} - U_{i,j}$ for a particle with the number (i, j) up to terms of $\varepsilon^{5/2}$-order inclusive (ε is a measure of the cell deformation, $\Delta u_i = (u_{i,j} - u_{i-1,j})/a \sim \Delta w_i \sim \varepsilon$,

$\Delta u_j = (u_{i,j} - u_{i,j-1})/b \sim \Delta w_j \sim \varepsilon,\ \varphi_{i,j} \sim \sqrt{\varepsilon},\ \Delta \varphi_i \sim \Delta \varphi_j \sim \varepsilon^{3/2})$. In this case, in the continuum approximation, the Lagrange function L of the considered medium consisting of anisotropic particles takes on the form:

$$
\begin{aligned}
L = &\ \frac{M}{2}\left(u_t^2 + w_t^2 + R^2\varphi_t^2\right) - \frac{M}{2}\left[c_1^2(u_x^2 + \delta_1 w_y^2) + c_2^2(w_x^2 + \delta_2 u_y^2)\right.\\
&+ R^2 c_3^2(\varphi_x^2 + \delta_3\varphi_y^2) + s^2(u_x w_y + \delta_4 u_y w_x)\\
&+ 2\beta_1(w_x - \delta_5 u_y)\varphi + 2\beta_2\varphi^2\\
&+ (\alpha_1 u_x^3 + \alpha_1' w_y^3) + (\alpha_2 u_y^3 + \alpha_2' w_x^3) + \alpha_3(au_x^2 u_y + bu_x u_y^2)\\
&+ \alpha_3'(aw_x^2 w_y + bw_x w_y^2) + \alpha_4(a^2 u_x^2 w_x + b^2 u_y^2 w_x + abu_x^2 w_y)\\
&+ \alpha_4'(b^2 u_y w_y^2 + a^2 u_y w_x^2 + abu_x w_y^2)\\
&+ (\alpha_5 u_x w_x^2 + \alpha_5' u_y^2 w_y) + \alpha_6 u_x u_y(aw_x + bw_y)\\
&+ \alpha_6' w_x w_y(au_x + bu_y) + (\alpha_7 - \alpha_8)u_x u_y\varphi - (\alpha_7' - \alpha_8)w_x w_y\varphi\\
&+ \alpha_9(a^2(w_x^2 - u_x^2) + b^2(w_y^2 - u_y^2))\varphi + (\alpha_{10}u_y + \alpha_{10}'w_x)\varphi^2\\
&+ (\alpha_{11} - \alpha_{12})u_x\varphi^2 + (\alpha_{11}' - \alpha_{12}')w_y\varphi^2\\
&+ (\alpha_{13} + \alpha_{14}a^2)u_x w_x\varphi + (\alpha_{13}' + \alpha_{14}b^2)u_y w_y\varphi\\
&\left. + \alpha_{15}(u_x w_y + u_y w_x)\varphi\right].
\end{aligned}
\tag{5.1}
$$

Using Hamilton's variational principle, differential equations of the first approximation that describe nonlinear dynamic processes in an anisotropic crystalline medium are derived from the Lagrange function (5.1):

$$
\begin{aligned}
u_{tt} = &\ c_1^2 u_{xx} + \delta_2 c_2^2 u_{yy} + \frac{1 + \delta_4}{2}s^2 w_{xy}\\
&- \delta_5\beta_1\varphi_y + \frac{1}{2}\frac{\partial F_1}{\partial x} + \frac{1}{2}\frac{\partial F_2}{\partial y},\\
w_{tt} = &\ c_2^2 w_{xx} + \delta_1 c_1^2 w_{yy} + \frac{1 + \delta_4}{2}s^2 u_{xy}\\
&+ \beta_1\varphi_x + \frac{1}{2}\frac{\partial F_3}{\partial x} + \frac{1}{2}\frac{\partial F_4}{\partial y},\\
R^2\varphi_{tt} = &\ R^2 c_3^2\left(\varphi_{xx} + \delta_3\varphi_{yy}\right)\\
&+ \ \beta_1\left(\delta_5 u_y - w_x\right) - 2\beta_2\varphi - F_5.
\end{aligned}
\tag{5.2}
$$

Here,

$$
\begin{aligned}
F_1 = &\ 3\alpha_1 u_x^2 + \alpha_3(2au_x u_y + bu_y^2)\\
&+ \alpha_4(2a^2 u_x w_x + abu_x w_y) + \alpha_4' abw_y^2 + \alpha_5 w_x^2\\
&+ \alpha_6 u_y(aw_x + bw_y) + \alpha_6' aw_x w_y
\end{aligned}
$$

$$+ (\alpha_7 - \alpha_8)u_y\varphi - 2\alpha_9 a^2 u_x\varphi + (\alpha_{11} - \alpha_{12})\varphi^2$$
$$+ (\alpha_{13} + \alpha_{14}a^2)w_x\varphi + \alpha_{15}w_y\varphi,$$
$$F_2 = 3\alpha_2 u_y^2 + \alpha_3(au_x^2 + 2bu_x u_y)$$
$$+ 2\alpha_4 b^2 u_y w_x + \alpha_4'(b^2 w_y^2 + a^2 w_x^2) + 2\alpha_5' u_y w_y$$
$$+ \alpha_6 u_x(aw_x + bw_y) + \alpha_6' bw_x w_y$$
$$+ (\alpha_7 - \alpha_8)u_x\varphi - 2\alpha_9 b^2 u_y\varphi + \alpha_{10}\varphi^2$$
$$+ (\alpha_{13}' + \alpha_{14}b^2)w_y\varphi + \alpha_{15}w_x\varphi,$$
$$F_3 = 3\alpha_2' w_x^2 + \alpha_3'(2aw_x w_y + bw_y^2)$$
$$+ \alpha_4(a^2 u_x^2 + b^2 u_y^2) + 2\alpha_4' a^2 u_y w_x$$
$$+ 2\alpha_5 u_x w_x + \alpha_6 au_x u_y + \alpha_6' au_x w_y$$
$$- (\alpha_7' - \alpha_8)w_y\varphi + 2\alpha_9 a^2 w_x\varphi + \alpha_{10}'\varphi^2$$
$$+ (\alpha_{13} + \alpha_{14}a^2)u_x\varphi + \alpha_{15}u_y\varphi,$$
$$F_4 = 3\alpha_4' w_y^2 + \alpha_3'(aw_x^2 + 2bw_x w_y)$$
$$+ \alpha_4 abu_x^2 + \alpha_4'(2b^2 u_y w_y + 2abu_x w_y)$$
$$+ \alpha_5' u_y^2 + \alpha_6 bu_x u_y + \alpha_6' w_x(au_x + bu_y)$$
$$- (\alpha_7' - \alpha_8)w_x\varphi + 2\alpha_9 b^2 w_y\varphi +$$
$$+ (\alpha_{11}' - \alpha_{12}')\varphi^2 + (\alpha_{13}' + \alpha_{14}b^2)u_y\varphi + \alpha_{15}u_x\varphi,$$
$$F_5 = (\alpha_7 - \alpha_8)u_x u_y - (\alpha_7' - \alpha_8)w_x w_y$$
$$+ \alpha_9(a^2(w_x^2 - u_x^2) + b^2(w_y^2 - u_y^2)) +$$
$$+ 2(\alpha_{10}u_y + \alpha_{10}'w_x)\varphi + 2(\alpha_{11} - \alpha_{12})u_x\varphi$$
$$+ 2(\alpha_{11}' - \alpha_{12}')w_y\varphi + (\alpha_{13} + \alpha_{14}a^2)u_x w_x$$
$$+ (\alpha_{13}' + \alpha_{14}b^2)u_y w_y + \alpha_{15}(u_x w_y + u_y w_x) \qquad (5.3)$$

are the nonlinearity functions.

The following notation is introduced in the Lagrange function (5.1) and Eq. (5.2): c_i ($i = 1, 2, 3$) are the velocities of the longitudinal, shear, and microrotation waves, respectively, s is the coefficient of linear coupling between the longitudinal and shear waves, β_1 and β_2 are the dispersion parameters, δ_i ($i = 1 \div 5$) are the correction coefficients arising due to the anisotropy of the medium at issue, and α_i are the nonlinearity coefficients.

The coefficients of the linear parts of Eq. (5.2) are expressed in terms of the force constants K_0, K_1, K_2, K_3, lattice parameters a and b, and particle sizes h_1 and h_2 according to formulas (3.9). The anisotropy parameters have the form (3.7). The nonlinearity coefficients depend on the microstructure parameters as follows:

$$M\alpha_1 = \frac{K_2}{r_1^4}a^3(a - h_1)h_2^2 + \frac{K_3}{r_3^4}a^3(a - h_1)(b - h_2)^2,$$

$$M\alpha_2 = \frac{K_3}{r_3^4}b^3(a - h_1)(b - h_2)^2, \quad M\alpha_3 = \frac{K_3}{r_3^4}ab(a - h_1)(b - h_2)^2,$$

$$M\alpha_4 = \frac{K_3}{r_3^4}a(b - h_2)\big((b - h_2)^2 - 2(a - h_1)^2\big),$$

$$M\alpha_5 = K_0 a^2 + K_1\frac{a^3}{a - h_1} + \frac{K_2}{r_1^4}a^3(a - h_1)\big((a - h_1)^2 - 2h_2^2\big)$$

$$+ \frac{K_3}{r_3^4}a^3(a - h_1)\big((a - h_1)^2 - 2(b - h_2)^2\big),$$

$$M\alpha_6 = \frac{2K_3}{r_3^4}ab(b - h_2)\big((b - h_2)^2 - 2(a - h_1)^2\big),$$

$$M\alpha_7 = \frac{4abK_3}{r_3^4}(b - h_2)^2(bh_1 - ah_2),$$

$$M\alpha_8 = \frac{4abK_3}{r_3^4}(a - h_1)(b - h_2)(h_1(a - h_1) + h_2(b - h_2)),$$

$$\alpha_9 = \frac{\alpha_8}{2ab},$$

$$M\alpha_{10} = \frac{K_3}{r_3^4}b(h_1(a - h_1) + h_2(b - h_2))^2,$$

$$M\alpha_{11} = K_1\frac{ah_1^2}{a - h_1} + \frac{K_2}{r_1^4}a(h_1^2 + h_2^2 - ah_1)$$

$$\big(2ah_2^2 + (a - h_1)(h_1^2 + h_2^2 - ah_1)\big)$$

$$+ \frac{K_3}{r_3^4}a(a - h_1)(h_1(a - h_1) + h_2(b - h_2))^2,$$

$$M\alpha_{12} = \frac{4aK_3}{r_3^4}(b - h_2)(bh_1 - ah_2)(h_1(a - h_1) + h_2(b - h_2)),$$

$$M\alpha_{13} = K_1\frac{2a^2h_1}{a - h_1} + \frac{2a^2}{r_1^4}$$

$$K_2\big((h_1^2 + h_2^2 - ah_1)(h_2^2 - (a - h_1)^2) - ah_2^2(a - h_1)\big),$$

$$M\alpha_{14} = \frac{2K_3}{r_3^4}[\big((a - h_1)^2 - (b - h_2)^2\big)(h_1(a - h_1) + h_2(b - h_2))$$

$$- 2(a - h_1)(b - h_2)(bh_1 - ah_2)],$$

$$M\alpha_{15} = \frac{2abK_3}{r_3^4}\big((a - h_1)^2 - (b - h_2)^2\big)(h_1(a - h_1) + h_2(b - h_2)). \tag{5.4}$$

The expressions for coefficients α_i' ($i = 1 \div 7, 10 \div 13$) are obtained from the formulas for the corresponding coefficients α_i by simultaneously replacing the parameters a with b, h_1 with h_2, b with a, h_2 with h_1, and r_1 with r_2. It should be noted that when the considered rectangular lattice consisting of ellipse-shaped particles

degenerates into a square lattice of round particles, some nonlinearity coefficients become equal to zero: $\alpha_7 = \alpha_{12} = \alpha_{14} = \alpha_{15} = 0$.

When a rectangular lattice degenerates into a square lattice of round particles, formulas (5.1)–(5.4) are significantly simplified. In this case, the Lagrange function of the considered medium with microstructure has the form [3]:

$$
\begin{aligned}
L = {} & \frac{M}{2}\left(u_t^2 + w_t^2 + R^2\varphi_t^2\right) \\
& - \frac{M}{2}\Big[c_1^2(u_x^2 + w_y^2) + c_2^2(w_x^2 + u_y^2) \\
& + R^2 c_3^2(\varphi_x^2 + \varphi_y^2) + s^2(u_x w_y + u_y w_x) \\
& + 2\beta^2(w_x - u_y)\varphi + 2\beta^2\varphi^2 \\
& + \alpha_1(u_x^3 + w_y^3) + \alpha_2\big(u_y^3 + w_x^3 + u_x^2 u_y + u_x u_y^2 \\
& + w_x^2 w_y + w_x w_y^2 - u_x^2 w_x - u_y^2 w_x - u_x^2 w_y \\
& \qquad\qquad\qquad -u_y w_y^2 - u_y w_x^2 - u_x w_y^2\big) \\
& - 2\alpha_2\big(u_x u_y(w_x + w_y) + w_x w_y(u_x + u_y)\big) \\
& + \alpha_3(u_x w_x^2 + u_y^2 w_y) + \alpha_4(w_x w_y\varphi - u_x u_y\varphi \\
& + \frac{1}{2}(w_x^2 - u_x^2 + w_y^2 - u_y^2)\varphi) \\
& + \alpha_5(u_y\varphi^2 + w_x\varphi^2) + \alpha_6(u_x\varphi^2 + w_y\varphi^2) \\
& + \alpha_7(u_x w_x\varphi + u_y w_y\varphi)\Big].
\end{aligned}
\tag{5.5}
$$

Here, expression (5.5) is obtained from Eq. (5.1) with accuracy up to a re-designation of the nonlinearity coefficients. The set of nonlinear differential equations describing dynamic processes in a two-dimensional crystalline medium with non-dense packing of particles has the form:

$$
\begin{aligned}
u_{tt} = {} & c_1^2 u_{xx} + c_2^2 u_{yy} + s^2 w_{xy} \\
& - \beta\varphi_y + \frac{1}{2}\frac{\partial F_1}{\partial x} + \frac{1}{2}\frac{\partial F_2}{\partial y}, \\
w_{tt} = {} & c_2^2 w_{xx} + c_1^2 w_{yy} + s^2 u_{xy} \\
& + \beta\varphi_x + \frac{1}{2}\frac{\partial F_3}{\partial x} + \frac{1}{2}\frac{\partial F_4}{\partial y}, \\
R^2\varphi_{tt} = {} & R^2 c_3^2(\varphi_{xx} + \varphi_{yy}) \\
& + \beta(u_y - w_x) - 2\beta\varphi - F_5.
\end{aligned}
\tag{5.6}
$$

The dependences of the linear coefficients of Eq. (5.6) on the force constants K_0, K_1, K_2, K_3, the lattice parameter a, and the particle size $h = d/\sqrt{2}$ (d is the particle diameter) are determined by formulas (3.10), and the nonlinearity functions have the form:

$$\begin{aligned}
F_1 = {} & 3\alpha_1 u_x^2 + \alpha_2(2u_x u_y + u_y^2 - 2u_x w_x - u_x w_y - w_y^2) \\
& + \alpha_3 w_x^2 - 2\alpha_2(u_y w_x + u_y w_y + w_x w_y) \\
& - \alpha_4(u_y\varphi + u_x\varphi) + \alpha_6\varphi^2 + \alpha_7 w_x\varphi,
\end{aligned}$$

$$\begin{aligned}
F_2 = {} & \alpha_2(3u_y^2 + u_x^2 + 2u_x u_y - 2u_y w_x - w_y^2 - w_x^2) \\
& + 2\alpha_3 u_y w_y - 2\alpha_2(u_x w_x + u_x w_y + w_x w_y) \\
& - \alpha_4(u_x\varphi + u_y\varphi) + \alpha_5\varphi^2 + \alpha_7 w_y\varphi,
\end{aligned}$$

$$\begin{aligned}
F_3 = {} & 3\alpha_2 w_x^2 + \alpha_2(2w_x w_y + w_y^2 - u_x^2 - u_y^2 - 2u_y w_x) \\
& + 2\alpha_3 u_x w_x - 2\alpha_2(u_x u_y + u_x w_y) \\
& + \alpha_4(w_y\varphi + w_x\varphi) + \alpha_5\varphi^2 + \alpha_7 u_x\varphi,
\end{aligned}$$

$$\begin{aligned}
F_4 = {} & 3\alpha_1 w_y^2 + \alpha_2(w_x^2 + 2w_x w_y - u_x^2 - 2u_y w_y - 2u_x w_y) \\
& + \alpha_3 u_y^2 - 2\alpha_2(u_x u_y + u_x w_x + u_y w_x) \\
& + \alpha_4(w_x\varphi + w_y\varphi) + \alpha_6\varphi^2 + \alpha_7 u_y\varphi,
\end{aligned}$$

$$\begin{aligned}
F_5 = {} & \alpha_4\left(w_x w_y - u_x u_y + \frac{1}{2}(w_x^2 - u_x^2 + w_y^2 - u_y^2)\right) \\
& + 2\alpha_5(u_y\varphi + w_x\varphi) + 2\alpha_6(u_x\varphi + w_y\varphi) \\
& + \alpha_7(u_x w_x + u_y w_y).
\end{aligned} \tag{5.7}$$

The nonlinearity coefficients α_i ($i = 1, \ldots, 7$) depend on the microstructure parameters:

$$M\alpha_1 = \frac{K_2}{r^4}a^3(a-h)h^2 + \frac{K_3}{4(a-h)}a^3,$$

$$M\alpha_2 = \frac{K_3}{4(a-h)}a^3,$$

$$\begin{aligned}
M\alpha_3 = {} & K_0 a^2 + K_1\frac{a^3}{a-h} \\
& + \frac{K_2}{r^4}a^3(a-h)(a^2 - 2ah - h^2) - \frac{K_3 a^3}{4(a-h)},
\end{aligned}$$

$$M\alpha_4 = \frac{2a^2 h K_3}{a-h}, \quad M\alpha_5 = \frac{K_3}{(a-h)^2}a^2 h^2,$$

$$\begin{aligned}
M\alpha_6 = {} & K_1\frac{ah^2}{a-h} + K_2\frac{ah^2}{r^4}(2h-a)(5ah - 2h^2 - a^2) \\
& + \frac{K_3}{(a-h)^2}a^2 h^2,
\end{aligned}$$

$$M\alpha_7 = K_1\frac{2a^2 h}{a-h} + \frac{2a^3 h}{r^4}K_2(5h^2 - 5ah + a^2). \tag{5.8}$$

Here, $r = \sqrt{(a-h)^2 + h^2}$ is the initial length of the springs with rigidity K_2.

5.2 Estimation of the Nonlinearity Coefficients of the Mathematical Model of the Square Lattice of Round Particles

Now, according to the similar procedure like it was done in Chap. 4, we will consider the low-frequency approximation of nonlinear Eq. (5.6), where the microrotations of the particles of a medium are not independent and are determined by a displacement field. The relationship between the microrotations φ and the displacements u and w can be found from the linear part of the third Eq. (5.6) by the method of successive approximations. In the first approximation, $\varphi(x,t) \approx \frac{1}{2}(u_y - w_x)$ and the Lagrange function L takes on the form:

$$
\begin{aligned}
L = {}& \frac{M}{2}\left(u_t^2 + w_t^2 + \frac{R^2}{4}(u_{yt} - w_{xt})^2 \right) \\
& - \frac{M}{2}\Big[c_1^2(u_x^2 + w_y^2) + c_2^2(w_x^2 + u_y^2) \\
& + \frac{R^2}{4}c_3^2\big((u_{xy} - w_{xx})^2 + (u_{yy} - w_{xy})^2\big) \\
& + s^2(u_x w_y + u_y w_x) - \frac{\beta}{2}(w_x - u_y)^2 \\
& + \alpha_1(u_x^3 + w_y^3) - \alpha_2\big(u_x^2 w_y + u_x w_y^2 + 2u_x u_y w_y + 2u_x w_x w_y\big) \\
& + \gamma_1(u_y^3 + w_x^3 - u_y w_x^2 - u_y^2 w_x) \\
& + \gamma_2(u_x u_y^2 + w_x^2 w_y) + \gamma_3 u_x w_x^2 + \gamma_4 u_y^2 w_y \\
& + \gamma_5(u_x^2 u_y + w_x w_y^2 - u_x^2 w_x - u_y w_y^2) \\
& - (2\gamma_5 + \gamma_6)u_x u_y w_x - (2\gamma_5 + \gamma_7)u_y w_x w_y \Big].
\end{aligned}
\tag{5.9}
$$

Here,

$$
\begin{aligned}
& \gamma_1 = \alpha_2 + \frac{\alpha_5 - \alpha_4}{4}, \quad \gamma_2 = \alpha_2 + \frac{\alpha_6}{4} - \frac{\alpha_4}{2}, \\
& \gamma_3 = \alpha_3 + \frac{\alpha_6}{4} - \frac{\alpha_7}{2}, \quad \gamma_4 = \alpha_3 + \frac{\alpha_6}{4} + \frac{\alpha_7}{2}, \\
& \gamma_5 = \alpha_2 - \frac{\alpha_4}{4}, \quad \gamma_6 = \frac{1}{2}(\alpha_6 - \alpha_7), \\
& \gamma_6 = \frac{1}{2}(\alpha_6 + \alpha_7).
\end{aligned}
\tag{5.10}
$$

From the Lagrange function (5.9), it is possible to obtain nonlinear equations of the higher-order gradient theory of elasticity [2, 4], which contain terms with the fourth-order derivatives:

$$u_{tt} - c_1^2 u_{xx} - \left(c_2^2 - \frac{\beta}{2}\right) u_{yy} - \left(s^2 + \frac{\beta}{2}\right) w_{xy}$$

$$= \frac{R^2}{4} \frac{\partial}{\partial y} \left[\frac{\partial^2}{\partial t^2}(u_y - w_x) - c_3^2 \Delta(u_y - w_x)\right]$$

$$+ \frac{1}{2} \frac{\partial H_1}{\partial x} + \frac{1}{2} \frac{\partial H_2}{\partial y},$$

$$w_{tt} - \left(c_2^2 - \frac{\beta}{2}\right) w_{xx} - c_1^2 w_{yy} - \left(s^2 + \frac{\beta}{2}\right) u_{xy}$$

$$= -\frac{R^2}{4} \frac{\partial}{\partial x} \left[\frac{\partial^2}{\partial t^2}(u_y - w_x) - c_3^2 \Delta(u_y - w_x)\right]$$

$$+ \frac{1}{2} \frac{\partial H_3}{\partial x} + \frac{1}{2} \frac{\partial H_4}{\partial y}. \tag{5.11}$$

Here, the symbol Δ denotes a two-dimensional Laplacian $\Delta = \partial^2/\partial x^2 + \partial^2/\partial y^2$ and $H_{1,2,3,4}$ are the nonlinearity functions:

$$H_1 = 3\alpha_1 u_x^2 - 2\alpha_2 \left(u_x w_y + \frac{1}{2} w_y^2 + u_y w_y + w_x w_y\right)$$

$$+ \gamma_2 u_y^2 + \gamma_3 w_x^2 + 2\gamma_5 (u_x u_y - u_x w_x)$$

$$- (2\gamma_5 + \gamma_6) u_y w_x,$$

$$H_2 = -2\alpha_2 u_x w_y + \gamma_1 (3u_y^2 - w_x^2 - 2u_y w_x)$$

$$+ 2\gamma_2 u_x u_y + 2\gamma_4 u_y w_y + \gamma_5 (u_x^2 - w_y^2)$$

$$- (2\gamma_5 + \gamma_6) u_x w_x - (2\gamma_5 + \gamma_7) w_x w_y,$$

$$H_3 = -2\alpha_2 u_x w_y + \gamma_1 (3w_x^2 - u_y^2 - 2u_y w_x)$$

$$+ 2\gamma_2 w_x w_y + 2\gamma_3 u_x w_x + \gamma_5 (w_y^2 - u_x^2)$$

$$- (2\gamma_5 + \gamma_6) u_x u_y - (2\gamma_5 + \gamma_7) u_y w_y,$$

$$H_4 = 3\alpha_1 w_y^2 - 2\alpha_2 (u_x w_y + \frac{1}{2} u_x^2 + u_x u_y + u_x w_x)$$

$$+ \gamma_2 w_x^2 + \gamma_4 u_y^2 + 2\gamma_5 (w_x w_y - u_y w_y)$$

$$- (2\gamma_5 + \gamma_7) u_y w_x. \tag{5.12}$$

In Chap. 4, a detailed analysis of the coefficients of the linear parts of Eq. (5.6) had been performed depending on the values of the microstructure parameters, as a result

of which, wave velocities c_1, c_2, and c_3, parameters β and s, as well as the model parameters of interparticle interactions K_0, K_1, K_2, and K_3 were calculated for some cubic crystals on the base of the known experimental data. The calculations were carried out for $K = K_0/K_1 = 10$ (the central interactions dominate) and $d/a = 0.9$. In this section, we will estimate the nonlinearity coefficients (5.8) (see Table 5.1), in which dependencies on microstructure parameters K and $p = h/a = d/a\sqrt{2}$ and the elasticity constants of the second order have the following form [3]:

$$\rho\alpha_1 = \frac{1-p}{(1-p)^2 + p^2}(C_{44} - C_{12}), \, \rho\alpha_2 = \frac{C_{12}}{4(1-p)},$$

$$\rho\alpha_3 = \frac{K(1-p)+1}{(2+K)(1-p)}\left[C_{11} - C_{12} - 2(C_{44} - C_{12})\frac{(1-p)^2}{p^2}\right]$$

$$+ (C_{44} - C_{12})\frac{(1-p)(1-2p-p^2)}{((1-p)^2 + p^2)p^2},$$

$$\rho\alpha_4 = \frac{2pC_{12}}{1-p}, \, \rho\alpha_5 = \frac{p^2 C_{12}}{(1-p)^2},$$

$$\rho\alpha_6 = \frac{1}{2+K}\left[(C_{11} - C_{12})\frac{p^2}{1-p} - 2(C_{44} - C_{12})(1-p)\right]$$

$$+ (C_{44} - C_{12})\frac{(2p-1)(5p-2p^2-1)}{(1-p)^2 + p^2},$$

$$\rho\alpha_7 = \frac{2}{2+K}\left[(C_{11} - C_{12})\frac{p}{1-p} - 2(C_{44} - C_{12})\frac{1-p}{p}\right]$$

$$+ 2(C_{44} - C_{12})\frac{(5p^2 - 5p + 1)}{p((1-p)^2 + p^2)}. \tag{5.13}$$

From (5.13), it follows that, if $p \to 0$, as shown in Ref. [5], the Cauchy relation $C_{12} = C_{44}$ is valid and, as a result, $\alpha_2 \to \frac{C_{12}}{4\rho}$, $\alpha_3 \to \frac{K+1}{(2+K)\rho}(C_{11} - C_{12})$, and all the other nonlinearity factors tend to zero, and $\alpha_1 \to 0$ because only a geometric nonlinearity is taken into account in this model. If physical nonlinearity is taken into account, α_1 would tend to some positive value.

For $p = 1/2$, the Cauchy relation is not valid and

$$\alpha_1 = \frac{C_{44} - C_{12}}{\rho}, \, \alpha_2 = \frac{C_{12}}{2\rho},$$

$$\alpha_3 = \frac{C_{11} + 2C_{12} - 3C_{44}}{\rho}, \, \alpha_4 = \frac{2C_{12}}{\rho},$$

$$\alpha_5 = \frac{C_{12}}{\rho}, \, \alpha_6 = \frac{C_{11} + C_{12} - 2C_{44}}{2(2+K)\rho},$$

$$\alpha_7 = \frac{C_{11} + 3C_{12} - 4C_{44}}{2(2+K)\rho}.$$

Table 5.1 Nonlinearity coefficients for crystals with cubic symmetry

	The structural parameters		Crystals			
			LiF	NaF	NaBr	C_{60}
Experimental data	Density (kg/m^3)	ρ	2600	2800	3200	1720
	Elasticity constants (GPa)	C_{11}	113.00	97.00	32.55	14.9
		C_{12}	48.00	25.60	13.14	6.9
		C_{44}	63.00	28.00	13.26	8.1
Calculated characteristics	Wave velocities (m/s)	c_1	6593	5890	3190	2943
		c_2	5477	3295	2045	2325
		c_3	5659	2896	1092	2036
	The coefficient of linear coupling between the longitudinal and shear deformations (m/s)	s	6076	4276	2866	2833
	The dispersion parameter (m/s)	$\sqrt{\beta}$	3396	1309	274	1180
	Parameters of force interactions between the particles (GPa)	K_0/a	46.01	58.19	16.11	6.01
		K_1/a	4.601	5.819	1.611	0.601
		K_2/a	19,897	3.183	0.159	1.592
		K_3/a	48.00	25.60	13.14	6.90
	The nonlinearity coefficients of the original model (10^6 m^2/s^2)	α_1	16.60	6.87	2.85	3.23
		α_2	12.69	6.29	2.82	2.76
		α_3	-34.75	0.38	-4.91	-7.37
		α_4	64.63	32.00	14.37	14.04
		α_5	56.65	28.01	12.58	12.29
		α_6	62.55	30.92	13.17	13.17
		α_7	0.90	6.49	1.73	0.58
	The nonlinearity coefficients of the two-mode model (10^6 m^2/s^2)	γ_1	10.68	5.29	2.37	2.32
		γ_1	-3.98	-1.99	-1.07	-0.97
		γ_3	-19.56	4.87	-2.49	-4.37
		γ_4	-18.66	11.36	-0.76	-3.79
		γ_5	-3.46	-1.71	-0.77	-0.75
		γ_6	30.83	12.22	5.72	6.29
		γ_7	31.72	18.70	7.45	6.87

Here, α_3 no longer depends on the parameter of interparticle interactions $K = K_0/K_1$ and all the nonlinearity coefficients do not tend to zero.

If, however, $p \rightarrow 1/\sqrt{2}$ (at $p = 1/\sqrt{2}$, particles will touch each other and their rotation will be difficult; therefore, only a limit transition to this case will be considered), then

$$\alpha_1 \rightarrow \frac{2(2\sqrt{2}-1)(C_{44}-C_{12})}{7\rho}, \alpha_2 \rightarrow \frac{(2+\sqrt{2})C_{12}}{4\rho},$$

$$\alpha_3 \rightarrow \frac{1}{\rho}\left(C_{11}\left(1+\frac{\sqrt{2}}{2+K}\right) + C_{12}\left(\frac{9}{2}-3\sqrt{2}+\frac{5\sqrt{2}-8}{2+K}\right)\right.$$

$$\left. -C_{44}\left(\frac{11}{2}-3\sqrt{2}+\frac{6\sqrt{2}-8}{2+K}\right)\right),$$

$$\alpha_4 \rightarrow \frac{2(1+\sqrt{2})C_{12}}{\rho}, \alpha_5 \rightarrow \frac{(3+2\sqrt{2})C_{12}}{\rho},$$

$$\alpha_6 \rightarrow \frac{(2+\sqrt{2})C_{11} + (\sqrt{2}-8+K(2\sqrt{2}-5))C_{12} + (6-2\sqrt{2}+K(5-2\sqrt{2}))C_{44}}{2(2+K)\rho},$$

$$\alpha_7 \rightarrow \frac{2\left(C_{11}(1+\sqrt{2}) + C_{12}(\sqrt{2}-3) + 2C_{44}(1-\sqrt{2}) + (2+K)(2\sqrt{2}-3)(C_{44}-C_{12})\right)}{(2+K)\rho}.$$

Numerical estimates of the nonlinearity factors presented in Table 5.1 show that only parameters γ_2 and γ_5 are negative for all considered crystals, whereas factors α_3, γ_3, and γ_4 can be both positive and negative. In the three-mode model, parameter α_4 is the greatest for all considered materials, and parameter γ_7 is maximal in the two-mode model. For the certain material, γ_7 exceeds the smallest absolute value of a factor γ_i up to 11 times, and for parameters α_i this ratio is greater—up to 72 times. Besides, some α_i can even surpass a square of the longitudinal wave velocity, c_1^2, that proves importance of the accounting of the nonlinear terms.

5.3 The Square Lattice of Nanotubes

All the models of media considered so far in the monograph contained particles with no more than 3 degrees of freedom. Now let us construct a model of the medium, in which particles have five degrees of freedom. This model is a generalization of the model of an oriented medium representing a chain of dumbbell-shaped particles (dipoles) considered in Refs. [6–8] to a two-dimensional case. It can be used to describe a layer of carbon nanotubes discovered by Ijima in 1991 [9, 10]. These extended cylindrical structures from one to several tens of nanometers in diameter and up to several microns in length consist of one or several hexagonal graphite layers rolled into a tube and usually end in a hemisphere, which can be considered as half of the C_{60} fullerene molecule. Because of this, a fullerene molecule can be considered as the limiting case of a carbon nanotube, in which two hemispheres are directly connected to each other. Thus, in their structure, CNTs occupy an intermediate position between graphite and fullerenes. However, many properties of CNTs do not

resemble either graphite or fullerenes [9, 10]. In this regard, it becomes relevant to study nanotubes as an independent advanced material with unique physical and mechanical characteristics, which has a significant potential for practical application.

5.3.1 The Discrete Model

Let us consider a layer of carbon nanotubes [9–13] modeled by a square lattice of homogeneous rods of length l and mass m [14]. The mass center of each nanotube coincides with the geometric center and in the initial state ($t = 0$) lies in the plane (x, y). Besides, in the initial states, the distance between the mass centers of neighboring rods (particles) along both the x-axis and y-axis is equal to a (Fig. 5.1) and all the particles are located perpendicular to the (x, y)-plane.

Each particle has five degrees of freedom: a displacement of the mass center of the particle with number $N = N(i, j)$ along the x-, y-, and z-axes (translational degrees of freedom $u_{i,j}$, $v_{i,j}$, and $w_{i,j}$) and rotation about the mass center that is described by two angles: $\theta_{i,j}$, which is measured from the z-axis in (x, z)-plane, and $\varphi_{i,j}$, which characterizes a rotation in (x, y)-plane with respect to the y-axis (rotational degrees of freedom) (Fig. 5.2). The kinetic energy of a particle $N(i, j)$ is equal to

$$T_{i,j} = \frac{m}{2}\left(\dot{u}_{i,j}^2 + \dot{v}_{i,j}^2 + \dot{w}_{i,j}^2\right) + \frac{J_1}{2}\dot{\theta}_{i,j}^2 + \frac{J_2}{2}\dot{\varphi}_{i,j}^2. \tag{5.14}$$

Here, $J_1 = ml^2/12$ is the moment of inertia of the particle relative to the y-axis, and $J_2 = ml^2\sin^2\theta_{i,j}/12$ is the variable moment of inertia of the rod relative to the z-axis. The dot above denotes the time derivative.
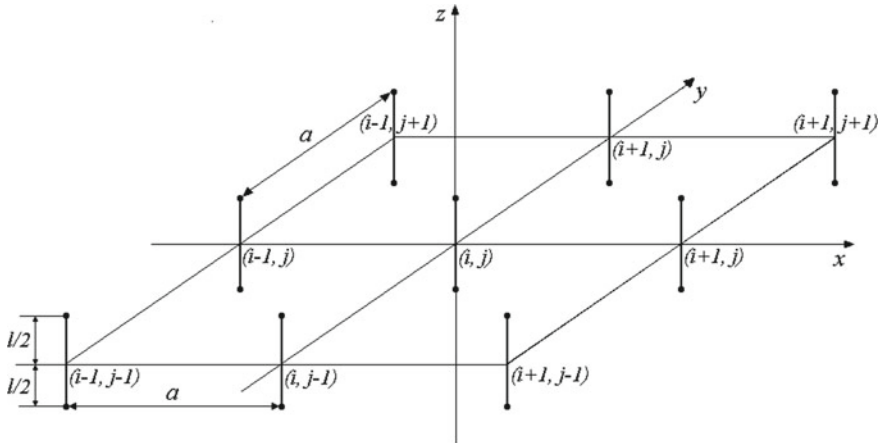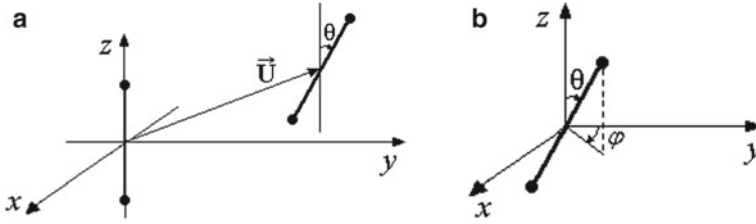

Fig. 5.1 A square lattice of nanotubes

Fig. 5.2 Kinematic scheme of a rod: translational displacements and rotation θ (**a**), rotations θ and φ (**b**)

We will consider small oscillations of particles near the lattice sites, when the displacements of the particles are small in comparison with sizes of the unit cell built on mutually perpendicular vectors directed along the x- and y-axes and having length a. Angles of the particle rotations are also assumed to be small. Under these conditions, the force and moment interactions of particles can be described by a potential representing a low-degree polynomial. In the harmonic approximation, the interaction potential is a quadratic form of the variables of a state of the system, whereas anharmonic effects are described by terms of the third (quadratic nonlinearity in the motion equations) and fourth (cubic nonlinearity in the motion equations) orders. In this model, we will assume that each particle interacts with eight nearest neighbors in the lattice, the mass centers of four of which lie on the horizontal and vertical lines, and of the other four—on the diagonals (Fig. 5.1). The first four particles, in which mass centers are located on a circle of radius a, will be hereinafter called *particles of the first coordination sphere*, and the rest of them will be called *particles of the second coordination sphere* (their centers are situated on the circle of radius $a\sqrt{2}$); the centers of both circles coincide with the particle N. Since all the particles are finite-sized, then the interaction between them has both force and moment components depending on the relative location and orientation of the particles.

The potential energy of a particle N that is caused by its interaction with eight nearest neighbors in the lattice is described by the formula

$$V_N = \frac{1}{2}\left(\frac{k_0}{2}\sum_{n=1}^{4} D_{0n}^2 + \frac{k_1}{2}\sum_{n=1}^{8} D_{1n}^2 + \frac{k_2}{2}\sum_{n=1}^{8} D_{2n}^2 \right.$$
$$\left. + \frac{k_0'}{2}\sum_{n=1}^{4} \tilde{D}_{0n}^2 + \frac{k_1'}{2}\sum_{n=1}^{8} \tilde{D}_{1n}^2 + \frac{k_2'}{2}\sum_{n=1}^{8} \tilde{D}_{2n}^2\right). \tag{5.15}$$

Here, D_{ln} and $\tilde{D}_{ln}$ ($l = 0, 1, 2$) are variations of the distances between the corresponding points of the particle $N(i, j)$ and its neighbors with numbers ($i + n, j + r$), where $n = \pm 1$ is the shift of the number along the horizontal axis, $r = 0, \pm 1$ is the shift of the number along the vertical axis, and factors k_0, k_1, and k_2 are the parameters of the force interactions: k_0 characterizes the central interactions during tension–compression of the material, k_1 describes non-central interactions during

Fig. 5.3 Scheme of force interactions between neighboring particles
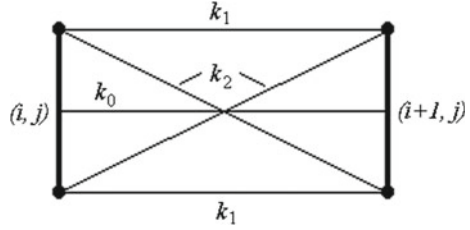
tension–compression of the material and moments during rotation of the particles, and k_2 stands for the force interactions of particles at shear deformations in the material. The parameters k_0', k_1', and k_2' determine similar interactions with the rods of the second coordination sphere [14]. With the viewpoint of a mechanical model, the parameters k_0, k_1, and k_2 can be interpreted as rigidity of the corresponding springs [15]: central (k_0), horizontal (k_1), and diagonal (k_2) ones (Fig. 5.3). The expressions for $D_{\ln}$ and $\tilde{D}_{\ln}$, calculated in the approximation of smallness of the quantities $\Delta u_i \sim \Delta v_i \sim \Delta u_j \sim \Delta v_j \sim \varepsilon$, $\Delta w_i \sim \Delta w_j \sim \theta_{i,j} \sim \varphi_{i,j} \sim \varepsilon^{3/4}$, $\Delta \theta_i \sim \Delta \theta_j \sim \Delta \varphi_i \sim \Delta \varphi_j \sim \varepsilon^{5/4}$, where $\varepsilon \ll 1$ is the measure of the cell deformation, are not given here because of their cumbersomeness. Expression (5.15), similar to Eqs. (2.2) and (3.1), contains an additional factor 1/2, since the potential energy of each spring is equally divided between two particles connected by this spring.

5.3.2 The Continual Approximation

In the case of the long-wavelength perturbations, when $\lambda \gg a$ (where λ is the characteristic spatial scale of deformation), one can pass from discrete variables i and j to continuous spatial variables $x = ia$ and $y = ja$ as it was done in Chaps. 2 and 3. As a result, it is possible to obtain the following expression for the surface density of the Lagrange function $L = (T - V)/a^2$:

$$\begin{aligned}
L = \frac{\rho}{2} &\left(u_t^2 + v_t^2 + w_t^2 + \frac{l^2}{12}(\theta_t^2 + \varphi_t^2 \sin^2 \theta) \right) \\
&- \frac{\rho}{2}\big[c_1^2(u_x^2 + v_y^2) + c_2^2(v_x^2 + u_y^2) \\
&+ \frac{l^2}{2}(c_{\theta x}^2 \theta_x^2 + c_{\theta y}^2 \theta_y^2) + s^2(u_x v_y + u_y v_x) \\
&+ c_3^2(w_x^2 + w_y^2) + \beta(\theta^2 + 2w_y \theta) \\
&+ \alpha_1(u_x w_x^2 + v_y w_y^2) \\
&+ \alpha_2(u_x w_y^2 + v_y w_x^2 + 2(u_y + v_x)w_x w_y) \\
&+ \alpha_3 u_x \theta^2 + \alpha_4 v_y \theta^2 + \alpha_5 w_x \theta \varphi + \alpha_6 v_x w_x \theta \\
&+ \alpha_7 v_y w_y \theta + \alpha_8(u_x w_y + u_y w_x)\theta \big].
\end{aligned} \tag{5.16}$$

The Lagrange function (5.16) is given with accuracy up to the terms of $\varepsilon^{5/2}$-order inclusively. The following notation is introduced here: $c_{1,2,3}$ are the velocities of the longitudinal, transverse, and bending waves, respectively, $c_{\theta x}$ and $c_{\theta y}$ are the rotational wave velocities with respect to x- and y-axes, correspondingly, s is the coefficient of linear coupling between the longitudinal and transverse waves, β is the dispersion parameter, α_i ($i = 1\ldots8$) are the nonlinearity coefficients, and $\rho = m/a^2$ is the average density of the two-dimensional medium in question.

Using Hamilton's variational principle, on the base of the Lagrange function (5.16), differential equations of the first approximation are derived that describe the dynamic processes in the considered nanotube layer [14]:

$$u_{tt} = c_1^2 u_{xx} + c_2^2 u_{yy} + s^2 v_{xy} + \frac{1}{2}\frac{\partial F_1}{\partial x} + \frac{1}{2}\frac{\partial F_2}{\partial y},$$

$$v_{tt} = c_2^2 v_{xx} + c_1^2 v_{yy} + s^2 u_{xy} + \frac{1}{2}\frac{\partial F_3}{\partial x} + \frac{1}{2}\frac{\partial F_4}{\partial y},$$

$$w_{tt} = c_3^2 (w_{xx} + w_{yy}) + \beta\theta_y + \frac{1}{2}\frac{\partial F_5}{\partial x} + \frac{1}{2}\frac{\partial F_6}{\partial y},$$

$$\frac{l^2}{12}\left(\theta_{tt} - \frac{1}{2}\varphi_t^2 \sin 2\theta\right)$$
$$= \frac{l^2}{2}(c_{\theta x}^2 \theta_{xx} + c_{\theta y}^2 \theta_{yy}) - \beta(\theta + w_y) - F_7,$$

$$\frac{l^2}{6}(\varphi_{tt} \sin^2 \theta + \varphi_t \theta_t \sin 2\theta) = -\alpha_6 w_x \theta. \tag{5.17}$$

Here,

$$F_1 = \alpha_1 w_x^2 + \alpha_2 w_y^2 + \alpha_3 \theta^2 + \alpha_8 w_y \theta,$$

$$F_2 = 2\alpha_2 w_x w_y + \alpha_8 w_x \theta,$$

$$F_3 = 2\alpha_2 w_x w_y + \alpha_6 w_x \theta,$$

$$F_4 = \alpha_1 w_y^2 + \alpha_2 w_x^2 + \alpha_4 \theta^2 + \alpha_7 w_y \theta,$$

$$F_5 = 2\alpha_1 u_x w_x + 2\alpha_2 (v_y w_x + (u_y + v_x) w_y)$$
$$+ \alpha_5 \theta\varphi + \alpha_6 v_x \theta + \alpha_8 u_y \theta$$

$$F_6 = 2\alpha_1 v_y w_y + 2\alpha_2 (u_x w_y + (u_y + v_x) w_x)$$
$$+ \alpha_7 v_y \theta + \alpha_8 u_x \theta$$

$$F_7 = \alpha_3 u_x \theta + \alpha_4 v_y \theta$$
$$+ \frac{1}{2}\big[\alpha_5 w_x \phi + \alpha_6 v_x w_x + \alpha_7 v_y w_y + \alpha_8 (u_x w_y + u_y w_x)\big]$$

are the nonlinearity functions.

Equation (5.17) differ from the equations of the classical theory of elasticity by the appearance of two additional equations for rotational motions. It should be remarked

that the last equation is non-wave in nature, since it does not contain the term φ_{xx}. "Freezing" of the rotational mode θ (i.e., if $\theta \equiv 0$) leads to disappearance of the equation for the second rotation mode φ.

Equation (5.17) have an essentially nonlinear nature, since the bending mode affects the longitudinal and transverse modes only due to nonlinear interactions. The longitudinal and transverse modes, as well as the bending mode and the rotational one θ, are linearly interlinked. In the linear approximation, the equations for the longitudinal and transverse waves have the form:

$$
\begin{aligned}
u_{tt} &= c_1^2 u_{xx} + c_2^2 u_{yy} + s^2 v_{xy}, \\
v_{tt} &= c_2^2 v_{xx} + c_1^2 v_{yy} + s^2 u_{xy}.
\end{aligned}
\tag{5.18}
$$

Equation (5.18) are analogs of the two-dimensional Lame equations for crystals with cubic symmetry (4.16).

5.3.3 Relationships Between the Macroparameters of the Material and the Parameters of Its Inner Structure

The coefficients of the linear parts of Eq. (5.17) are expressed in terms of the force constants $k_0, k_1, k_2, k_0', k_1', k_2'$, the length of the nanotubes l and the lattice period a as follows:

$$
\begin{aligned}
\rho c_1^2 &= k_0 + 2k_1 + \frac{2a^2}{r^2}k_2 + k_0' + 2k_1' + \frac{4a^2}{d^2}k_2', \\
\rho c_2^2 &= k_0' + 2k_1' + \frac{4a^2}{d^2}k_2', \ s^2 = 2c_2^2, \\
\rho c_{\theta x}^2 &= k_1' + \frac{2a^2}{d^2}k_2', \ \rho c_{\theta y}^2 \\
&= k_1 + \frac{a^2}{r^2}k_2 + k_1' + \frac{2a^2}{d^2}k_2', \\
\rho c_3^2 &= \rho\beta = 2\left(\frac{l^2}{r^2}k_2 + \frac{2l^2}{d^2}k_2'\right),
\end{aligned}
\tag{5.19}
$$

where $r = \sqrt{l^2 + a^2}$ and $d = \sqrt{l^2 + 2a^2}$ are the initial lengths of the diagonal springs of the first and second coordination spheres, respectively.

It should be noted that there is an equality $s^2 = 2c_2^2$ in Eq. (5.19). This is analog of the Cauchy relation $C_{12} = C_{44}$ for cubic crystals (see Sect. 4.2.1). Thus, the Cauchy relation is always fulfilled in the considered medium.

Moreover, from Eq. (5.19) it follows that in the linear parts of Eq. (5.17), only five coefficients are independent. From the second and third relations (5.19), it is

obviously that taking into account the interaction with particles of the second coordination sphere is necessary. If this interaction is not taken into account, then the quantity s^2 vanishes that, as it is visible from Eq. (5.18), contradicts the theory of elasticity. In addition, the first two equalities (5.19) imply that the longitudinal wave velocity c_1 exceeds the transverse wave velocity c_2 that is consistent with the data of classical solid-state physics [16–19], and the rotational wave θ propagates faster along y-axis than along x-axis. In the last conclusion, the principal thing is only the difference in the velocities of this wave along x- and y-axes, because if we count the angle φ from the x-axis, then $c_{\theta x} > c_{\theta y}$. It should be also noted that in the model under consideration $c_2 > c_{\theta x}$, and $c_{\theta y}$ can both exceed the transverse wave velocity c_2 and be less than it.

The dependences of the coefficients of the nonlinear parts of Eq. (5.17) on the parameters of the internal structure have the following form:

$$\rho\alpha_1 = k_0 + 2k_1 + \frac{2a^2(a^2 - 2l^2)}{r^4}k_2$$
$$+ k_0' + 2k_1' + \frac{8a^2(a^2 - 4l^2)}{d^4}k_2',$$
$$\rho\alpha_2 = k_0' + 2k_1' + \frac{8a^2(a^2 - 4l^2)}{d^4}k_2',$$
$$\rho\alpha_3 = \frac{2l^2}{r^2}k_2 + \frac{32l^4}{d^4}k_2',$$
$$\rho\alpha_4 = \frac{6l^2}{r^2}k_2 + \frac{24l^2(l^2 + a^2)}{d^4}k_2',$$
$$\rho\alpha_5 = \frac{4l^2}{r^2}k_2 + \frac{8l^2}{d^2}k_2',$$
$$\rho\alpha_6 = \frac{4l^2}{r^2}k_2 + \frac{16l^4}{d^4}k_2',$$
$$\rho\alpha_7 = \frac{4l^2(l^2 - a^2)}{r^4}k_2 + \frac{16l^4}{d^4}k_2',$$
$$\rho\alpha_8 = -\frac{24a^2l^2}{d^4}k_2'. \tag{5.20}$$

An inequality $\alpha_1 > \alpha_2$ follows from Eq. (5.20), and the last six coefficients α_i ($i = 3 \ldots 8$) depend on the parameters of force interactions of only one type— k_2 and k_2', which characterize the shear deformations in the material. When these parameters tend to zero, as well as in the case of the degeneration of the rods into material points ($l \to 0$) that corresponds to the limiting transition of the medium from nanotubes to the medium from fullerenes, the linear coefficients c_3 and β, as well as all factors α_i at $i = 3\ldots8$, vanish. Thus, the developed mathematical model (5.17) will change qualitatively that confirms the significant difference between the physical–mechanical properties of fullerenes and carbon nanotubes mentioned at the beginning of Sect. 5.3. In addition, it should be noted that the force parameters

k_2 and k_2' can be both positive and negative; therefore, the coefficients α_3, ..., α_8 can have different signs. For $k_2 > 0$ and $k_2' > 0$, the following estimates can be performed due to Eq. (5.20): $\alpha_4 > \alpha_3, \alpha_4 > \alpha_5$, and $\alpha_4 > \alpha_6 > \alpha_7$. The situation with the relation between α_6 and α_5 is less unambiguous. Since $\alpha_6 - \alpha_5 = \frac{8l^2(l^2 - 2a^2)}{d^4} k_2'$, then $\alpha_6 < \alpha_5$ for $l < a\sqrt{2}$ and $\alpha_6 > \alpha_5$ at $l > a\sqrt{2}$. The same applies to the coefficient α_3: Depending on the relationship between k_2 and k_2', it can take any value in comparison with α_5 and α_6.

5.4 Conclusions

In this chapter, using the structural modeling method, nonlinear mathematical models are obtained for two-dimensional media consisting of round particles (with 3 degrees of freedom) and of rods (with 5 degrees of freedom). The relationship between the macroparameters of such media and the parameters of their microstructure has been revealed.

In the first model, theoretical estimates of the nonlinearity coefficients have been performed for some materials with cubic symmetry.

In the second model, it is shown that, in the linear approximation, longitudinal and transverse waves are independent on the other vibration modes, and only bending mode w and rotational mode θ are dependent among all the translational and rotational modes. The equation for φ has a non-wave form. When one of the rotational modes is frozen (i.e., $\theta = 0$), the equation for the second rotational mode, φ, automatically disappears. When rods (nanotubes) degenerate into material points, as well as in the absence of interactions under shear deformations, all nonlinear terms proportional to the rotations θ disappear and the bending waves also become non-propagating. Thus, qualitative changes will occur in the developed mathematical model. This fact is consistent with the experimentally known significant difference between the physicomechanical properties of fullerenes and carbon nanotubes [9, 10].

References

1. Erofeev, V.I.: Wave Processes in Solids with Microstructure. World Scientific Publishing. New Jersey, London, Singapore, Hong Kong, Bangalore, Taipei (2003)
2. Lurie A.I.: Non-Linear Theory of Elasticity, 0. 617. Elsevier (2012)
3. Pavlov, I.S.: On estimation of the nonlinearity coefficients of a granular medium by the structural modeling method. Vestnik Nizhegorodskogo Universiteta (Nizhny Novgorod State University Proceedings) **6**, 143–152 (2012). (in Russian)

4. Vanin, G.A.: Gradient theory of elasticity. Mech. Solids **1**, 46–53 (1999)
5. Pavlov, I.S., Potapov, A.I., Maugin, G.A.: A 2D granular medium with rotating particles. Int. J. Solids Struct. **43**(20), 6194–6207 (2006)
6. Dragunov, T.N., Pavlov, I.S., Potapov, A.I.: Anharmonic interaction of elastic and orientation waves in one-dimensional crystals. Phys. Solid State. **39**, 118–124 (1997)
7. Potapov, A.I., Pavlov, I.S.: Nonlinear waves in 1D oriented media. Acoust. Lett. **19**(6), 110–115 (1996)
8. Potapov, A.I., Pavlov, I.S., Lisina, S.A.: Identification of nanocrystalline media by acoustic spectroscopy methods. Acoust. Phys. **56**(4), 588–596 (2010)
9. Dyachkov, P.N.: Carbon nanotubes. Structure, properties, applications. Publishing House Binom. Laboratory of Knowledge, Moscow (2006) 296 p. (in Russian)
10. Eletskii, A.V.: Mechanical properties of carbon nanostructures and related materials. Phys. Uspekhi **50**(3), 225–261 (2007)
11. Li, Chunyu, Chou, Tsu-Wei: A structural mechanics approach for the analysis of carbon nanotubes. Int. J. Solids Struct. **40**, 2487–2499 (2003)
12. Goldshtein, R.V., Chentsov, A.V.: A discrete-continual model for a nanotube. Mech. Solids **4**, 57–74 (2005)
13. Smirnov, V.V., Shepelev, D.S., Manevitch, L.I.: Localization of bending vibrations in the single-wall carbon nanotubes. Nanosyst. Phys. Chem. Math. **2**(2), 102–106 (2011)
14. Miloserdova, I.V., Pavlov, I.S.: The mathematical model of nonlinear oscillations of a layer of nanotubes. In: Proceedings of the First Russian Conference "Problems of Mechanics and Acoustics of Media with Micro- and Nanostructure: NANOMECH-2009", pp. 175–183. Nizhny Novgorod, Russia (2009) (in Russian)
15. Pavlov, I.S., Potapov, A.I.: Structural models in mechanics of nanocrystalline media. Doklady Phys. **53**(7), 408–412 (2008)
16. Fedorov, V.I.: Theory of Elastic Waves in Crystals. Plenum Press, New York, Nauka, Moscow, 1965, 1968
17. Kittel, C.: Introduction to Solid State Physics, 8th edn. John Wiley and Sons, Inc. (2005)
18. Pavlov, P.V., Khokhlov, A.F.: Physics of Solid Body: Textbook, p. 494. Visshaya School, Moscow (2000)
19. Tucker, J.W., Rampton, V.W.: Microwave Ultrasonics in Solid State Physics. North-Holland Publ. Comp, Amsterdam (1972)

Chapter 6
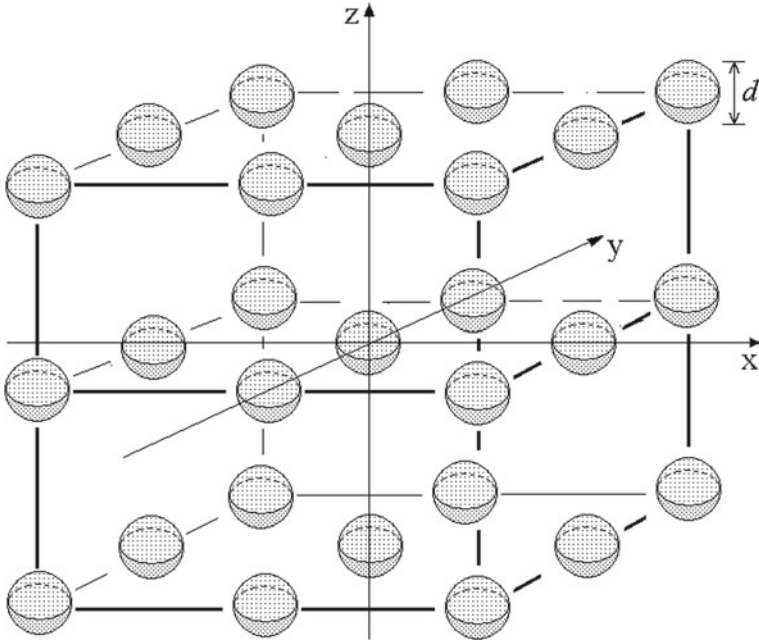# A Cubic Lattice of Spherical Particles

In the previous chapters, two-dimensional models of microstructured media were discussed, and the particles of which have three degrees of freedom. This chapter is devoted to the elaboration of a three-dimensional model of a crystalline medium consisting of spherical particles with six degrees of freedom. Such a medium is structurally similar to a fullerite crystal with a simple cubic lattice (see Sect. 1.2). The main objectives of this chapter are to obtain dynamic equations of a crystalline medium consisting of spherical particles by the method of structural modeling and to establish the relationships between the coefficients of these equations and the microstructure parameters of the material at issue.

6.1 A Discrete 3D Model of a Crystalline Medium of Spherical Particles

We consider a cubic lattice consisting of rigid spherical particles (grains) of mass M and having a shape of a sphere with diameter d. In the initial state, they are located in the sites of the lattice with a period a (Fig. 6.1). Each particle possesses six degrees of freedom: The center of gravity of a particle with number $N = N(i, j, k)$ can move along the x-, y-, and z-axes (translational degrees of freedom $u_{i,j,k}$, $v_{i,j,k}$, and $w_{i,j,k}$), and the particle itself can rotate around each of these axes (rotational degrees of freedom $\theta_{i,j,k}$, $\psi_{i,j,k}$, and $\varphi_{i,j,k}$) (Fig. 6.2). In this case, the kinetic energy of the Nth particle is described by the following formula:
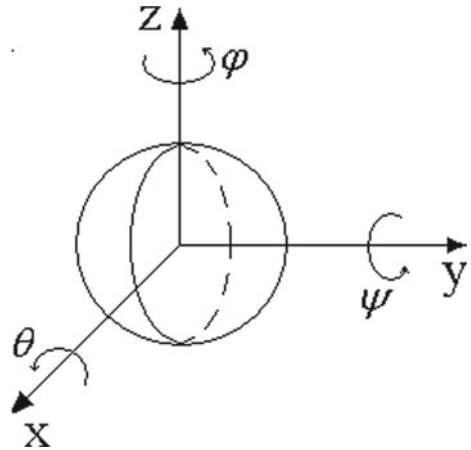
$$T = \frac{M}{2}\left(u_t^2 + v_t^2 + w_t^2\right) + \frac{J}{2}(\varphi_t^2 + \theta_t^2 + \psi_t^2), \tag{6.1}$$

where $J = \frac{2}{5}M\left(\frac{d}{2}\right)^2 = \frac{1}{10}Md^2 = \frac{2}{5}M\frac{3b^2}{4} = 0.3Mb^2$ is the moment of inertia of the particle with respect to each axis passing through its center of gravity.

Fig. 6.1 Simple cubic lattice consisting of spherical particles

**Fig. 6.2** Rotational degrees of freedom of the particle

As in the models discussed in the previous chapters, the space between the particles is an inertia-less elastic medium through which the force and moment effects are transmitted, which are modeled by elastic springs. The particles $N = N(i, j, k)$ is supposed to interact only with the nearest neighbors located at a distance a from it (particles of the first coordination sphere: $(i − 1, j, k)$, $(i, j − 1, k)$, $(i, j + 1, k)$, $(i +$

1, j, k)), $a\sqrt{2}$ (particles of the second coordination sphere: $(i-1, j-1, k)$, $(i-1, j+1, k)$, $(i+1, j-1, k)$, $(i+1, j+1, k)$) and $a\sqrt{3}$ (particles of the third sphere: $(i-1, j-1, k-1)$, $(i-1, j-1, k+1)$, $(i-1, j+1, k-1)$, $(i-1, j+1, k+1)$, $(i+1, j-1, k-1)$, $(i+1, j-1, k+1)$, $(i+1, j+1, k-1)$, $(i+1, j+1, k+1)$) (Fig. 6.1).

The central and non-central interactions of neighboring particles are modeled by elastic springs of five types: The central springs with rigidity K_0, the non-central springs with rigidity K_1 (Fig. 6.3), the diagonal springs (K_2), as well as the springs with stiffness K_3 and K_4, which connect the central particle with grains, respectively, of the second and third coordination spheres. The central springs K_0 connect the centers of neighboring particles. Points of connection of the springs K_1 and K_2 with the particles lie at the vertices of a cube with side b inscribed in a ball of diameter $d = b\sqrt{3}$ (in Fig. 6.3 A_2B_1', B_2A_1', E_2C_1', and C_2E_1' are the springs with rigidity K_1, whereas A_2C_1', E_2B_1', B_2E_1', and C_2A_1' are the springs of K_2-type). The springs with stiffness K_3 and K_4 are attached to the midpoints of the nearest edges of cubes, the geometric centers of which are located in the initial state at distances $a\sqrt{2}$ (Fig. 6.4) and $a\sqrt{3}$.

The springs with stiffnesses K_0, K_1, K_2, and K_3 describe the interactions of particles within one layer (Fig. 6.5). Thus, the central (K_0) and non-central (K_1) springs characterize interactions during tension-compression of the material. The springs K_1 also transmit torques when the particles rotate. Springs with stiffness K_1
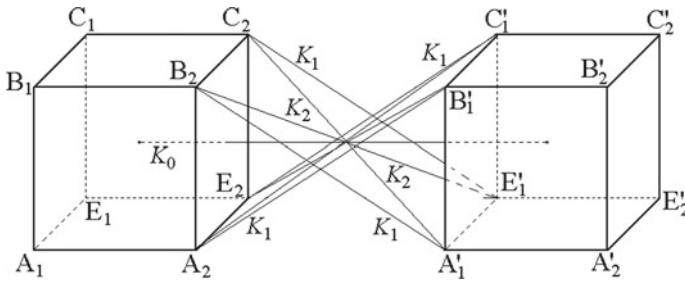
Fig. 6.3 Scheme of force interactions between the nearest neighbors in the lattice (particles of the first coordination sphere)

Fig. 6.4 Scheme of force interactions of the central particle with the particles of the second coordination sphere
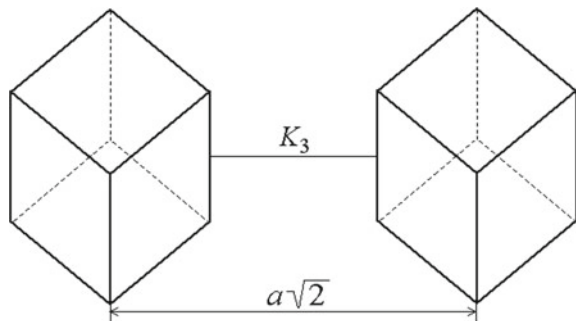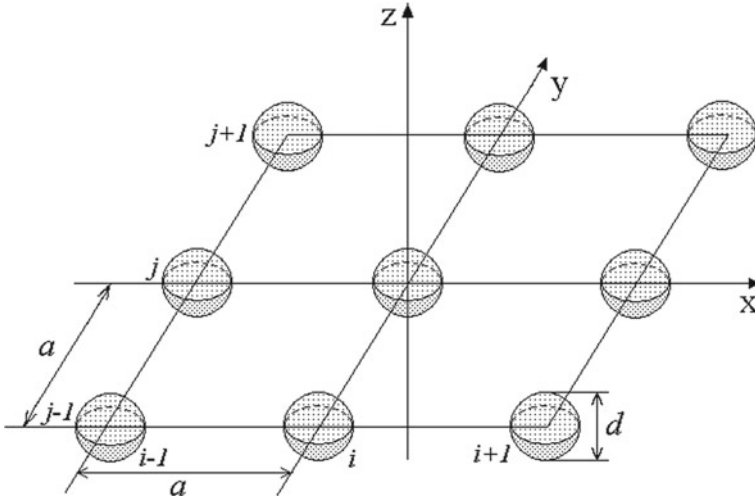
Fig. 6.5 Square lattice (a layer) of spherical particles

and K_2 characterize the force interactions of the particles during shear deformations in the material. It should be noted that the chosen scheme of force interactions inside one layer is similar to that introduced in a two-dimensional lattice of plane particles (see Chap. 3 and Refs. [1, 2]).

The displacements of the grains are assumed to be small in comparison with the sizes of the unit cell of the considered lattice. The interaction of the particles when they deviate from the equilibrium states is determined by the relative elongations of the springs. The potential energy due to the interaction of a particle N with eight nearest neighbors in the lattice is described by the formula

$$
U_N = \frac{1}{2}\left(\sum_{n=1}^{4} \frac{K_0}{2} D_{0n}^2 + \sum_{n=1}^{16} \frac{K_1}{2} D_{1n}^2 + \sum_{n=1}^{16} \frac{K_2}{2} D_{2n}^2 + \sum_{n=1}^{4} \frac{K_3}{2} D_{3n}^2 + \sum_{n=1}^{4} \frac{K_4}{2} D_{4n}^2 \right),
$$

$$(6.2)$$

where D_{ln} ($l = 0, 1, 2, 3, 4$) are the extensions of springs of five types, which are numbered in an arbitrary order and connect the particle with its neighbors. These extensions are determined by variations of the distances between the connection points of the respective springs (Fig. 6.3). The necessity to enter the mentioned above springs of all five types is justified in Sect. 6.2.2. Next, we will first consider the nonlinear dynamics of one layer [3] of spherical particles (when $K_4 \equiv 0$).

6.2 Nonlinear Model of a One-Layer Medium of Spherical Particles

In order to construct a mathematical model of a single-layer medium consisting of spherical particles, which is a generalization of two-dimensional models of media consisting of plane particles with three degrees of freedom and of rods with five degrees of freedom (they were considered, respectively, in Chap. 3 and Sect. 5.3 of this monograph), we first put in Eq. (6.2) $K_4 = 0$. Then, we substitute in Eq. (6.2) the expressions for the elongations D_{ln} that are calculated in the approximation of small quantities $\Delta u_i \sim \Delta v_i \sim \Delta u_j \sim \Delta v_j \sim \varepsilon$, $\Delta w_i \sim \Delta w_j \sim \varphi_{i,j} \sim \theta_{i,j} \sim \psi_{i,j} \sim \varepsilon^{3/4}$, $\Delta \varphi_i \sim \Delta \theta_i \sim \Delta \psi_i \sim \Delta \varphi_j \sim \Delta \theta_j \sim \Delta \psi_j \sim \varepsilon^{5/4}$, where $\varepsilon \ll 1$ is the measure of the cell deformation. These expressions are calculated according to the same algorithm as for the model in Sect. 5.1 (see Appendix 2), but they are not presented here because there are too many springs in this model. According to the procedure given in Sects. 3.1 and 3.2, one can obtain differential–difference equations describing the dynamics of a square lattice of spherical particles. However, in this chapter, we will consider in detail the continuum approximation of the proposed model.

6.2.1 The Continuum Approximation

In the case of the long-wavelength perturbations, when $\lambda \gg a$ (see Sects. 2.2 and 3.2), the Lagrange function L of the considered medium consisting of spherical particles takes on the form [4]:

$$
\begin{aligned}
L = {} & \frac{M}{2}\left(u_t^2 + v_t^2 + w_t^2\right) + \frac{J}{2}\left(\varphi_t^2 + \psi_t^2 + \theta_t^2\right) \\
& - \frac{M}{2}\Big[c_1^2\left(u_x^2 + v_y^2\right) + c_2^2\left(v_x^2 + u_y^2\right) + c_3^2\left((w_x - \psi)^2 + (w_y + \theta)^2\right) \\
& + b^2 c_4^2\left(\varphi_x^2 + \varphi_y^2\right) + b^2 c_5^2\left(\theta_x^2 + \psi_y^2\right) + b^2 c_6^2\left(\theta_y^2 + \psi_x^2\right) \\
& + s^2\left(u_x v_y + u_y v_x\right) + 2\beta\left(\varphi^2 + v_x \varphi - u_y \varphi\right) \\
& + \alpha_1\left(u_x w_x^2 + v_y w_y^2\right) + \alpha_2\left(u_x w_y^2 + v_y w_x^2 + 2(u_y + v_x)w_x w_y\right) + \alpha_3\left(u_x \varphi^2 + v_y \varphi^2\right) \\
& + \alpha_4\left(u_x \psi^2 + v_y \theta^2\right) + \alpha_5\left(u_x \theta^2 + v_y \psi^2\right) - \alpha_6 u_x w_x \psi + (\alpha_6 + \alpha_7)v_y w_y \theta \\
& + \alpha_7\left((u_x w_y + u_y w_x)\theta - (u_x w_y + u_y w_x + v_x w_x + v_y w_y)\psi\right) \\
& + \alpha_8\left(w_x \varphi\theta + w_y \varphi\psi\right) - \alpha_9\left(u_y + v_x\right)\theta\psi + (\alpha_7 + \alpha_{10})v_x w_x \theta - \alpha_{10} u_y w_y \psi\Big] \quad (6.3)
\end{aligned}
$$

The Lagrange function (6.3) contains only the terms up to the $\varepsilon^{5/2}$-order inclusive.

Using the Hamilton's variational principle, a set of differential equations describing nonlinear dynamic processes in a square lattice of spherical particles is derived from the Lagrange function (6.3):

$$u_{tt} = c_1^2 u_{xx} + c_2^2 u_{yy} + s^2 v_{xy} - \beta\varphi_y + \frac{1}{2}\frac{\partial F_1}{\partial x} + \frac{1}{2}\frac{\partial F_2}{\partial y},$$

$$v_{tt} = c_2^2 v_{xx} + c_1^2 v_{yy} + s^2 u_{xy} + \beta\varphi_x + \frac{1}{2}\frac{\partial F_3}{\partial x} + \frac{1}{2}\frac{\partial F_4}{\partial y},$$

$$w_{tt} = c_3^2 (w_{xx} + w_{yy} + 2\theta_y - 2\psi_x) + \frac{1}{2}\frac{\partial F_5}{\partial x} + \frac{1}{2}\frac{\partial F_6}{\partial y},$$

$$J\varphi_{tt} = M\big(b^2 c_4^2 (\varphi_{xx} + \varphi_{yy}) + \beta(u_y - v_x - 2\varphi) - F_7\big),$$

$$J\theta_{tt} = M\big(b^2 (c_5^2 \theta_{xx} + c_6^2 \theta_{yy}) - 2c_3^2(w_y + \theta) - F_8\big),$$

$$J\psi_{tt} = M\big(b^2 (c_6^2 \psi_{xx} + c_5^2 \psi_{yy}) + 2c_3^2(w_x - \psi) - F_9\big). \tag{6.4}$$

Here,

$$F_1 = \alpha_1 w_x^2 + \alpha_2 w_y^2 + \alpha_3 \varphi^2 + \alpha_4 \psi^2 + \alpha_5 \theta^2 - \alpha_6 w_x \psi + \alpha_7 w_y(\theta - \psi),$$

$$F_2 = 2\alpha_2 w_x w_y - \alpha_9 \theta\psi - \alpha_{10} w_y \psi + \alpha_7 w_x(\theta - \psi),$$

$$F_3 = F_2 + \alpha_{10}(w_x \theta + w_y \psi),$$

$$F_4 = \alpha_1 w_y^2 + \alpha_2 w_x^2 + \alpha_3 \varphi^2 + \alpha_4 \theta^2 + \alpha_5 \psi^2 + (\alpha_6 + \alpha_7)w_y \theta - \alpha_7 w_y \psi,$$

$$F_5 = 2\alpha_1 u_x w_x + 2\alpha_2 (v_y w_x + u_y w_y + v_x w_y) - \alpha_6 u_x \psi + \alpha_7 (u_y \theta - u_y \psi - v_x \psi)$$
$$\quad + \alpha_8 \varphi\theta + (\alpha_7 + \alpha_{10})v_x \theta,$$

$$F_6 = 2\alpha_1 v_y w_y + 2\alpha_2 (u_x w_y + u_y w_x + v_x w_x) + (\alpha_6 + \alpha_7)v_y \theta$$
$$\quad + \alpha_7 (u_x \theta - u_x \psi + v_y \psi) + \alpha_8 \varphi\psi - \alpha_{10} u_y \psi,$$

$$F_7 = 2\alpha_3 (u_x + v_y)\varphi + \alpha_8 (w_x \theta + w_y \psi),$$

$$F_8 = 2\alpha_4 v_y \theta + 2\alpha_5 u_x \theta + (\alpha_6 + \alpha_7)v_y w_y + \alpha_7 (u_x w_y + u_y w_x)$$
$$\quad + \alpha_8 w_x \varphi - \alpha_9 (u_y + v_x)\psi + (\alpha_7 + \alpha_{10})v_x w_x,$$

$$F_9 = 2\alpha_4 u_x \psi + 2\alpha_5 v_y \psi - \alpha_6 u_x w_x - \alpha_7 (u_x w_y + u_y w_x + v_x w_x + v_y w_y)$$
$$\quad + \alpha_8 w_y \varphi - \alpha_9 (u_y + v_x)\theta - \alpha_{10} u_y w_y$$

are the nonlinearity functions.

The following designations are introduced in the Lagrange function (6.3) and Eq. (6.4): c_1, c_2, and c_3 are the velocities of longitudinal, transverse, and bending waves, c_4, c_5, c_6 are the velocities of microrotation waves, s is the coefficient of linear coupling between the longitudinal and shear waves, β is the dispersion parameter, and α_i ($i = 1 \dots 10$) are the nonlinearity coefficients.

In the limiting case, when $w = \theta = \psi = 0$, Eq. (6.4) degenerate into the previously derived equations for the dynamics of a square lattice of round particles

(see Chap. 3), which, in turn, coincide with the equations of the two-dimensional
Cosserat continuum consisting of centrally symmetric particles [5, 6].

6.2.2   Dependency of the Macroparameters of a One-Layer Medium on the Parameters of Its Microstructure

The coefficients of linear parts of Eq. (6.4) are expressed in terms of the force
constants K_0, K_1, K_2, and K_3, the lattice period a, and the particle size $b = d/2\sqrt{3}$
as follows:

$$\rho c_1^2 = \frac{K_0}{a} + \frac{4(a-b)^2}{(a-b)^2 + b^2}\frac{K_1}{a} + \frac{4(a-b)^2}{(a-b)^2 + 2b^2}\frac{K_2}{a} + \frac{K_3}{a},$$

$$\rho c_2^2 = \frac{4b^2}{(a-b)^2 + 2b^2}\frac{K_2}{a} + \frac{K_3}{a},$$

$$\rho c_3^2 = \frac{4b^2}{(a-b)^2 + b^2}\frac{K_1}{a} + \frac{4b^2}{(a-b)^2 + 2b^2}\frac{K_2}{a},$$

$$\rho c_4^2 = \frac{(a-b)^2}{(a-b)^2 + b^2}\frac{K_1}{a} + \frac{a^2}{(a-b)^2 + 2b^2}\frac{K_2}{a},$$

$$\rho c_5^2 = \frac{b^2}{(a-b)^2 + b^2}\frac{K_1}{a},$$

$$\rho c_6^2 = \frac{a^2}{(a-b)^2 + b^2}K_1 + \frac{a^2}{(a-b)^2 + 2b^2}K_2,$$

$$\rho s^2 = \frac{2K_3}{a}, \quad \rho \beta = \frac{4b^2}{(a-b)^2 + 2b^2}\frac{K_2}{a} \tag{6.5}$$

where $\rho = M/a^3$ is the density of the medium.

From expressions (6.5), one can obtain the following relationships between the
macroparameters of the medium:

$$\beta + \frac{s^2}{2} = c_2^2,$$

$$c_4^2 = \frac{(a-b)^2 c_3^2 - (b^2 - 2ab)\beta}{4b^2},$$

$$c_5^2 = \frac{c_3^2 - \beta}{4}, \quad c_6^2 = \frac{a^2}{b^2}\left(\frac{c_3^2}{4}\right). \tag{6.6}$$

It should be noted that the first equality (6.6) is also valid for the square and
hexagonal lattices of plane round particles (see Eq. (2.11) and Ref. [7]).

The nonlinearity coefficients depend on the microstructure parameters as follows:

$$\rho\alpha_1 = \frac{K_0}{a} + \frac{4a^2(a-b)(a-2b)}{r_1^4}\frac{K_1}{a} + \frac{4a(a-b)^3}{r_2^4}\frac{K_2}{a} + \frac{a}{a-b}\frac{K_3}{a},$$

$$\rho\alpha_2 = \frac{a}{a-b}\frac{K_3}{a},$$

$$\rho\alpha_3 = \frac{b}{a}\left(\frac{4b(a-b)}{r_1^2}\frac{K_1}{a} + \frac{4b}{r_2^2}\left(a - 3b + \frac{4b^2(a+b)}{r_2^2}\right)\frac{K_2}{a} + \frac{3b}{2(a-b)}\frac{K_3}{a}\right),$$

$$\rho\alpha_4 = \frac{b}{a}\left(\frac{4b}{r_1^2}\left(a - b - \frac{ab^2+b^3}{r_1^2}\right)\frac{K_1}{a} + \frac{4b}{r_2^2}\left(a - 3b + \frac{4ab^2+4b^3}{r_2^2}\right)\frac{K_2}{a} + \frac{b}{a-b}\frac{K_3}{a}\right),$$

$$\rho\alpha_5 = \frac{b}{a}\left(\frac{4b(a-b)}{r_1^2}\frac{K_1}{a} + \frac{4b(a-b)}{r_2^2}\left(2 - \frac{b^2}{r_2^2}\right)\frac{K_2}{a} + \frac{b}{a-b}\frac{K_3}{a}\right),$$

$$\rho\alpha_6 = \frac{4b}{a}\left(\frac{a}{r_1^2}\left(2a - 3b - \frac{a^2b}{r_1^2}\right)\frac{K_1}{a} + \frac{2a}{r_2^2}\left(a - 2b + \frac{6b^3-2ab^2}{r_2^2}\right)\frac{K_2}{a}\right),$$

$$\rho\alpha_7 = \frac{2bK_3}{(a-b)a} = \frac{2b}{a}\rho\alpha_2,$$

$$\rho\alpha_8 = \frac{4b}{a}\left(\frac{2b^2}{r_1^2}\frac{K_1}{a} - \frac{b(a-b)}{r_2^2}\left(2 - \frac{b^2}{r_2^2}\right)\frac{K_2}{a}\right),$$

$$\rho\alpha_9 = \frac{2ab}{M}\left(\frac{4ab}{r_1^2}\frac{K_1}{a} + \frac{2b(a-b)}{r_2^2}\left(2 - \frac{b^2}{r_2^2}\right)\frac{K_2}{a} + \frac{b}{a-b}\frac{K_3}{a}\right),$$

$$\rho\alpha_{10} = \frac{8b^2}{(a-b)^2 + b^2}\frac{K_1}{a}. \tag{6.7}$$

Here, $r_1 = \sqrt{(a-b)^2 + b^2}$ and $r_2 = \sqrt{(a-b)^2 + 2b^2}$ are the lengths of springs K_1 and K_2 at the initial state. It should be noted that all the nonlinearity coefficients, except the factors α_1 and α_2, vanish, when the considered lattice of spherical particles degenerates into a lattice of material points (i.e., for $b \to 0$).

In Chap. 4 (see Table 4.1), it was shown that if the velocity of the longitudinal wave c_1 is greater than both the transverse wave velocity c_2 and the rotational wave velocity c_4 (in the model, such superiority of c_1 is provided by the central springs K_0), whereas c_2 can be either greater or less than c_4. In this medium, the bending wave velocity c_3 can also both exceed c_2 and be less than it. In particular, it follows from the second and third relations (6.5) that $c_3 > c_2$ for $K_1 > \left(\left(\frac{a}{2b} - \frac{1}{2}\right)^2 + \frac{1}{4}\right)K_3$. An analysis of expressions (6.5) and (6.6) shows that c_6 is the maximal velocity among all the rotational wave velocities c_4, c_5, and c_6. Moreover, as a rule, $c_4 > c_5$. The last inequality can be invalid only for large values of b (with respect to the lattice period a) and small values of K_2 (compared with K_1).

From Eq. (6.5), one can see the importance of taking into account springs of the types K_3, K_2, and K_1 in the model. In the absence of such springs, the terms vanish in Eq. (6.4), which are proportional, respectively, to s (and we would get a contradiction with the classical theory of elasticity), c_5 and β (that contradicts the equations of the Cosserat continuum, which consists of centrally symmetric particles [5, 6]).

It should be emphasized that when the linear parts of Eq. (6.4) degenerate into the dynamic equations for a square lattice of round particles, even the dependences of

their coefficients on the microstructure parameters coincide, if to take into account that in this case the amount of springs of K_1- and K_2-types has become twice greater as in the three-mode model.

Using Eq. (6.5) and the first relation (6.6), one can obtain the following expressions for the parameters of interparticle interaction in terms of the macroparameters of the medium:

$$\frac{K_3}{a} = \frac{\rho s^2}{2}, \quad \frac{K_2}{a} = \frac{\rho}{4}\left(c_2^2 - \frac{s^2}{2}\right)\left(\left(\frac{a}{b} - 1\right)^2 + 2\right),$$

$$\frac{K_1}{a} = \frac{\rho}{4}\left(c_3^2 - c_2^2 + \frac{s^2}{2}\right)\left(\left(\frac{a}{b} - 1\right)^2 + 1\right),$$

$$\frac{K_0}{a} = \rho\left(c_1^2 - \frac{s^2}{2} - \left(\frac{a}{b} - 1\right)^2 c_3^2\right). \tag{6.8}$$

Thus, if to determine experimentally the velocities of elastic waves c_1, c_2, and c_3 (in a three-dimensional medium with cubic symmetry $c_2 = c_3$, as it will be shown in the next section) and the parameter s, then due to the known density of the medium ρ and the relative particle size b/a, it is possible to calculate the parameters of interparticle interaction, which can be further used to estimate the rotational wave velocities and the nonlinearity coefficients. Examples of solving similar problems of parametric identification for the square and hexagonal lattices of plane round particles, as well as for the rectangular lattice of ellipse-shaped particles, are given in Chap. 4.

6.2.3 3D Model of a Crystalline Medium of Spherical Particles

Now, in contrast to Sect. 6.2, in expression (6.2), we take into account all terms, including the terms proportional to K_4. But we will retain only the linear terms in the expressions for the elongations D_{ln}. Further, according to the procedure described in Sects. 3.1 and 3.2, we will pass from the discrete model to the continual one.

6.2.4 Continuum Approximation

In the case of long-wavelength perturbations, when $\lambda \gg a$, the three-dimensional Lagrange function L of the considered medium of spherical particles, with accuracy up to quadratic terms, takes on the form:

$$L = \frac{M}{2}\left(u_t^2 + v_t^2 + w_t^2\right) + \frac{J}{2}\left(\varphi_t^2 + \theta_t^2 + \psi_t^2\right)$$

$$- \frac{M}{2}\left[c_1^2\left(u_x^2 + v_y^2 + w_z^2\right) + c_2^2\left(v_x^2 + v_z^2 + u_y^2 + u_z^2 + w_x^2 + w_y^2\right)\right.$$
$$+ s^2\left(v_y w_z + v_z w_y + u_x w_z + u_z w_x + u_x v_y + u_y v_x\right) + \beta_1^2\left(\varphi^2 + \theta^2 + \psi^2\right)$$
$$+ \beta_2^2\left(v_x \varphi - w_x \psi + w_y \theta - u_y \varphi + u_z \psi - v_z \theta\right)$$
$$+ b^2 c_3^2\left(\varphi_z^2 + \theta_x^2 + \psi_y^2\right) + b^2 c_4^2\left(\varphi_x^2 + \varphi_y^2 + \theta_y^2 + \theta_z^2 + \psi_x^2 + \psi_z^2\right)\bigg]. \tag{6.9}$$

Using the Hamilton's variational principle, it is possible to derive from the Lagrange function (6.9) that a set of linear differential equations describing the propagation of elastic and rotational waves in a cubic lattice of spherical particles:

$$u_{tt} - c_1^2 u_{xx} - c_2^2\left(u_{yy} + u_{zz}\right) - s^2\left(v_{xy} + w_{xz}\right) + \frac{\beta_2^2}{2}\left(\varphi_y - \psi_z\right) = 0$$

$$v_{tt} - c_1^2 v_{yy} - c_2^2\left(v_{xx} + v_{zz}\right) - s^2\left(u_{xy} + w_{yz}\right) + \frac{\beta_2^2}{2}\left(\theta_z - \varphi_x\right) = 0$$

$$w_{tt} - c_1^2 w_{zz} - c_2^2\left(w_{xx} + w_{yy}\right) - s^2\left(u_{xz} + v_{yz}\right) + \frac{\beta_2^2}{2}\left(\psi_x - \theta_y\right) = 0$$

$$\theta_{tt} - c_3^2 \theta_{xx} - c_4^2\left(\theta_{yy} + \theta_{zz}\right) + \frac{\beta_2^2}{2J}\left(w_y - v_z\right) + \frac{\beta_1^2}{J}\theta = 0$$

$$\psi_{tt} - c_3^2 \psi_{yy} - c_4^2\left(\psi_{xx} + \psi_{zz}\right) + \frac{\beta_2^2}{2J}\left(u_z - w_x\right) + \frac{\beta_1^2}{J}\psi = 0$$

$$\varphi_{tt} - c_3^2 \varphi_{zz} - c_4^2\left(\varphi_{xx} + \varphi_{yy}\right) + \frac{\beta_2^2}{2J}\left(v_x - u_y\right) + \frac{\beta_1^2}{J}\varphi = 0 \tag{6.10}$$

The following denotes are entered in the Lagrange function (6.9) and Eq. (6.10): c_1 and c_2 are the velocities of longitudinal and transverse waves, c_3 and c_4 are the velocities of rotation waves of different polarization, s is the coefficient of linear coupling between the longitudinal and shear deformations, β_1 and β_2 are the dispersion parameters (they relate microrotations with the longitudinal and transverse waves), and α_i ($i = 1 \ldots 10$) are the nonlinearity coefficients.

In the limiting case, when $w = \theta = \psi = 0$, Eq. (6.10), as well as the linear parts of Eq. (6.4) for a one-layer medium of spherical particles, degenerate into the previously derived equations for the dynamics of a square lattice of round particles (see Sect. 3.2), which, in turn, coincide with the equations of the two-dimensional Cosserat continuum consisting of centrally symmetric particles [5, 6].

6.2.5   Dependence of the Macroparameters of the 3D Medium on the Parameters of Its Microstructure

The coefficients of Eq. (6.10) are expressed in terms of the force constants K_0, K_1, K_2, K_3, and K_4, the lattice period a, and the particle size $b = d/2\sqrt{3}$ as follows:

$$c_1^2 = \frac{1}{\rho}\left(\frac{K_0}{a} + \frac{8(a-b)^2}{(a-b)^2+b^2}\frac{K_1}{a} + \frac{4(a-b)^2}{(a-b)^2+2b^2}\frac{K_2}{a} + \frac{K_3}{a\sqrt{2}} + \frac{2K_4}{3a}\right),$$

$$c_2^2 = \frac{1}{\rho}\left(\frac{4b^2}{(a-b)^2+b^2}\frac{K_1}{a} + \frac{4b^2}{(a-b)^2+2b^2}\frac{K_2}{a} + \frac{K_3}{2a\sqrt{2}} + \frac{2K_4}{3a}\right),$$

$$c_3^2 = \frac{K_1}{\rho a}\frac{2b^2}{(a-b)^2+b^2}, \quad c_4^2 = \frac{1}{\rho a}\left(\frac{K_1\left(a^2+(a-b)^2\right)}{(a-b)^2+b^2} + \frac{K_2 a^2}{(a-b)^2+2b^2}\right),$$

$$s^2 = \frac{1}{\rho}\left(\frac{K_3}{a\sqrt{2}} + \frac{4K_4}{3a}\right),$$

$$\beta_1^2 = \frac{8b^2}{\rho}\left(\frac{1}{(a-b)^2+b^2}\frac{K_1}{a} + \frac{1}{(a-b)^2+2b^2}\frac{K_2}{a}\right), \quad \beta_2^2 = \frac{K_2}{\rho a}\frac{8b^2}{(a-b)^2+2b^2}.$$

$$(6.11)$$

From relations (6.11), it follows that in a 3D medium with cubic symmetry, consisting of identical centrally symmetric particles with three translational and three rotational degrees of freedom, there is also a dependence of the acoustic and rotational wave velocities on the parameters of its microstructure. Due to this dependence, it is possible, in particular, to obtain two additional relationships between the macroparameters of the medium:

$$\beta_1^2 + s^2 = 2c_2^2, \; \beta_2^2 + 4c_3^2 = \beta_1^2. \tag{6.12}$$

It is interesting to note that the first of relations (6.12) is similar to relation (2.11), which was encountered for the two-dimensional models considered in Chaps. 2 and 3.

Let us find out how the microstructure of a crystalline material affects its physical and mechanical properties. To this purpose, we first write expressions (6.11) in the dimensionless form, i.e., we normalize all the wave velocities to the velocity $c_0 = a\sqrt{K_0/M}$. Next, we will analyze the dependences of the wave velocity c_i $(i = 1 \div 4)$ on the relative particle size d/a and the dimensionless parameters of the force and couple interactions between the particles $K_{i0} = K_i/K_0$ $(i = 1 \div 4)$.

Dependences of the wave velocities on the relative particle size d/a are plotted in Fig. 6.6. The figure shows that, when the particle size grows, the longitudinal wave velocity c_1 decreases monotonically, whereas all other wave velocities, on the contrary, increase monotonically. The velocity c_1 is maximal and the rotational wave velocity c_3 is the minimal. Note that in this case $c_4 > c_2$, however, decreasing of the parameters of the moment interactions K_{10} and K_{20}, as well as increasing of the parameters K_{30} and K_{40}, leads to the relation $c_2 > c_4$ (Figs. 6.7, 6.8, 6.9 and 6.10). Moreover, this inequality is more probably valid for the small $(d/a = 0.1)$ and large $(d/a = 0.9)$ particle sizes (Figs. 6.8, 6.9 and 6.10).

At small grain sizes, the wave velocities c_2 and c_3 are actually constant (Fig. 6.7a, b). But for the large particle sizes, a significant increase of these velocities is observed (Fig. 6.7c). The nature of the dependence of the longitudinal wave velocity on the

Fig. 6.6 Dependences of the
wave velocities on the
relative particle size at K_{10}
$= 0.3$, $K_{20} = 0.9$,
$K_{30} = 1$, $K_{40} = 1$
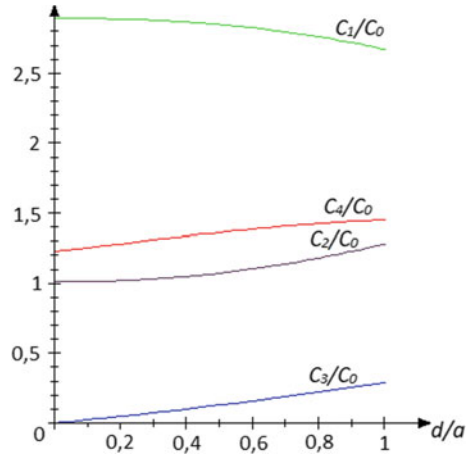
interaction parameters K_{i0} ($i = 1 \div 4$) differs from that shown in Fig. 6.6, as in
Figs. 6.7, 6.8, 6.9, and 6.10, the longitudinal wave velocity monotonically increases
with growing parameters K_{i0}.

6.2.6   Comparison of the Proposed Model with the 3D Cosserat Continuum

Let us compare the Lagrange function (6.9) with the Lagrange function for a 3D
isotropic Cosserat continuum:

$$
\begin{aligned}
L = {} & \frac{\rho}{2}\left(u_t^2 + v_t^2 + w_t^2 + I_1^2\theta_t^2 + I_2\psi_t^2 + I_3\varphi_t^2\right) \\
& - \frac{1}{2}\Big[(\lambda + 2\mu)\left(u_x^2 + v_y^2 + w_z^2\right) + (\mu + \alpha)\left(v_x^2 + v_z^2 + u_y^2 + u_z^2 + w_x^2 + w_y^2\right) \\
& + (\lambda + \mu - \alpha)\left(u_x v_y + u_y v_x + u_x w_z + u_z w_x + v_y w_z + v_z w_y\right) \\
& + 4\alpha\left(\theta^2 + \psi^2 + \varphi^2 + v_x\varphi - w_x\psi + w_y\theta - u_y\varphi + u_z\psi - v_z\theta\right) \\
& + (\beta + 2\gamma)\left(\theta_x^2 + \psi_y^2 + \varphi_z^2\right) + (\gamma + \varepsilon)\left(\varphi_x^2 + \varphi_y^2 + \theta_y^2 + \theta_z^2 + \psi_x^2 + \psi_z^2\right) \\
& + (\beta + \gamma - \varepsilon)\left(\theta_x\psi_y + \theta_y\psi_x + \theta_x\varphi_z + \theta_z\varphi_x + \psi_y\varphi_z + \psi_z\varphi_y\right)\Big] \qquad (6.13)
\end{aligned}
$$

Here, λ and μ are the Lamé parameters; α, β, γ, and ε are the constants of the
Cosserat medium. Thus, there are six independent macroconstants in the isotropic
Cosserat continuum. It is obvious that the degeneration of Eq. (6.13) into Eq. (6.9)
is possible only in the case when $\beta + \gamma = \varepsilon$.
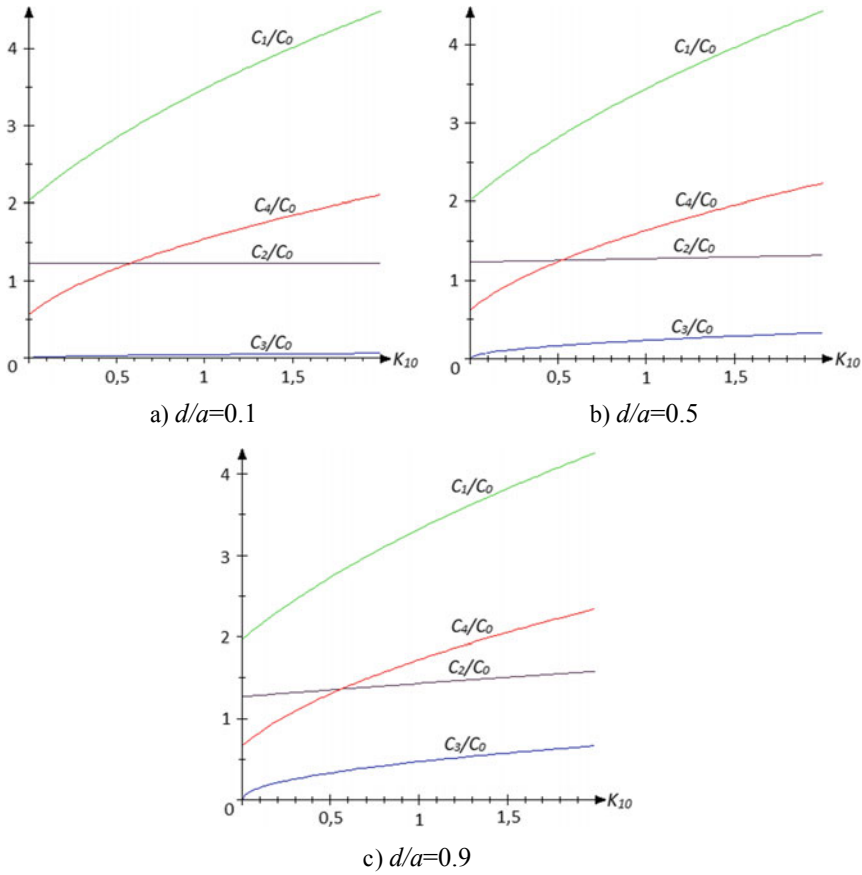
Fig. 6.7 Dependences of the wave velocities on parameter K_{10} at $K_{20} = 0.3$, $K_{30} = 1.2$, $K_{40} = 1.6$

Relations (6.12) show that in this anisotropic model there are only five independent macroconstants, and upon passing to an isotropic medium (see Sect. 4.2) only four constants remain. A similar result has been obtained for an isotropic medium in Ref. [8].

Consequently, the transition from the discrete model to the continuum does not lead to the Cosserat continuum.

6.3 Conclusions

A three-dimensional model of a crystalline medium that represents a simple cubic lattice resembling the lattice of fullerite at low temperatures (see Sect. 1.2.) has been

a) d/a=0.1

b) d/a=0.5

c) d/a=0.9
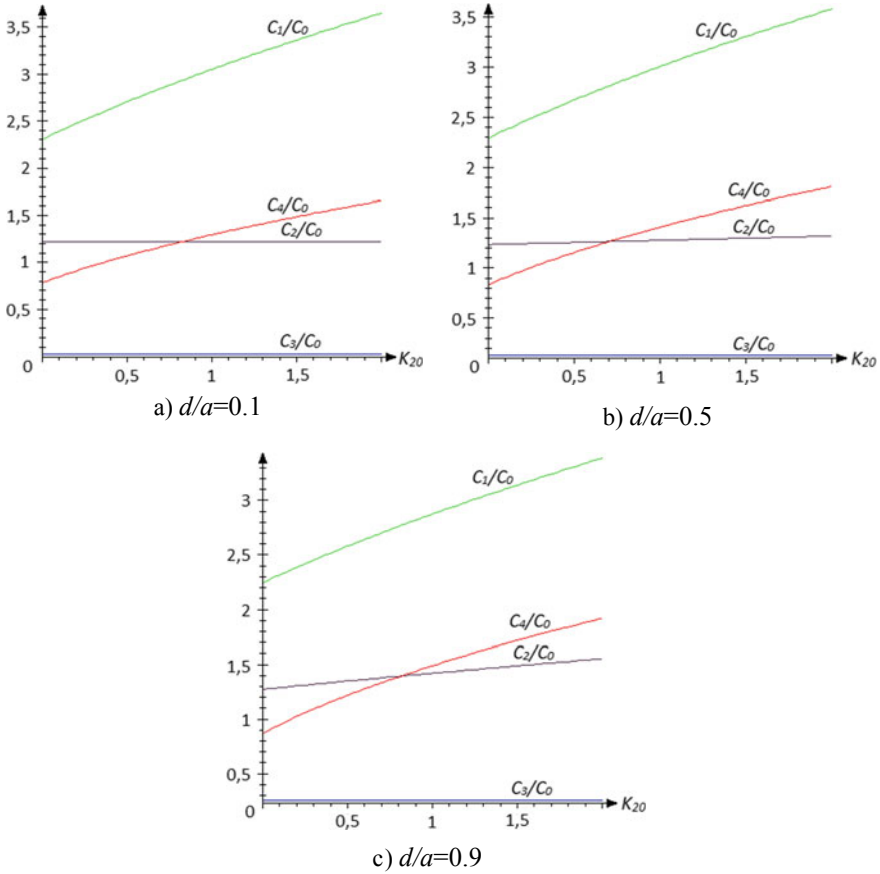
Fig. 6.8 Dependences of the wave velocities on parameter K_{20} at $K_{10} = 0.3$, $K_{30} = 1.2$, $K_{40} = 1.6$

elaborated in this chapter. It is shown that the three-dimensional model of a crystalline medium, in contrast to the Cosserat continuum model, enables one establishing of analytical dependences of the velocities of acoustic and rotational waves on the microstructure parameters of such a medium. The analysis of such dependences showed that the proposed model of the crystalline medium differs from the model of the Cosserat medium by a smaller number of independent macroconstants: If there are six independent constants in the isotropic Cosserat continuum, then in this anisotropic model there are only five of them, and upon passing to an isotropic medium, only four constants remain. Apparently, this indicates that it is not always possible to obtain the Cosserat continuum from a discrete model. Thus, a question arises: how to find conditions, when such transition is possible? Moreover, even the possibility of the existence of such conditions is not obvious. Certainly, such problems need further investigations.

a) $d/a=0.1$

b) $d/a=0.5$

c) $d/a=0.9$
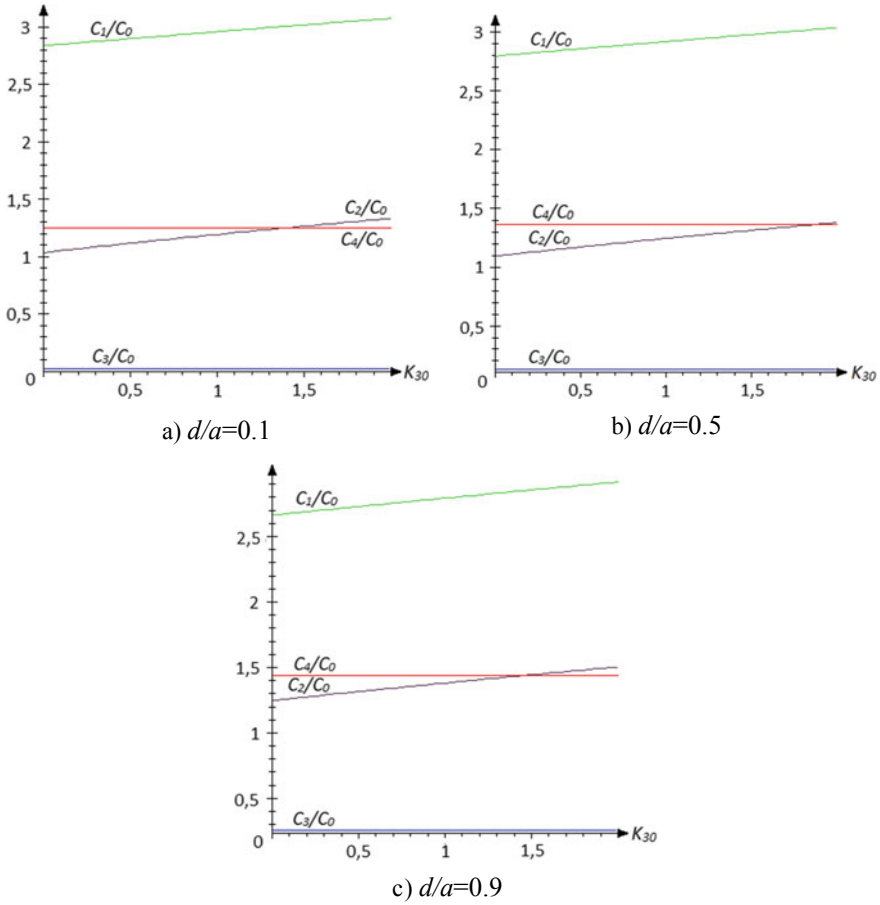
Fig. 6.9 Dependences of the wave velocities on parameter K_{30} at $K_{10} = 0.3$, $K_{20} = 0.9$, $K_{40} = 1.6$

It should be noted that if in this model interactions between particles are simulated by elastic springs of five types, then in the closely related work [9] a three-dimensional model of a granular medium of spherical particles contained springs of only three types. As a result, in [9], the springs largely duplicated each other and therefore the number of independent coefficients of the governing equations was even less than in the model proposed in this chapter.

The performed numerical analysis showed that in the considered medium, when the particle size grows, the longitudinal wave velocity c_1 decreases monotonically, whereas all other wave velocities, on the contrary, increase monotonically. The velocity c_1 is maximal among all the wave velocities and the rotational wave velocity c_3 is the minimal. The transverse wave velocity c_2 can either exceed the rotational wave velocity c_4 or be less than it.

a) d/a=0.1

b) d/a=0.5

c) d/a=0.9
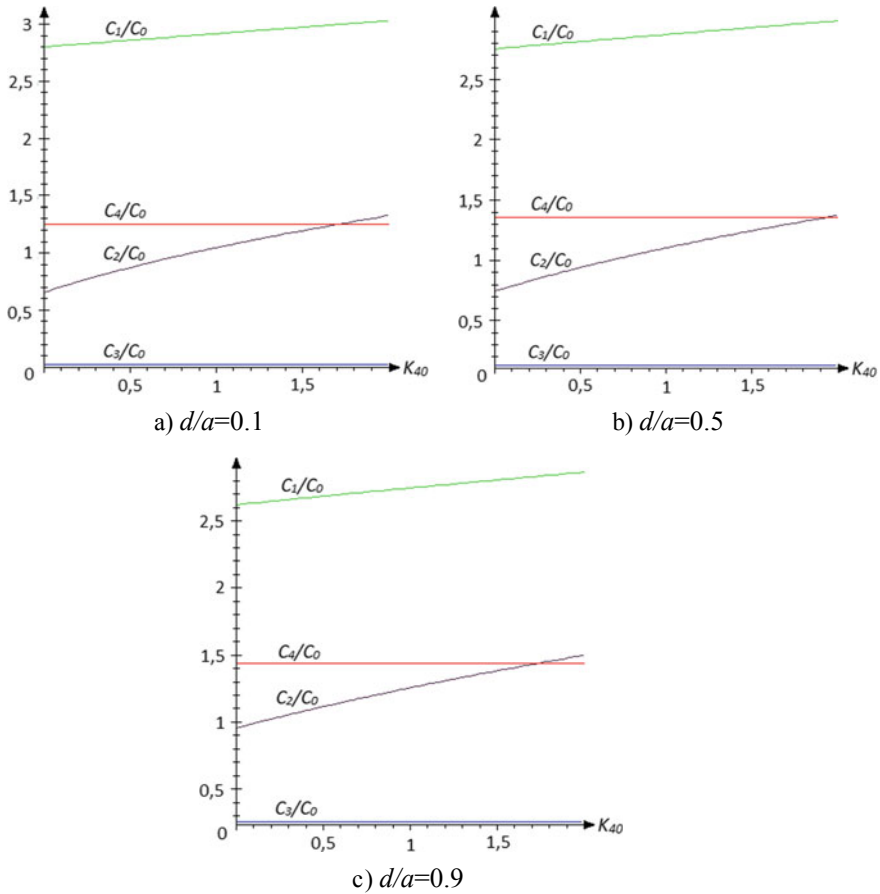
Fig. 6.10 Dependences of the wave velocities on parameter K_{40} at $K_{10} = 0.3$, $K_{20} = 0.9$, $K_{30} = 1.2$

References

1. Pavlov, I.S., Potapov, A.I.: Two-dimensional model of a granular medium. Mech. Solids **42**(2), 250–259 (2007)
2. Pavlov, I.S., Potapov, A.I., Maugin, G.A.: A 2D granular medium with rotating particles. Int. J. Solids Struct. **43**(20), 6194–6207 (2006)
3. Kuznetsova, E.L., Tarlakovskii, D.V., Fedotenkov, G.V.: Propagation of unsteady waves in an elastic layer. Mech. Solids **46**(5), 779–787 (2011)

4. Erofeev, V.I., Pavlov, I.S., Leontiev, N.V. A mathematical model for investigation of nonlinear wave processes in a 2D granular medium consisting of spherical particles. Compos. Mech. Comput. Appl. Int. J. **4**'3), 239–255 (2013)
5. Nowacki, W.: Theory of Micropolar Elasticity. J. Springer, Wien (1970)
6. Suiker, A.S.J., Metrikine, A.V., de Borst, R. Comparison of wave propagation characteristics of the cosserat continuum model and corresponding discrete lattice models. Int. J. Solids Struct. **38**, 1563–1583 (2001)
7. Potapov, A.I., Pavlov, I.S., Lisina, S.A.: Acoustic identification of nanocrystalline media. J. Sound Vib. **322**(3), 564–580 (2009)
8. Sadovskii, V.M.: Thermodynamically consistent equations of the couple stress elasticity. Dal'nevost. Mat. Zh. **16**(2), 209–222 (2016). (in Russian)
9. Berglund, K. Structural models of micropolar media. In: Brulin, O., Hsieh, R.K.T. (eds.) Mechanics of Micropolar Media, pp. 35–86. World Scientific, Singapore (1982)

Chapter 7
Propagation and Interaction of Nonlinear Waves in Generalized Continua

The main goal of the final chapter of the monograph is to study the features of the propagation of nonlinear elastic waves in metamaterials and constructions made of them [1]. Linear wave processes in generalized continua were considered, in particular, in Refs. [2–13].

7.1 Localized Strain Waves in a 2D Crystalline Medium with Non-dense Packing of the Particles

This section is devoted to revealing a possibility of the propagation of a plane strain soliton in a two-dimensional crystalline medium with non-dense packing of round particles, as well as to studying its stability with respect to two-dimensional perturbations and to determination of its polarity. In order to achieve these goals, at the first stage, the nonlinear differential equations (5.6) describing the propagation of longitudinal, transverse, and rotational waves in such a medium were obtained by the structural modeling method, as well as the dependences of linear and nonlinear macroparameters of the medium on particle sizes and interaction parameters between them were established in an analytical form (see Chap. 5). Next, in the low-frequency region, when the rotational wave does not propagate, the obtained three-mode set of equations (5.6) degenerates into the two-mode system (5.11), which will be reduced, using the multiscale method, to the Kadomtsev–Petviashvili evolution equation with respect to a shear strain. This equation has a solution in the form of a soliton. At the final stage, various scenarios of the behavior of a plane solitary wave will be analyzed in dependence on the initial conditions of the Kadomtsev–Petviashvili equation and its coefficients depending on the microstructure parameters of the medium under consideration.

Let us consider propagation of localized strain waves in the 2D granular medium with a non-dense packing of particles (see Chaps. 3 and 5), depending on parameters

of its microstructure. For this purpose, in Eq. (5.11), we introduce new coordinates and time: $\xi = x - vt$, $\eta = \sqrt{\varepsilon} y$, $\tau = \varepsilon t$; $u = \sqrt{\varepsilon} u$, $w = w$. So, Eq. (5.11) take on the form:

$$
\sqrt{\varepsilon} v^2 \frac{\partial^2 u}{\partial \xi^2} - 2\varepsilon \sqrt{\varepsilon} v \frac{\partial^2 u}{\partial \xi \partial \tau} - \sqrt{\varepsilon} c_1^2 \frac{\partial^2 u}{\partial \xi^2} - (c_2^2 - \tfrac{\beta}{2}) \varepsilon \sqrt{\varepsilon} \frac{\partial^2 u}{\partial \eta^2} - (s^2 + \tfrac{\beta}{2}) \frac{\partial^2 w}{\partial \xi \partial \eta} \sqrt{\varepsilon}
$$
$$
= \frac{R^2}{4} \sqrt{\varepsilon} \frac{\partial}{\partial \eta} \left[v^2 \frac{\partial^2}{\partial \xi^2} \left(\varepsilon \frac{\partial u}{\partial \eta} - \frac{\partial w}{\partial \xi} \right) - 2\varepsilon v \frac{\partial^2}{\partial \xi \partial \tau} \left(\varepsilon \frac{\partial u}{\partial \eta} - \frac{\partial w}{\partial \xi} \right) \right.
$$
$$
\left. -c_3^2 \left(\frac{\partial^2}{\partial \xi^2} + \varepsilon \frac{\partial^2}{\partial \eta^2} \right) \left(\sqrt{\varepsilon} \frac{\partial u}{\partial \eta} - \frac{\partial w}{\partial \xi} \right) \right] + \frac{1}{2} \frac{\partial H_1}{\partial \xi} + \frac{1}{2} \frac{\partial H_2}{\partial \eta},
$$
$$
v^2 \frac{\partial^2 w}{\partial \xi^2} - 2\varepsilon v \frac{\partial^2 w}{\partial \xi \partial \tau} - (c_2^2 - \tfrac{\beta}{2}) \frac{\partial^2 w}{\partial \xi^2} - \varepsilon c_1^2 \frac{\partial^2 w}{\partial \eta^2} - (s^2 + \tfrac{\beta}{2}) \varepsilon \frac{\partial^2 u}{\partial \xi \partial \eta}
$$
$$
= -\frac{R^2}{4} \frac{\partial}{\partial \xi} \left[v^2 \frac{\partial^2}{\partial \xi^2} \left(\varepsilon \frac{\partial u}{\partial \eta} - \frac{\partial w}{\partial \xi} \right) - 2\varepsilon v \left(\varepsilon \frac{\partial u}{\partial \eta} - \frac{\partial w}{\partial \xi} \right) \right.
$$
$$
\left. -c_3^2 \left(\frac{\partial^2}{\partial \xi^2} + \varepsilon \frac{\partial^2}{\partial \eta^2} \right) \left(\sqrt{\varepsilon} \frac{\partial u}{\partial \eta} - \frac{\partial w}{\partial \xi} \right) \right] + \frac{1}{2} \frac{\partial H_3}{\partial \xi} + \frac{1}{2} \frac{\partial H_4}{\partial \eta}.
$$

(7.1)

As various terms of Eq. (7.1) have different orders of smallness, we shall consider some approximations step by step.

Approximation of ε^0 order has the form: $\left(v^2 - (c_2^2 - \tfrac{\beta}{2}) \right) \frac{\partial^2 w}{\partial \xi^2} = 0$; hence

$$
v^2 = c_2^2 - \frac{\beta}{2}.
$$

(7.2)

Approximation of $\sqrt{\varepsilon}$ order: $(v^2 - c_1^2) \frac{\partial^2 u}{\partial \xi^2} - \left(s^2 + \tfrac{\beta}{2} \right) \frac{\partial^2 w}{\partial \xi \partial \eta} = 0$; therefore,

$$
\frac{\partial u}{\partial \xi} = \frac{s^2 + \beta/2}{v^2 - c_1^2} \frac{\partial w}{\partial \eta}.
$$

(7.3)

Approximation of ε order:

$$
- 2\varepsilon v \frac{\partial^2 w}{\partial \xi \partial \tau} - \varepsilon c_1^2 \frac{\partial^2 w}{\partial \eta^2} - \left(s^2 + \frac{\beta}{2} \right) \varepsilon \frac{\partial^2 u}{\partial \xi \partial \eta}
$$
$$
= -\frac{R^2}{4} \frac{\partial}{\partial \xi} \left[v^2 \frac{\partial^2}{\partial \xi^2} \left(\varepsilon \frac{\partial u}{\partial \eta} \right) - 2\varepsilon v \left(-\frac{\partial w}{\partial \xi} \right) - c_3^2 \left(\varepsilon \frac{\partial^2}{\partial \eta^2} \right) \left(-\frac{\partial w}{\partial \xi} \right) \right]
$$
$$
+ 3\gamma_1 \frac{\partial w}{\partial \xi} \frac{\partial^2 w}{\partial \xi^2}.
$$

(7.4)

After entering the designation $\frac{\partial w}{\partial \xi} = U$ in Eq. (7.4) and taking into account expressions (7.2) and (7.3), Eq. (7.4) is reduced to the following equation:

$$
2v U_{\xi \tau} + q_1 (U^2)_{\xi \xi} + \frac{R^2}{4} q_2 U_{\xi \xi \xi \xi} + q_3 U_{\eta \eta} = 0,
$$

(7.5)

where

$$\frac{3\gamma_1}{2\varepsilon} = q_1, \quad \frac{2c_2^2 - 2c_3^2 - \beta}{2\varepsilon} = q_2,$$

$$c_1^2 + \frac{(2s^2 + \beta)^2}{4(c_2^2 - c_1^2) - 2\beta} = c_1^2 + \frac{(4c_2^2 - 3\beta)^2}{4(c_2^2 - c_1^2) - 2\beta} = q_3. \tag{7.6}$$

Let us introduce designations $U/U_0 = W$, $\xi/\xi_0 = X$, $\tau/\tau_0 = T$, $\eta/\eta_0 = Y$. In terms of new variables, Eq. (7.5) takes on the form:

$$2\frac{\partial^2 W}{\partial X \partial T} + \frac{q_1}{v}\frac{\tau_0 U_0}{\xi_0}\frac{\partial^2 (W^2)}{\partial X^2} + \frac{R^2}{4v}q_2\frac{\tau_0}{\xi_0^3}\frac{\partial^4 W}{\partial X^4} + q_3\frac{\xi_0 \tau_0}{v\eta_0^2}\frac{\partial^2 W}{\partial Y^2} = 0 \tag{7.7}$$

If to put $U_0 = 1$ and $\eta_0 = \xi_0$ in Eq. (7.7), then $W = U$ and Eq. (7.7) yields:

$$2\frac{\partial^2 U}{\partial X \partial T} + \frac{q_1}{v}\frac{\tau_0}{\xi_0}\frac{\partial^2 (U^2)}{\partial X^2} + \frac{R^2}{4v}q_2\frac{\tau_0}{\xi_0^3}\frac{\partial^4 U}{\partial X^4} + q_3\frac{\tau_0}{v\xi_0}\frac{\partial^2 U}{\partial Y^2} = 0. \tag{7.8}$$

We choose scales ξ_0 and τ_0 so that the last coefficient in Eq. (7.8) would be equal to 1:

$$\frac{\tau_0}{\xi_0} = \frac{v}{q_3}.$$

Due to this relationship between ξ_0 and τ_0 Eq. (7.8) is transformed as follows

$$2\frac{\partial^2 U}{\partial X \partial T} + \frac{q_1}{q_3}\frac{\partial^2 (U^2)}{\partial X^2} + \frac{R^2 q_2}{4q_3}\frac{1}{\xi_0^2}\frac{\partial^4 U}{\partial X^4} + \frac{\partial^2 U}{\partial Y^2} = 0. \tag{7.9}$$

If to take $\xi_0 = R/2$ in Eq. (7.9), then this equation is transformed into well-known Kadomtsev–Petviashvili equation:

$$2\frac{\partial^2 U}{\partial X \partial T} + \frac{q_1}{q_3}\frac{\partial^2 (U^2)}{\partial X^2} + \frac{q_2}{q_3}\frac{\partial^4 U}{\partial X^4} + \frac{\partial^2 U}{\partial Y^2} = 0. \tag{7.10}$$

This equation has a solution in the form of a plane solitary strain wave (soliton) (Fig. 7.1):

$$U(\theta) = A_s ch^{-2}(\theta/\Delta), \tag{7.11}$$

where $\theta = X - kY - VT$ is the wave phase. The amplitude of the soliton, A_s, and its width Δ are determined by relations:

$$A_s = \left|\frac{3q_3(k^2 - 2V)}{2q_1}\right|, \quad \Delta = 2\sqrt{\left|\frac{q_2}{q_3(k^2 - 2V)}\right|}. \tag{7.12}$$
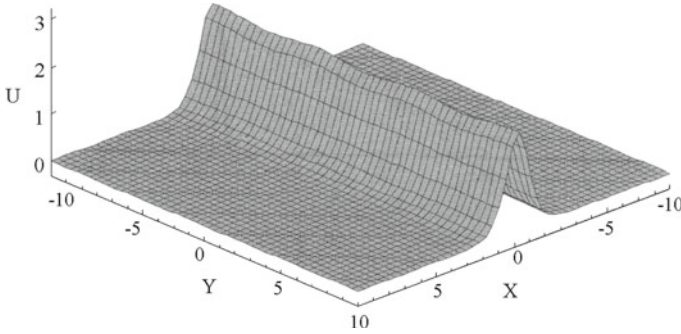
Fig. 7.1 Plane localized strain wave [14]

It should be noted that product

$$A_c \Delta^2 = \left| \frac{6q_2}{q_1} \right| = \left| \frac{2c_2^2 - 2c_3^2 - \beta}{\gamma_1} \right|$$

is the constant for each material.

The plane solitary wave (7.11) is known to be stable if $q_2/q_3 > 0$, and it is unstable with respect to transverse perturbations, when $q_2/q_3 < 0$ [14]. In this case, Kadomtsev–Petviashvili equation has an other precise solution [15]:

$$U(X, Y, T) = \frac{6q_2}{q_1} \frac{\partial^2}{\partial X^2} \ln[1 + \exp(2q\theta) + \exp(2p(\theta + \psi))$$
$$+ A \exp((q + p)\theta + p\psi) \cos kY]. \tag{7.13}$$

Here p and q are integration constants, $\theta = X - (1 + \frac{2q_2}{q_3}q^2)T$, $\psi = -4p\frac{q_2}{q_3}(p^2 - q^2)T$, $A = \frac{4\sqrt{pq}}{p+q}$, and $k = (q^2 - p^2)\sqrt{\frac{-3q_2}{q_3}}$.

Formula (7.13) describes a periodic chain of two-dimensional solitary strain waves (Fig. 7.2). If $q_2/q_3 < 0$, i.e., the condition of soliton instability, with respect to transverse perturbations takes place, the plane solitary wave (7.11) plotted in Fig. 7.1 will be transformed into Eq. (7.13).

Polarity of solitons (7.11) and (7.13) depends on sign of expression q_1/q_2. The solitons have a positive polarity (this case is represented in Figs. 7.1 and 7.2), when $q_1/q_2 > 0$, and their polarity is negative, if $q_1/q_2 < 0$.

Thus, existence and polarity of steady plane solitons of deformations depend on signs of coefficients q_1/q_2 and q_2/q_3. Let us analyze dependencies of these coefficients on the macroparameters of the medium, which were obtained from Eq. (7.6):
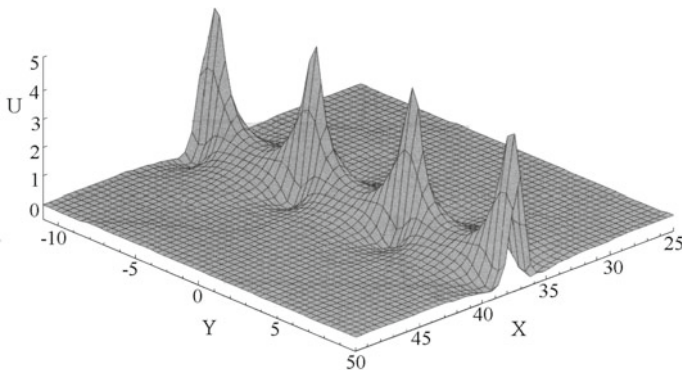
Fig. 7.2 Plane wave modulated in the transverse direction [14]

$$\frac{q_1}{q_2} = \frac{3\gamma_1}{2c_2^2 - 2c_3^2 - \beta},\tag{7.14}$$

$$\frac{q_2}{q_3} = \frac{(2c_2^2 - 2c_3^2 - \beta)(2c_2^2 - 2c_1^2 - \beta)}{\varepsilon(2c_1^2(2c_2^2 - 2c_1^2 - \beta) + (4c_2^2 - 3\beta)^2)}.\tag{7.15}$$

From (5.10) and (5.8) follows that

$$\gamma_1 = \alpha_2 + \frac{\alpha_5 - \alpha_4}{4} = \frac{K_3}{M}\left(\frac{a^3}{4(a-h)} + \frac{a^2h^2}{4(a-h)^2} - \frac{a^2h}{2(a-h)}\right)$$
$$= \frac{K_3 a^2(a^2 - 3ah + 3h^2)}{4M(a-h)^2} > 0,$$

hence, $q_1/q_2 > 0$ for $c_2^2 > c_3^2 + \beta/2$ and $q_1/q_2 < 0$ for $c_2^2 < c_3^2 + \beta/2$ [16].

According to the data presented in Table 5.1, for the media with such parameters as for cubic crystals of LiF, NaF, NaBr, and fullerite C_{60} with sc-lattice, it is possible to determine the signs of expressions q_1/q_2 and q_2/q_3. Since $q_2/q_3 > 0$ only for the first two of the four considered media, then stable plane strain solitons can exist only in them: the so-called *light* soliton (with negative polarity) can exist in the first medium, as $q_1/q_2 < 0$, and the "dark" soliton (with positive polarity)—in the second medium, as $q_1/q_2 > 0$.

Let us choose as an initial condition for Kadomtsev–Petviashvili equation a 2D soliton without plane front (Fig. 7.3), i.e., perturbation in the form [17]

$$U_0(X, Y) = 12\mathrm{sech}^2\left(\frac{X - 32}{4}\right)\mathrm{sech}(Y - 8).\tag{7.16}$$

In this case, we carried out the numerical simulation of Eq. (7.10) by means of the semi-implicit pseudo-spectral scheme [18] with parameters: 256×64 (dimension of a grid), $\Delta X = 0.25$ (a step length along x-axis), $\Delta Y = 0.25$ (a step length along
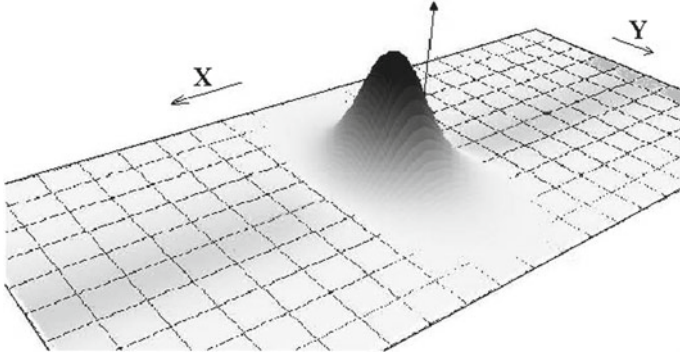
Fig. 7.3 2D soliton without a plane front ($T = 0$)
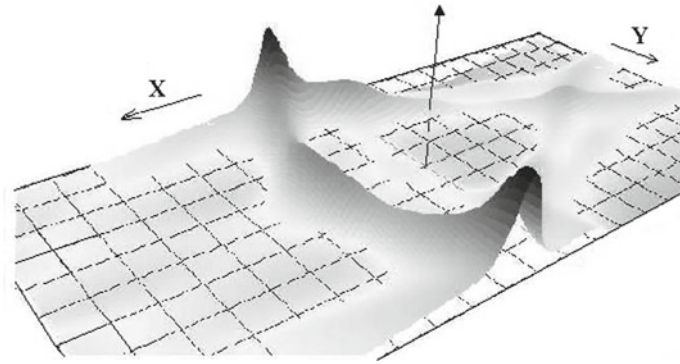
Fig. 7.4 Spreading of a 2D soliton ($T = 5$)

y-axis), $\Delta T = 0.003$ (a step length in T). As a result of these investigations, we have observed an other behavior of the solitary wave: In fact, the peak of excitations (7.16) moves forward (along x-axis) and simultaneously spreads to the sides (along y-axis), with prevailing of the latter effect. Eventually, the amplitude of excitation grows till a certain value ($A = 7.1$) near the boundaries, spreading aside and moving forward, that leads to appearance of the crosswise structures (Fig. 7.4).

7.2 A 1D Medium Consisting of Ellipse-Shaped Particles and with Internal Stresses

This section is auxiliary for further studies of the areas of modulation instability and the interaction of strain solitons propagating in a one-dimensional granular medium with internal (preliminary) stresses.

7.2.1 Mechanical Model of a 1D Medium with Internal Stresses

Let us consider a chain consisting of homogeneous particles (grains or granules) with the mass M having the shape of an ellipse with the axes d_1 and d_2. In the initial state, they are concentrated in the lattice sites and the distance between the mass centers of the neighboring granules along the x-axis equals a (Fig. 7.5). As in the rectangular lattice studied in Chap. 3, when moving in the plane, each particle has three degrees of freedom: the displacement of the mass center of the particle with the number $N = N(i)$ along the axes x and y (translational degrees of freedom u_i and w_i) and the rotation with respect to the mass center (rotational degree of freedom φ_i) (Fig. 7.6). The displacements of the grains are supposed to be small in comparison with the period a of the considered one-dimensional lattice.

It is assumed that the particle N interacts only with the two nearest neighbors in the chain, the mass centers of which are located at the distance a along the axis x from the particle N (Fig. 7.6). The central and non-central interactions of the neighboring granules are simulated, like in Sect. 2.1, by elastic springs of three types: central (with rigidity K_0), non-central (with rigidity K_1), and diagonal (K_2). The points of junctions of the springs with the particles are in the apexes of the rectangle of the maximum area, $ABCE$, inscribed in the ellipse (Fig. 7.6). Each rectangle has the size $h_1 \times h_2$, where $h_1 = d_1/\sqrt{2}$ and $h_2 = d_2/\sqrt{2}$. The elongations of the central springs are determined by the changes of the distances between the geometrical centers of the rectangles $ABCE$, and the tensions of other springs are characterized by the variations of the distances between the apexes of these rectangles.
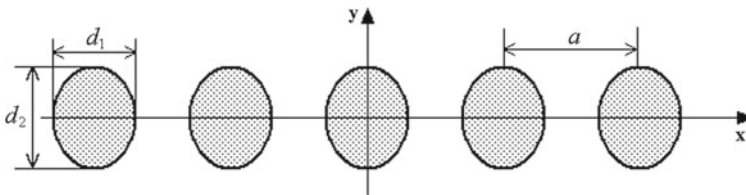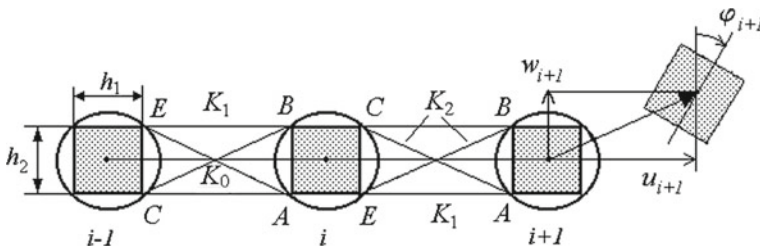

Fig. 7.5 Chain of ellipse-shaped particles

Fig. 7.6 Scheme of force interactions between the particles and kinematics

Note that, in contrast to the previously considered rectangular lattice of ellipse-shaped particles (see Chap. 3), this model does not contain springs with rigidity K_3 (that is natural, since the interaction with the second coordination sphere is not taken into account). It is supposed that in the initial state all the springs with rigidity K_0, K_1, and K_2 have been already deformed (stretched or compressed), accordingly, at quantities $\delta_0' \ll a$, $\delta_1' \ll a$, and $\delta_2' \ll a$ [19]. The initial deformations of the springs simulate internal (or preliminary) stresses in a medium [20, 21]. The elongations of these springs arising when the particles deviate from their equilibrium states are calculated in the same way as for a square lattice of round particles (see Sect. 5.1 and Appendix 2), but with one addition: δ_0' is added to the elongations of the central springs, δ_1' is added to the extensions of the non-central springs, and δ_2'—to the elongations of the diagonal springs.

In the approximation of smallness of the quantities

$$\Delta u_i = (u_i - u_{i-1}) \sim a\varepsilon_0, \quad \Delta w_i = (w_i - w_{i-1}) \sim a\varphi_i \sim a\sqrt{\varepsilon_0},$$
$$\Delta \varphi_i = (\varphi_i - \varphi_{i-1}) \sim \varepsilon_0^{3/2}, \tag{7.17}$$

where $\varepsilon_0 \ll 1$ is a deformation measure of the cell, and taking into account that

$$\Phi_i = (\varphi_{i-1} + \varphi_i)/2 = \varphi_i - (\varphi_i - \varphi_{i-1})/2 = \varphi_i - \Delta \varphi_i/2,$$

according to the algorithm described in Chaps. 2 and 3, one can obtain the following Lagrange function for the considered chain of round particles with accuracy up to the terms of ε_0^3 order [20]:

$$L = \frac{M}{2}(u_t^2 + w_t^2 + R^2\varphi_t^2) - \frac{M}{2}[c_1^2 u_x^2 + c_2^2 w_x^2 + R^2 c_3^2 \varphi_x^2 + 2\beta_1 w_x \varphi + 2\beta_2 \varphi^2$$
$$+ \alpha_1 u_x^3 + \alpha_2 u_x w_x^2 + \alpha_3 u_x \varphi^2 + \alpha_4 u_x w_x \varphi]. \tag{7.18}$$

The Lagrange function (7.18) is a one-dimensional analog of formula (5.1). The choice of relations (7.17), due to which Eq. (7.18) was derived, is explained by the fact that for stretching the chain in the longitudinal direction, more force is required than for its bending deformation.

A set of differential equations describing the nonlinear dynamic processes in the anisotropic granular medium is derived from the Lagrange function (7.18) in agreement with Hamilton's variational principle

$$u_{tt} - c_1^2 u_{xx} = \frac{1}{2}\frac{\partial}{\partial x}(3\alpha_1 u_x^2 + \alpha_2 w_x^2 + \alpha_3 \varphi^2 + \alpha_4 w_x \varphi),$$

$$w_{tt} - c_2^2 w_{xx} - \beta_1 \varphi_x = \frac{1}{2}\frac{\partial}{\partial x}(2\alpha_2 u_x w_x + \alpha_4 u_x \varphi), \tag{7.19}$$

$$R^2(\varphi_{tt} - c_3^2 \varphi_{xx}) + \beta_1 w_x + 2\beta_2 \varphi = -2\alpha_3 u_x \varphi - \alpha_4 u_x w_x.$$

Equation (7.19) are analogs of the equations for the nonlinear one-dimensional Cosserat continuum [22]. Here, the following notations are introduced: c_i ($i = 1$, 2, 3) are the propagation velocities, respectively, of the longitudinal, transverse, and rotational waves, β_1 and β_2 are the dispersion parameters, α_i ($i = 1$–4)—are the nonlinearity coefficients, $R = \sqrt{d_1^2 + d_2^2}/4$ is the inertia radius of the particle. Dependencies of the coefficients of Eq. (7.19) on the microstructure parameters (the force constants K_0, K_1, and K_2, the lattice period a and the grain sizes $h_1 = d_1/\sqrt{2}$ and $h_2 = d_2/\sqrt{2}$) have the following form:

$$\rho c_1^2 = a\left[K_0 + 2K_1 + \left(\frac{2(a - h_1)^2}{r^2} + \frac{2\delta_2 h_2^2}{r^3}\right)K_2\right],$$

$$\rho c_2^2 = a\left[\frac{\delta_0}{a}K_0 + \frac{2\delta_1}{a - h_1}K_1 + \frac{2}{r^2}\left(h_2^2 + \frac{2\delta_2(a - h_1)^2}{r}\right)K_2\right], \qquad (7.20a)$$

$$\rho c_3^2$$
$$= \frac{ah_2^2}{2R^2}\left[K_1 + \frac{a^2 K_2}{r^2} + \frac{\delta_1 h_1^2}{(a - h_1)h_2^2}K_1 + \frac{\delta_2}{r^3}K_2\left(h_2^2 + (a - h_1)^2\frac{h_1^2}{h_2^2} - 2h_1(a - h_1)\right)\right];$$

$$\rho\beta_1 = 2\left(\frac{ah_2^2}{r^2}K_2 + \frac{\delta_1 h_1}{a - h_1}K_1 + \frac{\delta_2(a - h_1)(ah_1 - h_1^2 - h_2^2)}{r^3}K_2\right),$$
$$\rho\beta_2 = \frac{ah_2^2}{r^2}K_2 + \frac{\delta_1 h_1^2}{a(a - h_1)}K_1 + \frac{\delta_2(h_2^4 + (a - h_1)^2 h_1^2 - 2h_1 h_2^2(a - h_1))}{ar^3}K_2; \qquad (7.20b)$$

$$\rho\alpha_1 = \frac{K_2}{r^4}a^2(a - h_1)h_2^2,$$

$$\rho\alpha_2 = K_0 a + K_1\frac{a^2}{a - h_1} + \frac{K_2}{r^4}a^2(a - h_1)((a - h_1)^2 - 2h_2^2),$$

$$\rho\alpha_3 = K_1\frac{h_1^2}{a - h_1} + \frac{K_2}{r^4}(h_1^2 + h_2^2 - ah_1)(2ah_2^2 + (a - h_1)(h_1^2 + h_2^2 - ah_1)),$$
$$\qquad (7.20c)$$

$$\rho\alpha_4 = K_1\frac{2ah_1}{a - h_1} + \frac{2a}{r^4}K_2((h_1^2 + h_2^2 - ah_1)(h_2^2 - (a - h_1)^2) - ah_2^2(a - h_1)),$$

where $\rho = M/a$ is the density of the one-dimensional medium per unit length.

From (7.20b), the relationship $\beta_1 = 2\beta_2$ follows, if there are no preliminary deformations of the springs. It should be noted that expressions (7.20c) are given without the preliminary deformations of the springs, since they are not significant for the further investigations.

It should also be noted that the Lagrange function for a chain of round granules without taking into account the preliminary stresses could be obtained avoiding the cumbersome procedure of derivation. For this purpose, first, it is necessary to exclude from the Lagrange function (5.1) all the terms containing derivatives with respect to y, and then to put $K_3 = 0$ and $h_1 = h_2 = h$ in the remaining coefficients. At first view,

it seems more effective to derive the Lagrange function for a chain of round granules without taking into account the preliminary stresses from the Lagrange function (5.5) for a square lattice of round particles. However, this path leads to an incorrect result, namely: If in expressions (3.9) for the dispersion parameters

$$\beta_1 = \frac{2a^2}{M}\left(\frac{h_2^2}{(a-h_1)^2 + h_2^2}K_2 + \frac{(b-h_2)(ah_2 - bh_1)}{a((a-h_1)^2 + (b-h_2)^2)}K_3\right),$$

$$\beta_2 = \frac{1}{M}\left(\left(\frac{a^2 h_2^2}{(a-h_1)^2 + h_2^2} + \frac{b^2 h_1^2}{(b-h_2)^2 + h_1^2}\right)K_2 + \frac{(ah_2 - bh_1)^2}{(a-h_1)^2 + (b-h_2)^2}K_3\right)$$

to pass first to a square lattice of round particles ($a = b$, $h_1 = h_2 = h$), then we get $\beta_1 = \beta_2$ (an extra term $\frac{b^2 h_1^2}{(b-h_2)^2 + h_1^2}K_2$ is added to β_2), whereas the initial transition to the one-dimensional case ($b = 0$, $K_3 = 0$) with the subsequent replacement $h_1 = h_2 = h$ eliminates the extra term and gives the correct result: $\beta_1 = 2\beta_2$.

7.2.2 Equations of the Gradient Theory of Elasticity for a 1D Medium with Internal Stresses

In the low-frequency approximation, when the rotational wave does not propagate, a relation between the microrotations φ and displacements w can be found from the linear part of the third equation (7.19) by a step-by-step approach. Since in this equation the term $\beta_1 w_x + 2\beta_2\varphi$ plays the main role (according to estimates (7.17), it has $\sqrt{\varepsilon_0}$ order of smallness), and the second term of the linear part of the equation, $R^2(\varphi_{tt} - c_3^2\varphi_{xx})$, has the next order of smallness—$\varepsilon_0^{3/2}$, then in the first approximation

$$\varphi(x, t) \approx -\frac{\beta_1}{2\beta_2}w_x, \tag{7.21}$$

and in the second approximation, the variable φ can be expressed in terms of w and its derivatives as follows [23]:

$$\varphi(x, t) \approx -\frac{\beta_1}{2\beta_2}\frac{\partial w}{\partial x} + \frac{R^2\beta_1}{4\beta_2}\left(\frac{\partial^3 w}{\partial x\,\partial t^2} - c_3^2\frac{\partial^3 w}{\partial x^3}\right).$$

Taking into account the constraint (7.21) leads to "freezing" of the rotational degree of freedom and, as a consequence, to exclusion of φ from Eq. (7.19). As a result, in the first approximation, Eq. (7.19) degenerate into a two-mode system, the Lagrange function of which has the form

$$L = \frac{M}{2}\left(u_t^2 + w_t^2 + \frac{R^2}{4}w_{xt}^2\right)$$

$$- \frac{M}{2} \left(c_1^2 u_x^2 + \left(c_2^2 - \frac{\beta_1^2}{2\beta_2} \right) w_x^2 + \frac{R^2}{4} c_3^2 w_{xx}^2 + \alpha_1 u_x^3 + \gamma\, u_x w_x^2 \right), \qquad (7.22)$$

where $\gamma = \alpha_2 + \frac{\alpha_3}{4} - \frac{\alpha_4}{2}$. It depends on the parameters of the microstructure as follows:

$$\gamma = \frac{a}{\rho} \left\{ K_0 + K_1 \frac{(2 - h_1/a)^2}{4(1 - h_1/a)} + \frac{K_2 a^4}{r^4} \left[\left(1 - \frac{h_1}{a} \right) \left(\left(1 - \frac{h_1}{a} \right)^2 - \frac{2h_2^2}{a^2} \right) \right. \right.$$

$$+ \frac{1}{4} \left(\frac{h_1^2 + h_2^2}{a^2} - \frac{h_1}{a} \right) \left(\frac{2h_2^2}{a^2} + \left(1 - \frac{h_1}{a} \right) \left(\frac{h_1^2 + h_2^2}{a^2} - \frac{h_1}{a} \right) \right)$$

$$\left. \left. - \left(\frac{h_1^2 + h_2^2}{a^2} - \frac{h_1}{a} \right) \left(\frac{h_2^2}{a^2} - \left(1 - \frac{h_1}{a} \right)^2 \right) + \frac{h_2^2}{a^2} \left(1 - \frac{h_1}{a} \right) \right] \right\}. \qquad (7.23)$$

Analysis of expression (7.23) shows that coefficient γ can be negative for $K_2 > K_0$ and enough large sizes of the particles (in comparison with the lattice period a). In particular, if to assume that $K_1/K_0 = 0.1$, $K_2/K_0 = 2.8$, then $\gamma < 0$ for

$$\frac{h_1}{a} = 0.7, \quad \frac{h_2}{a} \geq 0.47, \qquad (7.24a)$$

as well as for

$$\frac{h_1}{a} \geq 0.65, \quad \frac{h_2}{a} = 0.7. \qquad (7.24b)$$

It is possible to obtain from Lagrange function (7.22) the so-called *equations of the gradient elasticity theory* [24] containing terms with higher-order derivatives (in this case, the fourth-order):

$$u_{tt} - c_1^2 u_{xx} = \frac{1}{2} \frac{\partial \left(3\alpha_1 u_x^2 + \gamma\, w_x^2 \right)}{\partial x}, \qquad (7.25a)$$

$$w_{tt} - \tilde{c}_2^2 w_{xx} - \frac{R^2}{4} \frac{\partial}{\partial x} \left[\frac{\partial^2 w_x}{\partial t^2} - c_3^2 \frac{\partial^2 w_x}{\partial x^2} \right] = \frac{\partial (\gamma\, u_x w_x)}{\partial x}, \qquad (7.25b)$$

where $\tilde{c}_2^2 = c_2^2 - \frac{\beta_1^2}{2\beta_2}$. It should be noted that taking into account (7.25a) and (7.25b),

$$\tilde{c}_2^2 \approx \frac{\delta_0}{a\rho} K_0, \qquad (7.26)$$

whereas $\beta_1 = 2\beta_2$ and $\tilde{c}_2^2 = 0$ for $\delta_0 = \delta_1 = \delta_2 = 0$. Thus, all further analysis is possible only for a medium with internal stresses, which are simulated by the preliminary deformations of the springs [20].

7.3 Self-modulation of Shear Strain Waves Propagating in a 1D Granular Medium

The main goal of this section is to find a region of modulation instability (self-modulation) of a shear strain wave in a one-dimensional granular material with preliminary stresses. The boundaries of this region and the characteristics of the wave packet formed as a result of self-modulation of a quasiharmonic wave depend on the microstructure parameters of the material at issue.

7.3.1 The Modulation Instability Areas

We shall enter into consideration new independent variables and expansions of dependent variables in powers of the small parameter ε characterizing a ratio of the maximum amplitude of displacement to the wavelength:

$$\xi = x - Vt, \quad \tau = \varepsilon t; \tag{7.27}$$

$$w = w_0 + \sqrt{\varepsilon} w_1 + \cdots, \quad u = \varepsilon(u_0 + \varepsilon u_1 + \cdots). \tag{7.28}$$

The chosen asymptotics (7.27) and (7.28) corresponds to the case when the perturbation, slowly varying in time, propagates with a constant velocity along the x-axis. Introduction of new variables (7.27) and (7.28) is a basis of the multiscale method [22] that is used for derivation of evolution equations. At this stage, the main effects are separated from the secondary ones during the wave motion. Substituting (7.27) and (7.28) into Eqs. (7.25a) and (7.25b), one can receive relations of various orders of smallness with respect to ε. From the relationship containing ε in the zero power (or containing $\sqrt{\varepsilon}$), the velocity can be determined:

$$V = \tilde{c}_2 = \sqrt{c_2^2 - \frac{\beta_1^2}{2\beta_2}}. \tag{7.29}$$

One of the relations containing ε in the first power allows defining coupling between deformations in a wave:

$$\frac{\partial u_0}{\partial \xi} = \frac{\gamma}{2(\tilde{c}_2^2 - c_1^2)} \left(\frac{\partial w_0}{\partial \xi} \right)^2. \tag{7.30}$$

The second relation also containing ε in the first power, taking into account (7.30), represents an evolution equation of the following form:

$$\frac{\partial W}{\partial \tau} + b_1 W^2 \frac{\partial W}{\partial \xi} + b_2 \frac{\partial^3 W}{\partial \xi^3} = 0. \tag{7.31}$$

Here

$$W = \frac{\partial w_0}{\partial \xi}, \quad b_1 = \frac{3\gamma^2}{4(\tilde{c}_2^2 - c_1^2)\,\tilde{c}_2}, \quad b_2 = \frac{R^2(\tilde{c}_2^2 - c_3^2)}{8\,\tilde{c}_2}. \tag{7.32}$$

Equation (7.31) coincides with the modified Korteweg-de Vries (MKDV) equation [25, 26] that is well known in the nonlinear wave dynamics.

Thus, the velocity of perturbation and a ratio between the deformations in a wave have been determined at the first stage of application of the multiscale method. At the second stage, this information allowed obtaining the evolution equation for the main term of decomposition of the required dependent variable.

In order to find areas of the modulation instability of the shear wave of deformation $W = \partial w_0/\partial \xi$, we shall employ the standard procedure of obtaining the nonlinear Schrödinger equation [25]. We shall search for the solution of Eq. (7.31) as a harmonic wave with the amplitude and phase slowly varying in space and time (a quasiharmonic wave):

$$W = A(\varepsilon\xi,\ \varepsilon\tau)\exp(i(\omega\tau - k\xi)) + A*(\varepsilon\xi,\ \varepsilon\tau)\exp(-i(\omega\tau - k\xi)), \tag{7.33}$$

where A is the complex amplitude and $A*$ is the complex-conjugate amplitude. The frequency ω and the wavenumber k satisfy the dispersion equation of the linear problem

$$\omega = -b_2 k^3 \tag{7.34}$$

and the condition of smallness of amplitude-frequency modulation

$$\frac{\partial A}{\partial \xi} \cdot \frac{1}{kA} \sim \frac{\partial A}{\partial \tau} \cdot \frac{1}{\omega A} \sim \varepsilon \ll 1,$$
$$\frac{\partial^2 A}{\partial \xi^2} \cdot \frac{1}{kA} \sim \frac{\partial^2 A}{\partial \tau^2} \cdot \frac{1}{\omega A} \sim \varepsilon^2. \tag{7.35}$$

Using the method of averaging over the fast variables [25], it is possible to pass from Eq. (7.31) to the abridged equation of the quasiharmonic wave envelope. In the reference frame $\eta = \varepsilon(\xi - v_{gr}\tau)$, $T = \varepsilon\tau$ moving with the group velocity $v_{gr} = d\omega/dk$, the envelope evolution is described by the nonlinear Schrödinger equation

$$i\frac{\partial A}{\partial T} - \frac{1}{2}\frac{dv_{gr}}{dk} \cdot \frac{\partial^2 A}{\partial \eta^2} = \sigma|A|^2 A. \tag{7.36}$$

The last equation is frequently used in studying of wave processes in optics, plasma physics, acoustics, and electrodynamics [25]. Here

$$\sigma = \frac{b_1 k}{\varepsilon},$$ (7.37)

$$\frac{dv_{gr}}{dk} = -6b_2 k.$$ (7.38)

It should be noted that the nonlinear Schrödinger equation can be also obtained from Eqs. (7.25a) and (7.25b), but as we already have got MKDV Eq. (7.31), our way is shorter.

It is known that under certain conditions a quasiharmonic wave is unstable with respect to breaking up into individual wave packets (this effect is called *a modulation instability* or *a self-modulation*) [25]. The presence of such instability in a system is determined by the Lighthill criterion [26]:

$$\frac{dv_{gr}}{dk}\sigma < 0.$$ (7.39)

Speaking in spectral language, the modulation effect is characterized by increasing of side components in the modulated wave spectrum. The energy will be pumped into these components from the central part of the spectrum of perturbations.

Figure 7.7 schematically shows the self-modulation process of a quasiharmonic wave (a) and evolution of its spectrum (b).
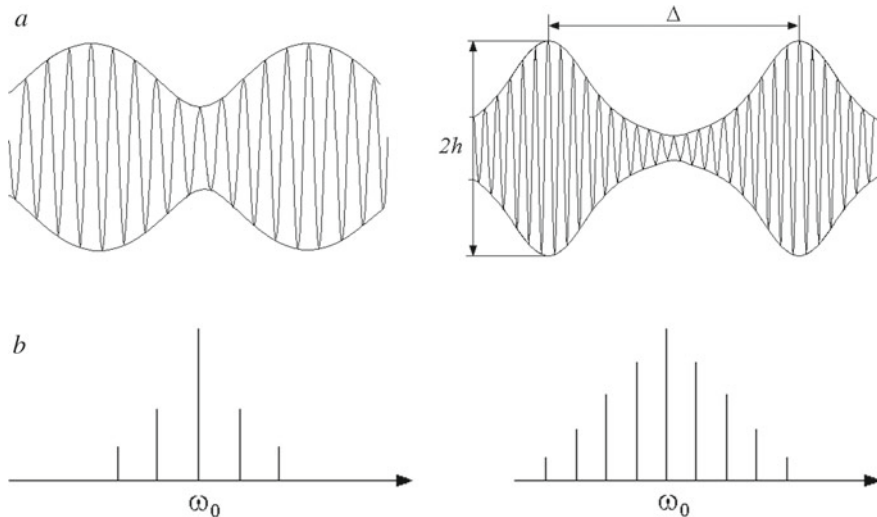
Fig. 7.7 Self-modulation of a quasiharmonic wave (**a**) and evolution of its spectrum (**b**)

In the case at issue, as follows from Eqs. (7.37) and (7.38), $\frac{\mathrm{d}v_{gr}}{\mathrm{d}k}\sigma = -\frac{6b_1b_2}{\varepsilon}k^2 = -\frac{9\gamma^2 R^2(c_3^2-\tilde{c}_2^2)}{16\varepsilon(c_1^2-\tilde{c}_2^2)\tilde{c}_2^2}k^2$. Since from Eqs. (7.26) and (7.20a), it is visible that $\tilde{c}_2^2 < c_3^2 < c_1^2$, then, according to the Lighthill criterion, the modulation instability will be observed in the considered medium for all the allowable values of the microstructure parameters [20].

7.3.2 Forms of Wave Packets in the Case of the Modulation Instability

Let us introduce the real amplitude a and phase θ instead of the complex amplitude A: $A = a\exp(i\theta)$. Then, Schrödinger equation (7.36) can be transformed into two coupled equations:

$$\frac{\partial}{\partial\tau}\left(\frac{a^2}{2}\right) - \frac{1}{2}\frac{\partial}{\partial\eta}\left(\frac{\mathrm{d}v_{gr}}{\mathrm{d}k}\frac{\partial\theta}{\partial\eta}a^2\right) = 0, \qquad (7.40)$$

$$a\frac{\partial\theta}{\partial\tau} + \frac{1}{2}\frac{\mathrm{d}v_{gr}}{\mathrm{d}k}\frac{\partial^2 a}{\partial\eta^2} - \frac{1}{2}\frac{\mathrm{d}v_{gr}}{\mathrm{d}k}a\left(\frac{\partial\theta}{\partial\eta}\right)^2 + \sigma a^3 = 0.$$

For determining the form of wave packets into which a quasiharmonic wave breaks up due to the modulation instability, we shall use the set of Eq. (7.40) and analyze the stationary wave envelopes.

We shall look for solutions of Eq. (7.40), depending on the single variable

$$z = \eta - v\tau,$$

where v is the stationary wave velocity: $a = a(z), \theta = \theta(z)$.

Then, Eq. (7.40) in partial derivatives is reduced to the set of two ordinary differential equations:

$$\frac{d}{dz}\left(\frac{v}{2}a^2 + \frac{1}{2}\frac{\mathrm{d}v_{gr}}{\mathrm{d}k}\frac{d\theta}{dz}a^2\right) = 0, \qquad (7.41)$$

$$\frac{1}{2}\frac{\mathrm{d}v_{gr}}{\mathrm{d}k}\frac{\mathrm{d}^2 a}{\mathrm{d}z^2} - va\frac{d\theta}{dz} - \frac{1}{2}\frac{\mathrm{d}v_{gr}}{\mathrm{d}k}a\left(\frac{d\theta}{dz}\right)^2 + \sigma a^3 = 0.$$

After integrating the first of Eq. (7.41), we obtain the relation of the phase and amplitude of the wave:

$$\frac{d\theta}{dz} = -2\left(\frac{\mathrm{d}v_{gr}}{\mathrm{d}k}\right)^{-1}\left(\frac{q}{a^2} + \frac{v}{2}\right) = 0, \qquad (7.42)$$

where q is the integration constant.

If to consider only the waves having the amplitude modulation, but without the phase modulation, then $q = 0$ and the amplitude variation will be described by Duffing equation:

$$\frac{d^2 a}{dz^2} + m_1 a + m_2 a^3 = 0, \tag{7.43}$$

where

$$m_1 = v^2 \left(\frac{dv_{gr}}{dk}\right)^{-2}, \quad m_2 = 2\sigma \left(\frac{dv_{gr}}{dk}\right)^{-1}. \tag{7.44}$$

It should be noted that coefficient m_1 of Eq. (7.43) is always positive, whereas the sign of factor m_2 can be both positive and negative. According to the Lighthill criterion (7.39), the negative value of this coefficient ($m_2 < 0$) corresponds to the considered area of the modulation instability.

For such signs of coefficients m_1 and m_2 Duffing equation has two types of finite solutions—the periodic solution and the solitary one. The periodic solution is expressed in terms of the elliptic sine:

$$a = a_0 sn(Kz, \ s), \tag{7.45}$$

where a_0 is the stationary wave amplitude, $K = \sqrt{(2m_1 + m_2 a_0^2)/2}$ is the nonlinear analog of the wavenumber, $s^2 = -m_2 a_0^2/(2m_1 + m_2 a_0^2)$ is the modulus of the elliptic function, which varies in the range $0 \le s \le 1$.

The periodic wave parameters are related as follows [20]:

$$a_0 = v \sqrt{\frac{s^2}{-\frac{dv_{gr}}{dk}\sigma(1 + s^2)}}, \quad K = \frac{v}{\frac{dv_{gr}}{dk}\sqrt{1 + s^2}}. \tag{7.46}$$

The wave amplitude grows in direct proportion to the velocity, whereas the wavelength $\Lambda = 4\mathbf{K}(s)/K$, where $\mathbf{K}(s)$ is the elliptic integral of the first kind, decreases in direct proportion to the velocity v.

The solitary wave, which is a limiting case ($s = 1$) of the periodic wave (7.45), is described by a hyperbolic tangent:

$$a = a_0 th(z/\Delta). \tag{7.47}$$

Its velocity v, amplitude a_0 and width Δ are related by the following formulas:

$$a_0 = \frac{v\sqrt{2}}{2}\left(-\sigma \frac{dv_{gr}}{dk}\right)^{-1/2}, \quad \Delta = \frac{\sqrt{2}}{v}\frac{dv_{gr}}{dk}. \tag{7.48}$$
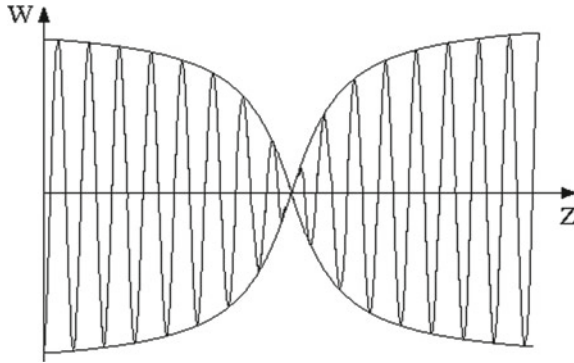
Fig. 7.8 Shear strain wave modulated by "kink" law

Function (7.47) describes the transition from one to another constant value (the difference). The shear strain wave modulated according to this law is shown in Fig. 7.8.

The profile of the periodic wave (7.45) is transformed from sinusoidal (for $s \to 0$) to close to meander (for $s \to 1$). The shear wave of displacement, modulated according to the periodic law, is shown (for $s \to 1$) in Fig. 7.9.

Let us reveal, how height (H) and width (D) of the wave packet formed as a result of the self-modulation of the quasiharmonic wave are related with the microstructure parameters of a material.

Identifying the height of the wave packet with the double amplitude, $H = 2a_0$, and its width with Δ: $D = \Delta$, according to Eq. (7.48), we find:

$$H = \frac{4\tilde{c}_2 v}{3R\gamma k}\sqrt{\frac{2\varepsilon(\tilde{c}_2^2 - c_1^2)}{\tilde{c}_2^2 - c_3^2}}, \quad D = \frac{3\sqrt{2}R^2(c_3^2 - \tilde{c}_2^2)}{4\tilde{c}_2 v}. \tag{7.49}$$

The similar dependences of H and D on parameter s can be obtained from Eq. (7.46) for a periodic sequence of wave packets (wave trains). In this case, the
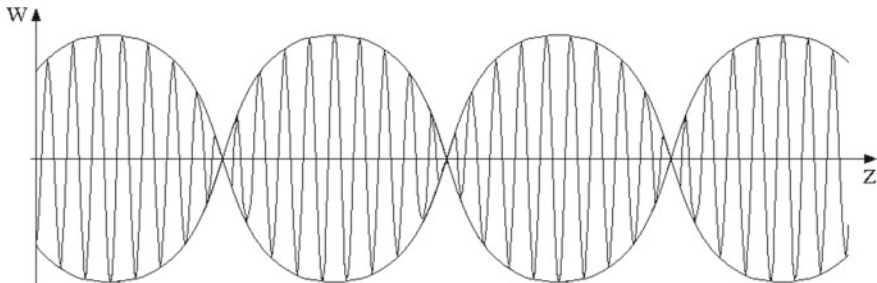
Fig. 7.9 Shear wave of displacement modulated according to the periodic law

width of the packet should be identified with a half of wavelength of the envelope $(D = \Delta/2)$ and the following formulas yield:

$$H = \frac{8vs}{3R\gamma k}\sqrt{\frac{\varepsilon(c_1^2 - \tilde{c}_2^2)}{(c_3^2 - \tilde{c}_2^2)(1 + s^2)}}, \quad D = \frac{3\mathbf{K}(s)R^2(c_3^2 - \tilde{c}_2^2)k\sqrt{1 + s^2}}{2\tilde{c}_2 v}. \quad (7.50)$$

Dependences (7.49) and (7.50) contain parameters R, c_1, $\tilde{c}_2$, c_3, and γ that, as it follows from expressions (7.20a), (7.23), and (7.26), are directly related to the microstructure parameters (the force constants K_0, K_1, K_2, the lattice period a and the grain sizes $h_1 = d_1/\sqrt{2}$ and $h_2 = d_2/\sqrt{2}$). Thus, these dependences enable one to estimate the influence of the material microstructure on the height and width of the propagating wave packets in it, into which the quasiharmonic shear wave breaks up as a result of its self-modulation.

7.4 Nonlinear Longitudinal Waves in a Rod Made of an Auxetic Material

Sections 4.4 and 4.5 discussed Mathematical models of auxetics—materials with a negative Poisson's ratio—were discussed in Sects. 4.4 and 4.5. Here we consider a rod made of an auxetic material [27].

At present, models and structures of auxetic rods [28–30] used as elements of a new class of composites [30–34] are actively developed, auxetic polymeric foams [35–37] and auxetic crystalline materials [30, 38–44] are synthesized and studied. Considerable attention is paid to the study of characteristic features of the propagation of elastic waves, primarily, of the ultrasonic range, in auxetics [5, 30, 45–52], since such studies will contribute to the development of methods for acoustic non-destructive testing of new advanced materials.

The aim of this section is an investigation of the propagation of longitudinal strain waves in a rod made from a material with a negative Poisson's ratio.

7.4.1 The Linear Mathematical Model. Dispersion Properties

In dynamics of rods, besides the engineering (classical) models, there are, so-called, refined or nonclassical models [53, 54]. These models either take into account additional factors affecting a dynamic process, or are free of some hypotheses accepted in the engineering theories and restricting their field of applicability.

The classical D. Bernoulli theory, which is usually used for description of longitudinal vibrations of a rod, is generalized by the Bishop model taking into account the kinetic energy of the transverse motions of rod particles and the potential energy of shear deformations:

$$\rho F \frac{\partial^2 u}{\partial t^2} - EF \frac{\partial^2 u}{\partial x^2} - \rho v^2 I_0 \frac{\partial^4 u}{\partial x^2 \partial t^2} + v^2 \mu I_0 \frac{\partial^4 u}{\partial x^4} = 0, \tag{7.51}$$

where $u(x, t)$ is a longitudinal displacement, ρ is a density, F is a cross-sectional area, I_0 is a polar moment of inertia, E is Young's modulus, μ is a shear modulus, and v is Poisson's ratio.

The longitudinal waves described by Eq. (7.51) possess dispersion, so the frequency ω and the wavenumber k of the harmonic wave $u = u_0 \exp(i(\omega t - kx))$ are interrelated as follows:

$$\omega = k \sqrt{\frac{c_0^2 + c_\tau^2 v^2 R^2 k^2}{1 + v^2 R^2 k^2}}, \tag{7.52}$$

where R is a polar radius of inertia.

The plot of Eq. (7.52) determines the dispersion curve in the (ω, k)-plane. This curve has an asymptote $\omega = c_0 k = k\sqrt{E/\rho}$ for small values of the wavenumber k, whereas for the large wavenumbers it asymptotically approaches the straight line $\omega = c_\tau k = k\sqrt{\mu/\rho}$. Thus, in a rod described by the Bishop model, low-frequency waves propagate with velocities close to the rod velocity c_0, whereas velocities of high-frequency waves are close to the shear wave velocity, c_τ, in an infinite medium. The relationship between these velocities can be expressed in terms of the Poisson's ratio as follows:

$$\frac{c_0}{c_\tau} = \sqrt{\frac{E}{\mu}} = \sqrt{\frac{2\mu(1 + v)}{\mu}} = \sqrt{2(1 + v)}. \tag{7.53}$$

For ordinary materials with positive values of the Poisson's ratio, the velocity c_0 of the longitudinal wave in a rod exceeds the shear wave velocity c_τ. In this case, the longitudinal wave dispersion is normal, i.e., the phase velocity is greater than the group velocity:

$$V_{ph} > V_{gr}, \tag{7.54}$$

where $V_{ph} = \omega/k$ and $V_{gr} = d\omega/dk$ are calculated due to Eq. (7.52).

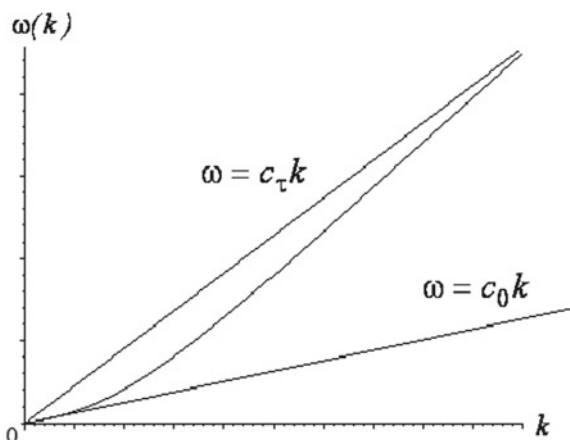The qualitative form of the dispersion curve (7.52) is plotted in Fig. 7.10.

Analysis of Eq. (7.53) shows that the difference between the velocities c_0 and c_τ decreases as the Poisson's ratio becomes negative. Dispersion of the longitudinal waves remains normal for $-0.5 < v < 0$, although the velocity variation becomes less noticeable with increasing frequency. In a rod with $v = -0.5$ the longitudinal waves do not possess dispersion, whereas for $-1 < v < -0.5$ dispersion becomes anomalous, i.e.,

$$V_{ph} < V_{gr}. \tag{7.55}$$

Fig. 7.10 Dispersion curves for the Bishop model
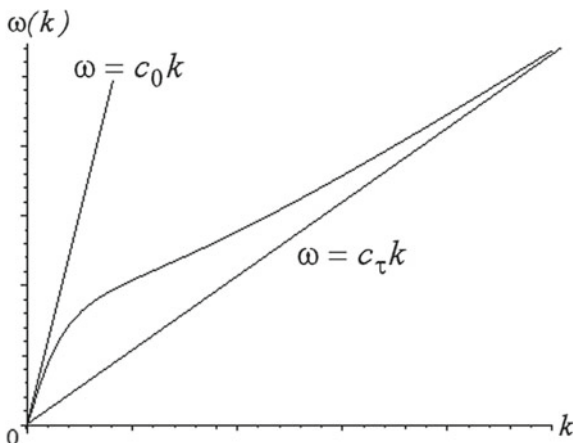
Fig. 7.11 Dispersion dependencies for $-1 < \nu < -0.5$—anomalous dispersion

In the latter case, the shear wave velocity exceeds the rod velocity c_0 in an infinite medium. The form of the dispersion curve is shown in Fig. 7.11.

Thus, the negative Poisson's ratio leads to a qualitatively different (anomalous) dispersion behavior of the linear waves propagating in a rod made of an auxetic material.

7.4.2   The Nonlinear Mathematical Model. Stationary Strain Waves

If to take into account the geometric and physical nonlinearities in a rod [55], then the equation for nonlinear longitudinal waves has the form [53]:

$$\frac{\partial^2 u}{\partial t^2} - c_0^2 \left(1 + \frac{6\alpha}{E} \frac{\partial u}{\partial x}\right) \frac{\partial^2 u}{\partial x^2} - v^2 R^2 \left(\frac{\partial^4 u}{\partial x^2 \partial t^2} - c_\tau^2 \frac{\partial^4 u}{\partial x^4}\right) = 0 \qquad (7.56)$$

Here R is the polar radius of inertia, and the coefficient α determining the contribution of the geometric and physical nonlinearities is equal to $\alpha = \frac{E}{2} + \frac{v_1}{6}(1 - 6v) + v_2(1 - 2v) + \frac{4}{3}v_3$, where $v_{1,2,3}$ are the third-order elastic constants.

Let us introduce dimensionless variables $t' = \frac{c_0 t}{R}$, $x' = \frac{x}{R}$, $u' = \frac{\alpha u}{R}$ in Eq. (7.56) and then omit dashes over the dimensionless variables:

$$\frac{\partial^2 u}{\partial t^2} - \left(1 + \beta \frac{\partial u}{\partial x}\right) \frac{\partial^2 u}{\partial x^2} - \frac{\partial^4 u}{\partial x^2 \partial t^2} + c^2 \frac{\partial^4 u}{\partial x^4} = 0 \qquad (7.57)$$

The dimensionless parameter β defines a rod with a "rigid" ($\beta = 1$) or a "soft" ($\beta = -1$) type of nonlinearity. For materials with a positive Poisson's ratio, it is known that the nonlinearity is "soft" for metal rods or rods made of alloys, whereas a "rigid" type of nonlinearity is possible for composite rods.

Any regularities similar to these ones have not yet been established for materials with a negative Poisson's ratio. Further, we shall consider both types of the nonlinear behavior.

In Eq. (7.57), the dimensionless parameter c is equal to the ratio of the velocities $c = c_\tau/c_0$. As it follows from expression (7.53), $c < 1$ for all the positive values of the Poisson's ratio. But if the Poisson's ratio is negative, various cases are possible, when the rod velocity c_0 exceeds the shear wave velocity c_τ ($c < 1$ for $-0.5 < v < 0$) or, vice versa, $c_\tau > c_0$ ($c > 1$ for $-1 < v < -0.5$). The degenerated case, when both velocities coincide, yields $c = 1$ for $v = -0.5$.

Both dispersion and nonlinearity will influence the propagation of longitudinal waves described by Eq. (7.57). Nonlinearity leads to the generation of new harmonics in a wave. This fact contributes to the appearance of sharp differences in the moving profile of the wave. But dispersion, on the contrary, decreases the differences due to distinguishes in the phase velocities of the harmonic components of the wave. The joint action of these factors can lead to the formation of stationary waves, which propagate with a constant velocity without changing the shape [56].

We shall search for solutions of Eq. (7.57) among stationary strain waves $U(\xi) = \frac{\partial u}{\partial \xi}$, where $\xi = x - Vt$ is the "traveling" coordinate and $V =$ const is the stationary wave velocity. Equation (7.57) is reduced to the ordinary differential equation:

$$\frac{d^2 U}{d\xi^2} + m_1 U + m_2 U^2 = 0, \qquad (7.58)$$

where $m_1 = \frac{V^2 - 1}{c^2 - V^2}$, $m_2 = \frac{\beta}{2(V^2 - c^2)}$.

Depending on the relationship between the nonlinear wave velocity, V, the parameter c that corresponds to the velocities c_0 and c_τ in the dimensional variables, and number 1, the behavior of the solutions of this equation will be qualitatively different.

Fig. 7.12 Periodic wave shape ("soft" nonlinearity; $c < V < 1$; $\nu > -0.5$)
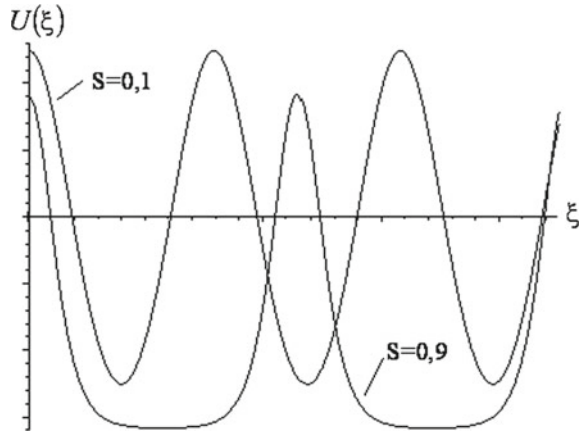
We will research only those cases, when there is no constant component in the strain wave, as only these cases are physically realizable.

"Soft" nonlinearity. Let us consider a rod with a "soft" nonlinearity that is typical for metals and alloys. If the Poisson's ratio of a material of a rod exceeds -0.5 (i.e., $c < 1$), then a nonlinear periodic wave propagates in the rod with velocities $c < V < 1$ (or $c_\tau < V < c_0$—in terms of the dimensional variables).

Such a wave is analytically described by the solution of Eq. (7.58):

$$U(\xi) = \frac{A}{3s^2}\left(\sqrt{1 - s^2 + s^4} - 1 - s^2\right) + A\,\mathrm{sn}^2(k\xi, s),\tag{7.59}$$

where A is a wave amplitude, k is a wavenumber, sn is the elliptic sine (elliptic Jacobi function), s is the modulus of the elliptic function that determines degree of distortion of the wave shape $U(\xi)$ in comparison with the sinusoidal one.

The qualitative form of the periodic wave (7.59) is shown for different values of s in Fig. 7.12.

The amplitude A of the wave is related to its velocity V and modulus s by the expression

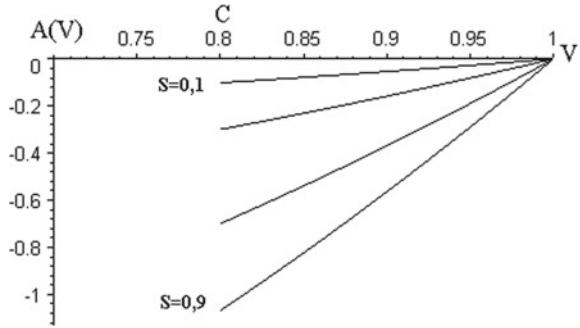$$A = 3\left(1 - V^2\right)\frac{s^2}{\sqrt{1 - s^2 + s^4}}.\tag{7.60}$$

These dependencies are shown in Fig. 7.13.

In its turn, the wave velocity V is expressed in terms of the wavenumber k and the modulus s as follows
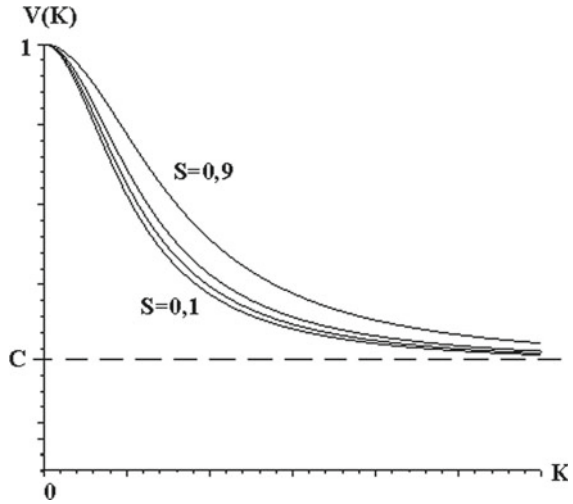
$$V = \sqrt{\frac{1 + 4c^2\sqrt{1 - s^2 + s^4}k^2}{1 + 4\sqrt{1 - s^2 + s^4}k^2}}.\tag{7.61}$$

Fig. 7.13 Wave amplitude versus the wave velocity ("soft" nonlinearity; $c < V < 1$; $\nu > -0.5$)

Fig. 7.14 Nonlinear dispersion law

The relationship (7.61) can be called *a nonlinear dispersion law* [57] and is plotted in Fig. 7.14. Obviously, if $s \to 0$, a dispersion curve yields for a linear wave.

In the velocity range $V < c$ and $V > 1$, where there are no linear waves, in the nonlinear case there exist soliton-like waves.
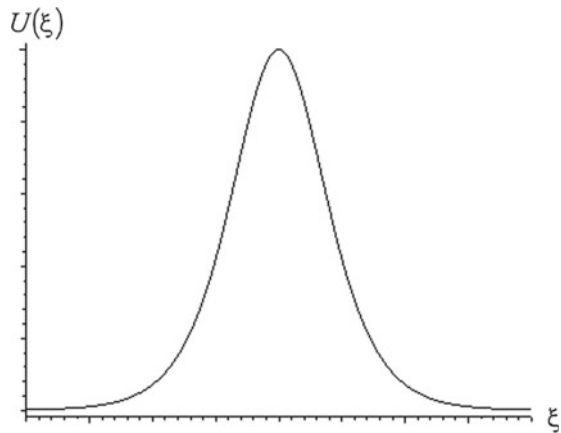
A wave propagating with velocity $V < c$ is described by the following solution of Eq. (7.58):

$$U(\xi) = \frac{A^*}{\text{ch}^2\left(\frac{x-Vt}{\Delta}\right)},\tag{7.62}$$

where A^* is the amplitude; Δ is the soliton width, ch is the hyperbolic cosine. The wave (6.62) has a bell shape (Fig. 7.15).

The amplitude A^* and the width Δ of the wave are related to its velocity V by the following relations [27]:

**Fig. 7.15** Wave propagating
with velocity $V < c$

$$A^* = 3(1 - V^2), \quad \Delta = 2\sqrt{\frac{c^2 - V^2}{1 - V^2}}. \tag{7.63}$$

Dependencies (7.63) are plotted in Figs. 7.16 and 7.17. The area $V < c$ corresponds to these dependencies in these figures. From these figures, it is visible that the behavior of a "subsonic" solitary wave is not classical for solitons: The wave of greater amplitude has a larger width and propagates with a slower velocity. Because of the limited velocity of the waves from this range, the soliton amplitude and width are also numerically restricted: $A \in (3(1 - c^2), 3)$, $\Delta \in (0, 2c)$.

A wave propagating with a velocity $V > 1$ is also described by Eqs. (7.62) and (7.63). These dependencies are plotted in Figs. 7.16 and 7.17 for $V > 1$. As distinct from the "subsonic" ($V < c$) solitary wave, "supersonic" ($V > 1$) solitons have a negative polarity and their amplitude can increase up to infinity. Waves of greater amplitude propagate with a higher velocity, and, when the velocity grows, their width decreases and approaches asymptotically number 2 ($\Delta \in (2, \infty)$).
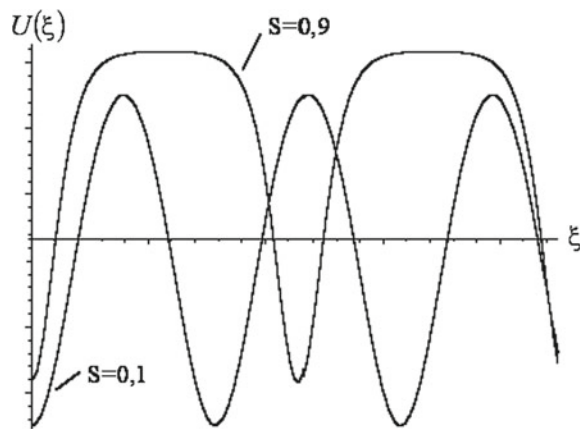
Fig. 7.16 Dependence of
the soliton amplitude on the
velocity for $V < c$ and $V > 1$
("soft" nonlinearity;
$\nu > -0.5$)
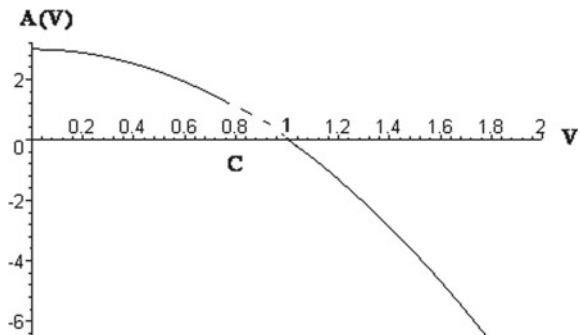
Fig. 7.17 Dependence of the wave width on the velocity for $V < c$ and $V > 1$ ("soft" nonlinearity; $\nu > -0.5$)
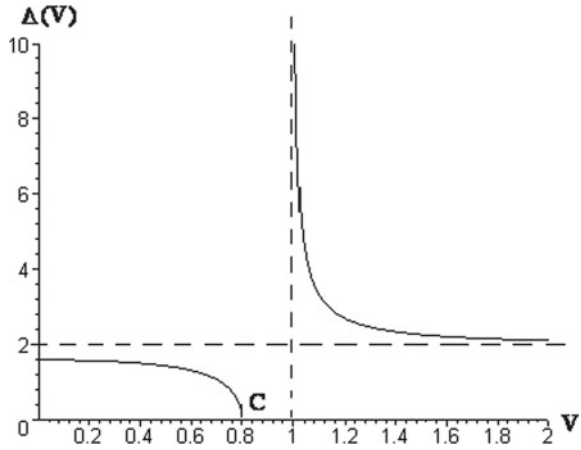
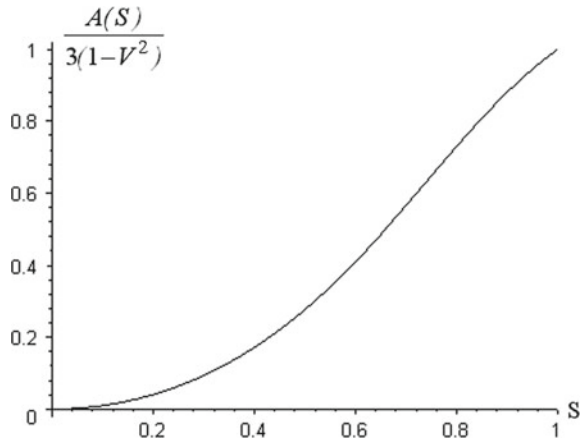Fig. 7.18 Periodic wave shape ("soft" nonlinearity; $1 < V < c$; $-1 < \nu < -0.5$)

As it was mentioned above, if Poisson's ratio varies in the interval $-1 < \nu < -0.5$, then the rod velocity c_0 becomes less than the shear wave velocity c_τ. In this case, $c > 1$ and the nonlinear periodic wave traveling with velocities $1 < V < c$ is described by the expression:

$$U(\xi) = \frac{A}{3s^2}\left(1 + s^2 - \sqrt{1 - s^2 + s^4}\right) - A sn^2(k\xi, s), \qquad (7.64)$$

where

$$A = 3(V^2 - 1)\frac{s^2}{\sqrt{1 - s^2 + s^4}}. \qquad (7.65)$$

Fig. 7.19 Normalized
amplitude versus the
nonlinear distortion
coefficient s ("soft"
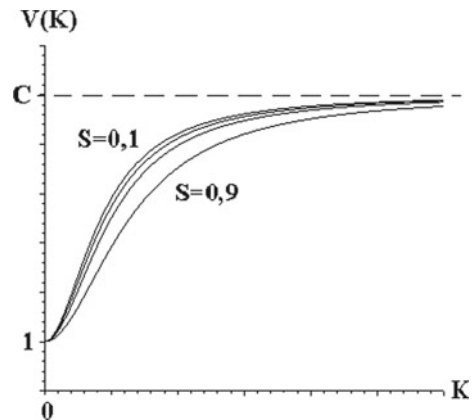nonlinearity; $1 < V < c$;
$-1 < v < -0.5$)

The periodic wave shape is shown for various values of s in Fig. 7.18, and the
dependence (7.65) scaled on $3(V^2 - 1)$ is plotted in Fig. 7.19.

The wave (7.64) satisfies the nonlinear dispersion law (7.61). The form of the
dispersion relations for this wave is shown in Fig. 7.20. Obviously, for small values
of the coefficient of nonlinear distortions ($s \to 0$) there exists a linear degeneracy
corresponding to the case, when the dispersion of linear waves is anomalous.

In a rod made from a material with $v \in (-1; -0, 5)$, the existence of "subsonic"
($V < 1$) and "supersonic" ($V > c$) solitary waves is possible. In this case, "subsonic"
solitons are described by expressions (7.62) and (7.63), like in the "subsonic" case for
$v > -0.5$, but their properties differ. Thus, the amplitude of these waves decreases
when the velocity grows, and it can be arbitrarily small for $V \to 1$. The soliton
width, on the contrary, infinitely grows, if the amplitude decreases. Dependences
of the amplitude and width on the wave velocity are plotted in Figs. 7.21 and 7.23,
respectively.

Fig. 7.20 Nonlinear
dispersion law for
"supersonic" waves

Fig. 7.21 Dependence of the soliton amplitude on the velocity for $V < 1$ and $V > c$ ("soft" nonlinearity; $-1 < \nu < -0.5$)
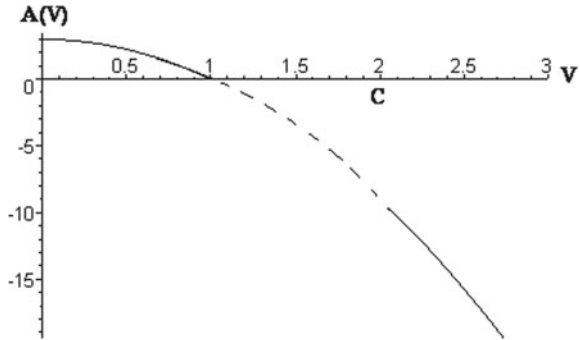
"Supersonic" solitary waves, as in the case $\nu > -0.5$, are described by expressions (7.62) and (7.63). They have a negative polarity; their amplitude starts with the value $3(1 - c^2)$ and increases indefinitely with growing velocity. The width of such a wave increases with growing amplitude, and it does not numerically exceed 2—it asymptotically approaches this value. Dependences of the amplitude and the width on the wave velocity are also shown in Figs. 7.21 and 7.22, respectively.

When the Poisson's ratio of a material equals $\nu = -0.5$, the rod and shear velocities coincide: $c_0 = c_\tau$, consequently, the region of existence of linear and, therefore, nonlinear periodic waves disappears. In this case, only solitary waves remain. They are described by Eqs. (7.62) and (7.63). The soliton width does not change, when the amplitude or velocity varies, and is equal to 2. When the velocity grows, the amplitude of the "subsonic" solitons decreases up to zero, whereas the "supersonic" soliton amplitude increases infinitely starting from zero. The dependence of the amplitude on the velocity is shown in Fig. 7.23.

"Rigid" nonlinearity. Let us consider a rod with a "rigid" nonlinearity. Formally, such type of nonlinearity causes a change of sign of the nonlinear term in Eq. (7.58) that, in its turn, leads to a change of the nature of the propagating waves. The areas

Fig. 7.22 Dependence of the soliton width on the velocity for $V < 1$ and $V > c$ ("soft" nonlinearity; $-1 < \nu < -0.5$)
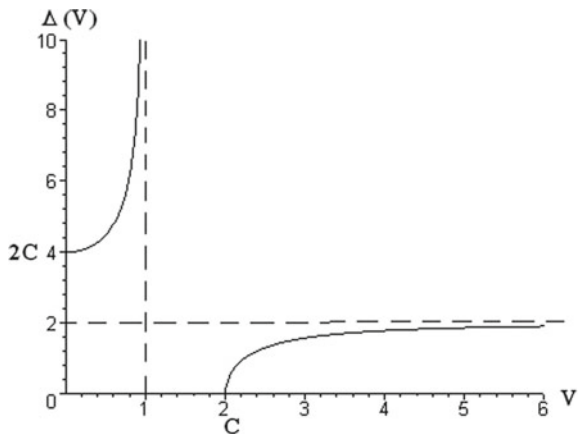
**Fig. 7.23** Dependence of the soliton amplitude on the velocity for $\nu = -0.5$ ("soft" nonlinearity)
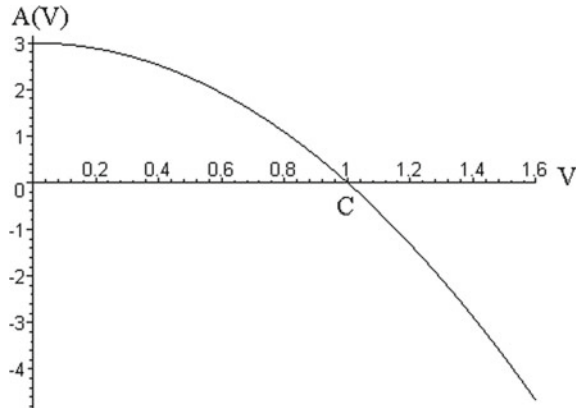
of existence of periodic and solitary waves remain the same as in a rod with a "soft" nonlinearity, but the polarity of these waves becomes another [27].

If the Poisson's ratio is positive or negative from the interval $\nu \in (-0.5;\ 0)$ (i.e., $c < 1$), then periodic waves propagate in a rod with a "rigid" nonlinearity with velocities $c < V < 1$. They are described by Eq. (7.64), whereas their parameters—the velocity, the amplitude and the coefficient of nonlinear distortions—are related by expression (7.65). In the "subsonic" ($0 < V < c$) and "supersonic" ($V > 1$) ranges, solitary waves are described by Eq. (7.62) and their parameters are determined by relations (7.63). As it was mentioned above, the waves in a rod with a "rigid" nonlinearity are distinguished by polarity, so the plots of the amplitude versus velocity are opposite to those shown in Fig. 7.16. They are shown in Fig. 7.24. The dependence of the soliton width on the velocity is plotted in Fig. 7.17.

When $\nu \in (-1;\ -0.5\,)$, the periodic waves propagate with velocities $1 < V < c$ and are described by Eq. (7.59), whereas their parameters are related by Eq. (7.60). As in the previous case, the "subsonic" (for $0 < V < 1$) and "supersonic" (for $V > c$)

Fig. 7.24 Soliton amplitude versus the velocity for $V < c$ and $V > 1$ ("rigid" nonlinearity; $\nu > -0.5$)
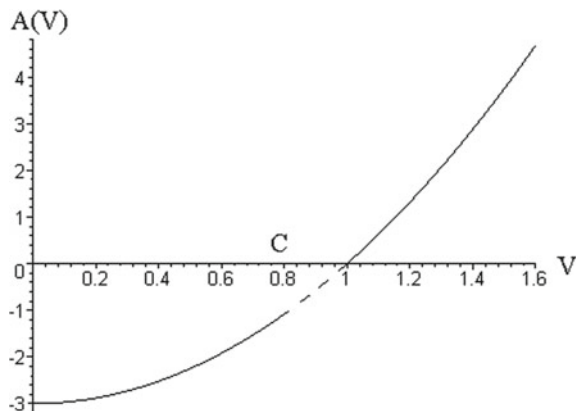
Fig. 7.25 Soliton amplitude versus the velocity for $V < 1$ and $V > c$ ("rigid" nonlinearity; $-1 < \nu < -0.5$)
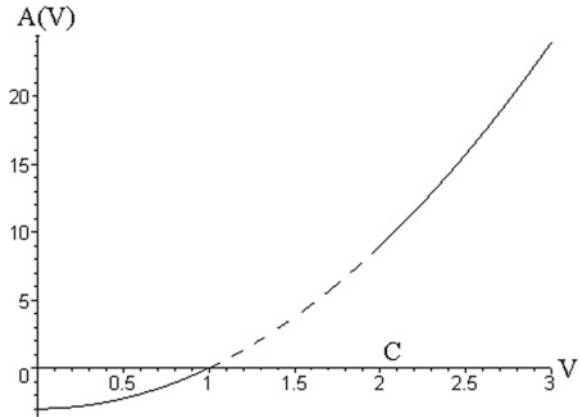
solitons have the form (7.62) and their parameters are related by Eq. (7.63). The plot of the soliton amplitude as a function of the velocity is shown in Fig. 7.25.

If $\nu = -0.5$, then the region of existence of periodic waves disappears and solitary "subsonic" and "supersonic" waves are saved and have the same relationships (7.63) between their parameters.

7.4.3 Numerical Simulation of Soliton Interactions

Mathematical models describing the propagation and interaction of nonlinear waves in distributed systems are usually subdivided into integrable and non-integrable ones by the inverse scattering transform (IST) [58]. In the slang of specialists, the mentioned models are called, respectively, "integrable" and "non-integrable" systems.

In many works (see, for example, [59, 60]), it has been shown analytically and numerically that in integrable systems, localized waves (solitons) behave like particles: upon collision, they retain their individuality and acquire only a phase shift (an elastic interaction takes place in this case). This fact is confirmed by experiments, where the studied objects were nonlinear waves in plasma, liquid with gas bubbles, and electromagnetic waves [61–63].

Equation (7.56) refers to a class of systems that are not integrable by IST, so features of the interaction of solitons described by this equation remain nowadays unexplored. However, it is known that for such systems, besides an elastic interaction, another scenario of the behavior of localized waves is possible. When overtaking each other, soliton-like waves emit part of their energy in the form of quasilinear wave packets (i.e., inelastic interaction is observed) [64].

In Ref. [65], there were experimentally observed not only the effects of inelastic interaction, but also the effects of splitting of strongly nonlinear waves, when additional soliton-like waves are separated from the wave packet after interaction. Splitting effects were obtained during a counter interaction of strongly nonlinear waves propagating along a rubber band.

Processes of soliton interaction will be studied here for the strain waves (7.62) and (7.63). Numerical simulation of Eq. (7.57) was carried out using the developed finite-difference algorithm realizing an implicit three-layer scheme with the approximation order $o(\tau^2, \xi^2)$, where τ is the time step and ξ is the space step of the grid. The difference scheme is uniformly stable for the following relation between the steps: $\tau \leq 0.85\xi^2/\sqrt{2\xi^2(1 + |W_x|) + 8c^2}$.

As a result of numerical simulation, it is shown that qualitatively different scenarios of interaction of solitons depend on the relative collision velocity. A collision of only "supersonic" solitons was considered, as any collision velocities can be realized for them. If the velocity is small, the collision occurs like the exchange interaction of the classical Korteweg-de Vries solitons. A fast soliton overtakes a slow soliton, they are not unified but they exchange their characteristics and continue to move with the just received velocities. In this case, the secondary solitons are completely identical to the primary solitons (Fig. 7.26).

The calculations for Fig. 7.26 have been performed for $v_1^2 = 1.2$ and $v_2^2 = 1.1$ (the relative collision velocity equals $\Delta v = v_1 - v_2 = 0.0466$). During the interaction, solitons pass a very long distance with respect to their width Δ. Due to this reason, one cannot display the whole process in one spatial scale. Figure 7.26 has been plotted using a tracking window; therefore, in this figure it is impossible to see the phase shift arising due to interaction of the solitons. This effect is well known and, in this case, is not interesting. Here, we would like to emphasize that even in non-integrable systems an elastic collision of solitons is possible, at least with accuracy up to errors of a numerical experiment. It should be also noted that the known analytical two-soliton solution of the KdV equation is not applicable here.

When the relative velocity is greater ($\Delta v = 0.1$), the collision of solitons is already inelastic (Fig. 7.27). During the interaction, solitons lose a part of their energy, which is realized in a packet of quasiharmonic waves moving behind the slowest "supersonic" soliton with the velocity of linear waves. The characteristics of the secondary solitons (7.62) completely coincide with Eq. (7.63). In Fig. 7.27, a packet of quasilinear waves is shown in a circle on an enlarged scale.

As a result of further increasing of the collision velocity ($\Delta v = 0.4$), the fast soliton overtakes the slow soliton and they are unified (Fig. 7.28). The amplitude of the unified soliton is less than the algebraic sum of the amplitudes of the interacting solitons. Then, the solitons go away from each other losing some part of the energy. This energy is distributed between two wave packets, one of which (it is shown in a circle on an enlarged scale) propagates in the opposite direction to the motion of the solitons with the velocity of quasilinear waves, and the other one (it is shown in a square frame on an enlarged scale) overtakes, with the same velocity, "supersonic" solitons.

Fig. 7.26 Elastic collision
of solitons with the relative
velocity
$\Delta v = v_1 - v_2 = 0.0466$
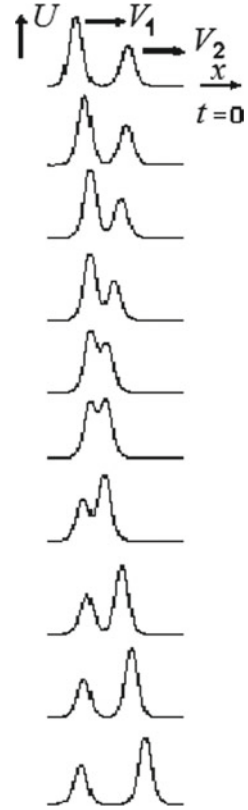
The great collision velocities ($\Delta v \geq 0.5$) lead to the effect of splitting of solitons, which means generation of a larger number of secondary solitons than in the beginning of interaction [23, 66]. Figure 7.29 demonstrates the process of splitting for collision of the solitons with velocities $v_1 = 3$ and $v_2 = 1.5$. From this figure, it is visible that a high-speed soliton, after overtaking a slow soliton, is rapidly removed from the interaction zone. And in this case, a wave packet arises that propagates in the opposite direction to the soliton motion. It is shown in the enlarged scale in the left circle and its evolution is demonstrated below. Next, a second soliton is extracted and a nonstationary wave packet (the right circle) follows for it (its evolution is shown below). Later, another supersonic soliton is formed from this packet. Then again, a quasilinear wave packet and a slow ("subsonic") soliton of negative polarity are generated. All the characteristics of the secondary solitons completely coincide with the solution (7.62) and (7.63). Since the amplitudes of the interacting solitons differ by almost two orders of magnitude, for the convenience of visual perception, Fig. 7.29 is executed in a logarithmic scale.

The soliton interaction occurring with very high speeds ($\Delta v > 2$) looks most effectively for the counter collision of identical solitons. In this case, the picture is

Fig. 7.27 Inelastic interaction of solitons with relative velocity $\Delta v = 0.1$
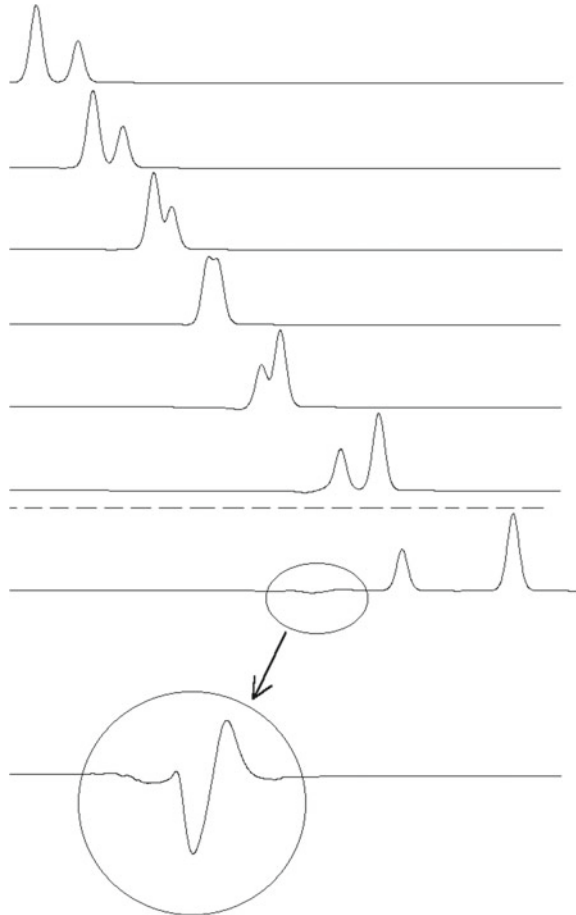
absolutely symmetric and the interaction region remains in the center as it is shown in Fig. 7.30. Because of the symmetry, it is sufficient to consider only one half of the figure.

After the collision, a high-speed secondary soliton with amplitude A_{11} is released. This amplitude is not much smaller than the amplitude A_0 of the primary soliton. A second secondary soliton is formed behind the soliton with amplitude A_{11}, the amplitude A_{12} of which is much smaller than A_0. Next, a nonlinear wave packet is formed (on an enlarged scale it is shown in the oval). If to observe the soliton interaction for a long time, it should be noticed that solitons can be further generated from this packet and, at last, the slow "subsonic" soliton, which amplitude A_{13} is almost equal to A_{12}, will travel behind them. In general, any number of "supersonic" solitons can arise from a wave packet, since their amplitude and energy can be practically zero.

Fig. 7.28 Passing collision of the solitons with the relative velocity $\Delta v = 0.4$
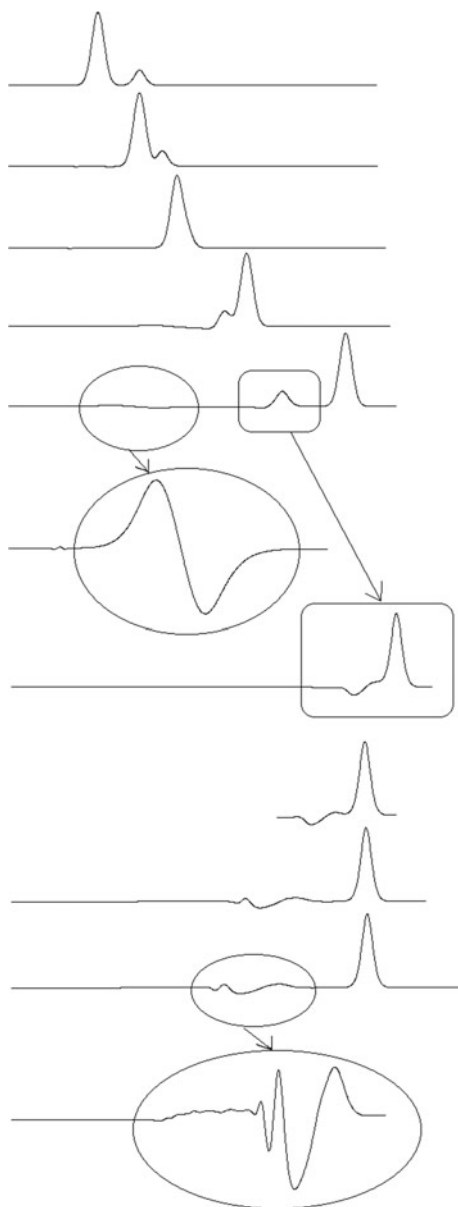
Fig. 7.29 Collision of the solitons with the relative velocity $\Delta v \geq 0.5$: the splitting effect

$v_1 = 3 \; v_2 = 1.5$
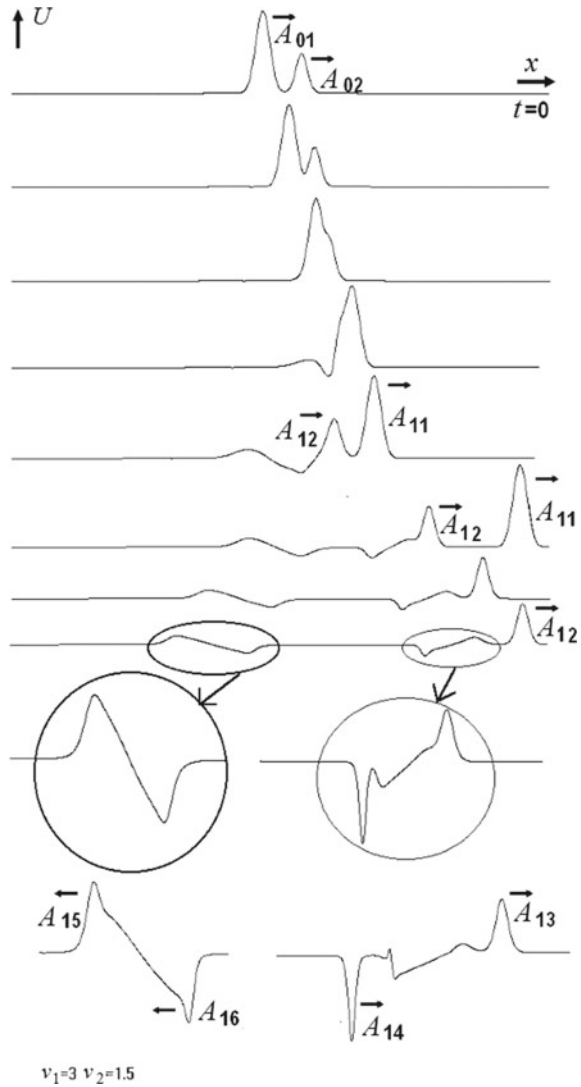
7.5 Application of an Alternative Continualization Method for Analysis of Nonlinear Localized Waves in a Gradient-Elastic Medium

Both discrete and continuum models of metamaterials have been discussed in the previous chapters. So, the problem of passing from a discrete description of a medium to a continuum model arises. In Chaps. 2 and 3, the discrete models have been

Fig. 7.30 Counter interaction of solitons with relative velocities $\Delta v > 2$
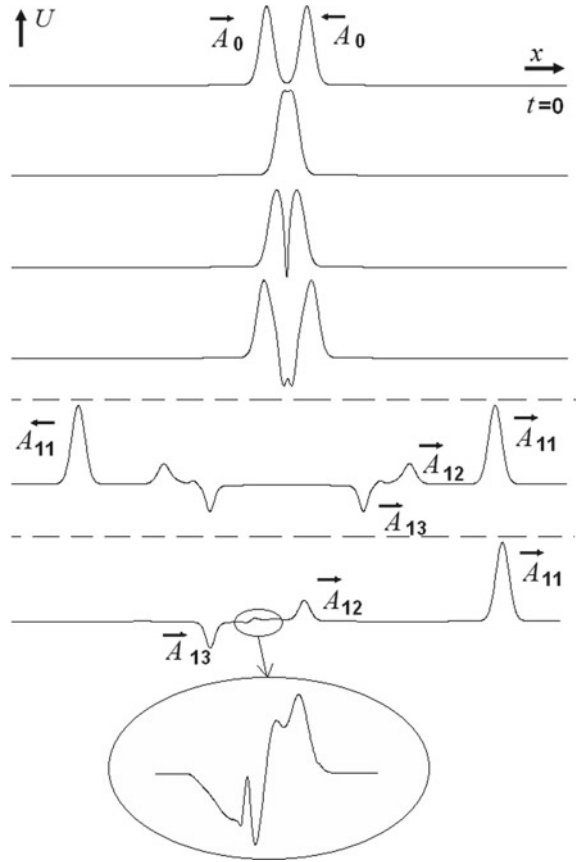
transformed into continuum ones due to expansion of displacements into Taylor's series. Here, we consider an alternative way of such a transformation.

7.5.1 One-Dimensional Model of a Nonlinear Gradient-Elastic Continuum

In order to obtain a dynamically consistent model of a nonlinear gradient-elastic continuum, we use the structural modeling method and the continualization method proposed by Askes and Metrikine [67], which consists in the assumption of a nonlocal connection between the displacements of lattice sites and the resulting continuum.

Let us consider a long one-dimensional chain of alternating identical masses and springs. We assume that the masses can move only along the chain. This direction we denote as Ox axis. Besides, the following designations are introduced: m is mass, k is

a spring rigidity, l is a distance between the masses, and $u_n = u_n(t)$ is a displacement of the nth mass.

The potential energy of the chain consists of potential energies $\phi(\xi_n)$ of all springs, which depends on their displacements $\xi_n = u_n - u_{n-1}$, and have the following form:

$$W = \sum_n \phi(\xi_n) = \sum_n \phi(u_n - u_{n-1}).$$

Since the aim of the work is to study nonlinear waves, we will consider cubical item in $\phi(\xi)$:

$$\phi(\xi) = \frac{k\xi^2}{2} + \frac{K\xi^3}{3}.$$

The equation of the dynamics of the mass has the following form:

$$m\frac{d^2 u_n}{dt^2} = -\frac{\partial W}{\partial u_n}.$$

or after transformations taking into account the previous relations

$$m\frac{d^2 u_n}{dt^2} = k(u_{n+1} - 2u_n + u_{n-1}) + K(u_{n+1} - u_{n-1})(u_{n+1} - 2u_n + u_{n-1}).$$

Let us construct an interpolation polynomial of the second degree with respect to x which coincides with function $u(x, t)$ in points $u(x_{n-1}, t) = u_{n-1}, u(x_n, t) = u_n, u(x_{n+1}, t) = u_{n+1}$.

$$\bar{u}(x, t) = u_{n-1}\frac{(x - x_n)(x - x_{n+1})}{2l^2} - u_n\frac{(x - x_{n-1})(x - x_{n+1})}{l^2}$$
$$+ u_{n+1}\frac{(x - x_{n-1})(x - x_n)}{2l^2}.$$

Let us calculate the values of the interpolation polynomial in points $x_n - \theta l$ and $x_n - \theta l$, here $0 < \theta < 1$.

$$\bar{u}(x_n + \theta l, t) = u_{n-1}\frac{\theta(\theta-1)}{2} + u_n(1 - \theta^2) + u_{n+1}\frac{\theta(\theta+1)}{2}$$
$$\bar{u}(x_n - \theta l, t) = u_{n-1}\frac{\theta(\theta+1)}{2} + u_n(1 - \theta^2) + u_{n+1}\frac{\theta(\theta-1)}{2}.$$

As a continuous function describing the motion of the continual model of masses and springs, we take the average value $\bar{u}(x_n + \theta l, t)$ and $\bar{u}(x_n - \theta l, t)$ We get the following

$$u(x, t) \approx \frac{\bar{u}(x_n + \theta l, t) + \bar{u}(x_n - \theta l, t)}{2} = u_{n-1}\frac{\theta^2}{2} + u_n(1 - \theta^2) + u_{n+1}\frac{\theta^2}{2}.$$

$$(7.66)$$

Note that the authors of the alternative continualization [67] consider a continuous function as the average between the displacement of three neighboring particles

$$u(x, t) \approx \frac{1}{1 + 2a_1}(a_1 u_{n-1} + u_n + a_1 u_{n+1}). \tag{7.67}$$

where dimensionless "weight" constant a_1 is in range $0 \leq a_1 < 1$. It is easy to see that relations (7.66) and (7.67) are identical, and the parameters a_1 and θ are connected with the following relations:

$$\theta^2 = \frac{2a_1}{1 + 2a_1}, a_1 = \frac{\theta^2}{2(1 - \theta^2)}.$$

When implementing the alternative continualization method, it is also assumed that

$$u_n(t) = u(x, t) + l^2 f_2(x, t) + l^4 f_4(x, t) + O(L^5),$$

where

$$f_2(x, t) = -\frac{a_1}{1+2a_1}u_{xx}(x, t) = -\frac{\theta^2}{2}u_{xx}(x, t),$$
$$f_4(x, t) = \frac{a_1}{12}\frac{10a_1-1}{(1+2a_1)^2}u_{xxxx}(x, t) = \frac{\theta^2}{24}(6\theta^2 - 1)u_{xxxx}(x, t).$$

Substituting (7.67) into (1.14) with account of

$$u_{n+1} = u(x + l, t) + l^2 f_2(x + l, t) + l^4 f_4(x + l, t) + O(L^5),$$
$$u_{n-1} = u(x - l, t) + l^2 f_2(x - l, t) + l^4 f_4(x - l, t) + O(L^5),$$

and expressing $u(x \pm l, t)$, $u_{xx}(x \pm l, t)$, $u_{xxxx}(x \pm l, t)$ through function $u(x, t)$ and its derivatives, using a Taylor series decomposition, we get

$$u_{tt} - \frac{l^2\theta^2}{2}u_{xxt} + \frac{l^4\theta^2(6\theta^2 - 1)}{24}u_{xxxxtt} - \frac{kl^2}{m}u_{xx} - \frac{(1 - 6\theta^2)kl^4}{12}\frac{1}{m}u_{xxxx}$$
$$= \frac{2Kl^3}{m}u_x u_{xx} + \frac{1 - 3\theta^2}{3}\frac{Kl^5}{m}u_{xx}u_{xxx} + \frac{1 - 6t}{6}\frac{w}{m}u_{xxxx}$$

7.5.2 Nonlinear Strain Waves

In terms of dimensionless variables, the equation can be written as follows:

$$\frac{\partial^2 U}{\partial \tau^2} - \frac{\partial^2 U}{\partial z^2} - \frac{\partial^4 U}{\partial z^2 \partial \tau^2} - d_1 \left(\frac{\partial^4 U}{\partial z^4} + \frac{\partial^6 U}{\partial z^4 \partial \tau^2} \right)$$

$$- d_2 \left(\frac{\partial U}{\partial z} \frac{\partial^2 U}{\partial z^2} + d_1 \frac{\partial U}{\partial z} \frac{\partial^4 U}{\partial z^4} + d_3 \frac{\partial^2 U}{\partial z^2} \frac{\partial^3 U}{\partial z^3} \right) = 0, \qquad (7.68)$$

where $U = u/u_0$, $z = x/X$, and $\tau = t/T$ are the dimensionless values of the displacement, the coordinate and time, respectively. Characteristic values of length and time are equal to

$$X^2 = \frac{l^2 \theta^2}{2}, \quad T^2 = \frac{m \theta^2}{2k},$$

dimensionless parameters have the following form:

$$d_1 = \frac{1}{\theta^2} \left(\frac{1}{6} - \theta^2 \right), \quad d_2 = \frac{2\sqrt{2} K u_0}{\theta k}, \quad d_3 = \frac{1}{\theta^2} \left(\frac{1}{3} - \theta^2 \right).$$

In terms of the traveling wave variables, Eq. (7.68) takes on the form:

$$W_{\chi\chi\chi\chi\chi} + \frac{(d_1 + v^2)}{d_1 v^2} W_{\chi\chi\chi} + \frac{(1 - v^2)}{d_1 v^2} W_\chi$$

$$+ \frac{d_2}{d_1 v^2} \left(W W_\chi + d_1 W W_{\chi\chi\chi} + d_3 W_\chi W_{\chi\chi} \right) = 0, \qquad (7.69)$$

where $\chi = z - v\tau$ is a traveling coordinate, v is a nonlinear wave velocity. The introduction of a new function $W = \frac{dU}{dx}$ allows us to reduce the order of the equation to the fifth.

By the method of the simplest equations [68], we can find the solution of Eq. (7.69):

$$W(\chi) = \frac{20 d_1 B_0 v^2}{d_2 (2d_1 + d_3)} \left(2 - 3 th^2 \left(\sqrt{B_0} \chi \right) \right) - \frac{d_1 d_3 - 3 d_1 v^2 + d_3 v^2 + 2 d_1^2}{d_1 d_2 (2d_1 + d_3)}, \qquad (7.70)$$

where $B_0^2 = -\frac{2 d_1^2 + d_1 d_3 - 3 d_1 + d_3}{16 d_1^2 (3 d_1 - d_3)}$.

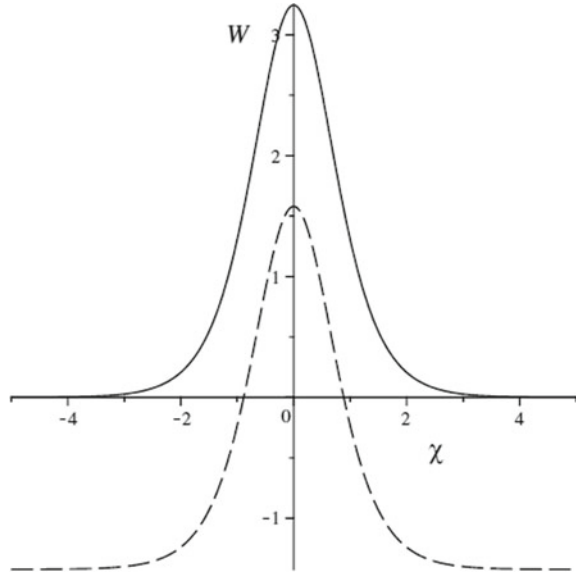Solution (7.70) has a profile in the form of a symmetric bell with a changing along the vertical axis offset (Fig. 7.31, dashed line). Fixing the sole of the bell at the zero mark (Fig. 7.31, solid line), we find the constraint imposed on the square of the wave velocity:

$$v^2 = -\frac{d_1 (2d_1 + d_3)}{20 d_1^2 B_0 - 3 d_1 + d_3}.$$

For such velocities, the solution (7.70) takes on the form:

Fig. 7.31 Dependencies $W(X)$

$$W(X) = -\frac{60d_1^2 B_0}{d_2(20d_1^2 B_0 - 3d_1 + d_3)\cosh^2(\sqrt{B_0}X)};$$

moreover, this solution has a physical meaning only in the interval $\frac{1}{6} < \theta^2 < \frac{2}{9}(\theta > 0)$. The dependences of the amplitude and width of the soliton on its velocity are shown in Fig. 7.32. When increasing the parameter θ within the considered interval, the velocity firstly increases, then decreases, the amplitude and width of the soliton monotonically increase. The curve $v(\theta)$ has a maximum point; i.e., soliton velocity is bounded from above.

The sign of the dimensionless parameter d_2 influences the polarity of the soliton. For positive values of the parameter (rigid nonlinearity), the soliton has a negative polarity. For negative parameter values (soft nonlinearity), the soliton possesses a positive polarity. The magnitude of the nonlinearity does not affect the speed of propagation of waves and their width, but affects their amplitude. The smaller the value of nonlinearity, the greater the amplitude of the wave, i.e., in weakly nonlinear media propagate waves of greater amplitude.

In the limiting case, when θ^2 is close to its bottom bound, the dimensionless parameters equal:

$$d_1 = 0, \quad d_2 = \frac{4\sqrt{3}Ku_0}{k}, \quad d_3 = 1,$$

and Eq. (7.69) has the following form:

$$W_{\chi\chi} + b_1 W + b_2(W^2 + W_\chi^2) = 0, \tag{7.71}$$

Fig. 7.32 Dependencies
$A(v)$ (solid), $\Delta(v)$ (dashed)
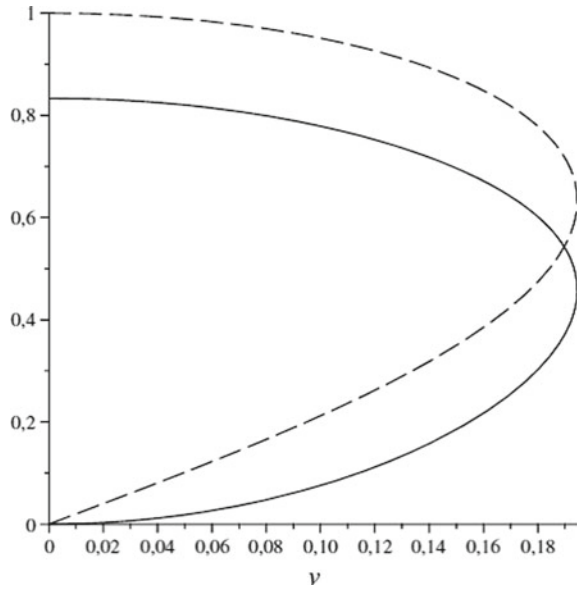
where $b_1 = \frac{1-v^2}{v^2}$, $b_2 = \frac{d_2}{2v^2} = \frac{2\sqrt{3}d}{v^2}$ are introduce to shorten the expressions, $d = \frac{Ku_0}{k}$—characterizes the elastic nonlinearity.

   Equation (7.71) is an equation of the anharmonic oscillator with two quadratic nonlinearities. Phase portrait of the equation when $b_1 > 0$ and $b_2 < 0$ is depicted in Fig. 7.33. It can be seen that there are two equilibrium states on the phase plane:

Fig. 7.33 Phase portrait (W, WX)
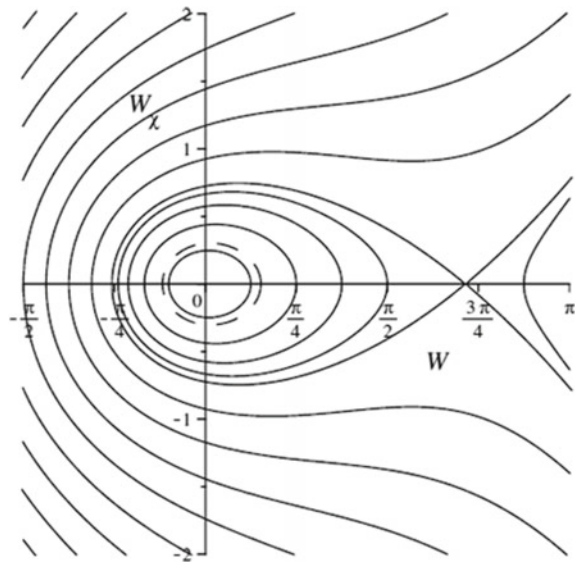
the "center," which is located at the origin of coordinates, and the "saddle," whose location (to the right or left of the center) depends on the type of nonlinearity. As in the classical case, anharmonic oscillator with quadratic nonlinearity [53], if the nonlinearity corresponds to "hard" ones, then the saddle is located to the left of the center. When $b_1 < 0$ the phase portrait is shifted along the horizontal axis, so that the saddle is located at the origin of coordinates.

Solitary soliton-type waves and periodic waves can propagate in the system as well. The exact analytical solution in the form of solitons for Eq. (7.71) cannot be found, the pole of this equation is zero [68].

In the case of a weak nonlinearity ($d \ll 1$), the solution of Eq. (7.71) can be found due to the asymptotic expansions [69]:

$$W(\chi) = A_0 \cos\left(\sqrt{b_1}\chi + \phi_0\right) + \varepsilon \frac{A_0^2 b_2}{2b_1}\left(\frac{(1-b_1)}{3}\cos 2\left(\sqrt{b_1}\chi + \phi_0\right) - (1+b_1)\right),$$

(7.72)

where the amplitude and the phase of oscillations are defined using the following expressions:

$$A_0 = \sqrt{w_1^2 + \frac{w_2^2}{b_1}} + \varepsilon \frac{b_2}{3\sqrt{b_1}} \frac{w_1\left(w_1^2 + 3w_2^2 + 2w_1^2 b_1\right)}{\sqrt{w_1^2 b_1 + w_2^2}},$$

$$\phi_0 = -\arctan\left(\frac{w_2}{\sqrt{b_1}w_1}\right) + \varepsilon \frac{b_2}{3\sqrt{b_1}} \frac{w_2\left(2w_2^2 + 3w_1^2 b_1 + w_2^2 b_1\right)}{b_1\left(w_1^2 b_1 + w_2^2\right)},$$

while w_1 and w_2 are set by initial conditions:

$$W(0) = w_1, \cdot W_\chi(0) = w_2.$$

A dotted line in Fig. 7.33 marks the approximate solution (7.72) near the stable equilibrium state. The found solution is valid only in the subsonic case and soft nonlinearity. With increasing rigidity, the amplitude of the waves (with fixed initial conditions) decreases, and the period increases. The closer the velocity of a nonlinear wave to the speed of sound, the smaller the amplitude of the periodic waves.

7.6 Conclusions

An influence of the microstructure of metamaterials on the features of the propagation of nonlinear localized strain waves in them has been investigated in this chapter.

So, due to the method of structural modeling used in this monograph, it was shown that in a crystalline medium with parameters as in NaBr or fullerite C_{60} with a simple cubic lattice, a plane soliton is unstable with respect to two-dimensional

perturbations, in a NaF crystal the soliton has a positive polarity, and in a LiF crystal, it has a negative polarity.

Within the scope of a one-dimensional model of a granular medium of ellipse-shaped particles with internal stresses, it has been shown, according to the Lighthill criterion, that modulation instability (self-modulation) of the shear deformation wave is observed for all admissible values of the microstructure parameters. The dependences of the height and width of a wave packet formed as a result of self-modulation of a quasiharmonic wave, as well as a periodic sequence of wave packets, on the parameters of the material microstructure have been determined.

A rod made of an auxetic material has been also considered in this chapter. It is shown that a negative Poisson's ratio leads to a qualitatively different (anomalous) dispersion behavior of linear waves. Nonlinearities of two types have been considered here: a "soft" nonlinearity and a "rigid" one. Accounting for such nonlinearities leads to the possibility of generating in a rod of stationary strain waves of a substantially non-sinusoidal profile—solitons and their periodic analogs. Depending on the nonlinearity type and on the value of a Poisson's ratio, propagation of "subsonic" or "supersonic" solitons is possible in a rod.

If the collision velocity is small, the interaction occurs according to the scheme of classical solitons, and it is described by Kortewege-de-Vries equation; i.e., the secondary solitons have the same velocity, amplitude, and width as the initial solitons had. When the relative velocity is higher, the soliton collision is inelastic in nature: Part of their energy is lost in the interaction and it is realized in the quasiharmonic packets of waves moving with the linear wave velocity. A further increase of the collision velocity leads to the splitting effect of solitons that means generation of a larger number of secondary solitons than before the interaction.

In addition, in this chapter, the features of the formation of spatially localized strain waves in a one-dimensional gradient-elastic medium are investigated, the dynamics equations of which have been obtained from a discrete model by the method of alternative continualization. Particularly, it has been shown that dispersion and nonlinearity influence on the propagation of plane longitudinal waves in such a medium. The nonlinearity leads to the generation of new harmonics in the wave. The energy is continuously pumped from the main perturbation to these harmonics. This effect contributes to the appearance of sharp differences in the moving profile. The dispersion, on the contrary, smoothes the distinguishes due to the difference in the phase velocities of the harmonic components of the wave. The combined effect of these two factors and their "competition" can contribute to the formation of stationary non-sinusoidal waves. Such waves propagate with a constant velocity without changing their shape.

References

1. Gerasimov, S.I., Erofeev, V.I., Soldatov, I.N.: Wave Processes in Continuous Media. Publishing of the Russian Federal Nuclear Center—All-Russian Research Institute of Experimental Physics, Sarov (2012) (in Russian)
2. Bobrovnitskii, YuI: An acoustic metamaterial with unusual wave properties. Acoust. Phys. **60**(4), 371–378 (2014)
3. Bobrovnitskii, YuI: Models and general wave properties of two-dimensional acoustic metamaterials and media. Acoust. Phys. **61**(3), 255–264 (2015)
4. Bobrovnitskii, YuI, Tomilina, T.M.: Sound absorption and metamaterials: a review. Acoust. Phys. **64**(5), 519–526 (2018)
5. Goldstein, R.V., Gorodtsov, V.A., Lisovenko, D.S.: Rayleigh and Love surface waves in isotropic media with negative Poisson's ratio. Mech. Solids **49**(4), 422–434 (2014)
6. Indeytsev, D.A., Naumov, V.N., Semenov, B.N.: Dynamic effects in materials of complex structure. Mech. Solids **42**(5), 672–691 (2007)
7. Kulesh, M.A., Grekova, E.F., Shardakov, I.N.: The problem of surface wave propagation in a reduced Cosserat medium. Acoust. Phys. **55**(2), 218–226 (2009). https://doi.org/10.1134/S1063771009020110
8. Kulesh, M.A., Matveenko, V.P., Shardakov, I.N.: Propagation of surface elastic waves in the Cosserat medium. Acoust. Phys. **52**(2), 186–193 (2006). https://doi.org/10.1134/s1063771006020114
9. Savin, G.N., Lukashev, A.A., Lysko, E.M.: Propagation of elastic waves in a solid with microstructure. Prikl. Mekh. (Appl. Mech.) **6**(7), 48–52 (1970) (in Russian)
10. Savin, G.N., Lukashev, A.A., Lysko, E.M., Veremeenko, S.V., Agas'ev, G.G.: Propagation of elastic waves in the Cosserat continuum with constrained particle rotation. Prikl. Mekh. (Appl. Mech.) **6**(6), 37–40 (1970) (in Russian)
11. Muhlhaus, H.-B., Oka, F.: Dispersion and wave propagation in discrete and continuous models for granular materials. Int. J. Solids Struct. **33**(19), 2841–2858 (1996)
12. Suiker, A.S.J., Metrikine, A.V., de Borst, R.: Comparison of wave propagation characteristics of the Cosserat continuum model and corresponding discrete lattice models. Int. J. Solids Struct. **38**, 1563–1583 (2001)
13. Suiker, A.S.J., Metrikine, A.V., de Borst, R.: Dynamic behaviour of a layer of discrete particles. Part 1: Analysis of body waves and eigenmodes. J. Sound Vib. **240**(1), 1–18 (2001)
14. Porubov, A.V.: Amplification of Nonlinear Strain Waves in Solids, p. 213p. World Scientific, Singapore (2003)
15. Pelinovsky, D.E., Stepanyants, Yu.A.: Self-focusing instability of plane solitons and chains of two-dimensional solitons in positive-dispersion media. J. Exp. Theor. Phys. **77**, 602–614 (1993)
16. Erofeev, V.I., Kazhaev, V.V., Pavlov, I.S.: Nonlinear localized strain waves in a 2D medium with microstructure. In: H. Altenbach et al. (eds.) Generalized Continua as Models for Materials. Advanced Structured Materials, vol. 91, pp. 91–110. Springer, Berlin, Heidelberg (2013)
17. Erofeev, V.I., Zemlyanukhin, A.I., Catcon, V.M., Sheshenin, S.F. Nonlinear waves in the Cosserat continuum with constrained rotation. In: Altenbach, H., Maugin, G.A., Erofeev, V. (eds.) Mechanics of Generalized Continua. Advanced Structured Materials, vol. 7, pp. 221–230. Springer, Heidelberg, Dordrecht, London, New York (2011)
18. Press, W.H., Teukolsky, S.L., Vetterling, W.T., Flannery, B.P.: Numerical Recipes in C. The Art of Scientific Computing, 680 p. Cambridge University Press, Cambridge (1992)
19. Potapov, A.I., Pavlov, I.S., Maugin, G.A.: Nonlinear wave interactions in 1D crystals with complex lattice. Wave Mot. **29**, 297–312 (1999)
20. Erofeev, V.I., Pavlov, I.S.: Self-modulation of shear waves of deformation propagating in a one-dimensional granular medium with internal stresses. Math. Mech. Solids **21**(1), 60–72 (2016)

21. Nikitina, N.Ye., Pavlov, I.S.: Specificity of the phenomenon of acoustoelasticity in a two-dimensional internally structured medium. Acoust. Phys. **59**(4), 399–405 (2013). https://doi.org/10.1134/s106377101304012x
22. Erofeev, V.I.: Wave Processes in Solids with Microstructure. World Scientific Publishing, New Jersey, London, Singapore, Hong Kong, Bangalore, Taipei (2003)
23. Erofeev, V.I., Kazhaev, V.V., Pavlov, I.S.: Inelastic interaction and splitting of strain solitons propagating in a one-dimensional granular medium with internal stress. Adv. Struct. Mater. **42**, 145–162 (2016)
24. Vanin, G.A.: Gradient theory of elasticity. Mech. Solids **1**, 46–53 (1999)
25. Rabinovich, M.I., Trubetskov, D.I.: Introduction to the Theory of Oscillations and Waves. SIC "Regular and Chaotic Dynamics", Moscow (2000)
26. Whitham, G.B.: Linear and Nonlinear Waves. Wiley, New York (1974)
27. Erofeev, V.I., Kazhaev, V.V., Pavlov, I.S.: Splitting of strain solitons upon their interaction in the auxetic rod. In: Matveenko, V.P. et al. (eds.) Dynamics and Control of Advanced Structures and Machines, pp. 57–64. Springer, Cham (2019)
28. Fozdar, D.Y., Soman, P., Lee, J.W., Han, L.-H., Chen, S.: Three-dimensional polymer constructs exhibiting a tunable negative Poisson's ratio. Adv. Funct. Mater. **21**(14), 2712–2720 (2011)
29. Kolken, H.M.A., Zadpoor, A.A.: Auxetic mechanical metamaterials. RSC Adv. **7**(9), 5111–5129 (2017)
30. Lim, T.-C.: Auxetic Materials and Structures. Engineering Materials, 588 p. Singapore, Heidelberg, New York, Dordrecht, London (2015)
31. Bilski, M., Wojciechowski, K.W.: Tailoring Poisson's ratio by introducing auxetic layers. Phys. Status Solidi B **253**(7), 1318–1323 (2016)
32. Goldstein, R.V., Gorodtsov, V.A., Lisovenko, D.S.: Longitudinal elastic tension of two-layered plates from isotropic auxetics–nonauxetics and cubic crystals. Eur. J. Mech. A: Solids **63**, 122–127 (2017)
33. Jopek, H.: Computer simulation of bending a fibrous composite reinforced with auxetic phase. Phys. Status Solidi B **253**(7), 1369–1377 (2016)
34. Zhou, L., Jiang, H.: Auxetic composites made of 3D textile structure and polyurethane foam. Phys. Status Solidi B **253**(7), 1331–1341 (2016)
35. Alderson, A.: A triumph of lateral thought. Chemistry & Industry, vol. 17, pp. 384–391 (1999)
36. Evans, K.E., Alderson, A.: Auxetic materials: Functional materials and structures from lateral thinking. Adv. Mater. **17**, 617–628 (2000)
37. Lakes, R.S.: Foam structures with a negative Poisson's ratio. Science **235**(4792), 1038–1040 (1987)
38. Goldstein, R.V., Gorodtsov, V.A., Lisovenko, D.S.: Auxetic mechanics of crystalline materials. Mech. Solids **45**(4), 529–545 (2010)
39. Alderson, K.L., Simkins, V.R., Coenen, V.L., Davies, P.J., Alderson, A., Evans, K.E.: How to make auxetic fibre reinforced composites. Phys. Status Solidi B **242**(3), 509–518 (2005)
40. Baughman, R.H., Shacklette, J.M., Zakhidov, A.A., Stafström, S.: Negative Poisson's ratios as a common feature of cubic metals. Nature **392**, 362–365 (1998)
41. Branka, A.C., Heyes, D.M., Mackowiak, Sz., Pieprzyk, S., Wojciechowski, K.W.: Cubic materials in different auxetic regions: linking microscopic to macroscopic formulations. Phys. Status Solidi B **249**(7), 1373–1378 (2012)
42. Goldstein, R.V., Gorodtsov, V.A., Lisovenko, D.S.: Average Poisson's ratio for crystals. Hexagonal auxetics. Lett. Mater. **3**(1), 7–11 (2013)
43. Goldstein, R.V., Gorodtsov, V.A., Lisovenko, D.S.: Classification of cubic auxetics. Phys. Status Solidi B **250**(10), 2038–2043 (2013)
44. Krasavin, V.V., Krasavin, A.V.: Auxetic properties of cubic metal single crystals. Phys. Status Solidi B **251**(11), 2314–2320 (2014)
45. Dinh, T.B., Long, V.C., Xuan, K.D., Wojciechowski, K.W.: Computer simulation of solitary waves in a common or auxetic elastic rod with both quadratic and cubic nonlinearities. Phys. Status Solidi B **249**(7), 1386–1392 (2012)

46. Drzewiecki, A.: Rayleigh-type wave propagation in an auxetic dielectric. J. Mech. Mater. Struct. **7**(3), 277–284 (2012)
47. Koenders, M.A.: Wave propagation through elastic granular and granular auxetic materials. Phys. Status Solidi B **246**(9), 2083–2088 (2009)
48. Kołat, P., Maruszewski, B.T., Tretiakov, K.V., Wojciechowski, K.W.: Solitary waves in auxetic rods. Phys. Status Solidi B **248**(1), 148–157 (2011)
49. Kołat, P., Maruszewski, B.T., Wojciechowski, K.W.: Solitary waves in auxetic plates. J. Non-Cryst. Solids **356**(37–40), 2001–2009 (2010)
50. Lim, T.-C., Cheang, P., Scarpa, F.: Wave motion in auxetic solids. Phys. Status Solidi B **251**(2), 388–396 (2014)
51. Malischewski, P.G., Lorato, A., Scarpa, F., Ruzzene, M.: Unusual behaviour of wave propagation in auxetic structures: P-waves on free surface and S-waves in chiral lattices with piezoelectrics. Phys. Status Solidi B **249**(7), 1339–1346 (2012)
52. Mikhailov, D.N., Nikolaevskiy, V.N.: Tectonic waves of the rotational type generating seismic signals. Izv. Phys. Solid Earth **36**, 895 (2000)
53. Erofeev, V.I., Kazhaev, V.V., Semerikova, N.P.: Waves in Rods. Dispersion. Dissipation. Nonlinearity, 208 p. Fizmatlit, Moscow (2002) (in Russian)
54. Grigolyuk, E.I., Selezov, I.T.: Nonclassical theories of rod, plate, and shell vibrations. In: Results in Science and Technology. Mechanics of Deformable Solids, vol. 5. VINITI, Moscow (1973) (in Russian)
55. Andrianov, I.V., Awrejcewicz, J., Danishevskyy, V.V., Markert, B.: Influence of geometric and physical nonlinearities on the internal resonances of a finite continuous rod with a microstructure. J. Sound Vib. **386**, 359–371 (2017)
56. Erofeev, V.I., Klyueva, N.V.: Solitons and nonlinear periodic strain waves in rods, plates, and shells (a review). Acoust. Phys. **48**(6), 643–655 (2002)
57. Erofeev, V.I., Kazhaev, V.V., Lisenkova, E.E., Semerikova, N.P.: Nonsinusoidal bending waves in Timoshenko beam lying on nonlinear elastic foundation. J. Mach. Manuf. Reliab. **37**(3), 230–235 (2008)
58. Novikov, S.P., Manakov, S.V., Pitaevskii, L.P., Zakharov, V.E.: Theory of Solitons: The Inverse Scattering Method. Consultants Bureau, New York and London (1984)
59. Dodd, R.K., Eilbek, J.C., Gibbon, J.D., Morris, H.C.: Solitons and Nonlinear Wave Equations. Academic, London (1982)
60. Scott, A.C., Chu, F.Y.F., McLaughlin, D.: The soliton: a new concept in applied science. Proc. IEEE **61**, 1443–1483 (1973)
61. Kadomtsev, B.B.: Collective Phenomena in Plasma. Fizmatlit Publishing House, Moscow (1976). (in Russian)
62. Lonngren, K.: Experimental investigations of solitons in nonlinear dispersive transmission lines. In: Lonngren, K., Scott, A.C. (eds.) Solitons in Actions, pp. 138–162. Academic, New York (1978)
63. Ostrovsky, L.A., Papko, V.V., Pelinovsky, E.N.: Solitary electromagnetic waves in nonlinear lines. Radiophys. Quantum Electron. **15**, 438–446 (1972)
64. Abdullow, Kh.O., Bogoloubsku, I.L., Makhankov, V.G.: One more example of inelastic soliton interaction. Phys. Lett. A **56**, 427–428 (1976)
65. Potapov, A.I., Vesnitsky, A.I.: Interaction of solitary waves under head-on collision. Experimental investigation. Wave Mot. **19**, 29–35 (1994)
66. Erofeev, V.I., Gerasimov, S.I., Kazhaev, V.V., Pavlov, I.S.: Splitting of strain solitons upon their interaction. Bull. Russ. Acad. Sci.: Phys. **80**(10), 1203–1208 (2016)
67. Askes, H., Metrikine, A.V.: One-dimensional dynamically consistent gradient elasticity models derived from a discrete microstructure. Part 1: Generic formulation. Eur. J. Mech. A/Solids **21**(4), 573–588 (2002)
68. Erofeev, V.I., Leontyeva, A.V., Malkhanov, A.O., Pavlov, I.S.: Structural modeling of nonlinear localized strain waves in generalized continua. In: Wolfgang, H., Altenbach, H., Muller, W.H., Abali, B.E. (eds.) Advanced Structured Materials. 2019. High Gradient Materials and Related Generalized Continua, pp. 55–68. Springer, Cham, Switzerland

69. Bogoliubov, N.N., Mitropolsky, YuA: Asymptotic Methods in the Theory of Non-linear Oscillations. Gordon and Breach, New York (1961)
70. Bayuk, I., Ammerman, M., Chesnokov, E.: Upscaling of elastic properties of anisotropic sedimentary rocks. Geophys. J. Int. **172**, 842–860 (2008)
71. Yalaev, T., Bayuk, I., Tarelko, N., Abashkin, A.: Connection of elastic and thermal properties of Bentheimer sandstone using effective medium theory (rock physics). In: ARMA-2016-128. 50th U.S. Rock Mechanics/Geomechanics Symposium, 26–29 June, Houston, TX, pp. 1–7 (2016)
72. Dubinya, N., Tikhotsky, S., Bayuk, I., Beloborodov, D., Krasnova, M., Makarova, A., Rusina, O., Fokin, I.: Prediction of physical-mechanical properties and in-situ stress state of hydrocarbon reservoirs from experimental data and theoretical modeling. In: SPE Russian Petroleum Technology Conference (SPE-187823-MS), pp. 1–15 (2017)
73. Rudenko, O.V.: Giant nonlinearities in structurally inhomogeneous media and the fundamentals of nonlinear acoustic diagnostic techniques. Phys. Uspekhi **49**, 69–87 (2006)
74. Nikitina, N.E.: Acoustoelasticity. Experience of practical application. TALAM, Nizhny Novgorod, 208 p (2005) (in Russian)
75. Yadawa, P., Singh, D., Pandey, D., Mishra, G., Yadav, R.: Acoustic wave propagation in nanocrystalline RuCo alloys. Adv. Mater. Phys. Chem. **1**(2), 14–19 (2011)
76. Destrade, M., Gilchrist, M.D., Saccomandi, G.: Third- and fourth-order constants of incompressible soft solids and the acousto-elastic effect. J. Acoust. Soc. Am. **127**(5), 2759–2763 (2010)
77. Walker, S.V., Kim, J.-Y., Qu, J., Jacobs, L.J.: Fatigue damage evaluation in A36 steel using nonlinear Rayleigh surface waves. NDT&E Int. **48**, pp. 10–15 (2012)
78. Strakaa, L., Yagodzinskyya, Yu., Landa, M., Hanninena, H.: Detection of structural damage of aluminum alloy 6082 using elastic wave modulation spectroscopy. NDT&E Int. **41**(7), 554–563 (2008)
79. Hirao, M., Ogi, H., Suzuki, N., Ohtani, T.: Ultrasonic attenuation peak during fatigue of polycrystalline copper. Acta Mater. **48**, 517–524 (2000)
80. Smirnov, A.N., Murav'ev, V.V., Khaponen, N.A.: Acoustic criterion of limiting state of long-lived metal of technical devices of hazardous facilities. Kontrol'. Diagnostika (Testing. Diagnost.) **5**, 19–23 (2004) (in Russian)
81. Ilyakhinskii, A.V., Rodyushkin, V.M.: The Dirichlet distribution in the metal-state evaluation problem by the acoustic-sensing method. Russ. J. Nondestr. Test. **51**(7), 396–399 (2015)
82. Rodyushkin, V.M., Mishakin, V.V.: Nonlinearity as the index of pre-defective state of a material. Bezopasn. Truda Promyshl. **7**, 48–53 (2009) (in Russian)
83. Kunin, I.A.: Elastic Media with Microstructure, vol. 2. Springer, Berlin (1983)
84. Cosserat, E., Cosserat, F.: Theorie des Corps Deformables. Librairie Scientifique A, 226p. Hermann et Fils, Paris (1909) (Reprint, 2009)
85. Nowacki, W.: Theory of Micropolar Elasticity. Springer, Wien (1970)
86. Leonov, M.G.: Tectonics of the consolidated crust. Nauka, Moscow (2008). (in Russian)
87. Nikolaevsky, V.N.: Geomechanics and Fluidodynamics. Kluwer Academic Publishers, Dordrecht (1996)
88. Milanovskii, E.E. (ed.): Rotational Processes in Geology and Physics. KomKniga, Moscow (2007) (in Russian)
89. Vikulin, A.V., Ivanchin, A.G.: Modern concept of block hierarchy in the structure of geomedium and its implications in geosciences. J. Min. Sci. **49**(3), 395–408 (2013). https://doi.org/10.1134/S1062739149030076
90. Vikulin, A.V., Ivanchin, A.G.: Model of a seismic process. Vychislit. Tekhnol. **2**(2), 20–25 (1997)
91. Vikulin, A.V., Makhmudov, K.F., Ivanchin, A.G., Gerus, A.I., Dolgaya, A.A.: On wave and rheidity properties of the Earth's crust. Phys. Solid State **58**(3), 561 (2016)
92. Kasahara, K.: Earthquake Mechanics. Cambridge University Press, Cambridge (1981)
93. Maslov, L.A.: Geodynamics of the Lithosphere of the Pacific Mobile Belt, 200 p. Dalnauka, Khabarovsk-Vladivostok (1996) (in Russian)

94. International Geological-Geophysical Atlas of the Pacific Ocean. Mezhpravit. okeanograf. komm. Saint-Petersburg, Moscow (2003) (in Russian)
95. Vikulin, A.V.: World of Vortex Motions. Kamchatka State Technical University, Petropavlovsk-Kamchatskii (2008). (in Russian)
96. Kuzikov, S.I., Mukhamediev, ShA: Structure of the present-day velocity field of the crust in the area of the Central-Asian GPS network. Izvest. Phys. Solid Earth **46**(7), 584–601 (2010). https://doi.org/10.1134/S1069351310070037

Discussion of the Results

The theoretical foundations of the structural modeling method are developed in this monograph. Using this method, a hierarchy of mathematical models of generalized continua for various periodic structures, frequencies and wavelengths is constructed. The main advantage of such models consists in their ability to establish in an analytical form a relationship between the microstructure parameters of a medium and its macroproperties. Thus, it becomes possible not only to get an idea of the qualitative influence of the internal structure of the medium on its effective elastic moduli, but also to find quantitative estimates of these quantities. The prerformed investigations can find application for designing of advanced metamaterials with predetermined physical and mechanical properties.

In addition, the method of structural modeling can be successfully used in geophysics and geology, since a lot of physical properties of rocks (elastic properties, thermal and electrical conductivity, hydraulic and dielectric constant) are different on various scales and are entirely determined by the internal structure of these rocks [1, 2]. It should be also noted that the method of structural modeling is used, as a rule, for crystalline media, and, for example, gas hydrates, as distinct from traditional hydrocarbons, have a crystalline structure. "Shale oil/gas" rocks are characterized by a rather high (over 30%) content of clay minerals, the crystal lattice of which contains intracrystalline water. Due to that, the elastic properties of clayminerals are drastically changed. Therefore, studies of processes, which occur at the level of the crystal lattices of such media and influence on their physical properties, are of great importance. When different-scale mathematical models of physical properties of such rocks are constructed, these studies should precede the study of properties on nano-and micro-scales [3].

The elaboration of new models is also necessary for the development of methods for acoustic diagnostics of materials with microstructure [4]. The key idea of these methods consists in describing the internal structure of a medium by means of the parameters of acoustic wave propagation in such a medium. In particular, in prestressed media (in this monograph, such media were considered in Sect. 7.2), the

phenomenon of *acoustoelasticity* is observed—the dependence of the phase velocities of ultrasonic vibrations on their polarization and the direction of a load generating stresses. The practical application of the acoustoelasticity phenomenon for studying the plane stress state of structural materials using the shear and longitudinal waves propagating along the normal to the plane of action of stresses is discussed in monograph [5], where a great attention is also paid to taking into account the microstructure of a material both in precision measurements of informative acoustic parameters and when interpreting their results for calculating of stress values. These studies are still relevant today. For example, in paper [6], the elastic moduli of the second and third orders were calculated using the Lenard-Jones potential and the propagation of elastic waves in a nanocrystalline anisotropic alloy of ruthenium with cobalt was considered. In Ref. [7], the specificity of the acoustoelastic effect in "soft" incompressible bodies is considered, where the wave velocity, even taking into account the "quadratic" acoustoelasticity, depends only on three elastic constants of the medium of the second, third and fourth orders, respectively.

The principal possibility of application of acoustic methods is provided by the fact that the conditions of propagation of an ultrasonic wave in a material vary depending on many factors: the chemical and phase composition, the grain size, the presence of inclusions, point defects, on the amount of pores and the dislocation density, on the internal and external stresses, and, including on accumulated structural damage. Naturally, there are also methods for studying the properties of materials based on the interaction of elastic waves with these structural features.

At present, the leading position among them is occupied by the nonlinear acoustic diagnostics of materials. In recent years, many works have appeared in which the damage of metals is estimated by acoustic methods [8, 9], where the measured parameter is often the velocity of elastic waves probing a metal [10, 11]. In order to estimate the state of a metal, in addition to the wave velocity, the results of measurements of some other parameters of the ultrasonic pulse (for example, the attenuation coefficient, dispersion, spectral components of the pulse, etc.), which are sensitive to the structure, are used. But again, a restricted part of information about changes that occurred in probing signal is employed for calculation of such parameters. The prospect of using the entire "array" of information obtained from an elastic wave passing through a bulk of a material with its structural features looks attractively [12]. By controlling the nonlinearity parameters of a medium, one can indirectly estimate the damage [13], as the nonlinearity grows with the appearance of "nuclei" of the destruction process. However, a more effective application of nonlinear acoustic diagnostics methods necessitates nonlinear models of materials with microstructure. In this monograph, such models are discussed in Chaps. 5 and 6.

Note that all the models elaborated in the monograph have two distinctive features. First, they consist of bodies-particles of finite dimensions, which, in contrast to the classical theory of elasticity, have both translational and rotational degrees of freedom. Secondly, the forces of interaction between the particles are simulated by elastic springs of various types. In this regard, two natural questions arise:

1. What role do springs play in these models, because in real media, of course, there are no springs? And how is it possible to interlink the rigidity of the springs with a potential of a real interaction, taking into account the type of coupling (ionic, covalent, metal)?

2. Is it necessary to take into account the rotational motions of the particles of the medium and the rotational waves associated with them, or is it enough to take into account only the translational degrees of freedom, i.e. to consider only the longitudinal and transverse waves to describe the majority of wave phenomena in microstructured media? This doubt is supported by the fact that so far nobody could observe the propagation of rotational waves in "laboratory conditions".

As for the respond to the first question, then springs and their rigidity play an exclusively auxiliary role. There are macroparameters of the medium that can be relatively easily determined experimentally (for example, the velocities of longitudinal and transverse waves), and, on the contrary, there are macroparameters that are not entirely clear how to measure experimentally (in particular, the velocity and threshold frequency of rotational waves, nonlinearity coefficients). But since both those and other macroparameters have been analytically interrelated with the rigidity of the springs due to the method of structural modeling, it is possible to find the rigidity of the springs using the known macroparameters of the first group, and using them, in turn, to calculate the macroparameters of the second group. Thus, the rigidity of the springs should be regarded as an abstract mathematical object that characterizes the force and couple interactions between the particles of a medium.

Unfortunately, it is impossible to interlink one-to-one the rigidity of the springs with a potential of a real interaction, taking into account the type of coupling (ionic, covalent, or metal). This is explained by the fact that the motion equations of the system and its energy are completely determined by setting the force constants, which, from this viewpoint, carry complete information about the system. However, the constants themselves are only effective characteristics of real compounds and do not determine the latter in a unique way. Indeed, to given force constants, firstly, there can correspond bonds inhomogeneous in the length, and secondly, bonds can involve complex connections (for example, unpaired bonds). And although they can be replaced by equivalent homogeneous pair bonds, the latter will take place only for some effective quantities. This is especially true for crystals, where physical fields of a different nature with a various nature of long-range action can correspond to the given force constants in the harmonic approximation [14].

In order to answer the second question, theoretical estimates of the threshold frequency of rotational waves in crystalline media were carried out in Chap. 4. They showed that for a grain size of about 100 nm in crystals with cubic and hexagonal symmetry, the threshold frequency of rotational waves lies in the range $10^{10} - 10^{11}$ s^{-1}. When considering wave phenomena in a lower-frequency range, as shown in this chapter, it is really possible not to take into account the rotational motions of particles of a medium, but the presence of particle sizes affects the velocities of longitudinal and transverse waves propagating in such a medium. However, when the particle size of the medium grows significantly, then the threshold frequency

decreases substantially and the range of propagation of rotational waves is drastically expanded. A similar result is achieved in the theory of the Cosserat continuum consisting of solid non-deformable material "particles" [15, 16]. Since rotations of particles relative to each other are taken into account in such a continuum, the microdisplacement tensor acquires an antisymmetric part, which can be expressed in terms of the vector of the "particle" rotation about its axis. The role of such rotations grows with increasing frequency, while with decreasing frequency, translational displacements of the centers of gravity of the medium elements (particles) acquire a major importance [14]. Thus, fail of the observation of the propagation of rotational waves is explained, most likely, by the fact that in "ordinary" solids the rotational interactions of grains with each other are very small in comparison with the other interactions.

The mentioned above data show that for a more complete and comprehensive understanding of the rotational mechanics of solids, it is necessary, first of all, to pass to such models, which particles have sufficiently large sizes and, therefore, the inertia moments. Our planet Earth is an example of such a medium, which elements are geophysical blocks or tectonic plates. They can rotate with respect to each other [17–20].

Recently, rotational waves are increasingly being studied in problems of geodynamics—one of the branches of the Earth sciences, which "elementary" structures reach the sizes of a planetary scale. Thus, V. N. Nikolayevskiy studied nonlinear interactions of longitudinal waves and rotational waves in the framework of the Cosserat model applying to seismoacoustic and geodynamic problems [18]. In the framework of a gradient-consistent model of a medium with complex structure, he attempted to explain an ultrasound generation during the propagation of seismic waves. Considering the lithosphere of the Earth in the framework of the Cosserat continuum, V. N. Nikolaevsky and his co-authors simulated a lot of geodynamic wave motions observed on the surface of the Earth, including global tectonic waves having, apparently, a rotational nature [21].

As an alternative to the Cosserat theory, A. V. Vikulin with his co-authors developed a "rotational" approach to solving geodynamic problems [22, 23]. This approach is based on the following assumptions: an elementary part of the rotating solid body— the Earth's crust block—is, first of all, a rigid non-deformable volume; secondly, its motion occurs under the action of its own moment; thirdly, such a motion leads to change of the stress state of the crust surrounding the block. In this model, in contrast to the Cosserat theory, the stress tensor is symmetric and the rotational motions of a block generating its own elastic field and interacting with the intrinsic elastic fields of other equal-sized blocks of a chain are described by the sine-Gordon equation in the dimensionless form [23].

In the framework of this rotational model it is possible to describe the whole range of geodynamic velocities of rotational waves that are typical both for geophysical and geological—processes from slow rotational waves (10^{-2} sm/s) characterizing redistribution of tectonic stresses up to fast seismic waves (1–10 km/s) [20, 23, 24].

Moreover, many geological and geophysical data can be explained in the scope of the rotational approach. For example, it has been shown that the entire Pacific

ocean plate, which area equals about 1/3 of the area of the entire planet, has made five oscillations over the past 30 million years around the "Hawaiian point" in the center of the ocean with an amplitude of about 10 degrees [25]. As there showed seismic, magnetometric, bathymetric and other observations carried out over a long period of time, Easter Island (163, 6 km^2) located in the south-eastern part of the Pacific Ocean during its existence (about five million years) has rotated by angle of almost 90° [26]. This corresponds to the angular velocity $0.5\pi/5 \times 10^6 \approx 3 \times 10^{-7}$ rad/year.

The analysis of orientations of preglacial and postglacial fissure eruptions in the southern part of Iceland made it possible to determine the angle of rotation of the island. For 10–12 thousand years this angle is approximately equal to 7° [27].

GPS observations in the Central Asian region (Tien Shan) showed that the entire area, as expected, is shifting to the North with a velocity of up to 20 mm/year. At the same time, blocks (domens) of area 150–500 km^2 were identified, which rotate in different directions with an angular velocity of up to 8 ms/year [28].

Thus, account of rotational motions of particles of a medium is necessary when either high-frequency wave processes are researched or a medium consisting of large rigid bodies is considered (especially it concerns geomedia). At present, rotational movements of blocks of the Earth's crust are no longer a hypothesis, but an experimentally established fact that is confirmed by lots of data obtained by various methods and by different groups of researchers in many regions of the Earth. And in geodynamics there is majority of experimental confirmations of the existence of rotational waves that were mathematically described back in 1909 by the Cosserat brothers.

Appendix A
Expressions for Elongation of the Springs in the Hexagonal Lattice

Expressions of the relative elongations of the springs $D_{l(m_1,m_2)}$ ($l = 1, 2, 3, 4, 5$ is the number of the spring in Fig. A.1) connecting the central particle N with its six neighbors, which have been calculated in the approximation of the smallness of the quantities $\Delta u_{m_1,m_2} = (u_{i+m_1,j+m_2} - u_{i,j})/a \sim \Delta w_{m_1,m_2} = (w_{i+m_1,j+m_2} - w_{i,j})/a \sim \sim \varphi_{i,j} \sim \varepsilon$ (here $\varepsilon \ll 1$ is the measure of the cell deformation, $m_1 = \pm 1$, $m_2 = 0, \pm 1$) and $\Phi_{m_1,m_2} = (\varphi_{i,j} + \varphi_{i+m_1,j+m_2})/2 = \varphi_{i,j} - 0, 5a\Delta\varphi_{m_1,m_2} \ll \pi/2$, with accuracy up to linear terms, have the form:
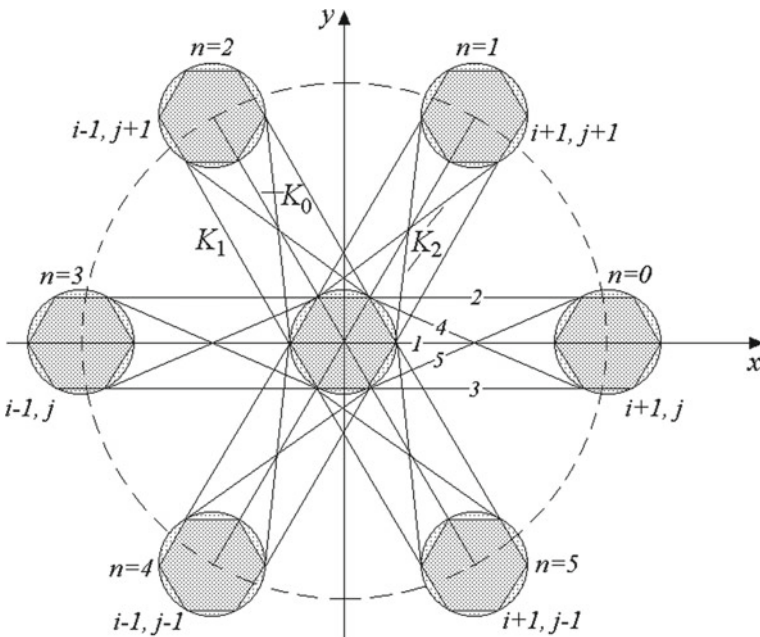
Fig. A.1 An elemenetary cell of the hexagonal lattice

$$D_{1(m_1,m_2)} = \frac{a}{2}\left(m_1\Delta u_{m_1,m_2} + m_2\sqrt{3}\Delta w_{m_1,m_2}\right), \quad D_{1(m_1,0)} = m_1 a\Delta u_{m_1,0},$$

$$D_{2,3(m_1,m_2)} = \frac{a}{4}\left(2m_1\Delta u_{m_1,m_2} + 2m_2\sqrt{3}\Delta w_{m_1,m_2} \mp m_2 d\sqrt{3}\Delta\varphi_{m_1,m_2}\right),$$

$$D_{2,3(p,0)} = m_1 a\left(\Delta u_{m_1,0} \pm \frac{d\sqrt{3}}{4}\Delta\varphi_{m_1,0}\right),$$

$$D_{4(m_1,m_1)} = \frac{m_1 a}{2r_0}\left((a-2d)\Delta u_{m_1,m_1} + a\sqrt{3}\Delta w_{m_1,m_1} + d\sqrt{3}\Phi_{m_1,m_1}\right),$$

$$D_{5(m_1,m_1)} = \frac{m_1 a}{2r_0}\left((a+d)\Delta u_{m_1,m_1} + (a-d)\sqrt{3}\Delta w_{m_1,m_1} - d\sqrt{3}\Phi_{m_1,m_1}\right),$$

$$D_{4,5(m_1,0)} = \frac{a}{2r_0}\left(m_1(2a-d)\Delta u_{m_1,0} \pm d\sqrt{3}\Delta w_{m_1,0} \pm m_1 d\sqrt{3}\Phi_{m_1,0}\right),$$

$$D_{4,5(\mp 1,\pm 1)} = \frac{a}{2r_0}\left(\mp(a+d)\Delta u_{\mp 1,\pm 1} \pm (a-d)\sqrt{3}\Delta w_{\mp 1,\pm 1} + d\sqrt{3}\Phi_{\mp 1,\pm 1}\right),$$

$$D_{4,5(\pm 1,\mp 1)} = \frac{a}{2r_0}\left(\pm(a-2d)\Delta u_{\pm 1,\mp 1} \mp (a-d)\sqrt{3}\Delta w_{\pm 1,\mp 1} - d\sqrt{3}\Phi_{\pm 1,\mp 1}\right).$$

$$(A.1)$$

Here $r_0 = \sqrt{a^2 - ad + d^2}$ is the initial length of springs K_2. In expressions for $D_{2,3}$ and $D_{4,5}$ the upper signs of the symbols $\pm$ and $\mp$ are taken for springs of types 2 and 4, wheareas the lower ones are used for 3 and 5.

Appendix B
Expressions for Elongation of the Springs in the Rectangular Lattice

Expressions for the extensions $D_{l(i+m_1, j+m_2)}$ of the springs (here the subscript $l = 0$, 1, 2, 3 denotes, respectively, the type of the spring - K_0, K_1, K_2, or K_3 (Fig. B.1)), connecting the central particle N with eight lattice neighbors (their numbers are designated by subscripts $m_1 = 0, \pm 1$ and $m_2 = 0, \pm 1$), which have been calculated in the smallness approximation quantities
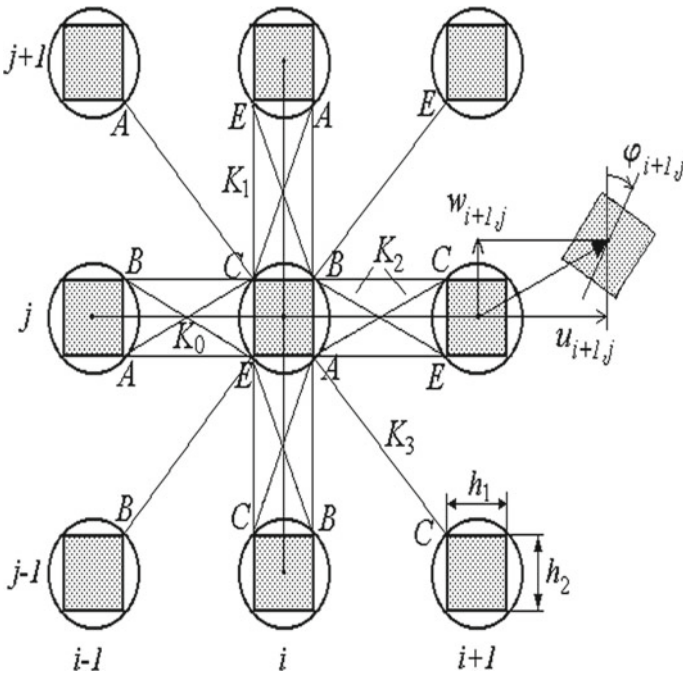
Fig. B.1 The rectangular lattice of ellipse-shaped particles

$$\Delta u_i = (u_{i+1,j} - u_{i,j}) \sim \Delta w_i = (w_{i+1,j} - w_{i,j}) \sim a\varphi_{i,j} \sim a\varepsilon,$$
$$\Delta u_j = (u_{i,j+1} - u_{i,j}) \sim \Delta w_i = (w_{i,j+1} - w_{i,j}) \sim b\varphi_{i,j} \sim b\varepsilon,$$

where $\varepsilon \ll 1$ is the measure of cell deformation, and

$$\Phi_{m_1,m_2} = \left(\varphi_{i,j} + \varphi_{i+m_1,j+m_2}\right)/2 = \varphi_{i,j} - 0,5a\,\Delta\varphi_{m_1,m_2} \ll \pi/2,$$

with accuracy up to quadratic terms, have the form:

$$D_{0(i-1,j)} = \Delta u_i + \frac{(\Delta w_i)^2}{2a} \sim D_{0(i+1,j)}, \quad D_{0(i,j-1)} = \Delta w_j + \frac{(\Delta u_j)^2}{2b} \sim D_{0(i,j+1)},$$

$$D_{1(i-1,j)}^{CB,EA} = \Delta u_i \pm \frac{h_2}{2}\Delta\varphi_i + \frac{(\Delta w_i + h_1\Phi_i)^2}{2(a-h_1)} \sim D_{1(i+1,j)}^{BC,AE},$$

$$D_{1(i,j-1)}^{EC,AB} = \Delta w_j \pm \frac{h_1}{2}\Delta\varphi_j + \frac{(\Delta u_j - h_2\Phi_j)^2}{2(b-h_2)} \sim D_{1(i,j+1)}^{CE,BA},$$

$$D_{2(i-1,j)}^{CA,EB} = \frac{1}{r_1}\left((a-h_1)\Delta u_i \pm h_2\Delta w_i \pm ah_2\Phi_i\right)$$
$$+ \frac{1}{2r_1^3}[h_2(\Delta u_i \pm h_2\Phi_i) \mp (a-h_1)(\Delta w_i + h_1\Phi_i)]^2 \sim D_{2(i+1,j)}^{AC,BE},$$

$$D_{2(i,j-1)}^{AC,EB} = \frac{1}{r_2}\left((b-h_2)\Delta w_j \pm h_1\Delta u_j \mp bh_1\Phi_j\right)$$
$$+ \frac{1}{2r_2^3}[(b-h_2)(\Delta u_j - h_2\Phi_j) + h_1(\mp\Delta w_i + h_1\Phi_i)]^2 \sim D_{2(i,j+1)}^{CA,BE},$$

$$D_{3(i-1,j-1)}^{EB} = \frac{1}{r_3}[(a-h_1)(\Delta u_i + \Delta u_j) + (b-h_2)(\Delta w_i + \Delta w_j)$$
$$+ (bh_1 - ah_2)\frac{\varphi_{i-1,j-1} + \varphi_{i,j}}{2}]$$
$$+ \frac{1}{2r_3^3}[(b-h_2)(\Delta u_i + \Delta u_j) - (a-h_1)(\Delta w_i + \Delta w_j)$$
$$- (h_1(a-h_1) + h_2(b-h_2))\frac{\varphi_{i-1,j-1} + \varphi_{i,j}}{2}]^2,$$
$$D_{3(i+1,j+1)}^{BE} \sim D_{3(i-1,j-1)}^{EB}. \tag{B.2}$$

$$D_{3(i+1,j-1)}^{AC} = \frac{1}{r_3}[(a-h_1)(u_{i+1,j-1} - u_{i,j}) - (b-h_2)(w_{i+1,j-1} - w_{i,j})$$
$$+ (ah_2 - bh_1)\frac{\varphi_{i+1,j-1} + \varphi_{i,j}}{2}]$$
$$+ \frac{1}{2r_3^3}[(b-h_2)(u_{i+1,j-1} - u_{i,j}) + (a-h_1)(w_{i+1,j-1} - w_{i,j})$$
$$+ (h_1(a-h_1) + h_2(b-h_2))\frac{\varphi_{i+1,j-1} + \varphi_{i,j}}{2}]^2,$$

$$D^{CA}_{3(i-1,j+1)} = \frac{1}{r_3}[(a - h_1)(u_{i,j} - u_{i-1,j+1}) - (b - h_2)(w_{i,j} - w_{i-1,j+1})$$

$$+ (ah_2 - bh_1)\frac{\varphi_{i-1,j+1} + \varphi_{i,j}}{2}]$$

$$+ \frac{1}{2r_3^3}[(b - h_2)(u_{i-1,j+1} - u_{i,j}) + (a - h_1)(w_{i-1,j+1} - w_{i,j})$$

$$- (h_1(a - h_1) + h_2(b - h_2))\frac{\varphi_{i-1,j+1} + \varphi_{i,j}}{2}]^2.$$

In expressions (B.2), the elongations of all the springs, except the central ones with stiffness K_0, also contain the third (upper) index displaying the vertices of the rectangles *ABCE*, which are inscribed in the ellipse-shaped particles and are connected by the corresponding spring (Fig. B.1). Note that the first is here the vertex of the central rectangle.

Expressions (B.2) for the elongations of springs with rigidity K_2 contain the signs $\pm$ and $\mp$, therefore the upper index of these formulas consists of two parts: first, the vertices of the rectangles connected by the first spring are indicated (for the extensions of such springs, the upper signs of the symbols $\pm$ and $\mp$ are taken) and after the comma—by the second spring (the lower signs of such symbols are taken for them). The extensions of the springs, which are marked with equivalence signs, are obtained by replacing all subscripts i with $i + 1$ and j with $j + 1$. However, it is necessary to take into account that if $\Phi_i = (\varphi_{i-1,j} + \varphi_{i,j})/2 = \varphi_{i,j} - (\varphi_{i,j} - \varphi_{i-1,j})/2 = \varphi_{i,j} - \Delta\varphi_i/2$, then $\Phi_{i+1} = (\varphi_{i+1,j} + \varphi_{i,j})/2 = \varphi_{i,j} + (\varphi_{i+1,j} - \varphi_{i,j})/2 = \varphi_{i,j} + \Delta\varphi_{i+1}/2$.

It should also be noted that the elongations of the springs of the second coordination sphere (with rigidity K_3) depend on the rotations of the particles in this approximation, but this dependence disappears when $b/a = h_2/h_1$, i.e. when the condition of the similarity of the particle shape to the lattice shape is satisfied.

References

1. Bayuk, I., Ammerman, M., Chesnokov, E.: Upscaling of elastic properties of anisotropic sedimentary rocks. Geophysical. J. Int. **172**, 842–860 (2008)
2. Yalaev, T., Bayuk, I., Tarelko, N., Abashkin, A.: Connection of elastic and thermal properties of Bentheimer sandstone using effective medium theory (rock physics). In: ARMA-2016-128. 50th U.S. Rock mechanics/geomechanics symposium, 26–29 June, Houston, Texas, pp. 1–7 (2016)
3. Dubinya, N., Tikhotsky, S., Bayuk, I., Beloborodov D., Krasnova M., Makarova A., Rusina O., Fokin, I.: Prediction of physical-mechanical properties and in-situ stress state of hydrocarbon reservoirs from experimental data and theoretical modeling. In: SPE Russian petroleum technology conference (SPE-187823-MS), pp. 1–15 (2017)
4. Rudenko, O.V.: Giant nonlinearities in structurally inhomogeneous media and the fundamentals of nonlinear acoustic diagnostic techniques. Phys. Usp. **49**, 69–87 (2006)
5. Nikitina, N.E.: Acoustoelasticity. Experience of practical application. Talam, Nizhny Novgorod, 208 p (2005). (in Russian)
6. Yadawa, P., Singh, D., Pandey, D., Mishra, G., Yadav, R.: Acoustic wave propagation in nanocrystalline RuCo alloys. Adv. Mater. Phys. Chem. **1**(2), 14–19 (2011)
7. Destrade, M., Gilchrist, M.D., Saccomandi, G.: Third- and fourth-order constants of incompressible soft solids and the acousto-elastic effect. J. Acoust. Soc. Am. **127**(5), 2759–2763 (2010)
8. Walker, S.V., Kim, J.-Y., Qu, J., Jacobs, L.J.: Fatigue damage evaluation in A36 steel using nonlinear Rayleigh surface waves. NDT & E Int. **48**, 10–15 (2012)
9. Strakaa, L., Yagodzinskyya, Y., Landa, M., Hanninena, H.: Detection of structural damage of aluminum alloy 6082 using elastic wave modulation spectroscopy. NDT & E Int. **41**(7), 554–563 (2008)
10. Stroscio, M.A., Dutta M.: Phonons in Nanostructures. Cambridge University Press, 274 p (2001)
11. Smirnov, A.N., Murav'ev, V.V., Khaponen, N.A.: Acoustic criterion of limiting state of long-lived metal of technical devices of hazardous facilities, Kontrol'. Diagn Testing. Diagn **5**, 19–23 (2004) (in Russian)
12. Ilyakhinskii, A.V., Rodyushkin, V.M.: The Dirichlet distribution in the metal-state evaluation problem by the acoustic-sensing method. Russ J Nondestr Testing. **51**(7), 396–399 (2015)
13. Rodyushkin, V.M., Mishakin, V.V.: Nonlinearity as the index of pre-defective state of a material. Bezopasn. Truda Promyshl. **7**, 48–53 (2009) (in Russian)
14. Kunin I.A.: Elastic Media with Microstructure, vol. 2, Springer, Berlin (1983)

15. Cosserat, E., Cosserat, F.: Theorie des Corps Deformables. Librairie Scientifique A. Hermann et Fils, Paris, 226p (1909). (Reprint, 2009)
16. Nowacki, W.: Theory of Micropolar Elasticity. J. Springer, Wien (1970)
17. Leonov, M.G.: Tectonics of the consolidated crust. Nauka, Moscow (2008). (in Russian)
18. Nikolaevsky, V.N.: Geomechanics and Fluidodynamics. Kluwer Academic Publishers, Dordrecht (1996)
19. Milanovskii, E.E.: Rotational processes in geology and physics. KomKniga, Moscow (2007). (in Russian)
20. Vikulin, A.V., Ivanchin, A.G.: Modern concept of block hierarchy in the structure of geomedium and its implications in geosciences. J. Min. Sci. **49**(3), 395–408 (2013). https://doi.org/10.1134/S1062739149030076
21. Mikhailov, D.N., Nikolaevskiy, V.N.: Tectonic waves of the rotational type generating seismic signals. Izv. Phys. Solid Earth **36**, 895 (2000)
22. Vikulin, A.V., Ivanchin, A.G.: Model of a seismic process. Vychislit. Tekhnol. **2**(2), 20–25 (1997)
23. Vikulin, A.V., Makhmudov, K.F., Ivanchin, A.G., Gerus, A.I., Dolgaya, A.A.: On wave and rheidity properties of the Earth's crust. Phys. Solid State. **58**(3), 561 (2016)
24. Kasahara, K.: Earthquake *Mechanics*. Cambridge University Press, Cambridge (1981)
25. Maslov, L.A.: Geodynamics of the lithosphere of the Pacific mobile belt. Khabarovsk-Vladivostok, Dalnauka, 200 p (1996). (in Russian)
26. International geological-geophysical atlas of the pacific ocean (Mezhpravit. okeanograf. komm., Moscow - Saint-Petersburg, 2003). (in Russian)
27. Vikulin, A.V.: World of Vortex Motions. Kamchatka State Technical University, Petropavlovsk-Kamchatskii (2008). (in Russian)
28. Kuzikov, S.I., Mukhamediev, ShA: Structure of the present-day velocity field of the crust in the area of the Central-Asian GPS network. Izvestiya. Phys. Solid Earth. **46**(7), 584–601 (2010). https://doi.org/10.1134/S1069351310070037

Bibliography

29. Belyaeva, I.Y., Zaitsev, V.Y., Ostrovsky, L.A., Sutin, A.M.: Elastic nonlinear parameter as an informative characteristic in problems of prospecting seismology. Izv. Acad. Sci. USSR, Phys. Solid Earth **30**, 890–894 (1994)
30. de Borst, R., van der Giessen, E. (eds.) Material Instabilities in Solids. Wiley, Chichester, New York, Wienheim, Brisbane, Singapore, Toronto, 556 p (1998)
31. Davydov, A.S.: Solitons in quasi-unidimensional molecular structures. Sov. Phys. Usp. **25**, 898–918 (1982)
32. Epishin, A.I., Lisovenko, D.S.: Extreme values of poisson's ratio of cubic crystals. Tech. Phys. **61**(10), 1516–1524.
33. Erofeev, V.I., Pavlov, I.S., Vikulin, A.V.: Do rotational waves really exist? Mater. Phys. Mech. **35**(1), 53–58 (2018).
34. Gusev, A.I.: Nanomaterials, Nanostructures, Nanotechnologies. Fizmatlit, Moscow (2005). (in Russian)
35. Kasterin, N.P.: On propagation of waves in heterogeneous media. Part 1. Sound waves. University Press, Moscow (1903). (in Russian)
36. Nikolaev, A.V.: Problems of Nonlinear Seismology. Nauka, Moscow (1987). (in Russian)
37. Panin, V.E. (ed.): Physical Mesomechanics of Heterogeneous Media and Computer-Aided Design of Materials. Cambridge International Science Publishing (1998)
38. Peive, A.V.: Tectonics and Magmatism. Izv. AN SSSR, Series: Geology, no. 3, pp. 36–54 (1961)

39. Sadovsky, M.A., Pisarenko, V.F. Seismic Process in the block medium. Nauka, Moscow, 96 p (1991). (in Russian).
40. Shorkin, V.S.: Nonlinear dispersion properties of high-frequency waves in the gradient theory of elasticity. Mech. Solids. **46**(6), 898–912 (2011)
41. Stovas, M.V.: Izbrannye trudy (selected papers). Nedra, Moscow (1975). (in Russian)
42. Truell, R., Elbaum, C., Chick, B.: Ultrasonic Methods in Solid State Physics. Academic Press, New York (1969)
43. Tyapkin, K.F., Dovbnich, M.M.: New rotation hypothesis of structure development and its geological mathematically ground. Knowledge, Donetsk (2009). (in Russian)
44. Vanyagin, A.V., Rodyushkin, V.M.: Measurement of acoustic nonlinearity of damaged metal. Measure. Tech. **60**, 1028–1031 (2018). https://doi.org/10.1007/s11018-018-1312-x